AD-A067 252 AIR FORCE GEOPHYSICS LAB HANSCOM AFB MASS F/G 14/2
REPORT ON RESEARCH AT AFGL JULY 1974-JUNE 1976.(U)
JUN 77 J F DEMPSEY
UNCLASSIFIED AFGL-TR-77-0137 NL

1 OF 3
AD A
067252

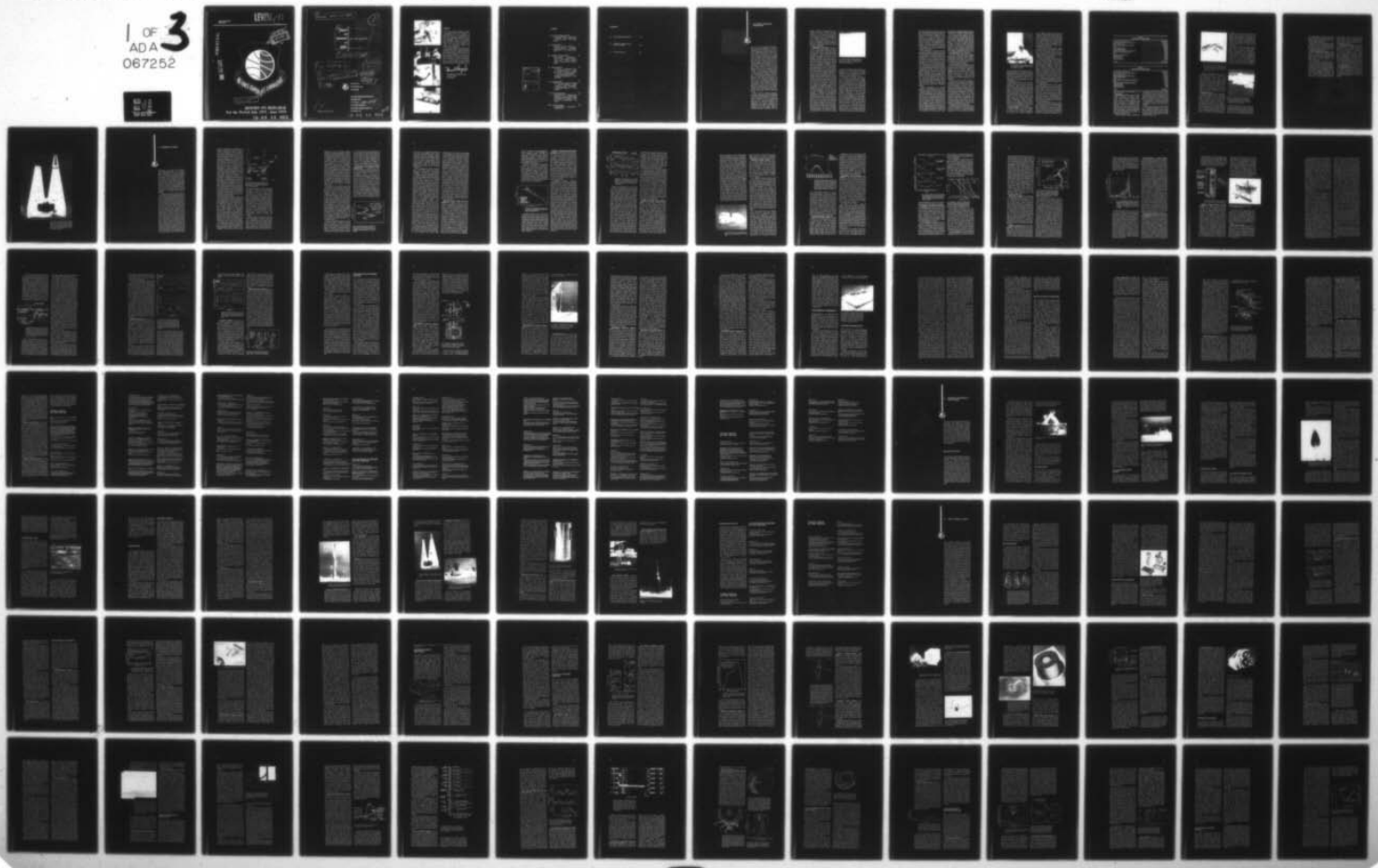

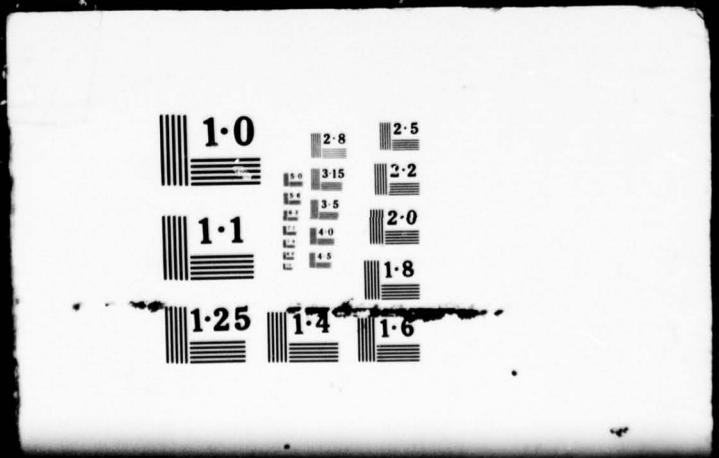

AFGL-TR-77-0137
JUNE 1977

LEVEL II

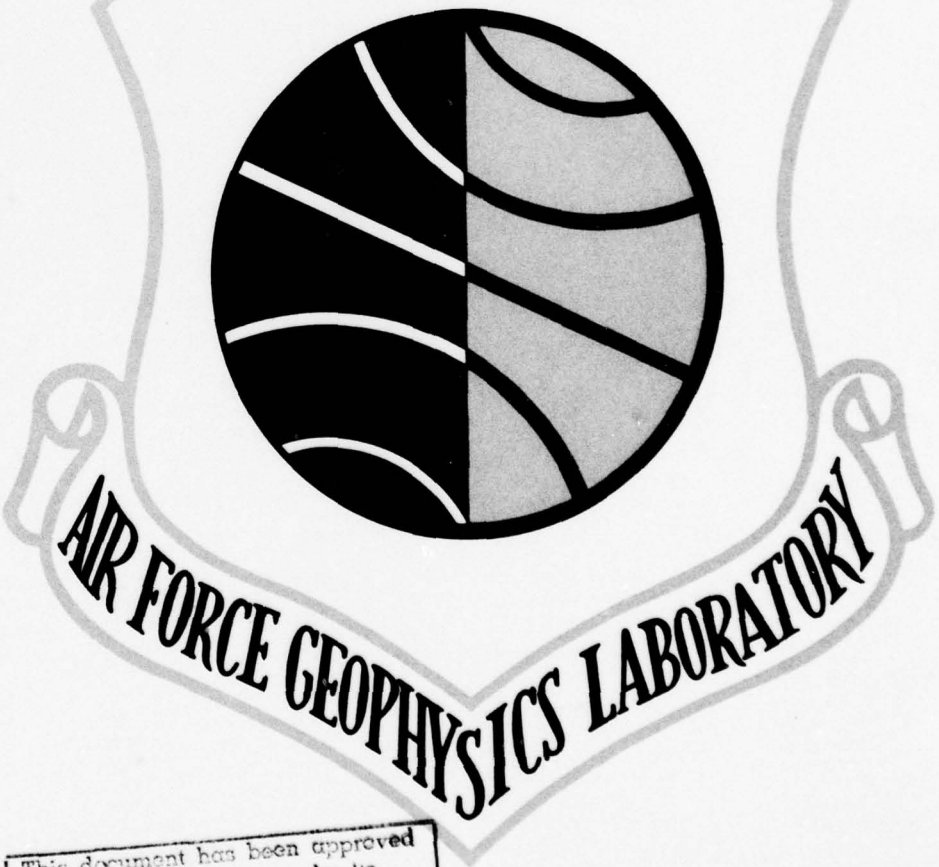

REPORT ON RESEARCH
For the Period July 1974 - June 1976

AFGL-TR-77-0137

AFGL-SR-204

Report on Research at AFGL

JULY 1974 — JUNE 1976

Interim Rept.

John F. Kennedy

June 77

9993

XX

109 p.

SURVEY OF PROGRAMS AND PROGRESS

THE AIR FORCE GEOPHYSICS LABORATORY
AIR FORCE SYSTEMS COMMAND
BEDFORD, MASSACHUSETTS

OCTOBER 1977

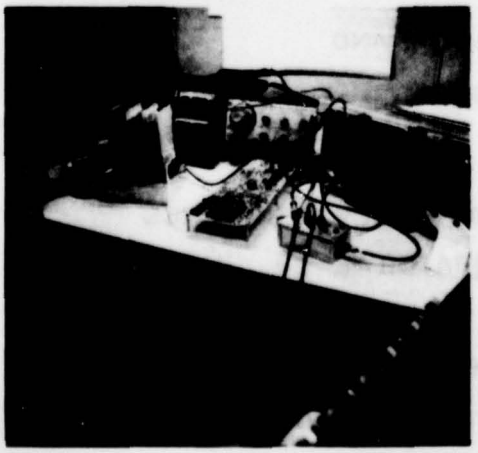

Foreword

The Air Force Geophysics Laboratory (AFGL) *Report on Research* is a continuation of a series published by AFGL's predecessor organization, the Air Force Cambridge Research Laboratories (AFCRL). The Air Force redesignated AFCRL to AFGL on January 15, 1976, in order to focus attention and effort into geophysics research and exploratory development.

The report reflects the strength and breadth of the AFGL scientific program in geophysics and its satisfaction of Air Force technological and/or system needs for geophysics R&D. It is written for DOD managers of research and development as well as the scientific community. It is a biennial report and documents progress and on-going programs during the period July 1974 through June 1976.

Bernard S. Morgan Jr.

BERNARD S. MORGAN, JR.
Colonel, USAF
Commander

Contents

Appendices

I AIR FORCE GEOPHYSICS LABORATORY

The Air Force Geophysics Laboratory came into being on January 15, 1976, by redesignation of its predecessor, the Air Force Cambridge Research Laboratories. This change reflected the Air Force policy of naming organizations according to their mission, and was made possible when the Microwave Physics Division, the Solid State Sciences Division, the Electromagnetic Environment and Ionospheric Radio Physics Branches of the Ionospheric Physics Division, and the Laser Physics Branch of the Optical Physics Division were transferred from AFCRL to the Rome Air Development Center, becoming RADC's Detachment 1, the Deputate for Electronic Technology. The remaining personnel and programs at AFGL are now devoted to exploratory and advanced development in those areas of geophysics which will meet known and anticipated military requirements. This report describes the programs, activities, and accomplishments of the organizations now comprising the Air Force Geophysics Laboratory for the period July 1, 1974 to June 30, 1976.

AFGL conducts technical programs covering a broad spectrum of disciplines in the environmental sciences. It is an in-house laboratory with a professional staff of more than 300 scientists and engineers. Its in-house programs are augmented by research conducted in universities and industry under contracts funded by the Air Force Office of Scientific Research (AFOSR). The pro-

grams of AFGL are summarized in the mission statement: Conducts research, exploratory and advanced development in those areas of the environmental sciences offering the greatest potential to the continued superiority of the Air Force's operational capability; participates in establishing advanced technologies whose exploitation will lead to new Air Force capabilities.

Organization and People: AFGL is one of 10 laboratories under the Director of Science and Technology, Headquarters, Air Force Systems Command, at Andrews AFB, Maryland. When AFCRL was merged into the Air Force Systems Command, the move was intended to focus its research and development activities more directly on evolving Air Force systems, technology, and research requirements. AFCRL's efforts had been coupled with both immediate and long-range Air Force needs, and a firm and extensive data and technology base was developed. Continuing pressure on the Air Force budget resulted in a need to utilize the available expertise in solving user-command problems, concentrating on those areas where technology can have the most rapid impact on the operational Air Force. When, in the summer of 1974, manpower restrictions were added to the budget restrictions, it was decided to change the mission of the organization. The previous mission, concentrating primarily on basic research, was to be changed to one concentrating primarily on exploratory and advanced development. AFOSR would fund basic research, giving most of the money to universities. In the early 1960's about 70 percent of the Air Force basic research funds went to universities, but attempts by research managers to preserve program continuity and stability of employment had caused more and more basic research money to be spent on in-house research programs. The manpower reductions imposed on the Air Force, while

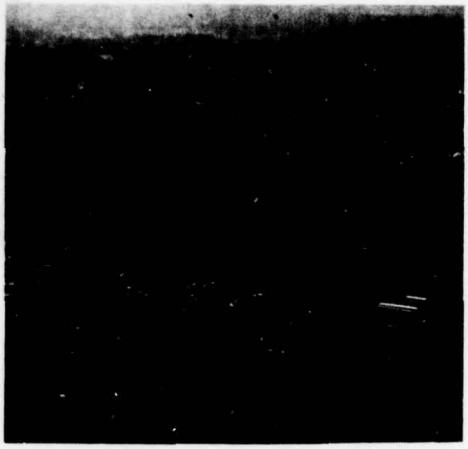

The AFGL laboratory complex is located 17 miles west of Boston at Hanscom AFB, Massachusetts, where it is a tenant of AFSC's Electronic Systems Division.

extremely unpleasant, were seen as an opportunity to re-establish the original funding ratios, while focusing in-house efforts even more sharply on the most immediate needs of the Air Force.

To execute this policy, the Department of Defense announced 111 realignments, on November 22, 1974. Included in this announcement was one directing that the geophysics research, then being conducted at the Air Force Cambridge Research Laboratories, be transferred to Kirtland AFB, New Mexico, and that civilian employment be reduced by 200 positions. Reaction to the proposed move was immediate and vocal, with a letter-writing campaign to the Massachusetts congressional delegation, and lobbying by the employees' union against both the move and the cutback. Two special select committees were formed by the Air Force, one to study the merits of transferring half of the Rome Air Development Center to Hanscom AFB (the other half was to go to Wright-Patterson AFB, Ohio) and the second, to study the

need for geophysics research in the Air Force and where it should be performed. This issue was finally resolved by the decision of Air Force Secretary John McLucas on August 15, 1975, not to move either the Rome Air Development Center or the Air Force Geophysics Laboratory. However, the 200-position reduction on civilian personnel was made effective June 30, 1976. The previous two reductions, in 1972 and 1974, had totaled 157 positions.

This reduction in authorized civilian manpower required a number of actions. The Sacramento Peak Solar Observatory was abolished as a separate Division, the facilities given to the National Science Foundation, and the employees paid by the Air Force reduced from 45 to 7. The Boundary Layer and Aerosol Interactions Branches of the Meteorology Division, the Spectroscopic Studies Branch of the Optical Physics Division, the Wave Propagation Branch of the Terrestrial Sciences Division, and the Polar Atmospheric Processes Branch of the Space Physics Division were abolished completely. The Chemical Physics Branch of the Aeronomy Division was reduced from 15 to 5 people and made a part of the Composition Branch. The rest of the reductions were taken by small reductions on other areas and in Research Services.

Other consolidations not directly caused by the reduction in force were: The Spectroscopic Studies Branch of the Aeronomy Laboratory was merged into the Ultraviolet Radiation Branch; Detachment 3 of the Aerospace Instrumentation Division at Chico Municipal Airport, California, was abolished, and its personnel, all military, were transferred; and the Energetic Particles Branch of the Space Physics Division was merged into the Geomagnetism Branch; and the Ionospheric Physics Division was abolished, two branches transferred to RADC, and the Ionospheric Dynamics and Trans-Ionospheric Propagation Branches incorporated into the Space Physics Division.

Six Divisions now comprise the Air Force Geophysics Laboratory: the Aeronomy Division, Aerospace Instrumentation Division, Meteorology Division, Optical Physics Division, Space Physics Division, and the Terrestrial Sciences Division. In addition, AFGL operates a small West Coast Office to focus AFGL support to the technology requirements and system development efforts of the AFSC Space and Missile Systems Organization (SAMSO), near Los Angeles.

The main AFGL laboratory complex is located at Hanscom AFB, Bedford, Massachusetts, 20 miles west of Boston. At Hanscom AFB, AFGL is a tenant of the Electronic Systems Division of the Air Force Systems Command.

Colonel Bernard S. Morgan, Jr., commanded AFGL during this entire reporting period, having assumed command in January 1974. Colonel Donald R. Wippermann, who had been Vice Commander since July 31, 1973, retired shortly after the end of the reporting period, on October 1, 1976. He was succeeded by Colonel Chester G. R. Czepyha.

In June 1976, 83 AFGL employees held the doctor's degree, 115 held master's degrees, and 133, bachelor's degrees. AFGL scientists are active in their respective professional societies. One scientist served as Editor of *Applied Optics* during the reporting period. Another was the Alternate U. S. Delegate to the Solar-Terrestrial Physics Group of the Pan-American Institute of Geography and History. Other AFGL scientists served as Associate Editors and referees for various professional journals, served on professional committees, and chaired professional meetings and symposia.

Examples of this type of activity include the Chairman of Working Group 4 of the Committee on Space Research, Chairman of the International Radia-

More than half of the 629 AFGL personnel are scientists or engineers. Of these, 80 have received the Ph. D degree.

tion Commission's Working Group on a Standard Radiation Atmosphere, and the Commander, who served on the editorial boards of the *Journal of Dynamic Systems, Measurement and Control,* and *Computers in Mathematical Sciences with Applications.*

During the two years covered by this Report, AFGL sponsored two scientific conferences. AFGL scientists and engineers authored 236 articles in scientific and professional journals, presented 306 papers at technical meetings, and wrote 129 in-house reports. These publications and presentations are listed at the conclusion of each division chapter. The solar physics and ionospheric physics efforts remaining in AFGL were transferred to the Space Physics Division; therefore, the publications and presentations in these disciplines are also listed following the Space Physics chapter.

Annual Budgets: The annual budgets for the two years covered in this report are shown in the accompanying tables. The totals cover salaries, equipment, travel, supplies, computer rental, service contracts, and those funds going into contract research. The largest expenditure is for salaries, which accounted for more than $22 million of an annual budget of $60.18 million. The annual budget increased from $56 million in FY-1974 to $57 million in FY-1975 and to $60 million in FY-1976.

Funds received from AFGL's higher headquarters, the AFSC Director of Science and Technology (DL), and to a lesser extent, those received from AFSC organizations other than DL, are used to conduct continuing programs.

AFGL receives support from the Electronic Systems Division, the host organization at Hanscom AFB, in accounting, personnel, procurement, security, civil engineering, and supply to the laboratory complex. Holloman AFB, New Mexico, provides services to the AFGL Balloon Detachment. AFGL provides support to RADC's Deputate for Electronic Technology (ET) in the areas of the Research Library, laboratory materials needed for the ET mission, computer, technical photography, mechanical and electrical engineering of laboratory layouts, electronic instrumentation, and woodworking.

A significant portion of the overall budget was spent for contract research. Of the $60.18 million FY-1976 budget, $12.75 million was devoted to contract research. As of June 30, 1976, AFGL had 210 contracts in effect. Of these, 105 were with U. S. industrial concerns, and 88 were with U. S. universities. The remaining 17 were with foreign universities, research foundations, and other government agencies.

AFGL contracts almost always call for work in direct support of the engineering and development carried out within AFGL. They are monitored by scientists who are themselves active, participating researchers, and who plan the research, organize the program, interpret the re-

TABLE 1
SOURCES OF FY-1975 FUNDS

Air Force Systems Command - DL	$44,157,000
Air Force Systems Command - Other than DL	4,413,640
Defense Nuclear Agency	4,141,265
Defense Advanced Research Projects Agency	3,697,898
Army	419,950
Defense Mapping Agency	296,696
Atomic Energy Commission	252,890
National Aeronautics and Space Administration	167,905
Air Force Test and Evaluation Center	38,500
Navy	35,000
Department of Transportation	33,814
Air Weather Service	26,000
Sandia Laboratories	20,000
Air Defense Command	6,500
TOTAL	$57,706,428

TABLE 2
SOURCES OF FY-1976 FUNDS

Air Force Systems Command - DL	$45,010,000
Air Force Systems Command - Other than DL	7,208,314
Defense Nuclear Agency	3,155,000
Defense Advanced Research Projects Agency	2,437,940
Defense Mapping Agency	1,118,000
Army	459,300
Energy Research and Development Administration	358,878
Navy	160,755
National Aeronautics and Space Administration	150,825
Air Weather Service	68,000
Sandia Laboratories	56,698
Air Defense Command	2,000
TOTAL	$60,185,710

sults, and share the workload of the actual research.

Field Sites: In addition to the 70 acres which it occupies at Hanscom AFB, AFGL operates several off-base sites, locally and at distant locations. The largest local site is the Sagamore Hill Radio Observatory at Hamilton, Massachusetts, which has an 84-foot radio telescope and several smaller telescopes. Other local sites are the Weather Radar Research Facility at Sudbury, Massachusetts, and the Weather Test Facility at Otis AFB, Massachusetts.

AFGL operates a balloon launch site at Holloman AFB, New Mexico. AFGL also maintains a seven-man branch of the Solar Physics Division at the Sacramento Peak Solar Observatory, at Sunspot, New Mexico, which it owned and operated for approximately 25 years, but which was transferred to the National Science Foundation, as part of the most recent cutback.

One very remote station is the Goose Bay Ionospheric Observatory at Goose Bay Air Station, Labrador, where studies of a variety of sub-arctic events are made, including polar cap absorption of high frequency radio waves.

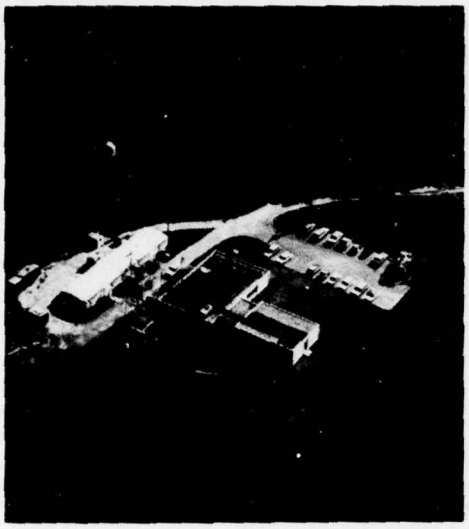

The AFGL Weather Radar Facility, at Sudbury, Massachusetts, is one of the larger off-base sites. It is used to study possible new ways to derive meteorological information from radar observations.

AFGL field programs utilize a number of military installations including the Fort Churchill, Canada, rocket range; Fort Wainwright and Eielson AFB, Alaska; Albrooke AFB, Canal Zone; Travis AFB, California; Vandenberg AFB, California, and the White Sands Missile Range, New Mexico. In addition to these military sites, AFGL has used other locations on a temporary basis. Commercial airports and the Poker Flat, Alaska, range are also used.

Research Vehicles: From its permanent balloon launch sites at Holloman AFB, New Mexico, and Chico Municipal Airport, California (now closed), and from temporary sites in several other locations, AFGL launched 111 large research balloons during the two-year period. Of these, 51 were launched during FY-1975. In addition, 27 tethered flights were conducted. These balloons carried test and experimental payloads for the Space and Missile Systems Organization (SAMSO), the Defense Nuclear Agency (DNA), the National Aeronautics and Space Administration, the Energy Research and Development Administration (ERDA), the Army, and university scientists with military contracts. AFGL scientists themselves, are, however, the largest users.

Rockets are used to examine almost every aspect of the earth's upper atmosphere and near-space environment—winds, temperatures and densities; the electrical structure of the ionosphere; solar ultraviolet radiation; atmospheric composition; the earth's radiation belts; cosmic ray activity, and airglow and aurora. The rockets most frequently used have been the Paiute Tomahawk, the Astrobee D, and the Ute Tomahawk.

Scientists studying geophysical phenomena must go to locations where they can observe these phenomena. Here, a crew has recovered a rocket-borne experiment from its landing point, north of Fairbanks, Alaska.

During the past two years, a total of 46 large research rockets were launched. The White Sands Missile Range was used most often (18 launches). Others were launched from Fort Churchill, Canada

(12); Wallops Island, Virginia (7); Poker Flat Rocket Range, Alaska (4); Woomera Rocket Range, Australia (3); and Vandenberg AFB, California (2).

During this reporting period, packages designed here were carried aboard two Air Force scientific satellites, the NASA Atmosphere Explorer D and E satellites, and the SOLRAD satellites.

AFGL Computation Center: AFGL operates a large scientific data processing facility consisting of two CDC 6600 computing systems which support AFGL, ESD, other government agencies and DOD contractors.

The CDC 6600 systems consist of a modular designed multiprocessor operation with extensive input-output devices, peripheral equipment and communications equipment. The systems provide remote batch, interactive graphics and conversational capabilities through a network of approximately 50 remote stations located within the laboratory complex and at off-base locations. The decommutation facility processes data from satellites, rockets, aircraft, balloons and from laboratory data collection systems, using two special purpose Honeywell computer systems.

AFGL Research Library: The breadth and quality of the technical collection maintained by the AFGL Research Library are surpassed by few libraries in the country. Available to AFGL scientists are the scientific journals of Bulgaria, Czechoslovakia, Holland, France, Germany, Hungary, Italy, Japan, Poland, Russia and Sweden. The collection of Chinese science journals and monographs is one of the most comprehensive in the U. S. Associated with the foreign periodical collection are translation services.

Classified Program: A portion of the research program is classified because of its relation to operational systems. Publications or presentations resulting from this classified research have not been included in the listings at the end of each chapter.

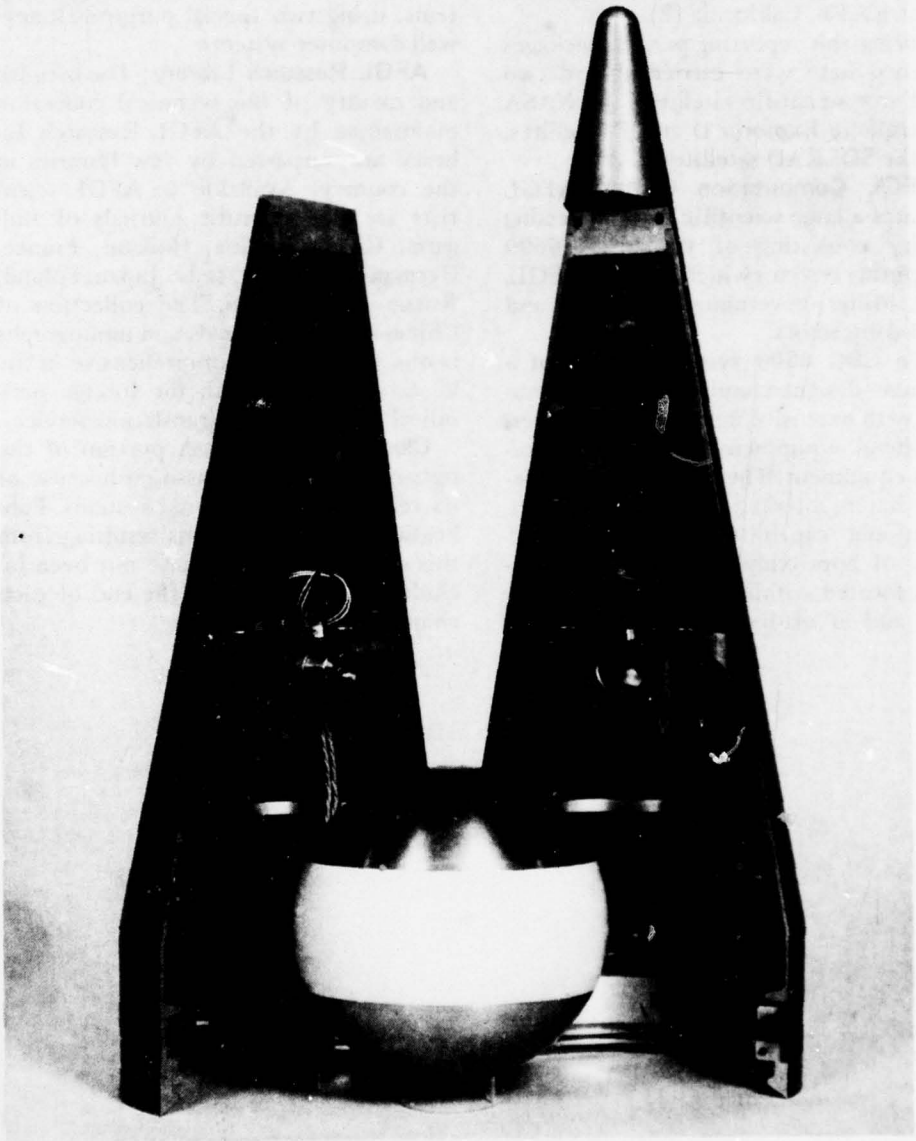

AFGL PZL densitometer (10-inch diameter falling sphere instrumented with a triaxial piezoelectric accelerometer) shown with the split nose cone deployment assembly. Installed behind the white equatorial band of the sphere are antennas for S-band PCM telemetry and C-band radar transponder.

II AERONOMY DIVISION

Aeronomy is the study of the physical and chemical properties of the earth's upper atmosphere. It deals principally with the atoms, molecules, ions and photons present in the atmosphere and how they interact with one another. The lowest region of the atmosphere, the troposphere, which extends from the ground to about 10 to 15 km, is investigated primarily by the Meteorology Division. The Aeronomy Division's principal investigations are in the regions above this—the stratosphere, mesosphere and thermosphere.

A major area of activity of the Division is the study of the stratospheric environment. The National Environmental Policy Act of 1969 requires the Air Force to provide environmental impact statements for its operations such as flying the B-1 and F-15 aircraft. Questions which must be answered include: What will aircraft emissions do to the ozone content of the stratosphere? How will this affect the amount of ultraviolet radiation reaching the earth? What will this do to the environment around us at ground level and what effect will this have on us? To answer questions such as these, the Division is engaged in a cooperative program with other government agencies such as Army, Navy, National Aeronautics and Space Administration, National Oceanic and Atmospheric Administration, Energy Research and Development Agency, Environmental Protection Agency, National Science Foundation and the Department of Transportation. The Division is per-

forming experiments, principally by means of high-altitude balloons, to determine the composition of the stratosphere, with special emphasis on those constituents that react chemically with the ozone in the stratosphere. The solar ultraviolet radiations impinging on the top of the stratosphere and their absorption as they pass through the stratosphere are being measured by means of spectrometers flown on balloons and sounding rockets. Stratospheric winds, temperature and turbulence are being measured in order to develop models for predicting the dispersion, spreading and lifetime of aircraft and missile exhaust products in the stratosphere. Laboratory chemistry experiments are being performed to measure the reactions and properties of important molecules in the stratosphere, both natural constituents and pollutants from aircraft operations. Models of the stratosphere with and without the perturbation of various pollutants are being developed for determining the environmental impact of Air Force operations. In particular, models for predicting the effect of aircraft traversing a given region of the stratosphere are being developed.

Another major area of activity is the study of ultraviolet radiations. In addition to the importance of these radiations in stratospheric research, as indicated above, the ultraviolet radiations from the sun are a principal source of energy for the earth's upper atmosphere and as such have a major influence on atmospheric composition, density and ionization. Also, the atmospheric background radiations in the ultraviolet region of the spectrum impose a limit on surveillance capabilities. These ultraviolet radiations are measured by means of optical spectrometers flown on rockets and satellites.

Another major area is the development of improved models of the properties of the earth's upper atmosphere for predicting space vehicle trajectories. For example, the Division has had a major

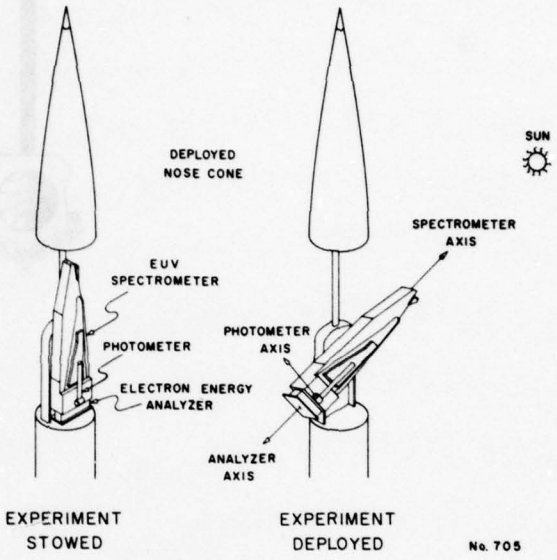

Rocket payload to measure solar UV fluxes, photoelectron energy distributions, and airglow radiation as a function of altitude in the earth's upper atmosphere.

role in the development of *U.S. Standard Atmosphere, 1976*, a cooperative effort involving the Air Force, the National Aeronautics and Space Administration and the National Oceanic and Atmospheric Administration. In systems operations, the Division is working on atmospheric density models and on geopotential models for the Aerospace Defense Command to be used in its tracking operations of all space objects, both friendly and unfriendly. The atmospheric data necessary for the development of these models is obtained by means of mass spectrometers, ionization gauges and accelerometers flown on rockets and satellites.

Another major area is the study of disturbed atmospheres. Systems operating in or through the earth's upper atmosphere may be affected by both natural disturbances such as polar cap absorption events, auroral events, and sudden ionospheric disturbances, and by atmospheric nuclear detonations. The Division, in co-

operation with the Defense Nuclear Agency, is measuring atmospheric properties during natural disturbances and developing models which are used as inputs to computer codes for predicting the atmospheric effects to be expected from nuclear detonations. Among the properties measured are the ion and neutral composition of the upper atmosphere. This is accomplished by means of mass spectrometers flown on sounding rockets with the atmospheric regions investigated being principally the D and E regions of the ionosphere. In addition, laboratory chemistry experiments are performed on the various reactions that may take place in the upper atmosphere such as positive ion-negative ion neutralization, photodissociation, photodetachment, ion-molecule reactions and reactions involving cluster ions.

The Division's investigations are being performed by means of theoretical studies, laboratory experiments and experiments by means of aircraft, balloons, sounding rockets and satellites. The satellite experiments are performed both on Air Force satellites and on satellites of the National Aeronautics and Space Administration (NASA). The Division is heavily involved with the Defense Meteorological Satellite Program. The Division has experiments on the NASA Atmosphere Explorer satellites. There are plans for participating in the national SPACELAB program. Among the experiments being proposed for SPACELAB is one in which a laser beam will probe the earth's upper atmosphere as far down as the stratosphere to determine atmospheric properties, primarily density, on a world-wide basis.

Neutral atmospheric density and temperature have been obtained by falling spheres launched by rocket, accelerometers aboard satellites, and ionization gauges on satellites. A parallel laboratory effort in theoretical density studies, atmospheric modeling, and measurements of ion-neutral reaction rates has improved understanding of the chemical processes in the upper atmosphere. The development of a system to eject charged particles from a rocket or satellite will allow control of vehicle potential, simplifying the collection of atmospheric samples by rockets, and possibly helping to protect spacecraft from high voltage discharges.

Rocket-borne Accelerometer Density Measurements: A rocket-borne measurements program, sponsored jointly by the Atmospheric Structure Branch of the Aeronomy Division and the Army's Atmospheric Sciences Laboratory at White Sands Missile Range, New Mexico, was carried out at White Sands Missile Range on December 13, 1974 to investigate the short-term variability of neutral density and temperature during a period of the so-called winter storm season. Four density measurements were made at intervals of approximately 30 minutes. A 10-inch diameter MICRO-G falling sphere payload was instrumented by AFGL and three ROBIN inflatable (passive) spheres by ASL. Up to 70 km, all sphere densities agreed well with corresponding values

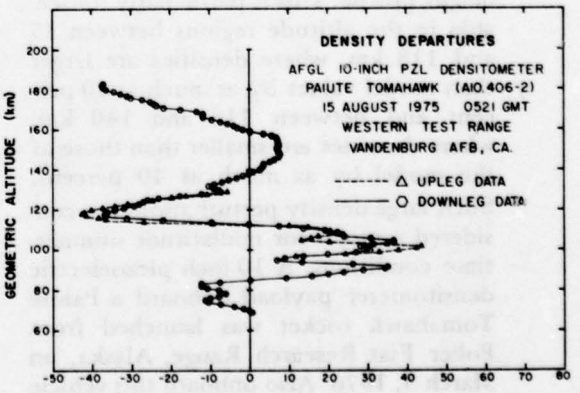

Curve of density ratios relative to CIRA 1972 (p/p CIRA 72) acquired by PZL densitometer. Comparison of upleg and downleg data show amplitude and phase changes in the wavelike structure.

from the *U. S. Standard Atmosphere, 1962* and the variability did not exceed 5 percent between successive flights. However, between 70 and 90 km, density values were observed to be about 30 percent less than corresponding model values, which is consistent with previous measurements made at White Sands Missile Range during quiet wintertime conditions.

Three rocket-borne density measurements were made using the recently developed piezoelectric densitometer consisting of a triaxial accelerometer in a 10-inch diameter aluminum sphere. The improved falling sphere instrumentation provides data over an extended altitude range (approximately 50-170 km) with greater accuracy (2 percent) and height resolution (approximately 15 meters) than was previously possible. The first operational flight of the piezoelectric densitometer was made from the Western Test Range, Vandenberg AFB, California, on August 15, 1975 and provided a continuous measurement from 70 to 170 km. The density departures relative to the COSPAR International Reference Atmosphere (CIRA) 1975 indicate considerable structure in the height profile. This is particularly noticeable in the altitude regions between 85 and 118 km, where densities are larger than model values by as much as 40 percent and between 118 and 140 km, where densities are smaller than those of the model by as much as 40 percent. Such large density perturbations are considered unusual for midlatitude summertime conditions. A 10-inch piezoelectric densitometer payload onboard a Paiute Tomahawk rocket was launched from Poker Flat Research Range, Alaska, on March 3, 1976. Also onboard this vehicle was a group of optical experiments used to determine simultaneously the vertical distributions of O_2, O_3, and total density by means of absorption measurements of solar ultraviolet and X-rays. The measurements were made near the peak of a geomagnetic substorm and following an auroral breakup. Preliminary analysis of data shows large amplitude structure in the mesosphere and lower thermosphere which may be related to Joule heating and particle precipitation. A radar transponder was first flown onboard a piezoelectric densitometer launched from Kwajalein Missile Range on August 30, 1976 to enable an independent radar track to be made of the sphere. This is an important technical advance since the accuracy of the density results depend upon the accuracy of the sphere position data. A shallow trajectory was selected for this launch in order to allow a qualitative evaluation of temporal and spatial variability of density by comparing upleg and downleg data during the period of measurement. It was assumed that there was no significant temporal variability for conjugate points along the sphere trajectory because of the short duration of the flight. However, at an altitude of 82 km the conjugate points have a horizontal separation of approximately 100 km and the apparent spatial variability is about 10 percent.

Molecular Oxygen, Ozone, and Total Density: Mesospheric ozone was measured by two different techniques during Project ALADDIN (Atmospheric Layering and Density Distribution of Ions and Neutrals) '74 on June 29 and 30, 1974, at Wallops Island, Virginia. The airglow of molecular oxygen at 1.27 micrometers and the absorption of solar ultraviolet radiation near 2950 angstroms are complementary methods that have not been compared adequately in the past. The agreement is generally good, but some of the structural difference, particularly the inversion near 77 km, is believed to reflect differences in solar elevation angle between midafternoon on June 29 and early morning on June 30. Other ozone data at lower altitudes show negligible differences between these two measure-

ments in contrast to some model predictions. A summary of the ALADDIN '74 ozone results, including four different techniques covering a 90-km altitude range, was presented at a Committee on Space Research/International Association of Geomagnetism and Aeronomy (COSPAR/IAGA) symposium.

A system to determine thermospheric density by measuring the backscatter from a laser was launched from White Sands Missile Range on June 10, 1975. The experiment utilizes the Rayleigh scattering of the laser light by atmospheric molecules. In the first flight using this novel technique, the dye laser operated perfectly, showing that such systems can be used for accurate measurements from a rocket or space platform.

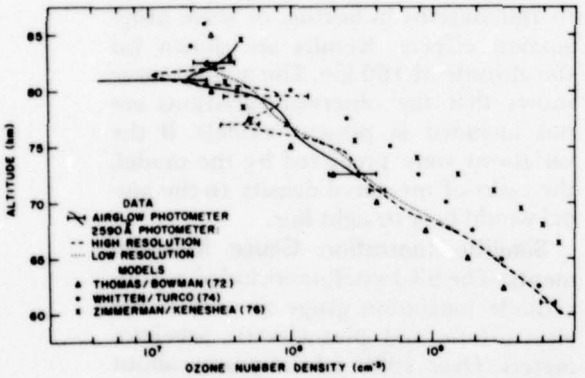

Comparison of UV and airglow techniques for ozone during ALADDIN 74, with some representative model predictions.

Additional rockets were launched in February and March 1976 as part of the Infrared Chemistry Experiments for the Coordinated Auroral Program (ICECAP) '76 program at Poker Flat Rocket Range, Alaska. Excellent data were obtained from ultraviolet sensors and the falling sphere. The data show the density, molecular oxygen and ozone environment at high latitudes related to variable geomagnetic conditions.

Satellite Accelerometer Density Measurements: A major effort has been directed toward the collection and reduction of accelerometer density measurements required to develop an accurate understanding of atmospheric variations. Data were obtained from accelerometers on five satellites during this reporting period. The NASA Atmosphere Explorer-C, D and E satellites each carried triaxial accelerometer systems consisting of three single-axis units mounted at right angles to each other. The Air Force S3-1 satellite carried a single-axis electrostatic accelerometer and a triaxial piezoelectric accelerometer being flight tested. A piezoelectric sensor was also flown on the Air Force S3-2 satellite.

Atmosphere Explorer C/(AE-C), launched December 1973 into a 68-degree inclination orbit, remained in an elliptical orbit for one year. Over 1,000 density profiles were obtained during this phase of the mission. These results, along with data from other Atmosphere Explorer experiments, were put into a central computer for use in scientific investigations. An empirical model was developed using this data base. This analysis showed that the semiannual and geomagnetic variations are in good agreement with the Jacchia 1971 models. However, individual magnetic storm responses often exceed average representations of the geomagnetic effect by more than a factor of two. The density was also found to be more variable with respect to the daily 10.7-cm solar flux than the Jacchia models predict. The sub-solar bulge has only about half the effect assumed in present models. The very low perigee altitude of AE-C permitted analysis of over 700 density values at 140 km. Increases in density as high as 50 percent were observed during geomagnetic storms and appeared to correlate with invariant latitude. A considerable amount of data was acquired near 250 km after AE-C was put into a circular orbit.

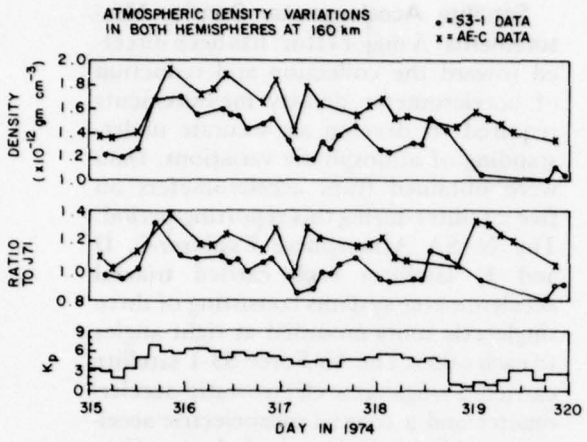

Atmospheric density variations at 160 km measured by accelerometers on the AE-C satellite in the Southern Hemisphere and Air Force research satellite S3-1 in the Northern Hemisphere.

AE-D was launched into a polar orbit in October 1975 and AE-E was launched into a near equatorial orbit in November 1975. All three accelerometers on both satellites performed normally. A spacecraft power system failure terminated AE-D operations in February 1976. However, approximately 1,000 orbits of data were obtained between 150 and 250 km before that time. These data provide global coverage of the neutral atmosphere. AE-E data were obtained throughout the elliptical orbit phase in the lower thermosphere. Data from about 300 orbits have been reduced to date. The AE-E data will permit studies of local time variations and atmospheric tides. The Air Force satellite S3-1 was launched into a near polar orbit with perigee at 155 km and apogee at 3850 km in the last quarter of 1974. Approximately 1500 orbits of density data from an electrostatic accelerometer onboard were acquired and are being reduced. Comparisons were made between this flight-proven instrument and the piezoelectric triaxial accelerometer being flight tested. The piezoelectric instrument performed well. This sensor possesses the advantages of lower cost, weight and power consumption. It has less inherent accuracy than the electrostatic accelerometer and is usable only on spinning satellites. A second Air Force satellite, S3-2, was launched into a near polar orbit with perigee near 250 km in late 1975. The piezoelectric accelerometer worked normally and data are being reduced.

The response of the neutral atmosphere to a large geomagnetic storm was studied by comparing results from AE-C when it was in the Southern Hemisphere and from S3-1 when it was in the Northern Hemisphere. A global component of the storm is observed with the density increasing by about 50 percent in both hemispheres. As the storm progresses the density fluctuations, as measured by each satellite, become out of phase, possibly due to fluctuations in heating or wave propagation effects. Results are shown for the altitude of 160 km. The middle curve shows that the observed variations are not included in present models. If the variations were predicted by the model, the ratio of measured density to the model would be a straight line.

Satellite Ionization Gauge Measurements: The S3-1 satellite included a cold-cathode ionization gauge as well as the electrostatic and piezoelectric accelerometers. Over 1900 orbital passes, about perigee, were acquired during which successful gauge measurements were obtained. During the six-month lifetime of the satellite, perigee precessed around the earth, thereby providing latitudinal sampling on a global scale. Reduction of the measurements to atmospheric densities has been accomplished and results are currently being compiled for use in analysis and correlation studies. Of particular interest are the results obtained during two moderately large geomagnetic storms which occurred while the satellite was in orbit. The extensive measurements from these periods will

make it possible to extract added information and detail about the morphology of storm development, progress and decay insofar as it affects atmospheric structure. Phenomena such as wave propagation were seen to occur during geomagnetic storms, usually near the polar regions of the earth. The Air Force research satellite S3-2 also carried ionization gauges onboard. S3-2 was placed into a less eccentric orbit with an initial perigee at 207 km and apogee at 1344 km. This satellite is still in orbit and is providing data of high quality. Instrumentation is being developed and fabricated for flights onboard the S77-2 spacecraft scheduled for launch in the fourth quarter of 1977. In addition to atmospheric neutral density measurements, the S77-2 instrumentation will provide information concerning atmospheric ambient temperature, winds and spacecraft aspect referenced to the flight vector. The additional measured parameters will be monitored by means of a motor-driven baffle extension. The baffle extension interrupts the airstream flow into the ionization gauge sensor producing a signal dropout. From analysis of the rise and fall times of the signal dropout waveform, atmospheric temperature and winds can be inferred.

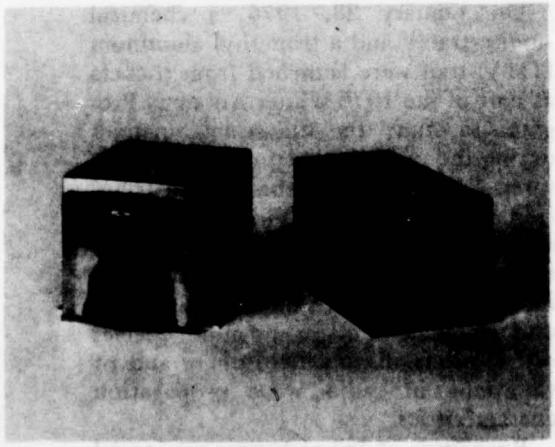

Cold cathode ionization gauge flight units, sensor on left with operating electronics at right.

Theoretical Density Studies: Derivation of density values from radar observations of the orbital motions of satellites has continued. Data from three Doppler Beacon satellites, as well as from some other low perigee Air Force satellites have been used to derive density data. The results of two computer programs for determining the orbit and atmospheric drag of the Doppler Beacon satellites were compared.

Two empirical density models based on drag analyses of 22 low-perigee satellites were developed for use in predicting low-altitude satellite ephemerides. A stepwise multiple regression analysis was performed with density at 145 km as the dependent variable, and a number of independent variables chosen to represent variations with solar cycle, geomagnetic activity, latitude, season, day of year and time of day. Densities between 120 and 500 km were determined from the hydrostatic law in a simple but realistic analytic form. The two models compared very well with the 1971 Jacchia model. The main advantage of such models is that they represent major savings in both computer storage and run time making improvement in operational systems possible.

The solar diurnal tide in the thermosphere excited by absorption of EUV and UV solar radiation for equinox conditions was determined by numerically integrating the linearized tidal equations for a spherical, rotating, viscous atmosphere. The model takes into account eddy viscosity, Newtonian cooling, molecular viscosity and conductivity, Coriolis acceleration and anisotropic ion drag. Because height and latitude terms are inseparable in the mathematical system, vertical structures of all tidal fields were found to vary with latitude; or equivalently, the horizontal structures

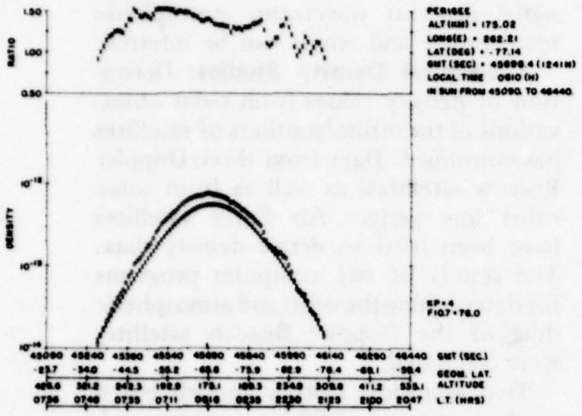

Data obtained from satellite ionization gauge illustrating wavelike structure observed over south polar region. In the lower portion of the figure the open circles are gauge determined densities and crosses are Jacchia 71 model values. In the upper portion of the figure crosses represent the ratio values of the gauge determined densities to the J71 values.

vary with height, contrary to classical inviscid tidal theory. Tidal structures also vary with the level of solar activity, since the altitudes where diffusion and hydromagnetic ion drag dominate the momentum balance depend upon the background temperature and ionospheric structures. Increased ion drag associated with more active solar conditions inhibits acceleration of the neutral winds via transfer of momentum to the (denser) ionospheric plasma; however, the suppression of subsidence heating, which is nearly in antiphase with the EUV heat source, gives rise to increased temperature amplitudes.

Geopotential Model Studies: The performance of several geopotential models in predicting the orbital ephemerides has been evaluated for some low-altitude SAMSO satellites and three Doppler Beacon satellites (perigee height approximately 160 km) as well as for a medium perigee height satellite, OV1-17 (perigee height approximately 300 km) and a higher perigee height satellite, OV1-21 (perigee height approximately 800 km).

Inasmuch as the larger geopotential models were quite time-consuming on the computer, a geopotential optimization scheme was devised which selects only the important geopotential terms in the ephemeris computation for a particular satellite. These tests showed that geopotential models can be optimized to save approximately 50 percent of the computer time with negligible loss in accuracy. Geopotential models that have been studied include the Gaposchkin 8x8, Standard Earth III, and WGS 72.

Mesospheric and Thermospheric Turbulence: To determine the structure and occurrence rates of turbulence between 30 and 90 km altitude, rocket grenade data taken between 1961 and 1967 have been utilized. These data were obtained at four latitudes: Barrow, Alaska, (71.3 degrees North); Churchill, Canada (58.7 degrees North); Wallops Island, Virginia (37.8 degrees North) and Natal, Brazil (6 degrees South). The results show that the rate of occurrence of turbulence increases with altitude approximately exponentially. A solar cycle relation proportional to the sunspot number and the 10.7 cm flux was noted at 70 to 90 km over Wallops Island, Virginia.

On January 28, 1976, a chemical smoke tracer and a trimethyl aluminum (TMA) trail were launched from rockets as part of the 1976 Winter Anomaly Program to study the fine-scale dynamics during the quiet period following a measured "anomalous" event. The distribution and intensity of turbulence determined from the fine-scale winds and from the density fluctuations observed in the TMA trail are important for the understanding of major and minor species distributions in the mesosphere and of variations in radio wave propagation characteristics.

Reanalysis of the nighttime equatorial electron density turbulent fluctuations from 86 to 115 km suggests that the electron density fluctuations follow the

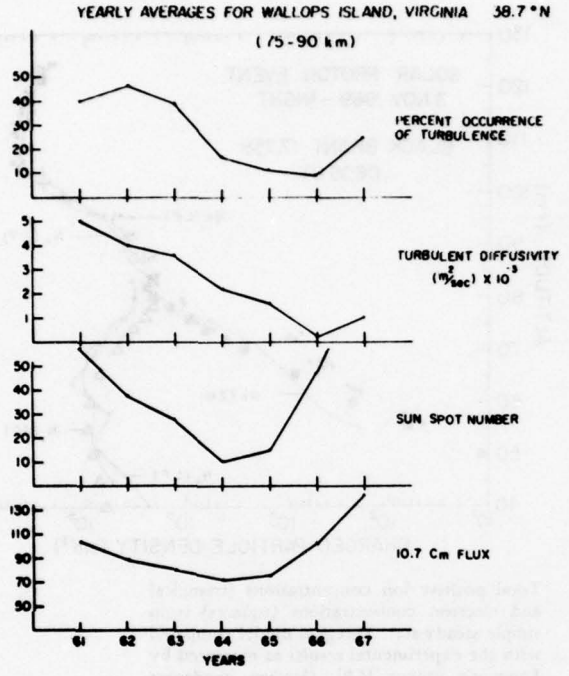

The cyclical behavior of the yearly averaged percent occurrence of turbulence and the turbulent diffusivities. These are compared to the yearly averaged values of sunspot number and 10.7 cm flux.

neutral turbulence, and does not support equatorial electrojet turbulence theory.

Atmospheric Dynamics and Models: The time-dependent model calculations of ALADDIN II were corrected to conform to the amended mass density from 110 to 135 km. The resulting calculations more accurately describe the neutral species distributions over the altitude range of measurements than did the original calculations for the altitude region 90 to approximately 150 km.

The ALADDIN I calculations were extended to 400 km to provide the model with better boundary conditions and to include a more comprehensive approach to the description of atomic hydrogen. This extension produced a better description of the hydrogenic dynamics in coupled calculations and showed good to excellent agreement with the hydrogen distribution determined from thermospheric ionic measurements.

The ALADDIN I calculations were again expanded to include the ionic species and the additional neutral species necessary for their description. The initial calculations of this amended model included the motion of molecular nitrogen with the mean mass motion assumed to be zero. The ionic distributions resulting from this calculation reproduced well the measured distributions of the major F-region ionic constituents.

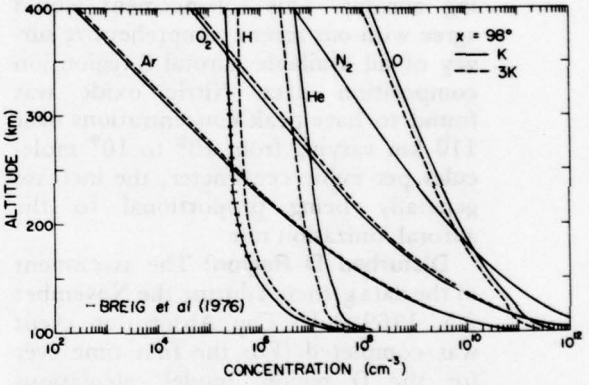

The ALADDIN I major and some minor thermospheric theoretical species distributions from 100 to 400 km. Included in the figure are the measured atomic hydrogen data from Breig et al (1976) for comparison purposes.

Thermospheric dynamics were analyzed by applying the coupled equations of motion including the effects of thermal diffusion of all species. The results of these calculations were applied to the measurements of rocket-borne neutral mass spectrometer data in the altitude region from 120 to approximately 200 km. The results showed that atomic oxygen flow does exhibit a reversal from downward to upward motion between 155 and 190 km, and that the velocity determined can be in error by a factor of 2 if thermal diffusion effects are ignored.

Auroral Chemistry: A study of auroral chemistry has led to the conclusion that

the charge transfer process between molecular oxygen ions and nitric oxide in the auroral E region, a major source of nitric oxide ions, may leave the oxygen in an electronically excited state. This mechanism could contribute to an explanation of the 1.27-micrometer emission greater than that predicted by theory sometimes observed in auroras. Formation of molecular nitrogen in its triplet A electronic state during auroras and its subsequent reaction with atomic oxygen may yield nitric oxide and thus substantially enhance the ambient nitric oxide concentration in the E region during auroras. This enhancement would agree with our recent comprehensive survey of all available auroral E-region ion composition data. Nitric oxide was found to have peak concentrations near 110 km varying from 10^8 to 10^9 molecules per cubic centimeter, the increase generally being proportional to the auroral ionization rate.

Disturbed D Region: The assessment of the data garnered during the November 2-5, 1969 Polar Cap Absorption event was completed. For the first time ever for the D region, model calculations agreed with the positive ion measurement data. (The quiet D-region structure is unsolved to date.) A detailed comparison for the nighttime was made for a relatively simple, but fast, steady-state model that was constructed. The daytime positive ion data were generally compatible with an earlier provisional model. A high-precision determination of the daytime electron loss rate as a function of altitude was also determined. The nighttime electron loss rate had been previously solved.

Laboratory Measurements of Ion Dissociation: Molecular ions in the atmosphere may dissociate following photon absorption or as the result of an energetic collision with a neutral species. Studies of each of these reactions are carried out in the Aeronomy Division using double

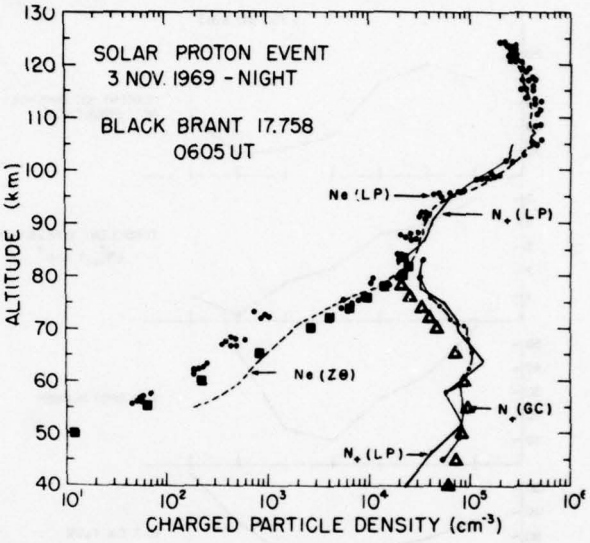

Total positive ion concentrations (triangles) and electron concentrations (squares) from simple steady-state D-region model compared with the experimental results as measured by Langmuir probes (LP), Gerdien condenser (GC) and Z-Theta ($Z\theta$) probe.

mass spectrometer systems to produce mass analyzed beams of the desired reactant ions and to analyze the products of the ion-photon or ion-neutral collisions. In ion photodissociation, the ion beam collides with a pulsed photon beam from a tunable dye laser. The wavelength of the photons is restricted to a bandwidth of about 0.1 nanometer in the range from 260 to 700 nanometers. Absolute cross sections are measured for photodissociation processes occurring in this range. In addition, time-of-flight analyses of the product ions provide information on the bond dissociation energy and on the vibrational levels of the reactant ions. This technique has so far been used to measure photodissociation cross sections for H_2^+ and its isotopes and for N_2O^+. Photon absorption excites the ions to a repulsive upper state which immediately dissociates, and the photodissociation spectrum is a continuum. In contrast, photon absorption by N_2O^+ in the wave-

length range from 300 to 340 nanometers excites a long-lived upper state which may decay by dissociation to NO^+ and N, as observed in these experiments, or by fluorescence, as previously observed by other workers. The N_2O^+ photodissociation spectrum in this wavelength range is highly structured.

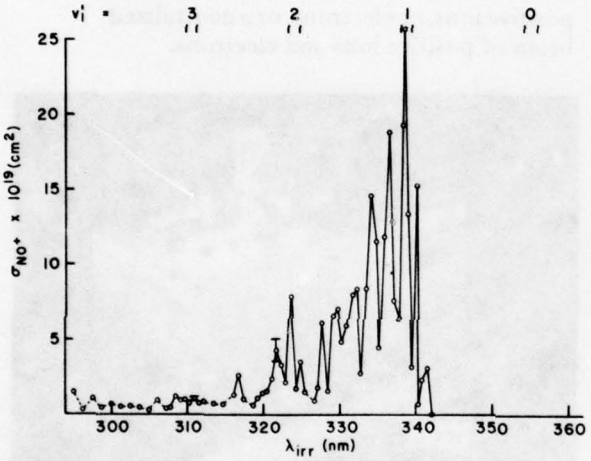

The photodissociation spectrum of N_2O^+. The photon absorbing state is the 2π ground electronic state. Vibrational levels for the symmetric stretching mode of this state are indicated by vertical lines across the top of the figure.

Collisional dissociation of ions may occur in the nuclear or natural perturbed atmosphere. In addition to measurements of the cross sections for these processes, laboratory studies on collisional dissociation provide information on bond dissociation energies and on the occurrence of competitive reaction channels. For example, in the reaction of CO_3^- with O_2, the observed ionic products are O^- resulting from collisional dissociation of CO_3^-, and O_3^- resulting from transfer of an O^- ion from CO_3^- to O_2. Cross sections for these reactions and for the dissociation of NO_2^- and NO_3^- in collisions with important atmospheric neutral molecules have been measured.

Thermochemistry of Metal Oxides: During this reporting period a high-temperature mass spectrometer was successfully refurbished and put into operation. This instrument has been used and will continue to be used to study the thermochemical properties of various metal oxides. These species are studied because they are formed following nuclear detonations and they may be sources of intense optical radiation as well as sources of ionization resulting in interference with radio and radar communications. Towards this end the dissociation energies and ionization potentials of thorium, zirconium and europium gaseous oxides were measured. In addition to the thermochemical studies some work has been performed to study the kinematics of ion-neutral collisions at energies between approximately 1 eV and 100 eV. For these experiments a double mass spectrometer system has been used, and so far cross sections have been measured for the reaction of N^+ and N_2^+ with N_2O and of N^+ with O_2. Isotopically labeled projectiles have been used to study the reaction of N^+ and N_2^+ with N_2O. From these experiments it is concluded that N_2^+ and N_2O undergo charge exchange reactions solely by electron transfer. It was found that in the reaction of N^+ with N_2O, charge transfer proceeds via both ion-atom exchange and electron transfer.

Charged Particle Ejection from Rockets and Satellites: An electron beam rocket payload was constructed, calibrated in a laboratory vacuum system, and flown to an apogee of 173 km at White Sands Missile Range, New Mexico, on August 6, 1975. The purpose of the flight was to measure the ambient atmospheric density, molecular nitrogen concentration, and the vehicle potential during beam emission. The payload instrumentation included two electron beam guns, three photometers with 3914 angstrom filters, two proportional counters with 2-mil beryllium windows, and a retarding po-

tential analyzer. All the payload instrumentation operated successfully during ascent and descent. Measurements were made from 110 km to 173 km on ascent, and from 173 km to 80 km on descent. Useful density results were obtained.

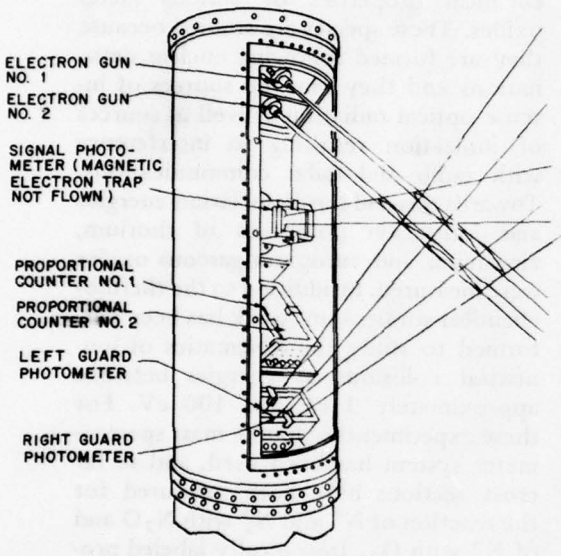

Sensor layout on electron beam payload, rocket borne Bremsstrahlung density experiment.

Satellite Charged Particle Ejection Systems: Two charged particle ejection systems have been developed and built for use on the SCATHA (Spacecraft Charging AT High Altitudes) satellite. These systems will be used to test a variety of techniques of controlling vehicle potential. The Satellite Electron Beam System utilizes a triode electron gun and allows for the ejection of currents from one microampere to 13 milliamperes, and particle energies from 50 eV to 6 keV. Continuous and pulsed beams can be obtained with a number of different focus conditions. In all, 250 combinations of different modes can be obtained by ground commands. The other instrument is the Satellite Positive Ion Beam System which will allow for the controlled ejection of xenon ions. Beam currents from 0.3 mA to 2.0 mA, and beam particle energies of 1.0 and 2.0 keV will be commandable from the ground. A neutralizer will be available which can be used either in conjunction with the beam or separately. The neutralizer can be biased from -1 kV to + 1 kV with respect to satellite ground. The Satellite Positive Ion Beam System can be commanded from the ground to emit positive ions, or electrons, or a neutralized beam of positive ions and electrons.

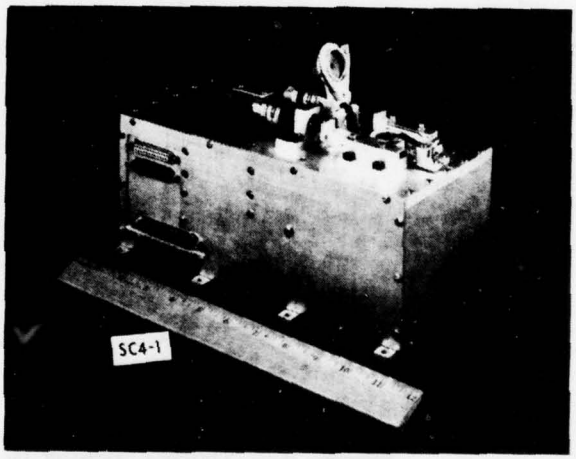

Satellite Electron Beam System (SC4-1) showing opened electron gun.

From July 1974 to June 1976, seven major Air Force and DOD rocket programs and two satellite programs were carried out. Generally these efforts were conducted to determine the ion and neutral compositions of the upper atmosphere during natural and man-made disturbances and their effects on Air Force systems.

Rocket Measurements: A total of 11 rocket payloads were launched in 7 different efforts to define the ionospheric conditions for communications, navigation and detection systems and also to define atmospheric conditions for calculations of infrared backgrounds and satellite ephemerides.

A coordinated auroral studies program designated ICECAP '75 was carried out from Poker Flat, Alaska, on March 3, 1975 by the Air Force and the Defense Nuclear Agency. A dual-mode quadrupole mass spectrometer that was programmed to measure the positive ion and neutral composition on alternate mass scans was included in a multi-instrumented Sergeant-Hydac rocket. The rocket was launched into a strong auroral arc and measurements were obtained in the E and F regions. The most interesting of the results was the finding that the positive ion plasma seemed to contain a significant component that was not thermal but had energies in excess of several electron volts. This could have important implications in the creation of disturbed ionospheres. It was the subject of a later rocket program.

Another program was part of a coordinated effort (Project AEOLUS, for Auroral Excitation of Oscillation and Layering of the Underlying Species) conducted at Fort Churchill, Canada, to study polar ionospheric structure and dynamic processes, especially those induced by an auroral electrojet and an auroral arc. Three Paiute-Tomahawk rockets were launched, along with other rockets containing various chemical releases in three separate events. The first rocket, containing a positive ion mass spectrometer, plasma frequency probe, electron energy deposition scintillator and electric field probes, was launched during an enhanced electrojet of about 700 kA at 0400 Central Standard Time on April 10, 1975. Measurements were obtained between 104 km and 211 km on ascent and down to 79 km on descent. The major ions measured in decreasing abundance were NO^+, O_2^+, O^+, N_2^+ and N^+. Ionized atomic oxygen attained a maximum relative concentration of only about 20 percent at the peak altitude with the NO^+/O_2^+ ratio about 3.5 ± 0.5 above 120 km. Significant O_2^+ signals were observed down to 82 km which require a source of ionization to explain. The O_2^+ ions were found to be due to a small amount of particle ionization as determined from the electron scintillator results. Water cluster ions were measured below 86 km. The second rocket carried a dual-mode ion-neutral quadrupole mass spectrometer and no electric field sensor was included. The rocket was launched at 0312 Central Standard Time on April 21 during very quiet conditions (less than 50 kA electrojet) for comparative purposes. Measurements were obtained between 108 and 222 km on ascent and down to 93 km. on descent. Compared to the first rocket, there was a stark decrease in the O_2^+ abundance with NO^+/O_2^+ ratios decreasing from about 100 near 120 km, to 10 at 175 km and to 2 at 220 km. Further, O^+ became the dominant ion above 215 km. Aluminum ions which resulted from a trimethylaluminum release from a rocket were also measured above 175 km allowing a tracer study of ionic motions. Excellent measurements of the neutral composition were obtained above 115 km. The third rocket, with a payload similar to that of the second one, was launched into an auroral arc of approximately class 2^+ to 3 at 2218 Central Standard Time on April 24. Measurements were obtained from 108 km to 217 km on upleg and to 84 km downleg. NO^+ was the major ion above 90 km. However, reflecting the auroral ionization, O^+ was significantly enhanced such that the O^+/O_2^+ ratio was near unity above 140 km while the NO^+/O_2^+ ratio was almost constant at 3.5 ± 0.5 above 115 km. Water cluster ions were observed below 87 km.

Project AEOLUS was highly successful and significant results on the polar ionosphere structure and dynamics were obtained. The results are being examined to determine the possible sources and effects of Traveling Ionospheric Disturbances.

A rocket payload consisting of a positive ion mass spectrometer, plasma frequency probes and an energetic electron scintillator was launched from Fort Churchill, Canada, on April 28, 1976, into a strong auroral form. The mass spectrometer was programmed to measure the energetic spectrum of the ionospheric species which from earlier experiments seemed to have energies in excess of several electron volts. In this particular flight there was no evidence that the major ionospheric species had more than their normal thermal energies; however, there was some evidence that the minor ions, H^+ and He^+, had suprathermal energies.

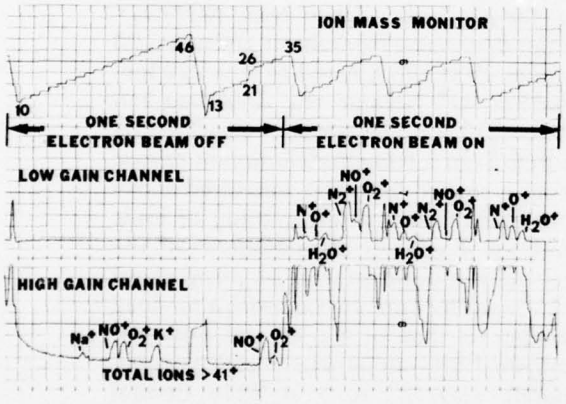

EXCEDE: SWIR. Positive Ion Mass Spectrometer Data–note the change in the relative concentrations of the major ions (N^+, O^+, H_2O^+, N_2^+, NO^+ and O_2^+) as a function of the beam on and off time. The dynamic range of the low gain channel extends from 10^{-11} to 10^{-6} amps, the high gain channel from 10^{-16} to 10^{-11} amps.

The Air Force/Defense Nuclear Agency EXCEDE: SWIR rocket experiment was primarily designed to measure the spatial, spectral and temporal nature of the visible and infrared atmospheric emissions induced by a pulsed rocket-borne energetic electron gun (3 kV, 1 ampere). A specially programmed positive ion mass spectrometer was included as part of this payload that was launched on a Sergeant rocket into a quiet night atmosphere from Poker Flat, Alaska, on February 28, 1976.

The positive ion mass spectrometer was initiated simultaneously with the electron gun turn-on and recorded data of excellent quality for approximately 120 seconds in the altitude range 68 to 99 km. The sensitivity of the instrument was sufficient to measure ambient nighttime ion concentrations to densities on the order of 10^{10} per cubic centimeter. The actual measurements recorded densities from approximately 10 to 10^8 ions per cubic centimeter. The mass spectrometer included a bias plate at the instrument sampling point maintained at a potential that was periodically stepped in the range of -30 to -260 volts. Initial analysis of the data indicates the vehicle potential of the electron emitting payload was seldom greater than 60 volts positive with a potential substantially less than this magnitude for the major portion of the experiment. Complete interpretation of the data should determine: the time-dependent build-up and decay of ionic species as produced by the pulsed electron beam; the ionization content of the near field plasma; the variation of the time-dependent abundances as a function of altitude; and ionization production yields, charge transfer processes and steady-state concentrations of the beam-induced positive ions.

The rocket-borne pulsed electron beam technique, as demonstrated in this experiment, provides a controlled ionization source capable of measuring detailed ionic production and loss processes in addition to the steady-state concentrations typically produced during nuclear and natural disturbances.

In January 1975, rocket measurements of the neutral composition of the atmospheric region between 80 and 150 km were made at Wallops Island. Other rocket measurements included density, winds and turbulence. This represented the first successful flight of an improved cryosorp-

tion pumped mass spectrometer. These data are being used to analyze the effects of dynamic processes on the structure of the turbopause region.

Two recently developed liquid helium cryosorption pumped mass spectrometer payloads used to study mesospheric neutral composition between 60 and 140 km were launched at local times of 1:46 p.m. and 11:15 p.m. on September 18, 1975 from White Sands Missile Range. The instruments performed quite well and the results will be used to make the first evaluations of the diurnal variations of the neutral species in the mesosphere.

A coordinated rocket program including NASA, Air Force and universities was conducted at Wallops Island, Virginia, in January 1976 to study a Winter Absorption Anomaly, when anomalous absorption in HF occurs during certain winter days. Neutral composition measurements were made in the mesosphere and lower thermosphere during a quiet day on January 23 to provide background atmospheric conditions prior to a winter anomaly.

Satellite Measurements: The Air Force S3-1 research satellite launched late in 1974 provided high quality data until its atmospheric reentry in May 1975. The satellite was designed to study atmospheric and ionospheric structure in the low-altitude region between 150 and 500 km. Data from the mass spectrometers were collected on about 2,000 orbits. Early results on the effects of geomagnetic storms have been reported. The results from the satellite have contributed substantially to our understanding of variations in the upper atmosphere during periods of enhanced geomagnetic activity.

The Air Force S3-2 research satellite was launched late in 1975. The set of experiments is intended to study the coupling between the neutral and ionized parts of the upper atmosphere and to provide basic data on atmospheric physical processes. The satellite includes 14 instruments to study the neutral and ionized species, the electric and magnetic fields, and the energetic particles. The experiments are from the Aeronomy Division and Space Physics Division of AFGL and the Aerospace Corporation Laboratories. All of the experiments have been providing good data to date. Among the instruments from the Aeronomy Division is a mass spectrometer to measure the composition and densities of the neutral and ion species. The data are collected by a programmed sequencer on the satellite from altitudes below the F-region peak

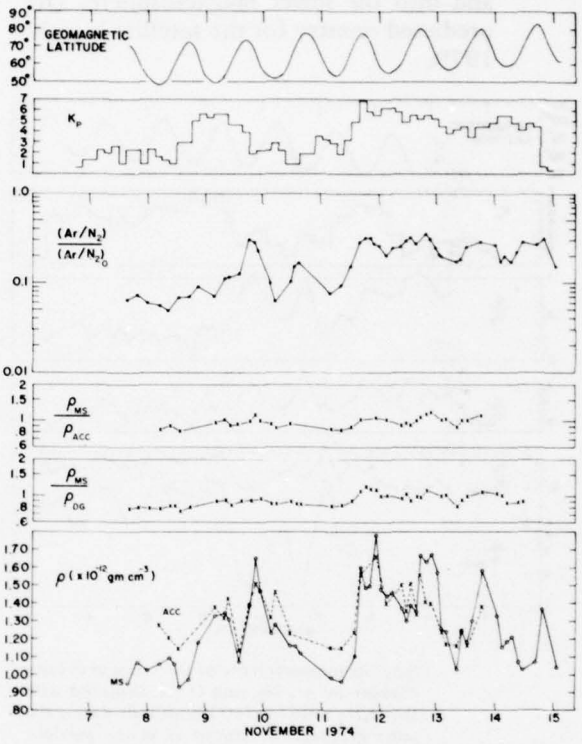

The mass density measured by a satellite mass spectrometer and accelerometer shown together with the density ratios of the mass spectrometer to the density gauge and accelerometer. The ground-level separation ratios of AR/N_2 during the magnetic storm period are displayed. All of the data applies to 160 km altitude.

and into the lower magnetosphere. The predicted reentry for the satellite is early 1979.

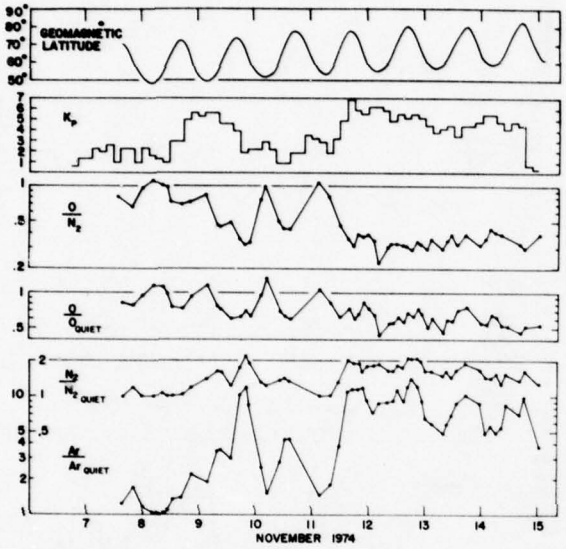

Satellite measurements of the ratios of density changes in Ar, N_2, and O are displayed with the O/N_2 ratio for 160 km altitude during the same geomagnetic storms as in the previous figure.

Ionospheric Models: Two unique models were developed for disturbed ionospheric conditions. A numerical model for a blanketing sporadic E layer composed of meteoric ions was formulated and validated with rocket measurements of ion composition and neutral winds during a sporadic-E event. The calculations support the hypothesis that midlatitude sporadic-E layers are caused mainly by neutral wind-induced compression of metallic ions resulting from meteor ablation in the lower E region.

Another model was developed for a strong (Class III) aurora and shown to be in good agreement with the measurements of ion composition and ionizing particle fluxes. Models have now been completed for Class I, II and III auroral forms. In all cases it was possible to deduce the concentrations of nitric oxide, a strong IR emitter. There is some evidence that the nitric oxide concentrations increase with the strength of the aurora. The largest nitric oxide concentrations obtained are about 10^9 per cubic centimeter near 110 km. These models have been used for both optical and communications computer codes for Department of Defense systems.

Mass Spectrometer Sampling: An extended series of Monte Carlo calculations related to the problem of sampling positive ions in the ionosphere has been carried out during the last two years. The problem of sampling is to relate the individual species currents ultimately detected after passage through a mass spectrometer to the ambient ionic densities which give rise to these currents. This relation may be broken into two components: first, that between the ambient densities and ion flux into the entrance of the spectrometer; and second, that between the entering flux and the current detected after passage through the spectrometer. The second of these may be handled by a combined theoretical/laboratory calibration procedure. Because the ionosphere cannot be simulated in the laboratory, the first problem must be treated theoretically and it is this problem with which the Monte Carlo calculations deal.

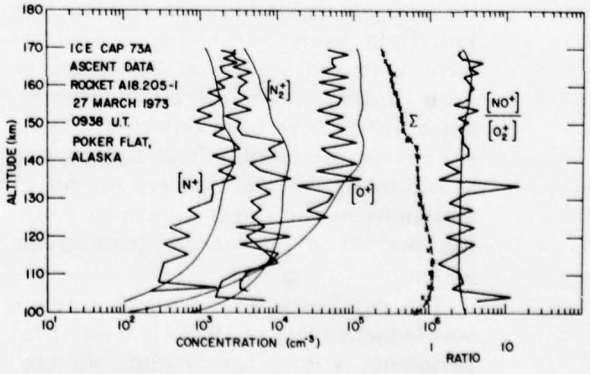

Model (smooth curves) and measurements for a Class III auroral ionosphere. The sum, Σ, symbol refers to total ion concentrations.

In drawing the ambient ions into a sample orifice, an electric field is used to enhance the sampled flux. The calculations then find the relationship between the ambient density and the orifice flux as a function of the following parameters: ambient Debye length and mean free path, vehicle velocity, and applied electric potential. For each set of parameters a distinct calculation is made.

It is planned in the future to extend these calculations to the negative ion spectrometer.

As currently operated, negative ion spectrometers require relatively large draw-in potentials to overcome the repelling effect of a negatively charged vehicle. This large potential tends to fragment the negative ions, resulting in a partial degradation of the composition measurements. One way of avoiding this problem is to stabilize the whole vehicle at some small positive potential with respect to the ambient plasma. Over the past two years a system for accomplishing this end has been designed and tested. Two payloads fabricated for this purpose consisted of a main emission system which emitted a stream of low-energy electrons into the ambient and of several diagnostic instruments used to measure the vehicle potential.

The first of two Ute-Tomahawk rocket payloads launched from the White Sands Missile Range under this program suffered a malfunction of the main emission system and essentially no data were obtained. The second payload was launched on August 16, 1974. The main emission system as well as most of the diagnostic instruments functioned properly and indications are that the vehicle was driven to a positive potential. With appropriate modifications such an emission system could be incorporated into negative ion spectrometer payloads and thus reduce the incidence of negative-ion fragmentation.

STRATOSPHERIC ENVIRONMENT PROGRAM

The stratosphere has attracted much interest and concern during the last few years because it is becoming evident that man's activities can cause significant changes in his natural environment. In particular, much concern has been given to the production of nitrogen oxides from supersonic aircraft exhaust, and chlorine and bromine released from certain halocarbons. The Air Force is concerned about the stratosphere and its ozone because some of its weapons systems operate in the stratosphere and careful evaluations must be made to avoid inadvertent modification of the environment.

The stratosphere is commonly defined to be that region of the lower atmosphere which has a positive temperature gradient, typically lying between 12 and 50 km. Both its existence and importance are due to the minor constituent ozone. Stratospheric ozone is directly important to man as a protective shield against harmful solar ultraviolet radiation. Although its maximum concentration is only about a few parts per million, ozone is the only atmospheric constituent capable of filtering out solar radiation between 200 and 300 nanometers. Ozone has an even more important indirect influence on the atmosphere because the radiation balance between the sun, ozone and carbon dioxide is responsible for the natural stratospheric temperature inversion. A modification of this inversion could have a severe impact on global climate.

The positive temperature gradient of the stratosphere creates a very stable region which minimizes vertical motion. It is precisely this strong vertical stability which makes it very difficult to see how gaseous pollutants ever find their way out of the stratosphere. Pollution remains in the stratosphere for years, all

the time chemically reacting to reduce the ozone concentration. Thus, even small quantities of pollution can have a large effect on the ozone.

The stratospheric environment program has the important task of predicting what environmental changes can occur from USAF missile and aircraft operations in the stratosphere. The program is proceeding in an orderly fashion to measure heretofore unknown minor stratospheric constituents, solar energy deposition and pollution transport properties and residence times in the stratosphere. These measurements will be conducted with unique, state-of-the-art instruments flown on large balloon systems. With these measurements, predictive models are being developed and tested. During the next several years, this effort will develop a respected scientific technology base and predictive tools necessary to determine quantitative changes in the stratosphere occurring from USAF pollution emissions. The Air Force will then have the capability for producing scientifically defensible environmental assessments of Air Force systems and flight operations in the stratosphere as required.

Stratospheric Composition Measurements: Stratospheric composition is studied through a series of balloon flights carrying a cryogenically cooled container that is opened at altitude to capture and freeze one mole of air for subsequent laboratory analysis. Obtaining air samples permits a more comprehensive diagnostics program than is possible with *in-situ* experiments. Cryogenic sampling both allows larger sample quantities to be obtained and inhibits potential chemical changes within the sample. Liquid helium is used as the primary cryogen to freeze out whole air samples.

The sampler and electronic control and monitoring circuitry are mounted in a protective frame or gondola. The sampler valve is remotely activated and the dimensions of the air inlet tube on the sample chamber are varied for each altitude investigated to provide a flow rate conducive to the molecules freezing on first contact with the sampler walls. The sampler is suspended 60 meters below the balloon, a large diameter extension of the air inlet tube extends 6 meters below the gondola and sampling is activated during descent, all to ensure that the air being sampled has not been contaminated by the flight package.

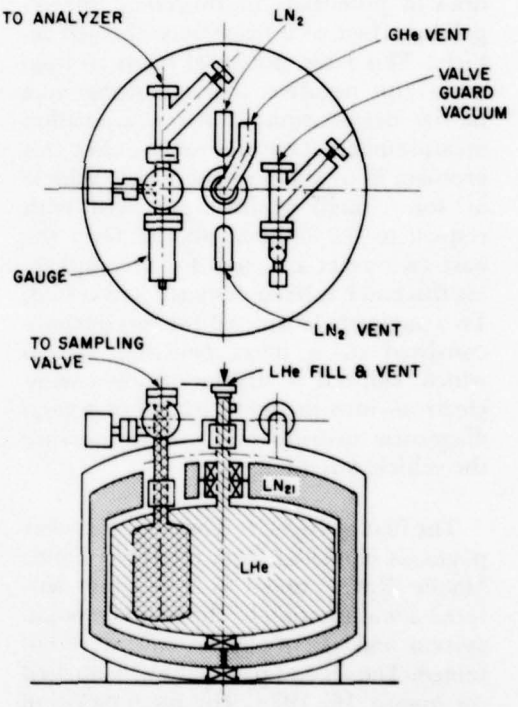

The cryogenically cooled container used to study stratospheric composition. It is opened at altitude to capture and freeze one mole of air for subsequent laboratory analysis.

Upon retrieval, the sample is allowed to warm to room temperature and then is injected into a chemiluminescence

analyzer for nitric oxide and nitrogen dioxide measurements and into a gas chromatograph and mass spectrograph for analysis of total sample components. Multiple diagnostics improve the range and accuracy of measurements. Since the trace constituents are present typically in the parts per trillion to parts per billion range, special care has to be taken in the choice of and conditioning of all surface materials with which the samples come in contact so that the container will not add to, subtract from or chemically alter the sample.

Flights were conducted at two middle latitudes (California and New Mexico) and one high-latitude (Alaska) and at three altitudes (15, 20 and 30 km). These ranges will be extended to include five latitudes and six altitudes. The sampling flights will be repeated each year and a correlation will be attempted between any trace gas variations and increased aircraft use of the stratosphere. The concentrations of nitric oxide, nitrogen dioxide, nitrous oxide and fluorocarbons 11 and 12 have been measured. The values lie within the ranges obtained by other investigators and will be considered baseline values for future comparisons.

Stratosphere UV Radiation Measurements: The solar radiation in the wavelengths between 200 and 310 nanometers will be measured at heights up to 40 km in the stratosphere. The solar energy deposition rate will be calculated from the variation of the solar flux with altitude. The absorption spectrum will be examined to determine ozone density as well as other minor species. These measurements will be made by a grating spectrometer mounted on a biaxial solar pointing control. The spectrometer has a spectral resolution of 0.015 nanometer and will complete the designated scan in nine minutes. The spectrometer will be carried aloft on a high-altitude balloon, with measurements made as a function of altitude during a sunrise ascent and descent at local noon.

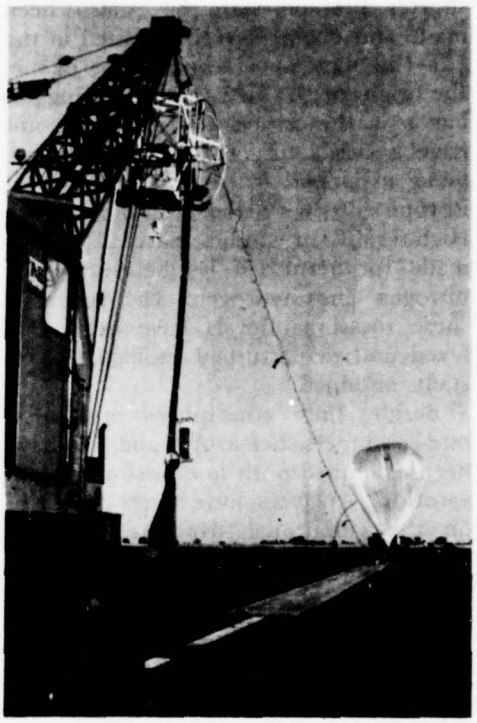

The cryogenic air sampler ready for launch. The sampler is suspended 60 meters below the balloon, and the air inlet tube can be seen extending 6 meters below the balloon.

UV Spectroscopy: Gaps of information still exist for certain energy ranges in the ultraviolet and vacuum ultraviolet region for molecules such as ozone, oxygen, nitric oxide and nitrogen. By the analysis of high-resolution spectra, classification of some of these energy levels has been made. For example, rotational analyses have been made for the first time of oxygen absorption bands at wavelengths less than 100 nanometers. This was done by studying the 80-90 nanometer absorption bands of a long-lived

metastable species of molecular oxygen which is relatively abundant in the upper atmosphere. In addition, high-resolution absorption studies of oxygen from a shorter lifetime state have also been made and energy levels classified in the 128-160 nanometer region. For ozone, the origin of the diffuse Hartley-Huggins bands in the critical UV region do not have a satisfactory explanation and are being examined in terms of vibrational isotope shifts with respect to pure $^{18}O_3$. High-resolution studies have also been made for perturbed Rydberg states of nitrogen and hydrogen. The shifts of these rotational levels have been analyzed and de-perturbed molecular constants obtained.

Besides these atmospheric molecules, rare gas dimers such as Ar_2 and Xe_2 have been examined both in emission and absorption. Analyses have been primarily on the vibrational structure of these bands due to the weakly bound nature of the ground state. Some rotational analysis, however, has been made for Ar_2. The rare gas energy levels are important for elucidating the energy transitions in vacuum ultraviolet lasers and for fundamental studies of cluster formation in the upper atmosphere.

Stratospheric Turbulence Measurements: Turbulence in the stratosphere is the mechanism by which the constituents are mixed and pollution transported out of the stratosphere. How long pollution remains in the stratosphere is determined from measurements of the turbulence present. Several measurement techniques are being used to define the turbulence characteristics—persistence, altitude distribution and latitudinal and seasonal variations. The altitude distribution is measured by analysis of vertical smoke trails deposited from rockets. The smoke trails are photographed repeatedly to record the position changes caused by the winds. The photographs can be analyzed to a remarkably high altitude resolution of 10 meters using newly developed techniques. This permits identification of thin, pancake-like layers of turbulence, several hundred meters in thickness. A second method of measuring turbulence is accomplished using a turbulence sensor mounted on a balloon. With this *in-situ* measurement of turbulence, the balloon sensor can be allowed to float in a turbulence layer for long periods of time to record the lifetime of the turbulence layer. Seasonal and latitudinal dependence of turbulence has been studied through analysis of rocket grenade data. Existing data between 30 and 90 km, covering the latitude region from 5 degrees South to 70 degrees North and the winter and summer seasons have been examined. The results demonstrate that the winter Northern Hemisphere is significantly more turbulent, in the upper stratosphere and upper mesosphere, than in the summer Northern Hemisphere. The equatorial regions display little or no turbulence in the stratosphere or lower mesosphere, around 70 km, and intensifying significantly by 90 km. These results are more indicative of diurnal tidal effects, as contrasted to what appears to be an internal gravity wave contribution to turbulence in the more northern latitudes.

Stratospheric Turbulence Model: The structure of turbulence in the stratosphere appears to be rather strange, at first sight, to someone who has not studied atmospheric dynamics. It has the form of large horizontal pancakes that are on the order of 25 km in the horizontal dimensions but quite thin in the vertical dimensions (100 meters to 1,000 meters being values quoted in the literature). These turbulent layers seem to form and decay at random heights and random times. Most of the stratosphere is essentially non-turbulent and the volume occupied by turbulent layers is probably well under 5 percent on the average.

The question addressed by this work is whether these random "mixing layers" can, in time, have the effect of bringing pollution out of the stratosphere. To answer this question, a computer model was created which related residence time (or the "vertical effective diffusivity" coefficient which determines residence time) to vertical profiles of the horizontal winds. The latter were obtained from rocket-laid smoke trails which served as fluid markers. The computer model was based on the theory that the stratospheric turbulent layers are caused by the so-called Kelvin-Helmholtz instability. This instability is generated by high wind shears in a statically stable environment and it is responsible for that type of tropospheric turbulence known as CAT (clear air turbulence). The upshot of this study was that within the context of certain assumptions, stratospheric turbulence may indeed play a significant role in pollution fallout. The calculated residence times were in the same general range as those found from radioactive fallout measurements. The assumptions of the model are now being tested with the field experiments. The same phenomenon causes the pancake-shaped turbulence layers in the ocean and it now seems that in many ways, the ocean does a good job of imitating the motions of the stratosphere.

Stratospheric Model Development: A new, more complete, one-dimensional model of the stratosphere and troposphere is currently being developed at AFGL. This model will include many of the feedback mechanisms which are important to the maintenance of the current natural environment by coupling together radiation, chemistry, and dynamics. Such a model is needed because the internal coupling in the atmosphere can be strong enough to substantially magnify or reduce the overall impact of a particular perturbation. This would represent a major step in the development of atmospheric models since present models are not flexible enough to include all three systems.

A new mathematical method has been developed for solving the linear photon transport equation in plane-parallel geometry. It allows a number of formal mathematical properties of the scalar flux to be derived. A computer program based upon this method has been written and tested which calculates the amount of solar ultraviolet light transmitted, absorbed and reflected by the earth's stratosphere if the average ozone concentration and the absorption and scattering cross sections are known.

Scientists in AFGL's Meteorology Division have also contributed to the development of stratospheric models. Their work in atmospheric modeling has direct application to the development of a global stratospheric model.

The turbulence which eventually removes pollutants from the stratosphere is limited, and ultimately damped out, by small-scale diffusion and viscous dissipation. The problem of modeling diffusion and viscous dissipation is the same in the stratosphere and the troposphere. If diffusion and dissipation are not strong enough, noise coming from errors in the initial data, model inadequacies from improper treatment of boundaries and from inadequate resolution will grow, producing inaccuracies which limit the length of time the model is valid, and possibly making the model unstable and the results meaningless. But if the important cyclone-scale waves in the atmosphere are damped along with the noise, the predictions become too smooth and fail to forecast adequately newly developing disturbances. Reducing the grid size of the model helps, but this is costly in computer time and dissipation occurs on a scale too small to be represented explicitly in any computer model.

Meteorology Division scientists have devised a digital filter which appears to

have the right properties to control noise, yet not suppress physically meaningful information in the model. It has been applied in a variety of numerical models ranging from fine-mesh limited area models and channel models with solid walls to large-scale general circulation models. In a test run, an idealized cyclonic storm which produced strong frontal zones as it matured was followed. In the unfiltered run, energy increasing in the smallest scales caused short wavelength waves to form parallel to the frontal zones. The filtered run maintained the same large-scale growth of the storm and the frontal zones while removing the unrealistic smaller scale waves and noise, thus modeling more realistically atmospheric diffusion processes on a subgrid scale.

ENVIRONMENTAL ASSESSMENTS

Detailed studies were conducted on the modifications to the natural stratospheric environment which could be expected to result from the operations of the B-1, F-15, and F-16 aircraft. The quantities of nitric oxide exhausted by these aircraft were found to be small enough to be not only insignificant, but also undetectable after mixing with the atmosphere.

Carbon tetrachloride (CCl_4) has long been used in fire extinguishers, in addition to its commoner use as a cleaning agent. A fire suppressant system using the related chemical bromofluoromethane (CF_3Br), which is more effective than carbon tetrachloride, was planned for the F-16 aircraft. But bromine is an extremely effective catalyst for destroying ozone; therefore, a study was conducted to assess the potential environmental hazard of this fire suppressant system. The results showed that the amount of bromine released would be much less than the amounts released by natural sources, and furthermore would not be sufficient to cause a detectable change in the natural ozone distribution.

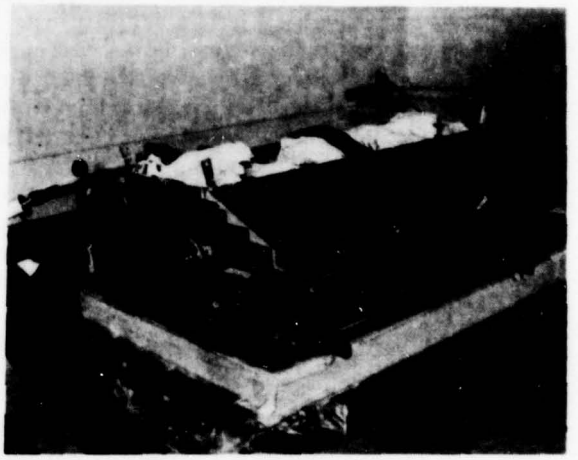

The S3 series of satellites carried several AFGL-designed experiments, including 3-axis accelerometers, a mass spectrometer, density gauges and electrostatic and retarding potential analyzers to determine the density and composition of the upper atmosphere. Other experiments measured energetic particles, electric fields, and magnetic fields.

EXERCISE PARADISE AEOLUS

AFGL planned and conducted an experiment known as Exercise PARADISE AEOLUS (Auroral Electrojet Oscillations and Layering of the Underlying Species) to investigate the production of Traveling Ionospheric Disturbances (TIDs) by *in situ* measurements near (but not within) the region of the atmosphere directly perturbed by the auroral electrojet. TIDs affect UHF radars, such as COBRA DANE, by causing range and angle errors and by modulating the auroral clutter.

Particle precipitation in the auroral zone lower thermosphere produces oscillations of the neutral temperature, density, wind, etc., either through Lorentz

force momentum transfer or Joule heating. These neutral gas waves spread out from the source region with propagation velocities that are anisotropic and frequency dependent, producing corresponding waves in the ionized constituents by which they are detected. Acoustic, buoyancy and gravity waves should all be detectable near the source, but as the distance increases the dominant contribution is due to the gravity waves. Most, if not all, of the published TID observations have been made at low to mid-latitudes, well away from the auroral zone, and hence have displayed the characteristics of gravity wave pulses and wave trains. These observations made by radio probing of the mid-latitude ionosphere have been associated with auroral zone sources by measuring the TID velocities, extrapolating back to an auroral zone source and searching for magnetometer events near the source at the appropriate time which seem capable of having initiated the TID. These studies have not provided quantitative, detailed, direct evidence on the auroral zone source mechanism, its coupling to the ionosphere, or the identification of highly correlated, routinely observable parameters or indices of auroral activity which could be used for predictive purposes. The AEOLUS experiment was designed to provide just such evidence.

AEOLUS was a cooperative venture of several groups at AFGL, their contractors, and the Churchill Research Range of the National Research Council of Canada. The basic idea was to search for ionospheric waves *in situ* using rocket-borne measurement techniques both in the presence and absence of a significant auroral electrojet, hopefully providing a Yes/No answer to the question of whether the waves are produced this way. Six chemical release rockets and three mass spectrometer rockets constituted the primary rocket experiments. Secondary experiments carried on board various of these rockets were: neutral density by falling sphere, electric field by multiple probe; hydroxyl radical and molecular oxygen emissions by photometers; thermal and energetic electron density by plasma frequency probes and scintillators. The primary ground-based experiments were the real-time monitoring of the location and strength of the auroral electrojet, and the time-lapse photographic observation of the chemical releases. Secondary ground experiments were: spectrometric determination of chemical release temperatures, and all-sky camera, auroral photometer and ionosonde observations carried out by the Churchill Research Range.

The program was divided into three nearly identical experiments, each involving the launch of three rockets. The three experiments were designated Disturbed, Quiet, and Auroral. Three criteria had to be met before launching each of the experiments: 1) appropriate electrojet conditions; 2) clear skies at each of the optical sites, and 3) illumination of the TMA puffs by the sun against a dark sky (twilight) for Disturbed and Quiet. When it was determined that the launch criteria were met, the first chemical rocket was launched, the second was launched 30 seconds later, and the mass spectrometer rocket 300 seconds later. The first rocket released, on descent, trimethylaluminum (TMA) puffs from apogee with a single barium release near 200 km. The second rocket released a trail on ascent and releases identical to the first rocket on descent. Both rockets were designed to be launched on azimuths of 120 degrees and 150 degrees true to enable horizontal variations of the atmospheric parameters to be measured. The third rocket made composition measurements on ascent and descent and was designed to be launched on an azimuth of 135 degrees in an attempt to penetrate one of the ionized barium clouds from the first two rock-

ets. The Disturbed experiment was launched at morning twilight after the electrojet current had reached 500 kiloamp and moved 100-200 km away from the experiment position and the Quiet experiment after the electrojet current had been quieter than 50 kiloamp for three hours preceding launch.

The Disturbed rockets were launched at twilight near 1000 Universal Time on April 10, 1975 into a region 150 km away from an electrojet which fluctuated but peaked near 1 megamp during the minutes preceding launch. All major experiments functioned. The Quiet rockets were launched at twilight near 0915 Universal Time on April 21, 1975 after three hours with no electrojet current above 50 kiloamp, and again, all major experiments functioned. The auroral rockets were launched at night into a Class 3 aurora near 0415 Universal Time on April 25, 1975. All three sets of launches were apparently made under optimum conditions and good to excellent data were obtained from all the major experiments.

Analysis of data is continuing at the present time. The results are expected to characterize the atmospheric perturbations induced by the auroral electrojet during the Disturbed and Quiet AEOLUS experiments. Three principal results are being sought. First, the chemical release experiments will determine a dynamical model of the atmospheric perturbations, giving the space-time variations of the neutral and ion winds, shears and diffusion, neutral temperatures and densities, and electric fields. Second, the space-time variations of the atmospheric parameters measured will be searched for wavelike motions, and detectability bounds will be determined. Finally, the dynamical model will be correlated with the other experimental parameters measured, including the neutral and ion mass spectra, the probe electric fields, the neutral density profile measured by falling sphere and by satellite as available, the ground-based magnetic field perturbations and ionograms. These and other routinely observed indicators of auroral, geomagnetic, ionospheric and magnetospheric activity will be searched for predictive relations between them and the characteristics of the electrojet perturbations.

SOLAR ULTRAVIOLET RADIATION

Only a small fraction of the sun's radiation is emitted in the ultraviolet (UV), the wavelength region from 30 to 3500 angstroms, but it is all absorbed by atoms and molecules in the atmosphere. For this reason, it is the principal source of heating in the stratosphere, mesosphere, and thermosphere and has an important influence on the photochemistry and composition of these atmospheric regions. Most of the energy used to produce the ionosphere, and much of the energy radiated by the atmospheric airglow envelope surrounding the earth, comes from solar UV absorbed by the atmosphere.

Quantitative models of the earth's upper atmosphere and ionosphere are constructed to predict neutral and charged particle density distributions and global radiation backgrounds. They require accurate measurements of the absolute intensity and spectral distribution of solar radiation incident on the earth's upper atmosphere as input data, as well as the rate at which this energy is absorbed within the atmosphere. Measurements of the variation with time of the intensity of solar UV during periods of changing solar activity and during solar flares are also required to develop these models. Photometrically calibrated optical spectrometers mated with solar pointing controls are carried by rockets and satellites well above 100 km to make these measurements.

Rocket Measurements of Solar UV: The altitudes achieved by high performance sounding rockets are essentially outside of the earth's atmosphere. The optical entrance aperture of the spectrometer carried on the rocket is pointed at the center of the solar disk during data acquisition. Photomultipliers are operated as photon counters to record the solar intensities, and the signals are telemetered to ground receiving stations.

During this reporting period, measurements of solar UV in the 1200 to 3500 angstrom range have been emphasized, because this radiation is important to the stratosphere and mesosphere. On May 18, 1976, an Ebert-Fastie spectrometer that scanned from 1800 to 3500 angstroms wavelength with a spectral resolution of 0.1 angstrom was flown for the first time from White Sands Missile Range, New Mexico. The experiment was highly successful, and the data obtained are currently being analyzed. The entire rocket payload was also recovered intact. This spectrometer will be flown again in a rocket during October 1976, while a similar solar pointed spectrometer is flown in a balloon. The rocket spectrometer will measure the solar UV intensity incident on top of the stratosphere, while the balloon spectrometer will measure the rate at which this radiation is absorbed within the stratosphere. These kinds of data, taken simultaneously, are essential for the study of photochemical processes occurring in the stratosphere and for the development of stratospheric models. Several of these coordinated rocket and balloon experiments are planned to establish a data base for solar UV fluxes for stratospheric studies. A new Ebert-Fastie spectrometer has been designed to expand the wavelength coverage and use the rocket payload capacity more efficiently. It will be flown in the near future. This spectrometer will measure the solar spectrum over the entire 1200 to 3500 angstrom range with a resolution of 0.1 angstrom.

Future DMSP satellites will measure atmospheric densities remotely. Instruments on the satellite will measure the intensities of the atmospheric emission of the molecular nitrogen second positive band at 3371 angstroms and the atomic oxygen intercombination line at 1356 angstroms. These airglow emission signals measured at the satellite will be deconvoluted to infer the airglow emission profiles of molecular nitrogen and atomic oxygen in the earth's atmosphere. To verify the remote measurement capability of the DMSP satellite, experiments flown on rockets will be coordinated with overhead passes of the DMSP satellite. The rocket will measure several atmospheric parameters while the satellite observes airglow radiation emitted in the atmospheric region probed by the rocket. The rocket experiment will measure solar UV absorption, neutral particle densities, photoelectron energy distributions and densities, and molecular nitrogen and atomic oxygen airglow radiation at 3371 and 1356 angstroms, respectively. These atmospheric processes and parameters are closely interrelated. Photoionization of atmospheric gases by solar UV produces photoelectrons with energies between 0 and 100 electron volts. The photoelectrons collisionally excite the atomic and molecular species, and these excited species emit the atmospheric airglow. Both the molecular nitrogen radiation at 3371 angstroms and the atomic oxygen radiation at 1356 angstroms are produced only by photoelectron excitation. The emission intensities depend on the densities of molecular nitrogen and atomic oxygen and the number and energy distribution of the atmospheric photoelectrons.

The rocket payload was test flown from White Sands Missile Range, New Mexico, on February 24, 1976. This payload included a grazing-incidence spectro-

meter that measured the atmospheric absorption of four particular solar UV emission lines. The absorption data, when combined with absorption cross sections of the atmospheric constituents, allow the vertical density distribution of the atmospheric constituents to be determined. The energy distribution of atmospheric photoelectrons having 0 to 100 electron volts energy was obtained with an electron energy analyzer with a 10 percent resolution in energy. This analyzer was mounted at the rear of the solar pointed spectrometer so that its entrance aperture viewed away from the sun. This orientation shields the aperture of the analyzer from the extraneous photoelectrons that direct solar radiation would produce. This rocket payload also included a narrowband photometer to measure the molecular nitrogen airglow band near 3371 angstroms. It was equipped with a collimator and sunshade, and was pointed to view the atmosphere near zenith. Although high levels of stray light degraded the measurements of nitrogen airglow radiation, excellent data were obtained on photoelectron densities and energy distributions, and on neutral particle densities. These data are now being analyzed. On future flights, a photometer to measure the 1356 angstrom oxygen airglow radiation will be included.

Satellite Measurements: Satellite-borne optical spectrometers allow nearly continuous measurements of solar UV intensities during extended periods of time. The data collected allow long-term variations of solar UV, caused by changing solar activity levels, to be studied. The nearly continuous time coverage also increases the probability of measuring solar UV enhancement during solar flares, which are unpredictable and last only a few minutes. The satellite spectrometer can also measure the attenuation of solar UV by the earth's atmosphere when the satellite penetrates the atmosphere as well as during periods of solar occultation at satellite sunrise and sunset.

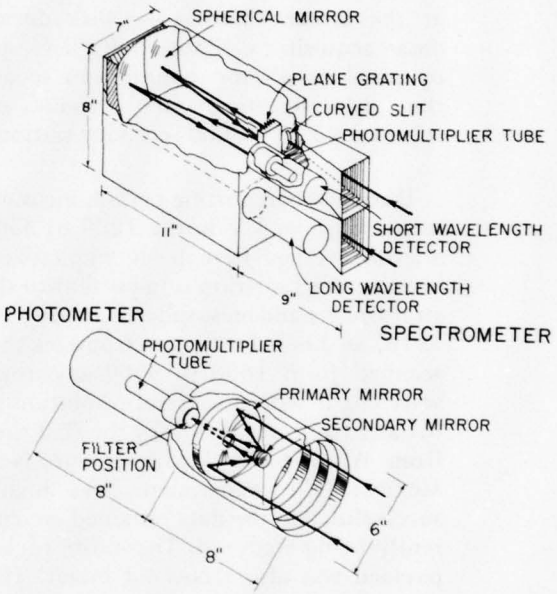

Schematic of AFGL satellite experiment CRL-246 to measure global UV radiation levels by using an Ebert-Fastie spectrometer (top) and a broad-band photometer (bottom).

AFGL has designed and supplied three solar UV spectrometers as part of the NASA Atmosphere Explorer (AE) series satellites. The first satellite, AE-C, was successfully launched into an orbit having an inclination of 65 degrees on December 16, 1973. This experiment is still returning data. Two additional satellites, AE-D and AE-E, were launched on October 6 and November 19, 1975, in near-polar and near-equatorial orbits. The UV spectrometers in both of these satellites operated satisfactorily, although the polar-orbiting AE-D satellite became inoperative approximately one month after launch.

The spectrometers on the Atmosphere Explorer satellites are composed of 24 individual grazing-incidence monochromators, making up a single instrument to obtain solar UV intensity data from 140 to 1850 angstroms as well as at several fixed wavelengths. Each orbit of the satellite has a nominal perigee of 150 km and an apogee of 4,000 km. The satellite has a motor that can be fired at apogee, allowing occasional perigee passes down to 120 km. The low perigee altitude permits the attenuation of particular solar emission lines by the earth's atmosphere to be determined. The measured attenuation, combined with absorption cross sections of atmospheric gases, yields a determination of the composition, density, and temperature of the upper atmosphere. Similar atmospheric parameters can be determined by solar occultation of the earth's atmosphere at satellite sunrise and sunset. During that part of the orbit when the satellite is above the absorbing region of the earth's atmosphere but below the energetic particle belts, the UV spectrometers can measure the unattenuated solar intensities and their temporal variations incident on the earth's atmosphere.

During this reporting period, a considerable amount of data on solar UV intensities within and above the absorbing region of the earth's atmosphere have been acquired and analyzed to study the relation between solar UV variations and changes in the atmosphere between 100 and 400 km. These satellite experiments have made it possible to determine, in detail, variations of solar UV in different bands and emission lines, which occur over several solar rotations. These variations are notably different for different wavelength regions, since the radiation is emitted from different regions in the solar atmosphere. Data are still being acquired from these satellites and analyzed, and it is anticipated that more significant information of the relationship of solar UV and conditions in the earth's upper atmosphere will be accumulated.

Missile Plumes: Surveillance, threat warning and technical intelligence can all use the ultraviolet radiation emitted by missile exhaust plumes. AFGL's Multispectral Measurements Program (MSMP) includes both ultraviolet and infrared sensors. The Aeronomy Division will supply the ultraviolet photometers and spectrometers which will be flown in rockets to measure the spatial, spectral, and temporal characteristics of the plume radiation. A previous program, Project Chaser, measured the radiation from large missile engines. The MSMP will use specially developed sensors with one and two dimensional detector arrays to obtain spatial and spectral readouts electronically. The missile targets will have the altitudes, velocities, and aspect angles of actual missile systems, which will nearly eliminate "scaling" from measurement to operational conditions. The first MSMP flight is scheduled for October 1977.

Atmospheric UV Measurements: To improve satellite detection, tracking, and attack assessment, the atmospheric emission must be known in detail because it forms the background against which missile targets must be observed. An experiment to measure global UV radiation has been largely fabricated, and will be launched on an Air Force satellite in 1977. The experiment will achieve spectral resolution of 1 angstrom by using an Ebert-Fastie spectrometer, and spatial resolution of 1 km by using a broad-band photometer. The work is closely related to previous missile plume radiation measurements. The results of the two efforts will allow a complete and reasonably definitive statement on surveillance uses of ultraviolet.

Ultraviolet limb horizon profiles will be measured to provide information for development of UV horizon sensors for spacecraft attitude control. The primary

unknown is the strength and global distribution of the Lyman-Birge-Hopfield bands of molecular nitrogen, which occur in a wavelength region which otherwise has a low atmospheric radiance, because the Schumann-Runge continuum band of molecular oxygen absorbs the radiation. In addition, the intensities and distribution of the oxygen emission lines at 1304 and 1356 angstroms will be correlated with atmospheric, ionospheric, and auroral parameters, so that passive sensors of quantities such as the electron density profile can be developed. Where feasible, missile target measurements will be conducted.

Reaction Cross Sections: The interaction of ultraviolet photons with atmospheric gas molecules determines the extent and severity of blackouts from atmospheric nuclear detonations, as well as ionospheric and stratospheric characteristics. Values for these interaction cross sections are being determined both by in-house work and critical reviews of the literature. Reports of cross section values at solar emission lines and at emission lines produced by nuclear detonations are being prepared for the Defense Nuclear Agency and other users. These photon cross sections are especially important in predicting the effects of high-altitude nuclear bursts, where the UV fireball is a dominant feature. They are also primary inputs to computer codes such as ROSCOE, RANC IV, and WEPH, which model the blackout and return to ambient conditions.

Molecular Nitrogen Spectra: The lack of high-resolution spectroscopic data has kept our knowledge of the high energy Rydberg states of molecular nitrogen incomplete. During this reporting period, measurement and analysis of high-resolution absorption spectra in the 680-950 angstrom wavelength region has provided additional information on these Rydberg states of nitrogen. The upper states in these optical transitions are Rydberg states converging on the first excited state of the molecular ion, N_2^+. Two distinct series were identified with rotational quantum numbers up to 40 and vibrational quantum numbers up to 7. Accurate values for the convergence limits for the Rydberg states were obtained.

JOURNAL ARTICLES
JULY 1974 - JUNE 1976

BASS, J. (Math. Dept., Univ. of Paris, Fr.), and MOSES, H. E.
Construction of a Model of a Turbulent Velocity Field Which is Homogeneous and Isotropic
J. de Mecanique (October 1974)

BERNSTEIN, W., LEINBACH, H. (NOAA, Space Envmt. Lab., Boulder, Colo.), COHEN, H., WILSON, P. S., DAVIS, T. N., and HALLINAN, T. (Geophys. Inst., Univ. of Alaska), BAKER, B. (NASA Marshall Space Flight Ctr., Huntsville, Ala.), MARTZ, J., ZEIMKE, R. (NASA Plum Brook Station, Lewis Res. Ctr., Sandusky, Ohio), HUBER, W. (Tri-Con Assoc., Inc., Cambridge, Mass.)
Laboratory Observations of RF Emissions at ω_{pe} and $(n + \frac{1}{2})\,\omega_{ce}$ in Electron Beam-Plasma and Beam-Beam Interactions
J. of Geophys. Res., Vol. 80, No. 31 (1 November 1975)

BEST, G. T., and HOFFMAN, H. S.
The Initial Behavior of High Altitude Barium Releases: X. The Particulate Ring
J. of Atm. and Terrestrial Phys. (September 1974)

CALO, J. M., CAPT.
Heteromolecular Clusters of H_2O, SO_2, CO_2, CO and NO
Nature, Vol. 248 (1974)
Dimer Formation in Supersonic Water Vapor Molecular Beams
J. of Chem. Phys., Vol. 62, No. 12 (15 June 1975)

CALO, J. M., and BAILEY, A. D.
Phase-Sensitive Pulse Counting in Modulated Beam Mass Spectrometry
Rev. of Sci. Instm. (November 1974)

CALO, J. M., and BROWN, J. H.
The Calculation of Equilibrium Mole Fractions of Polar-Polar, Nonpolar-Polar, and Ion Dimers
J. of Chem. Phys., Vol. 61 (1974)

CHAMPION, K. S. W.

Dynamics and Structure of the Quiet Thermosphere
J. of Atm. and Terrestrial Phys., Vol. 37 (1975)

The Earth's Neutral Atmosphere and Aeronomy
Chap. IV of State of the Art and Assessment of Sci. and Technol. Dev. in the Exploration and Practical Uses of Outer Space Within an Intl. Framework, Pub. by UN Gen. Asbly. (26 January 1976)

CORMIER, R. V.

The Behavior of Vertically Integrated Boundary Layer Winds
Boundary Layer Met., Vol. 9 (1975)

The Horizontal Variability of Vertically Integrated Boundary Layer Winds
J. of Geophys. Res., Vol. 80, No. 24 (20 August 1975)

DEWAN, E. M., and ROSENBERG, N. W.

Analysis of Vertical Profiles of Horizontal Winds
Appendix B of Chap. 6, CIAP Mono. I (September 1975)

DRAPER, J. S., BIEN, F. (Aerodyne Res., Inc., Burlington, Mass.), HUFFMAN, R. E., and PAULSEN, D. E.

Rocket Plumes in the Thermosphere
AIAA J., Vol. 13 (June 1975)

FAIRE, A. C., CORBIN, V. L., (GCA Corp., Bedford, Mass.), and CHAMPION, K. S. W.

Diurnal Variations in Neutral Density and Temperature Observed at Natal, Brazil
Space Res. XVI, Akademie-Verlag, Berlin, Ger. (1976)

Solar Diurnal Tide in the Thermosphere
J. of Atm. Sci., Vol. 33, No. 11 (1976)

FORBES, J. M. (Ctr. for Earth and Planetary Phys., Harvard Univ.), and GARRETT, H. B.

Variations in the Atmospheric Neutral Density at 145 Km
Planetary and Space Sci. (November 1975)

FREEMAN, D. E., and ALIX, A. J. (Univ. of Rheims, Fr.), MULLER, A. (Univ. of Dortmund, Ger.)

On the Definitions of Characteristic Molecular Vibrations and the Distribution of Vibrational Energy
Zeitschrift fur Naturforschung, Vol. 29a (1974)

FREEMAN, D. E., YOSHINO, K., and TANAKA, Y.

Vacuum Ultraviolet Absorption Spectrum of the van der Waals Molecule Xe_2. I. Ground State Vibrational Structure, Potential Well Depth and Shape
J. of Chem. Phys., Vol. 61 (1974)

GALLAGHER, C. C., and LEVINE, M. A.

Observation of Hydrogen and Helium Satellites in a Turbulent Plasma
J. of Quant. Spectros. Radiative Transfer, Vol. 15 (1975)

GALLAGHER, C. C., LEVINE, M. A., and BOOZER, A. H.

Wave Heating of Plasma in a Toroidal Cusp (Tormac)
Bull. of Am. Phys. Soc., Ser. II, Vol. 19, No. 9 (1 October 1974)

GOLOMB, D., and BROWN, J. H.

Dimer Mechanism of Termolecular Reactions – The Temperature Dependence of the NO-O Chemiluminous Reaction
J. of Chem. Phys. (15 December 1975)

GOLOMB, D., HOFFMAN, H. S., and BEST, G. T.

Chemiluminescence of Sodium Released at Night and Its Relation to the Sodium Nightglow
J. of Geophys. Res. (1 March 1975)

GOOD, R. E.

Determination of Atomic Oxygen Density from Rocket Borne Measurement of Hydroxyl Airglow
Planetary and Space Sci., Vol. 24 (1976)

GRINGORTEN, I. I.,

A Statistical Study of PPT Scope Radar Pictures
Proc. of 4th Conf. on Probability and Stat. in Atm. Sci., Tallahassee, Fla. (21 November 1975)

HEROUX, L., COHEN, M., and HIGGINS, J. E.

Electron Densities Between 110 and 300 Km Derived from Solar EUV Fluxes of August 23, 1972
J. of Geophys. Res., Vol. 79 (1974)

Reply to Nisbet's "Comments on the Paper, Electron Densities Between 110 and 300 Km Derived from Solar EUV Fluxes of August 23, 1972, by L. Heroux et al"

Improved Calculations of Electron Densities Between 110 and 300 Km Derived from Solar EUV Fluxes of August 23, 1972
J. of Geophys. Res., Vol. 80 (December 1975)

HEROUX, L., and SWIRBALUS, R. A.

Full-Disk Solar Fluxes Between 1230 and 1940 A
J. of Geophys. Res., Vol. 81 (February 1976)

HIGGINS, J. E.

The Solar EUV Flux Between 1220Å-230Å
J. of Geophys. Res., Vol. 81, No. 7 (1 March 1976)

HILDENBRAND, D. L. (Stanford Res. Inst., Menlo Pk., Calif.), and MURAD, E.
The Ionization Potential of Thorium
J. of Chem. Phys., Vol. 61, No. 12 (15 December 1974)

HOFFMAN, H. S., and BEST, G. T.
The Initial Behavior of High Altitude Barium Releases — II: The Expanding Vapor Cloud
J. of Atm. and Terrestrial Phys. (September 1974)

JASPERSE, J. R.
Boltzmann-Fokker-Planck Model for the Electron Distribution Function in the Earth's Ionosphere
Planetary and Space Sci., Vol. 24 (1976)

KATAYAMA, D. H., HUFFMAN, R. E., and TANAKA, Y.
O_2 ($a\,^1\Delta_g$) Absorption Bands in the Vacuum Ultraviolet
J. of Chem. Phys., Vol. 62, No. 8 (15 April 1975)

LUND, I. A.
Cloud-Free Lines-of-Sight Through the Atmosphere
Natl. Telecomm. Conf. Record (San Diego, Calif., 2-4 December 1974)

LUND, I. A., and GRANTHAM, D. D.
Estimating Hourly Persistence and Recurrence Probabilities of Temperature
Proc. of 4th Conf. on Probability and Stat. in Atm. Sci., Tallahassee, Fla. (21 November 1975)

MAC LEOD, M. A., KENESHEA, T. J., and NARCISI, R. S.
Numerical Modeling of a Metallic Ion Sporadic-E Layer
Rad. Sci., Vol. 10, No. 3 (1975)

MANSON, J. E.
The Solar Extreme-Ultraviolet Between 30 and 205 Å on 9 November 1971 Compared with Previous Measurements in this Spectral Region
J. of Geophys. Res., Vol. 81, No. 10 (1 April 1976)

MINZNER, R. A., REBER, C. A. (NASA Goddard Space Flight Ctr., Greenbelt, Md.), JACCHIA, L. J. (Smithsonian Astrophys. Obsv., Cambridge, Mass.), HUANG, F. T. (NASA Goddard Space Flight Ctr.), COLE, A. E., KANTOR, A. J., KENESHEA, T. J., ZIMMERMAN, S. P., and FORBES, J. M. (Boston Coll., Chestnut Hill, Mass.)
Defining Constants, Equations and Abbreviated Tables of the 1976 U.S. Standard Atmosphere
NASA TRR-459 (May 1976)

MOSES, H. E.
The Exact Electromagnetic Matrix Elements and Selection Rules for Relativistic Hydrogenic Atoms
Phys. Rev. A, Vol. 9 (January 1975)
An Integral Equation for the Gelfand-Levitan Kernel in Terms of the Scattering Potential in the One-Dimensional Case
J. of Math. Phys. (May 1975)
Derivation of the Dipole Approximation from the Exact Transition Probabilities for Hydrogen Atoms
Phys. Rev. (June 1975)

MURAD, E., and HILDENBRAND, D. L. (Stanford Res. Inst., Menlo Pk., Calif.)
Mass Spectrometric Studies of Gaseous THO and THO_2
J. of Chem. Phys., Vol. 61 (1974)
Redetermination of the Dissociation Energy of Europium Monoxide and its Bearing on Atmospheric Release Experiments
Zeitschrift fur Naturforschung, Vol. 30a (1975)
Thermochemical Properties of Gaseous ZrO and ZrO_2
J. of Chem. Phys., Vol. 63 (1975)
Thermochemical Properties of Gaseous EuO
J. of Chem. Phys., Vol. 65 (1976)

NARCISI, R. S.
Planetary Ionospheres
Book, NATO Adv. Study Inst. on Ion-Mol. Interactions, Plenum Pub. Corp. (1 February 1975)

NARCISI, R. S., SHERMAN, C., WLODYKA, L. E., and ULWICK, J. C.
Ion Composition in an IBC Class II Aurora, 1. Measurements
J. of Geophys. Res. (September 1974)

NARCISI, R. S., and SWIDER, W.
Mesospheric Neutral Constituents Deduced from PCA Ion Composition Measurements
J. of Geophys. Res. (1 February 1975)

OGAWA, M., YAMAWAKI, K. R. (Univ. of So. Calif.). HASHIZUME, A. (Natl. Chem. Lab. for Ind., Tokyo, Jap.), and TANAKA, Y.
Vibrational Isotope Shifts of Absorption Bands of $^{16}O_2$ and $^{18}O_2$ in the Region 1130-1300 A
J. of Mol. Spectros., Vol. 55 (1975)

ROSENBERG, N. W., and DEWAN, E. M.
Stratospheric Turbulence and Vertical Effective Diffusion Coefficients
Proc. of Climatic Impact Assessment Program Mtg., Feb. 1974 (November 1974)

ROSENBERG, N. W., GOOD, R. E., VICKERY, W. K., and DEWAN, E. M.
Experimental Investigation of Small Scale Transport Mechanisms in the Stratosphere
AIAA J., Vol. 12, No. 8 (August 1974)

SHERMAN, C.
Barium Zirconate Thermionic Cathodes
Rev. of Sci. Instms. (September 1974)

SMITH, E. R.
Electron-Impact Excitation of Atomic Oxygen
Phys. Rev. A, Vol. 13 (1976)
Angular Distributions of Photoelectrons from Atomic Oxygen
The Phys. Rev., Vol. 13, No. 3 (March 1976)

SWIDER, W.
Chemical Excitation of O_2 ($^1\Delta g$) in Auroras
J. of Geophys. Res., Vol. 79, No. 22 (August 1974)
The D- and E-Regions
Atm. of Earth and the Planets, Ed. by B. M. McCormac, D. Reidel Pub. Co. (1975)
Atmospheric Formation of NO from N_2 ($A^3\Sigma$)
Geophys. Res. Ltrs., Vol. 3, No. 6 (1 June 1976)

SWIDER, W., and DEAN, W. A. (U. S. Army Ballistic Res. Lab., Aberdeen, Md.)
Effective Electron Recombination Coefficient of the Disturbed Daytime D-Region
J. of Geophys. Res., Vol. 80 (1 May 1975)

SWIDER, W., and NARCISI, R. S.
Ion Composition of a Class II Aurora. 2. Model
J. of Geophys. Res., Vol. 79, No. 19 (July 1974)
A Study of the Nighttime D-Region During a PCA Event
J. of Geophys. Res. (February 1975)

TAKEZAWA, S., and TANAKA, Y.
The Absorption Spectrum of D_2 in the Vacuum-UV Region, Rydberg Bands, npa $^1\Sigma_u^+ + X\ ^1\Sigma_g^+$ and $np\pi\ ^1\Pi_u X\ ^1\Sigma^+$ with n = 4 - 6, and the Ionization Energy
J. of Mol. Spectros., Vol. 53, No. 3 (15 March 1975)

TANAKA, Y., YOSHINO, K., and FREEMAN, D. E.
Vacuum Ultraviolet Absorption Spectrum of the van der Waals Molecule Xe_2. Part I. Excited Electronic States
J. of Chem. Phys., Vol. 61 (1974)
Emission Spectra of Heteronuclear Diatomic Rare Gas Positive Ions
J. of Chem. Phys., Vol. 62 (1975)

TATTLELMAN, P. I.
Surface Gustiness and Wind Speed Range as a Function of Time Interval and Mean Wind Speed
J. of Appl. Met., Vol. 14, No. 7 (October 1975)

VAN TASSEL, R. A., and PAULSEN, D. E.
Rayleigh, the Unit for Light Radiance: Comment
Appl. Opt., Vol. 14 (March 1975)

WEEKS, L. H.
Observation of O_2 Variability at Midlatitudes from 1450 Å Measurements
J. of Geophys. Res., Vol. 80 (1975)
Determination of O_2 Density from Lyman-a Ion Chambers
J. of Geophys. Res., Vol. 80 (1975)

YOSHINO, K., TANAKA, Y., and CARROLL, P. K., MITCHELL, P. (Phys. Dept., Univ. Coll., Dublin, Ire.)
High Resolution Absorption Spectrum of N_2 in the Vacuum-UV Region, O_3. $4^2\ ^1\Pi_u X\ ^1\Sigma_g^+$ Bands
J. of Mol. Spectros., Vol. 54, No. 1 (January 1975)

ZIMMERMAN, S. P.
Turbulence Observed in Electron Density Fluctuations in the Equatorial E-Region Over Thumba, India-A Reanalysis
J. of Geophys. Res., Vol. 81 (1976)

ZIMMERMAN, S. P., and KENESHEA, T. J.
Appendix 3 to U. S. Standard Atmosphere – 1976
U. S. Govt. Prtg. Off., Wash., D. C. (1976)

PAPERS PRESENTED AT MEETINGS JULY 1974 - JUNE 1976

BERTONI, E. A.
USAF In-Flight Line-of-Sight Program
11th Mtg. of NATO AC/225 (Panel XII), NATO Hq., Brussels, Belgium (16-18 September 1974)

BRACE, L. H., MAYR, H. G., HOEGY, W. R. (NASA Goddard Space Flt. Ctr., Greenbelt, Md.), and HINTEREGGER, H. E.
The Thermospheric Electron Heat Balance from AE-C Measurements
AM. Geophys. Union 1974 Fall Ann. Mtg., San Francisco, Calif. (12-17 December 1974)

CHAMPION, K. S. W.
Some Highlights of Atmosphere Explorer-C Investigations
18th Plenary Comm. on Space Res. (COSPAR) Mtg., Varna, Bulgaria (29 May - 7 June 1975)

COLE, A. E.
International Standards Organization (ISO) Reference Atmospheres
5th Mtg. of the Intl. Stds. Orgn. Working Gp. on Std. and Ref. Atm., London, Eng. (27-29 November 1974)

CORBIN, V. L., OLSEN, R. (White Sands Missile Range, N. M.), and FAIRE, A. C.
Atmospheric Structure Parameters During Disturbed Wintertime Conditions at White Sands
56th Ann. Am. Geophys. Union Mtg., Wash., D. C. (16-20 June 1975)

DEWAN, E. M.
Ball Lightning
Dept. of Atm. Sci., State Univ. of N. Y. at Albany, N. Y. (12 May 1975)

FAIRE, A. C., CORBIN, V. L., and CHAMPION, K. S. W.
Diurnal Variations in Neutral Density and Temperature Observed at Natal, Brazil
Comm. on Space Res. (COSPAR) Mtg., Varna, Bulgaria (29 May – 7 June 1975)

FREEMAN, D. E.
Electronic Spectra of Weakly Bound Diatomic Rare Gas Molecules
Sem., Mass. Inst. of Technol., Cambridge, Mass. (6 May 1975)

FREEMAN, D. E., YOSHINO, K., and TANAKA, Y.
Vacuum Ultraviolet Absorption Spectra of Heteronuclear Diatomic Rare Gas Molecules
28th Ann. Gaseous Elect. Conf., Univ. of Mo. -Rolla, Mo. (21-24 October 1975)

GALLAGHER, C. C.
Wave Heating of Plasma in a Toroidal Cusp (Tormac)
Am. Phys. Soc. Mtg., Albuquerque, N. M. (28-31 October 1974)

GARRETT, H. B., 1ST LT., and FORBES, J. M. (Harvard Univ., Cambridge, Mass.)
Observations of a Zonal Wavenumber Two Variation in Total Mass Density Near 145 Km
56th Ann. Am. Geophys. Union Mtg., Wash., D. C. (16-20 June 1975)

GRINGORTEN, I. I.
On the Use of Stochastic Models of Simultaneous Critical Weather Condition in an Area
4th Conf. on Stochastic Processes, York Univ., Toronto (Downsview), Ont., Can. (4-9 August 1974)
A Statistical Study of PPT Scope Radar Pictures
4th Conf. on Probability and Stat. in Atm. Sci., Tallahassee, Fla. (18-21 November 1975)
To Find Computer Algorithms for Models of the Extent of Weather Conditions in Time and Space
Symp. on Appl. of Stat., Wright State Univ., Dayton, Ohio (14-18 June 1976)

HINTEREGGER, H. E.
EUV Fluxes in the Solar Spectrum Below 2000 A°
1975 Intl. Assn. for Geomag. and Aeron. (IAGA) Symp., Grenoble, Fr. (25 August – 6 September 1975)

HINTEREGGER, H. E., BEDO, D. E., and MANSON, J. E.
Solar Extreme Ultraviolet Measurements for Aeronomical Objectives
AIAA 13th Aerosp. Sci. Mtg., Pasadena, Calif. (20-22 January 1975)

HINTEREGGER, H. E., HEROUX, L. J., BEDO, D. E., MANSON, J. E., and HIGGINS, J. E.
Satellite-Observed Variations of Solar EUV Fluxes in 1974 and Spectrophotometric Calibration by a Rocket Experiment
Am. Geophys. Union 1974 Fall Ann. Mtg., San Francisco, Calif. (12-17 December 1974)

INNES, F. R.
Adjointure and Phases for Spherical Functions and Operators
Atomic Spectros. Symp., Natl. Bur. of Stds., Gaithersburg, Md. (23-26 September 1975)

KANTOR, A. J.
Character of the Meteorological Equator in the Stratosphere and Mesosphere
6th Conf. on Aerosp. and Aero. Met., El Paso, Tex. (12-14 November 1974)

KENESHEA, T. J., and ZIMMERMAN, S. P.
Dynamical Calculations of a Major and Minor Neutral Species from 50 to 400 Km Using Measured Transport Coefficients
56th Ann. Am. Geophys. Union Mtg., Wash., D. C. (16-20 June 1975)

LUND, I. A.
Cloud-Free Lines-of-Sight Through the Atmosphere
Natl. Telecomm. Conf., San Diego, Calif. (2-4 December 1974)

LUND, I. A., and GRANTHAM, D. D.
A Model for Estimating Joint Probabilities of Cloud-Free Lines-of-Sight from Unconditional Probabilities
6th Conf. on Aerosp. and Aero. Met., El Paso, Tex. (12-14 November 1974)
Estimating Hourly Persistence and Recurrence Probabilities of Temperature
4th Conf. on Probability and Stat. in Atm. Sci., Tallahassee, Fla. (18-21 November 1975)
A Model for Estimating Joint Probabilities of Weather Events
Mil. Ops. Res. Soc. Mtg., Ft. Bliss, Tex. (22-24 June 1976)

MAC LEOD, M. A., KENESHEA, T. J., and NARCISI, R. S.
Numerical Modeling of a Metal Ion Sporadic E Layer
Recent Adv. in the Phys. and Chem. of the E-Region Mtg., Boulder, Colo. (13-15 August 1974)

MANSON, J. E.
Solar Spectral Irradiance Between 10 and 300 Angstroms
NASA and NCAR/High Alt. Obsv. Solar Output Wkshp., Univ. of Colo., Boulder, Colo. (26-28 April 1976)
Radiometric Calibration in the 160-304 Å Region
4th Wkshp. on VUV Radiometric Calibration of Space Exp., NCAR, Boulder, Colo. (29-30 April 1976)

MARCOS, F. A.
Neutral Density Variations from Simultaneous Accelerometer Measurements on Two Satellites
56th Ann. Am. Geophys. Union Mtg., Wash., D. C. (16-20 June 1975)

MARCOS F. A., CHAMPION, K. S. W., and POTTER, W. E., KAYSER, D. C. (Univ. of Minn.)
Density and Composition of the Neutral Atmosphere at 140 Km from Atmosphere Explorer-C Satellite Data
1976 Spring Ann. Mtg. of the Am. Geophys. Union, Wash., D. C. (12-16 April 1976)
19th Plenary Mtg. of Comm. on Space Res. (COSPAR), Univ. of Pa., Philadelphia, Pa. (8-19 June 1976)

MARCOS, F. A., GARRETT, H. B., and FORBES, J. M. (Boston Coll., Chestnut Hill, Mass.)
Lower Thermospheric Density Variations from the Atmosphere Explorer-C Accelerometer Experiment
Am. Geophys. Union Fall Mtg., San Francisco, Calif. (8-12 December 1975)

MARCOS, F. A., PHILBRICK, C. R., and RICE, C. J. (Aerosp. Corp., El Segundo, Calif.)
Correlative Satellite Measurements of Atmospheric Mass Density by Accelerometers, Mass Spectrometers and Ionization Gauges
19th Plenary Mtg. of Comm. on Space Res. (COSPAR), Univ. of Pa., Philadelphia, Pa. (8-19 June 1976)

MURAD, E.
The Reaction of N+ and N_2^+ with N_2O
Spring Mtgs. of the Am. Chem. Soc., Philadelphia, Pa. (6-11 April 1975)

MURAD, E., and HILDENBRAND, D. L. (Stanford Res. Inst., Menlo Pk., Calif.)
The Dissociation Energy of Europium Monoxide
Am. Chem. Soc. Mtg., Chicago, Ill. (24-29 August 1975)

MURPHY, E. A., and ZIMMERMAN, S. P.
Stratospheric and Mesospheric Turbulence
19th Plenary Mtg. of Comm. on Space Res. (COSPAR), Univ. of Pa., Philadelphia, Pa. (8-19 June 1976)

MOSES, H. E.
A Two-Level Approximation to the Resonance Scattering of Lyman-a Radiation by H Atoms in the Ground State
Mtg. of Am. Phys. Soc., New York, N. Y. (2-5 February 1976)

NARCISI, R. S.
Negative Ion Composition of the D and E Regions
16th Gen. Asbly. of the Intl. Union of Geod. and Geophys. (IUGG), Grenoble, Fr. (25 August - 6 September 1975)
Lower Ionosphere Physics
AIAA 4th Sounding Rocket Technol. Conf., Boston, Mass. (23-25 June 1976)

NARCISI, R. S., BAILEY, A. D., SHERMAN, C., and WLODYKA, L.
On Associative Electron Detachment Processes in the Ionospheric D Region
56th Ann. Am. Geophys. Union Mtg., Wash., D. C. (16-20 June 1975)

PAULSON, J. F., and GALE, P. J., HENCHMAN, M. J. (Brandeis Univ., Waltham, Mass.)
A Quantitative Investigation of the Role of Franck Condon Factors in Charge Transfer Reactions
23rd Ann. Conf. on Mass Spectrom. and Allied Topics, Houston, Tex. (May 1975)

PHILBRICK, C. R.
Recent Satellite Measurements of Upper Atmospheric Composition
Comm. on Space Res. (COSPAR) Mtg., Varna, Bulgaria (29-31 May 1975)

PHILBRICK, C. R., MC ISAAC, J. P., and FAUCHER, G. A.
Variations in the Atmospheric Composition and Density During a Geomagnetic Storm
19th Plenary Mtg. of Comm. on Space Res. (COSPAR), Univ. of Pa., Philadelphia, Pa. (8-19 June 1976)

QUESADA, A. F., DEWAN, E. M., GOOD, R. E., ROSENBERG, N. W., and VICKERY, W. K.
Stratospheric Winds and Turbulence Measurements from Smoke Trails
19th Plenary Mtg. of Comm. on Space Res. (COSPAR), Univ. of Pa., Philadelphia, Pa. (8-19 June 1976)

QUESADA, A. F., ZIMMERMAN, S. P., and ROSENBERG, N. W.
Tidal Motions in the Thermosphere and Realistic Viscosities
56th Ann. Am. Geophys. Union Mtg., Wash., D. C. (16-20 June 1975)

ROSENBERG, N. W., QUESADA, A. F., and ZIMMERMAN, S. P.
High Resolution Stratospheric Winds from Chemical Trail Data
56th Ann. Am. Geophys. Union Mtg., Wash., D. C. (16-20 June 1975)

SWIDER, W.
The D- and E-Regions
Summer Adv. Study Inst., Phys. and Chem. of Atm., Univ. of Liege, Belgium (29 July-9 August 1974)
Generation of NO from N_2 (A) + O
1976 Spring Ann. Mtg. of the Am. Geophys. Union, Wash., D. C. (12-16 April 1976)
Minor Mesospheric Constituents at High Latitudes
19th Plenary Mtg. of Comm. on Space Res. (COSPAR), Univ. of Pa., Philadelphia, Pa. (8-19 June 1976)

SWIDER, W., and NARCISI, R. S.
Nitric Oxide at 100-200 Km in Aurora
Am. Geophys. Union Mtg., San Francisco, Calif. (8-12 December 1975)

SWIDER, W., and ULWICK, J. C. (Opt. Phys. Lab.), DEAN, W. A. (U. S. Army/BRL, Aberdeen, Md.)
Electron Recombination in the Disturbed D-Region
1974 USNC/URSI-IEEE Mtg., Boulder, Colo. (14-17 October 1974)

TANAKA, Y.
The Electronic Absorption Spectra of Diatomic Van der Waals Rare Gas Molecules
Am. Chem. Soc. Ann. Mtg., Symp. on van der Waals Molecules, Atlantic City, N. J. (8-13 September 1974)

TATTELMAN, P. I.
Surface Wind Speed Range as a Function of Time and Mean Wind Speed
6th Conf. on Aerosp. and Aero. Met., El Paso, Tex. (12-14 November 1974)

THOMAS, T. F., and PAULSON, J. F.
Photodissociation of Ion Beams in a Tandem Mass Spectrometer Using a Tunable Dye Laser
Am. Soc. for Mass Spectrom. 24th Ann. Conf., San Diego, Calif. (9-14 May 1976)
Photodissociation Spectra of Positive Ions with Time-of-Flight Analysis
12th Informal Conf. on Photochem., Natl. Bur. of Stds., Gaithersburg, Md. (28 June-1 July 1976)

WEEKS, L. H., DOIRON, C., and MC INERNEY, R. E. (AFCRL Comp. Branch), DELAY, S. H. (Boston Coll., Mass.)
Observations of Mesospheric Ozone from a Nighttime-Daytime Rocket Series
56th Ann. Am. Geophys. Union Mtg., Wash., D. C. (16-20 June 1975)

WEEKS, L. H., GOOD, R. E., and RANDHAWA, J. S. (U. S. Army Atm. Sci. Lab., White Sands Missile Range, N. M.), and TRINKS, H. (Physikalisches Inst. der Univ. Bonn, Fed. Rep. of Ger.)
Ozone Measurements in the Stratosphere, Mesosphere, and Lower Thermosphere During ALADDIN '74
19th Plenary Mtg. of Comm. on Space Res. (COSPAR), Univ. of Pa., Philadelphia, Pa. (8-19 June 1976)

YOSHINO, K.
High Resolution VUV Spectroscopy of Diatomic Molecules
31st Symp. on Mol. Spectros., Ohio State Univ., Columbus, Ohio (14-18 June 1976)

YOSHINO, K., and TANAKA, Y.
High Resolution Absorption Spectra of Kr I and Xe I in the VUV Regions
Atomic Spectros. Symp., Natl. Bur. of Stds., Gaithersburg, Md. (23-26 September 1975)

ZIMMERMAN, S. P.
Turbulence Observed in Electron Density Fluctuations in the Equatorial E Region Over Thumba, India
Recent Adv. in the Phys. and Chem. of the E Region Mtg., Boulder, Colo. (13-15 August 1974)

ZIMMERMAN, S. P., and KENESHEA, T. J.
The Effects of Small Scale Dynamics Upon the Distribution of Minor and Major Neutral and Ionic Constituents in the Mesosphere and Thermosphere
19th Plenary Mtg. of Comm. on Space Res. (COSPAR), Univ. of Pa., Philadelphia, Pa. (8-19 June 1976)

ZIMMERMAN, S. P., QUESADA, A. F., and TROWBRIDGE, C. A. (Photomet., Inc., Lexington, Mass.)
Small Scale Turbulent and Wave Structure in the Stratosphere
56th Ann. Am. Geophys. Union Mtg., Wash., D. C. (16-20 June 1975)

TECHNICAL REPORTS JULY 1974 - JUNE 1976

CHAMPION, K. S. W.
Dynamics and Structure of the Quiet Thermosphere
AFCRL-TR-74-0318 (17 July 1974)

CHAMPION, K. S. W., FORBES, J. M., and BRAMSON, A. S. (IBM, Burlington, Mass.), BHAVNANI, K. H. (Logicon, Bedford, Mass.), SLOWEY, J. W. (Smithsonian Astrophys. Obsv., Cambridge, Mass.), GILLETTE, D. F., and HUSSEY, I. (Off. of Res. Svc.)
Densities Near 160 Km Obtained from Orbital Analysis of Satellite 1973-14A
AFCRL-TR-75-0253 (2 May 1975)

COLE, A. E., and KANTOR, A. J.
Periodic Oscillations in the Stratosphere and Mesosphere
AFCRL-TR-74-0504 (8 October 1974)

CORMIER, R. V.
World-Wide Extremes of Humidity with Temperatures Between 85° and 120°F
AFCRL-TR-74-0603 (5 December 1974)

GARRETT, H. B., 2ND LT.
An Updated Empirical Density Model for Predicting Low-Altitude Satellite Ephemerides
AFCRL-TR-75-0158 (19 March 1975)

JASPERSE, J. R.
Electron Distribution Function in a Nonuniform, Magnetized, Weakly Photoionized Gas Application to a Model Ionosphere
AFCRL-TR-75-0266 (12 May 1975)

KANTOR, A. J.
A Comparison Between Observed and Deduced Mean Monthly Winds from 700 mb to 200 mb
AFCRL-TR-76-0044 (22 January 1976)

KANTOR, A. J., and COLE, A. E.
The Meteorological Equator in the Stratosphere and Mesosphere
AFCRL-TR-74-0604 (5 December 1974)
Monthly Midlatitude Atmospheres, Surface to 90 Km
AFGL-TR-76-0140 (23 June 1976)

LUND, I. A., GRANTHAM, D. D., and ELAM, C. B., JR. (USAF Envmt. Tech. Appl. Ctr., Scott AFB, Ill.)
Atlas of Cloud-Free Line-of-Sight Probabilities
AFCRL-TR-75-0261 (8 May 1975)

MANSON, J. E.
Satellite Measurements of Solar UV During 1974
AFCRL-TR-76-0006 (6 January 1976)

MAPLETON, R. A., and SCHNEEBERGER, M. F., STEELE, C. A., JR. (RDP, Inc., Bedford, Mass.)
Electron Capture from $Tl^+(6s^2)$ and Li^+ by Protons
AFCRL-TR-75-0053 (28 January 1975)

MARCOS, F. A., CHAMPION, K. S. W., MC INERNEY, R. E., and DELOREY, D.
Atmospheric Density Variations in the Southern Hemisphere at Low Satellite Altitudes
AFCRL-TR-75-0254 (5 May 1975)

MARCOS, F. A., and MENDILLO, J. L. (Boston Coll., Chestnut Hill, Mass.)
Lower-Thermosphere Neutral Density Profiles Derived from Satellite Accelerometer Data
AFGL-TR-76-0045 (4 March 1976)

MC ISAAC, J. P., CHAMPION, K. S. W., MC INERNEY, R. E., and DELOREY, D. (Boston Coll., Chestnut Hill, Mass.)
Ionization Gauge Measurements of Atmospheric Density from a Low Altitude Satellite
AFGL-TR-76-0113 (24 May 1976)

MOSES, H. E.
Probes in a Plasma from a Gas Dynamic Point of View with Application to the Problem of Satellite Charging
AFCRL-TR-76-0005 (6 January 1976)

QUESADA, A. F.
Vector Evaluation of Triangulation Camera Parameters from Star Photographs
AFCRL-TR-75-0451 (21 August 1975)

ROSENBERG, N. W., and DEWAN, E. M.
Stratospheric Turbulence and Vertical Effective Diffusion Coefficients
AFCRL-TR-75-0519 (29 September 1975)

SHERMAN, C.
Vehicle Potential Control by Means of Electron Emission
AFCRL-TR-75-0445 (18 August 1975)

SMITH, E. R.
The Effect of Several Configuration Interaction Target States on the Elastic Scattering of Low-Energy Electrons by Complex Atoms
AFCRL-TR-75-0054 (28 January 1975)

SWIDER, W.
The D- and E- Regions
AFCRL-TR-74-0493 (12 September 1974)
Composite PCA '69 Study: Final Report
AFCRL-TR-75-0149 (17 March 1975)

SWIDER, W., and CHIDSEY, I. L., JR. (U. S. Army Ballistic Res. Lab., Aberdeen Proving Ground, Md.)
Calculated and Measured HF/VHF Absorption for the 2-5 November 1969 Solar Proton Event
AFGL-TR-76-0053 (9 March 1976)

SWIDER, W., and FOLEY, C. I. (Boston Coll., Chestnut Hill, Mass.)
Computer Program for the Disturbed Steady-State Nighttime D-Region
AFCRL-TR-75-0150 (13 March 1975)

TATTELMAN, P., and KANTOR, A. J.
Atlas of Probabilities of Surface Temperature Extremes
AFGL-TR-76-0084 (16 April 1976)

VICKERY, W. K.
Techniques for Depositing Visible Smoke Trails in the Stratosphere for Measurement of Winds and Turbulence
AFCRL-TR-75-0221 (21 April 1975)

III AEROSPACE INSTRUMENTATION DIVISION

The Air Force Geophysics Laboratory is concerned with obtaining a thorough knowledge of the environment in which Air Force systems must operate. Atmospheric and space probes play an important role in this mission. The Aerospace Instrumentation Division provides balloon, rocket, and satellite system support to the other AFGL Divisions and also conducts research and development programs to ensure that the most reliable and cost effective vehicles and instruments are available to scientists to meet their objectives.

BALLOON ACTIVITIES

A permanent balloon launch facility is located at Holloman AFB, New Mexico. Another site, manned until the end of this reporting period, but now unmanned, is located at the Chico, California, Municipal Airport for scientists requiring long duration flights or operations at a latitude other than Holloman. A permanent tethered balloon launch site is maintained at the northern end of the White Sands Missile Range, New Mexico. The Range provides the use of precision radar, optical instrumentation, telemetry and restricted airspace to scientists conducting experiments involving free fall, explosive bursts or high altitude tethering.

The balloon expertise of the Division is frequently called on to support other Air Force organizations, the Army, Navy, and NASA. The Division also supports the Energy Research and Development Administration's air sampling program (Project Ash Can) by flying collectors on balloons launched from Alaska, and Panama, as well as from Holloman AFB.

In July 1974, several successful tethered balloon flights at Holloman AFB showed the feasibility of using a small tethered balloon supporting a special antenna to serve as an emergency backup to a tower mounted tactical LORAN antenna disabled by enemy action or a severe storm. As a result, the Tactical LORAN Special Projects Office of the Air Force Systems Command, ESD, sponsored a program to develop several operational units.

Two heavy load, high altitude single parachute system flight tests were also flown in 1974. These tests were made to investigate the possibility of replacing the cluster of three 100-foot diameter parachutes normally used for recovery of payloads over 4,000 pounds by a single parachute. A payload of 4,035 pounds was released from a balloon at 92,000 feet in September to test a 135-foot diameter flat circular cargo parachute. In November, a 120-foot diameter, flat circular parachute was tested by releasing a load of 4,565 pounds at 92,000 feet. The instrumentation at the White Sands Missile Range was used to get performance data. Both tests were successful.

A series of balloon flights in June 1975 tested a cryogenic whole air sampler operating at altitudes of 20 to 30 km. The sampler was used in the Stratospheric Environment program, which has provided data and models from which environmental impact statements for aircraft such as the F-15 may be written.

Two balloon flights also conducted in 1975 carried experiments to measure aerosol size and concentration and to determine the variability in optical scattering properties of the atmosphere.

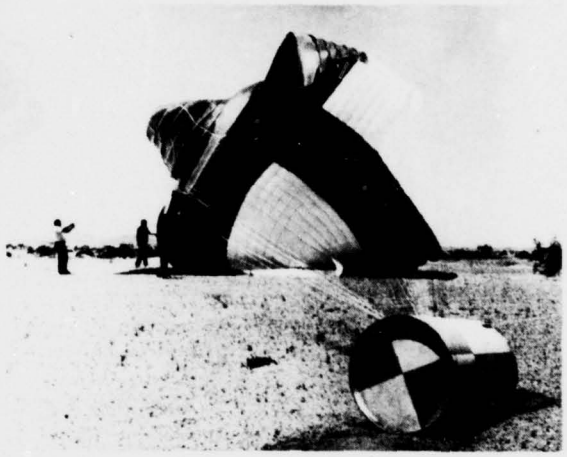

Sixty-six-foot paraform parachute after successful drop test.

Still another series of balloon flights carried a 50-inch mirror telescope to determine the infrared radiance of Venus and Mars. Later flights in the series carried a high quality gamma-ray telescope which could be pointed by ground commands at likely celestial sources of gamma rays.

Finally, a series of balloon flights carried aloft experiments to measure microscale fluctuations of wind and temperature, and the distribution of ozone to determine stratospheric dynamics.

FREE BALLOONS

The free balloon development program progressed in three areas during the past two years: balloon capability, recovery systems reliability, and non-dynamic launch technique development.

A mathematical model of balloon capability, relating payload, altitude, duration and maneuverability (alteration of

the balloon's vertical position or velocity) was defined and examined for a 23-year period. The results were reported in the "Proceedings (Supplement) of the Eighth Scientific Balloon Symposium, 30 September to 3 October 1974." The capability trend was extrapolated and interpreted, and recommendations to accelerate the capability growth were made and related to present and planned research and development.

Many balloon missions require the recovery of a delicate payload for success. The standard balloon payload recovery system is an in-line (between balloon and payload) parachute. Traditional models of parachute performance (relating opening time, opening shock, etc.) were developed to explain and predict parachute deployment from moving aircraft. One of these recent models has been theoretically extended to cover the deployment of in-line parachutes at balloon altitudes up to 120,000 feet.

The third flight in a series to develop a non-dynamic launch technique for single-cell balloons was attempted. Release of more balloon material than was needed for the state of inflation at the time resulted in balloon failure while the system was still tethered to the ground. The examination of the failed balloon revealed problems that would have caused failure later in flight, but which would have been undetectable had the balloon been flown. Results of this flight have served as the basis for a redesign of the balloon reefing sleeve which has been incorporated in a balloon now awaiting test.

AIR-LAUNCHED BALLOON SYSTEM

Significant progress has been made on the development of an Air-Launched Balloon System (ALBS) which will satisfy the Tactical Air Command requirement for a lighter-than-air tactical communications relay platform. One critical subsystem, the cryogenic gas storage and heat transfer unit, was successfully developed through the assistance of the Cryogenics Division of the National Bureau of Standards (NBS). In November 1975, the NBS unit, in a test at Holloman AFB, inflated a balloon which carried a 300-pound payload to 75,000 feet. This is believed to be the first balloon flight ever to use liquid helium as the gas source. Flight tests of a complete ALBS are now possible.

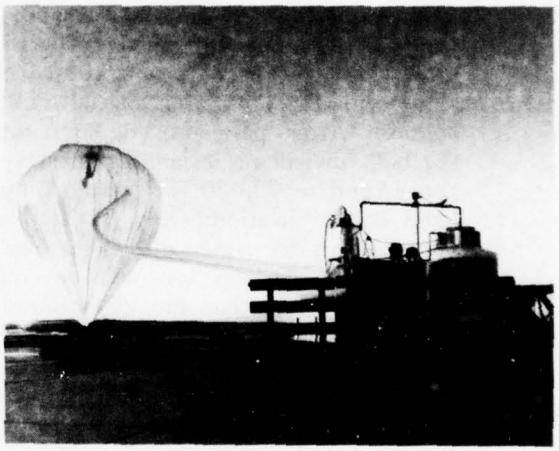

Balloon payload preparation, inflation, and launch from Holloman AFB, November 11, 1975.

Progress has been made on other portions of the system. The design of the special balloon required for the ALBS mid-air inflation process was completed and fabrication was begun. The working agreement with the NBS was extended and a new, lighter weight cryogenic gas storage and heat transfer unit, more suited to flight tests, was designed and built. The complicated ALBS parachute deployment subsystem was designed in-house, and reviewed at the National Parachute Test Range (NPTR).

A verification test program to be conducted at El Centro, California, from November 1976 to October 1977, with ALBS system mockups, will determine the final design of the parachute system, thus allowing subsequent drop tests of the overall system to be made.

An in-house drop-platform analysis led to the choice of a scientific balloon as the release vehicle for the first complete system test. In this test, scheduled for July 1978, the lightweight cryogenic unit will be dropped from 20,000 feet along with the uninflated special ALBS balloon. After parachute deployment, the balloon will be inflated, pull away, and ascend to 70,000 feet with a simulated communications relay. To resolve uncertainties discovered during the analysis, a second drop test will be conducted using system mockups, about three months prior to the July 1978 tests of the "live" configuration.

In addition to several briefings on lighter-than-air platforms and the ALBS system, two in-house reports were written. "An Investigation of the Applicability of High Altitude, Lighter-Than-Air (LTA) Vehicles to the Tactical Communications Relay Problem" (AFCRL-TR-74-0399) was published, and "The Flight Test Aspects of the Air Launched Balloon System (ALBS) Development Program" (AFGL-TR-76-0196) will be published in August 1976.

POWERED BALLOONS

For many years, the Division has studied the concept of propelling a free balloon to counter the wind. Basic feasibility and parametric studies were completed and a simplified flight system fabricated. A flight of the system demonstrated the feasibility of powering a balloon against the wind at high altitude. A more sophisticated streamlined system was then designed under contract, and manufacturing drawings completed.

The Navy has a need to fly certain sensors in a regime that can be reached by a powered balloon. For this reason, the U. S. Naval Surface Weapons Center contacted the Division and initiated a powered balloon program in 1974, based on the preliminary work completed by the Air Force. The Navy asked for, and funded, assistance from the Division on this High Altitude Superpressure Powered Aerostat (HASPA) program.

In 1975, the Division designed and fabricated special launch equipment and vehicles for the HASPA program. A complete ground station, and an airborne control and telemetry system, were also designed and fabricated in-house for the program.

In November 1975 the Division fielded a 10-man launch team to Kennedy Space Center to assist the Navy in the launch of the first, unpowered HASPA balloon. The system was launched on November 5, 1975, but a reefing collar did not release at the proper time, preventing the system from reaching its design altitude of 65,000 feet.

A second flight, in March 1976, was aborted when the balloon material failed at launch. It appears that the Kevlar fiber used for fabric reinforcement is degraded by light. The Navy is now reviewing the program, with emphasis on the balloon material problem. Testing will continue as soon as this problem is resolved.

BALLOON INSTRUMENTATION

The modular concept for instrumentation system assembly has continued to provide the increased flexibility and measurement capability needed to meet the

rapidly expanding scientific and operational requirements of balloon-using scientists.

Manning and budget reductions have made it increasingly important not only to refurbish and reuse system components but to design systems that can be used with many different experiments whenever possible.

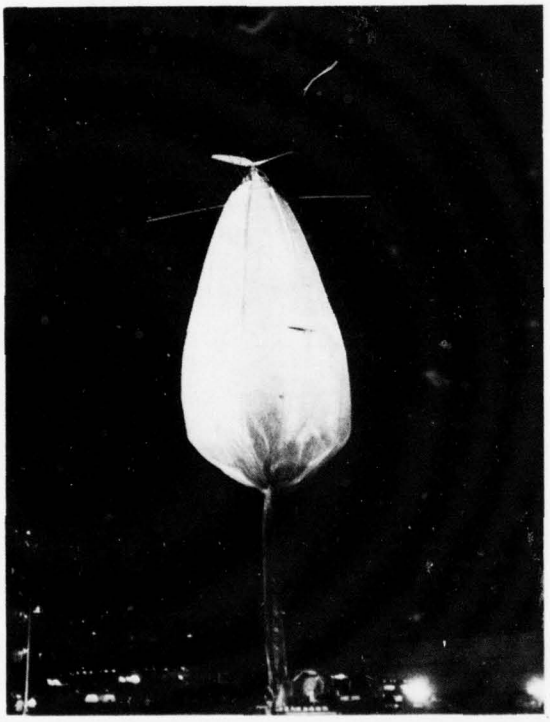

High Altitude Super Pressure Aerostat (HASPA) being reeled up for launch. Stern mounted propeller can be seen at top of picture.

A new ground station terminal and a minicomputer have been installed at the Holloman AFB facility to receive PCM telemetry signals from balloons. The system allows a user to examine selected data channels within the standardized pulse code modulated telemetry signal in real time. The computer also can accept a user's programs to manipulate the data and transfer blocks of data to a teleprinter output.

The high altitude atmospheric sampling program for the Energy Research and Development Administration (ERDA) has continued. The Atomic Energy Commission began this program to collect atmospheric nuclear debris in 1956. Responsibility for balloon operations was transferred from the Air Weather Service to the Aerospace Instrumentation Laboratory in July 1972. Since then, the program has expanded to include investigation of the gaseous and particulate atmospheric constituents with various types of sampling devices. Some of these devices are specifically designed for aerial recovery by C-130 aircraft after the samples have been collected and the payload is separated from the balloon.

In the spring of each year, an annual sampling cross section is made beginning at Albrook AFB, Canal Zone, in March, proceeding to Holloman AFB, New Mexico, in April, and concluding at Eielson AFB, Alaska, in May. Sampling is normally conducted at altitudes of 70,000, 80,000 and 90,000 feet above mean sea level (MSL). However, in 1973, additional sampling was conducted at altitudes of 105,000 and 120,000 feet MSL. At Holloman AFB, sampling is conducted quarterly at altitudes of 70,000, 80,000 and 90,000 feet MSL. There were also research and development flights to update the sampling hardware and support instrumentation, and to qualify a nitric oxide sensing system for flight.

Special balloon instrumentation was developed for the whole air sampling program conducted by the Air Force. A 24-channel command system developed for this program controls all balloon and experiment operations. Every command issued is verified by a coded reply mes-

sage before actuation of the command, and every reply code is repeated once. Highly stable sequentially activated tone decoders ensure security of this command system. Both S-band and HF data transmitters are used. S-band provides a high data rate while the balloon is within line-of-sight of the ground monitoring station. The HF provides a lower data rate, but is usable beyond line-of-sight.

TETHERED BALLOONS

The 450A Tactical LORAN Special Project Office (SPO), Electronic Systems Division, is in the process of developing and installing a series of LORAN D antenna and transmitter sites around the world. These sites are required for precise navigation of aircraft. The SPO is concerned that sabotage, severe weather, or wartime actions could knock down one or more of the 400-foot high antenna towers being used in the LORAN D system. It has been proposed, to have a packaged tethered balloon system at these sites that could be used to hoist a backup antenna to keep the station operating should the primary antenna be inoperable.

The Aerospace Instrumentation Division has conducted two series of flights in support of this effort to determine basic aerodynamic stability of the pyramid moored system. Balloon tether length was varied and cine-theodolite data was gathered under various wind conditions, indicating that a 500-foot tether results in the best antenna stability. Analysis and flight testing were also conducted to determine the optimum angle that the tri-tether cables make with the ground. Greatest antenna stability was observed when this angle was 40°. Torque balanced Kevlar fiber tether cables have been developed and tested for this application. These cables have tensile strengths comparable to steel at less than 20 percent its weight.

Further testing of the 450A tethered system will take place in January 1978 at an operational LORAN antenna site.

The Division's development of Kevlar cables has also made possible the tethering of balloons at altitudes above 50,000 feet. The first demonstration of a tether system at 60,000 feet is scheduled to take place in July 1978 at the AFGL Tethered Balloon site on White Sands Missile Range, New Mexico.

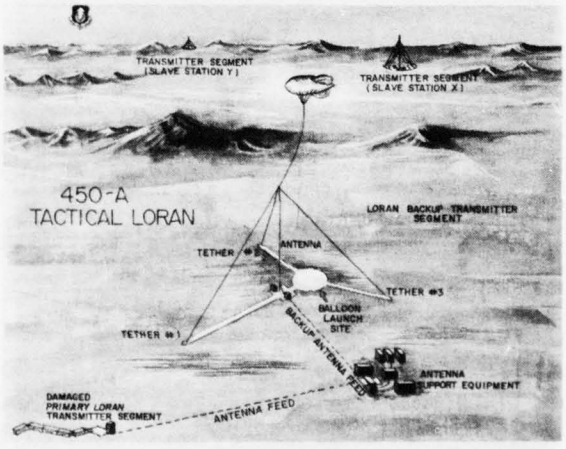

Tri-tether balloon system to temporarily replace damaged LORAN antenna.

Another research effort that has taken place over the last two years involved the development of lightning warning criteria for tethered balloon operations. Atmospheric electrical activity associated with thunderstorms presents a variety of hazards to tethered balloon operations. Lightning strikes can burn small holes in the balloon hull, may destroy the balloon control instrumentation or a scientific payload, or

may sever the tether cable. Lightning strikes also pose a serious hazard to ground crew personnel. Thus it is desirable to be able to assess the possibility of a lightning strike and forecast approximately when it will occur.

Using a lightning warning system developed by the Meteorology Division of AFGL as the data source, criteria were developed to insure safe balloon flight procedures during periods of thunderstorm activity.

PROJECT BAMM

The Balloon Altitude Mosaic Measurements (BAMM) Program is designed to make temporal, spatial, and spectral measurements of earth backgrounds in the infrared for use in the design of advanced sensors. Measurements will be made from a stabilized balloon-borne platform at an altitude of 100,000 feet. Scenes to be viewed for background radiation are cirrus clouds, high altitude lakes and snowfields, ocean effects (glint, land-sea interface, etc.) and temporal buildup of cumulus clouds. Seven flights are scheduled: from Chico, California; Holloman AFB, New Mexico; and Eglin AFB, Florida. Flight durations will average about ten hours and the payload is being designed for air-to-air recovery by helicopter.

The Optical Physics Division has the responsibility for the scientific aspects of this program sponsored by SAMSO.

The Aerospace Instrumentation Division has the responsibility for the balloon flight operation, flight control and data recovery instrumentation, and aerial recovery of the scientific package during descent by parachute following completion of the scientific mission.

RESEARCH ROCKETS

For many years, sounding rockets have been a useful tool for conducting atmospheric and exoatmospheric research. Within AFGL, the Aerospace Instrumentation Division is responsible for the engineering support and range coordination of the research rocket program. To fulfill this responsibility, the Division provides payload engineering, fabrication, test, launching support, data collection and trajectory information. To keep current with state-of-the-art advances, the Division also conducts engineering research towards improving instrumentation and flight systems.

During this reporting period, there has been a decrease in the number of sounding rockets flown, from 93 in the previous two years to 54 during this period. However, at the same time, there has been a definite move toward more complex payloads, more advanced instrumentation, broader use of attitude control systems for more efficient data collection, and increasing use of PCM telemetry for higher resolution, faster sampling and increased data capacity. In contrast to earlier requirements for data retrieval, it has become an economic necessity to retrieve multi-million dollar payloads and sensors. Twenty-one of 54 sounding rockets used recovery systems. Of the 33 that did not use recovery systems, 23 were chemical release, falling sphere or Astrobee D types that do not lend themselves to recovery.

The Division was responsible for payload integration and launching of 54 research rocket vehicles from six different sites. From White Sands Missile Range, New Mexico, 18 rocket vehicles were launched: 7 from the NASA Wallops Flight Center, Virginia; 12 from Churchill Research Range, Manitoba, Canada; 12 from Poker Flat Research Range, Alaska; 2 from Western Test Range, Vandenberg AFB, California; and 3 from Woomera

Range in Australia. These launches were typical examples of the Division's capability to conduct launch operations from any geographical area in the world under diverse work and climatic conditions. Most of these rocket payloads were for AFGL scientific projects, but several launches were conducted in cooperation with other agencies. For example, nine of these rockets were instrumented and launched in support of programs sponsored by the Defense Nuclear Agency. In addition to this work, the Division has provided varying degrees of technical support to other agencies during joint launch programs.

Of the 54 rocket flights, 44 were total successes, 8 returned less than 100 percent data, and only 2 were failures. One sounding rocket failed when a second stage did not ignite and another had a short second stage burn leaving 52 good sounding rockets for a success rate of 96 percent. Of the 21 recovery systems flown, one parachute did not deploy and one deployed too early for a recovery system success rate of 90 percent. Good recovery has resulted in the reflight of many of these payloads, some payloads several times.

Hi Star South: Seven Aerobee 170's were flown from the White Sands Missile Range during 1970 and 1971 in support of Project Hi Star to map the celestial sphere in the infrared using a cryogenic infrared telescope. Hi Star *South* was a continuation of this program with the purpose of completing the IR mapping in the Southern Hemisphere. Hi Star South was a program of three Aerobee 200 flights from Woomera, Australia, in September 1974, using two IR sensors and many payload parts that had been recovered from the Hi Star flights and refurbished. One of these sensors was flown at Woomera, refurbished in the field and reflown in the third payload, a first for the Division, which provided a significant dollar saving.

To obtain precise coordinates of celestial objects observed, a star tracker locked the scan axis to a pre-selected star transiting near the zenith. This star was acquired using a roll stabilized inertial attitude control system (ACS). Once the star was acquired the star tracker provided the error signal for fine control using a reaction gas system. The payload was then rolled around the scan axis at a fixed rate. The IR telescope was rotated from its stowed position in the payload to look up at an angle to the scan axis. At the completion of each rotation the sensor was stepped 1.1 degrees to enable it to search another ring of the sky. After 39 of these rotations the sensor was stowed for reentry and recovery. The star tracker controlled pointing within ± 1 arc minute. The sensor was stepped to a similar accuracy. To obtain this precision, the payload principal axis was aligned to the star tracker axis within 30 arc seconds by dynamic balancing. This not only reduced disturbance torques to those that could be handled by the ACS, but also kept gas consumption at a minimum.

To provide a fast sampling rate and a large data capacity, an encoder with a rate of 600,000 bits per second was used.

Since the IR telescope was capable of detecting very low energy sources, particulate contamination was a real threat to proper data gathering. Because of this, the payload features were designed for cleanliness and preparation techniques were developed to make these the cleanest payloads ever flown by the Division.

Bremsstrahlung Density: This successful Aerobee 170 flight measured atmospheric density by emitting a beam of electrons and measuring the Bremsstrahlung glow created when the electrons interacted with the surrounding oxygen and nitrogen.

Prior to flight, the entire payload was operated in the NASA Plumbrook vacuum facility to provide an electron beam so NASA and Army scientists could con-

duct charging studies. The development of a leakproof pressure seal for a staircase shaped structural section of the payload airframe and significant advances in electron gun handling procedures and technology contributed to the success of the experiment. These advances are being incorporated into current experiments and space flights dealing with spacecraft charging.

Hi-Star South payload, atop Aerobee 200, ready for launch from Woomera, Australia.

Exercise PARADISE AEOLUS: Nine Paiute-Tomahawks were flown from Ft. Churchill, Canada, in April 1975 for this program. These rockets were launched in three series of three, each series into different atmospheric conditions. The first series was launched into disturbed magnetic conditions, the second into quiet and the third into an active aurora. Complementary measurements were made using combinations of mass spectrometer, E-field probe, falling sphere, photometer and chemical release techniques. To make data comparable, it was necessary to launch all three vehicles in each series within 5 minutes. Two payloads were recovered for later reuse.

Laser Backscatter: An Aerobee 150 was successfully flown in June of 1975 carrying the first rocket-borne, high power dye laser. Backscatter from aerosols illuminated by the laser was collected on a 14-inch diameter mirror and measured with a high sensitivity photometer. The payload design accommodated a super clean mirror compartment, a very large ejectable door and high power dissipation with associated high voltage and RF noise problems. The payload was recovered and will be refurbished and reflown.

ICECAP: This program, sponsored by the Defense Nuclear Agency, was successfully concluded during launch campaigns in both 1975 and 1976 at Poker Flat Research Range, Alaska. The 1975 series of nine rockets was flown to obtain diagnostic chemistry of infrared emissions in the February-March period. AFGL provided all of the instrumented payloads: four 6-inch, four 12-inch and one 17-inch. The 17-inch payload was a complex, multi-instrumented, attitude controlled, 860-pound payload, the heaviest AFGL has flown to date. This payload and the 12-inch ones were successfully recovered from the Arctic tundra.

ICECAP 76 consisted of the refurbished Defense Nuclear Agency 17-inch diameter payload which was originally flown in 1975, plus two AFGL density (X-ray composition and falling sphere) payloads. All of the experiments were flown successfully. Additional DNA vehicles were originally scheduled as part

of this series, but bad weather and lack of required auroral conditions caused a reduction in the number of payloads flown.

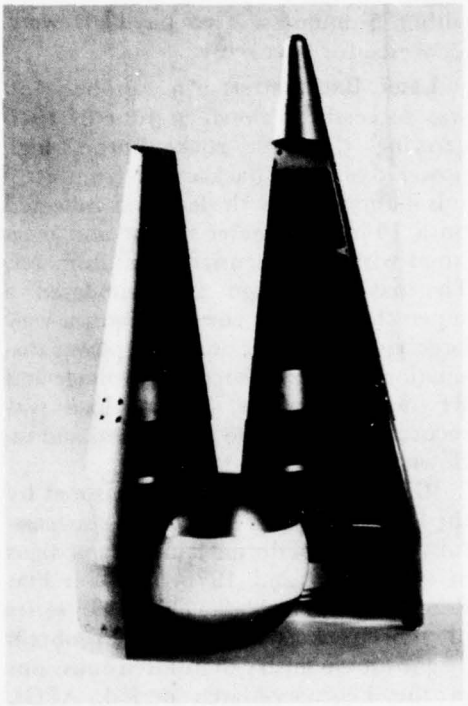

Ten-inch instrumented sphere payload with integrated telemetry and transponder beacon system.

Mid Latitude Twilight D-Region Studies: Six Astrobee D vehicles were launched within a 13-hour period from White Sands Missile Range, New Mexico, in December 1975. Infrared measurements of hydroxyl (OH) emissions were made by payload instrumentation prior to, during and after both sunrise and sunset transitions. In conjunction with these studies, a mobile laboratory located at the payload preparation area conducted synoptic measurements with ground based sensors.

Engineering Research: The Division has conducted a continuing effort to provide for advanced instrumentation and flight systems. This project has resulted in several unique accomplishments. Two different telemetry tracking systems have been developed. The first system, known as TRATEL/TRADAT, consists of a transportable UHF telemetry auto track system (TRATEL) combined with a VHF ranging and trajectory determining system (TRADAT). This system was successfully tested during the ICECAP 75 Program at Poker Flat Research Range, Alaska. The TRATEL/TRADAT System can be deployed to any type of remote rocket launch site and is capable of providing reliable telemetry data reception and accurate rocket vehicle trajectory data, replacing the need for a much more complex radar system.

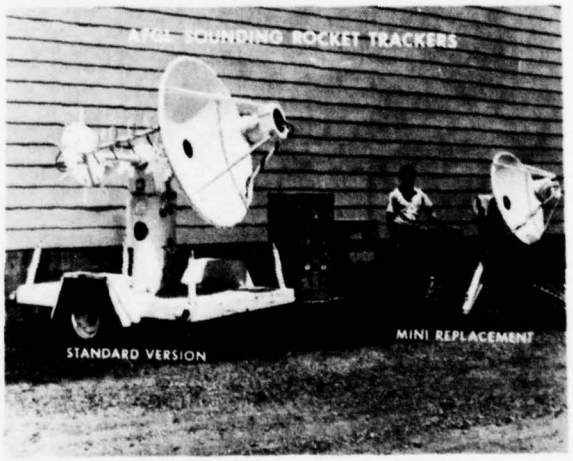

Comparison of the standard TRATEL/TRADAT telemetry tracker with the recently developed MINI-TRACKER.

Another addition to the Division's capability is a recently developed Minitracker. This system is unique in that it is small enough to be brought to a remote site on an airplane as baggage, if required. This highly reliable system is ready for

acceptance testing and for use in support of future AFGL launch missions. It will provide complete UHF telemetry, auto tracking and data reception. The design permits the future addition of the capability for determining a trajectory. Only one man is required to set up and operate the tracker. An integrated, flush mounted antenna system was developed for use with the Ute/Paiute-Tomahawk rockets. This system provides for an interchangeable strip-line antenna section which can be fabricated for either S-Band telemetry and S-Band beacon application or for use with a C-Band beacon and S-Band telemetry system. The technology developed has many aerospace vehicle applications. A typical example was the instrumentation of a 10-inch sphere for a density measurement program. The sphere contains an integral S-Band PCM telemetry system and a miniature C-Band transponder for trajectory. The first operational test of this complete system will be at Kwajalein Missile Range in August 1976.

Work is also progressing to provide computer controlled PCM telemetry data collection at remote sites. A prototype system is being developed that will be used with future AFGL research rockets instrumented with complex PCM equipment.

Dispersion Control System: High altitude sounding rockets have always presented a problem to small test ranges, such as White Sands Missile Range, New Mexico, because of their large impact dispersion. As previously reported, the Division developed a strap-on dispersion control system that can be added to existing payloads without modification. Recent technological advances permit the design of a light, relatively inexpensive package.

The heart of the system is a 16 bit microprocessor that does all the calculations and transformations in the control program. A commonly used digital gyro platform provides attitude reference information while the aerodynamic fins are controlled by a modified pneumatic package from an existing tactical missile. The design was successfully proven by a test flight in October 1975.

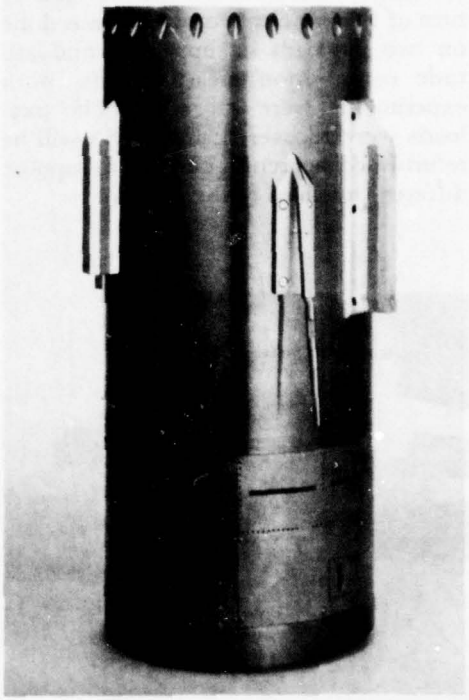

New, flush-mounted UHF telemetry and C-Band beacon antenna mounted underneath older types of antennas.

Zero Angle of Attack Attitude Control System: As experiments become more sophisticated, the payload angle of attack (angle between the payload longitudinal centerline and the velocity vector) becomes more critical for good data collection by some experiments. To reduce this angle of attack to near zero, AFGL used an attitude control system (ACS) on a small, 12-inch diameter payload flown in September 1975. The three-axis ACS, using Freon 14 as the reaction gas, was preprogrammed to pitch

the 300-pound payload at a constant rate to closely match the expected gravity turn of the velocity vector. This was done on two payloads in support of mid-latitude composition measurements. Both experiments were successful. The payloads were recovered; the ACS's will be refurbished and reprogrammed to support different missions in the future.

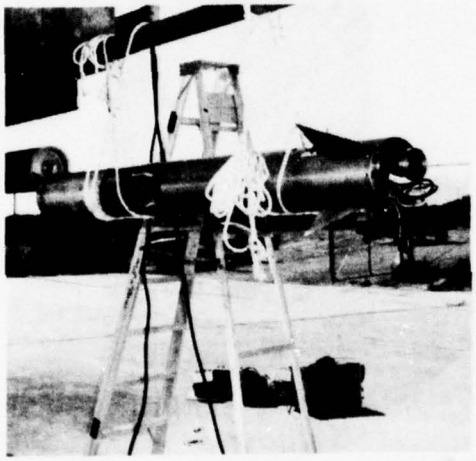

Dispersion control system test payload undergoing pre-launch checks.

Aries Recovery System: A 66-foot paraform parachute recovery system, the largest of its type ever tested, was successfully drop-tested at El Centro, California, on May 13, 1976. The recovery system, using actual Aries flight hardware for deployment and a 1500-pound cylinder for payload simulation was dropped from 18,000 feet by a C-130 aircraft.

The paraform design is a significant improvement over conventional designs. It has all of the desirable features of a ring sail parachute: a wide tolerance of deployment conditions, low opening loads, good stability, and in addition, is a much simpler, lighter weight design. This system will be used for recovery of payloads flown on the Multispectral Measurements Program.

AIAA Fourth Sounding Rocket Technology Conference: In June 1976, the Division hosted, for the first time, the AIAA-sponsored Sounding Technology Conference. This conference was highlighted by its commemoration of the 50th anniversary of Dr. Robert H. Goddard's historic first rocket flight in Auburn, Massachusetts, on March 16, 1926.

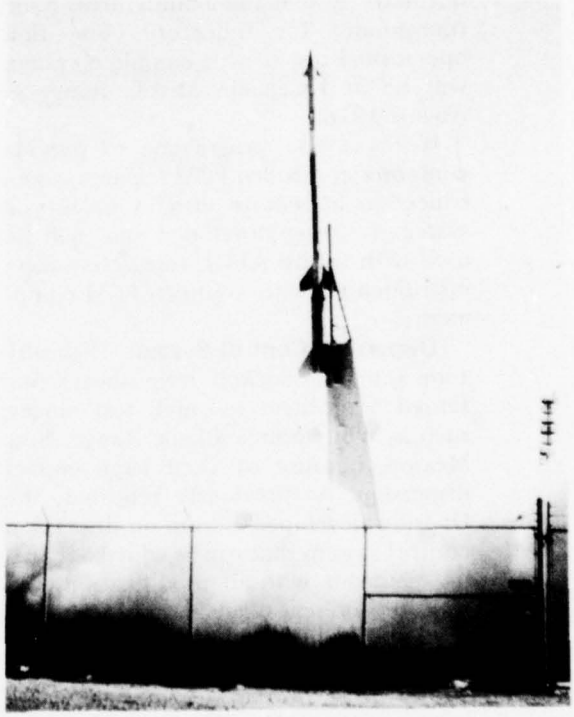

Dispersion control test flight leaving launcher at WSMR.

RESEARCH SATELLITES

In recent years, the Division has been responsible for technical management of research satellites and has designed and fabricated the spacecraft. One of these, the OV5-6, a small satellite designed to measure solar radiation, was flown piggyback on a Titan III in May 1969 and achieved an orbit of 10,000 by 60,000 nautical miles. All systems are still working in the satellite but early in 1976 data taking was curtailed after making comparison measurements on the recently launched SOLRAD II which has similar experiments of a more recent design. The OV5-6 performed well for a period four times its design life of 18 months and supplied much valuable scientific data to experimenters of the Space Physics Division.

Presently, the Division is providing technical assistance to AFGL scientists who are piggybacking experiments on satellites. The Division serves as a focal point for these programs and interfaces with the military program office and the spacecraft contractor. Division engineers conduct environmental and electronic tests to certify the experiments and coordinate integration and tests of the instruments at the satellite manufacturer's plant. Assistance is provided from experiment conception through data collection. During this report period, three research satellites were successfully launched. All 12 AFGL experiments on board the satellites were successful and much valuable data have been obtained.

JOURNAL ARTICLES JULY 1974 - JUNE 1976

NOLAN, G. F. (Contributing Author)
Manual of Remote Sensing,
Vol. 1, Theory, Instm., and Techniques, The Am. Soc. of Photogram. (1975)

PAPERS PRESENTED AT MEETINGS JULY 1974 - JUNE 1976

CORDELLA, R. H., JR., CAPT.
A Control and Telemetry System for a Balloon Borne Air Sampling Package
8th AFCRL Sci. Balloon Symp., Hyannis, Mass.
(30 September - 3 October 1974)

DOHERTY, F. X.
The USAF Geophysics Laboratory Balloon Program
19th Plenary Mtg. of Comm. on Space Res. (COSPAR), Univ. of Pa., Philadelphia, Pa. (8-19 June 1976)

DWYER, J. F.
Free Balloon Capabilities: A Critical Perspective
8th AFCRL Sci. Balloon Symp., Hyannis, Mass.
(30 September - 3 October 1974)

GILDENBERG, B. D.
Computer Techniques for Balloon Operations
8th AFCRL Sci. Balloon Symp., Hyannis, Mass.
(30 September - 3 October 1974)

KORN, A.
Unmanned Powered Balloons
8th AFCRL Sci. Balloon Symp., Hyannis, Mass.
(30 September - 3 October 1974)

LAPING, H, and GRIFFIN, A. R.
An Advanced Balloon Locating System
8th AFCRL Sci. Balloon Symp., Hyannis, Mass.
(30 September - 3 October 1974)

LE CLAIRE, R. C., 1ST LT., and SCHUMACHER, H. L., JR., 2ND LT.
Local Motions of a Payload Supported by a Nolaro Tri-tethered Balloon
8th AFCRL Sci. Balloon Symp., Hyannis, Mass.
(30 September - 3 October 1974)

MARCUCCI, M. G., CAPT.
Sphere Design for a Static Detonable Gas Experiment-GEST
8th AFCRL Sci. Balloon Symp., Hyannis, Mass.
(30 September - 3 October 1974)

TECHNICAL REPORTS
JULY 1974 - JUNE 1976

CARTEN, A. S. JR., Ed.
Proceedings, Eighth AFCRL Scientific Balloon Symposium, 30 September to 3 October 1974
AFCRL-TR-74-0393 (21 August 1974)
An Investigation of the Applicability of High Altitude, Lighter-Than-Air (LTA) Vehicles to the Tactical Communications Relay Problem
AFCRL-TR-74-0399 (20 August 1974)
Ed.,
Proceedings (Supplement), Eighth AFCRL Scientific Balloon Symposium, 30 September to 3 October 1974
AFCRL-TR-74-0596 (2 December 1974)

CORDELLA, R. H., JR., CAPT.
A Control and Telemetry System for a Balloon Borne Air Sampling Package
Proc., 8th AFCRL Sci. Balloon Symp., 30 Sept. to 3 Oct. 1974, AFCRL-TR-74-0393 (21 August 1974)

DWYER, J. F.
Free Balloon Capabilities: A Critical Perspective
Proc. (Suppl.), 8th AFCRL Sci. Balloon Symp., 30 Sept. to 3 Oct. 1974, A. S. Carten, Jr., Ed., AFCRL-TR-74-0596 (2 December 1974)

GILDENBERG, B. D.
Computer Techniques for Balloon Operations
Proc., 8th AFCRL Sci. Balloon Symp., 30 Sept. to 3 Oct. 1974, AFCRL-TR-74-0393 (21 August 1974)

JACKSON, D. E., CAPT., and RICE, C. B.
Motions of a Payload on a Tethered, Aerodynamic-Shape Balloon Using Various Cable Lengths
AFCRL-TR-75-0148 (17 March 1975)

KORN, A.
Unmanned Powered Balloons
Proc., 8th AFCRL Sci. Balloon Symp., 30 Sept. to 3 Oct. 1974, AFCRL-TR-74-0393 (21 August 1974)

LAPING, H., and GRIFFIN, A. R.
An Advanced Balloon Locating System
Proc., 8th AFCRL Sci. Balloon Symp., 30 Sept. to 3 Oct. 1974, AFCRL-TR-74-0393 (21 August 1974)

LE CLAIRE, R. C., 1ST LT., and SCHUMACHER, H. L. JR., 2ND LT.
Local Motions of a Payload Supported by a Nolaro Tri-tethered Balloon
Proc., 8th AFCRL Sci. Balloon Symp., 30 Sept. to 3 Oct. 1974, AFCRL-TR-74-0393 (21 August 1974)

MARCUCCI, M. G., CAPT.
Sphere Design for a Static Detonable Gas Experiment-GEST
Proc., 8th AFCRL Sci. Balloon Symp., 30 Sept. to 3 Oct. 1974, AFCRL-TR-74-0393 (21 August 1974)

MILLER, P. L., JR., CAPT.
A Method for the Calculation of Parachute Opening Forces for High Altitude Balloon Payloads
AFCRL-TR-75-0260 (7 May 1975)

PICKELL, J. R., CAPT.
Dispersion Control System for Sounding Rockets
AFGL-TR-76-0044 (4 March 1976)

STEEVES, R. G., MIRANDA, H. A., and DULCHINOS, J. (Epsilon Labs., Bedford, Mass.)
Celestial Aspect Sensor System
AFCRL-TR-75-0596 (20 November 1975)

WILTON, R. E.
Antenna Developments for Aerospace Research Vehicles
AFCRL-TR-75-0239 (30 April 1975)

IV SPACE PHYSICS DIVISION

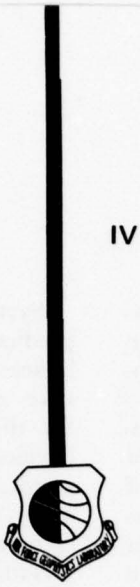

The technical program of the Space Physics Division is concerned with space environment effects on Air Force systems. Space affects operational systems because it is a dynamic environment with daily and seasonal variations and with naturally occurring disturbances. These variations and disturbances are caused by the sun. Therefore, the Division's program deals with the phenomenon of solar activity and how to predict it. It is concerned with the radio and particle emissions resulting from such activity and with the propagation of solar particles through the interplanetary medium to the vicinity of the earth. It deals with the interaction of such particles with the earth's magnetosphere, and with the particle fluxes and energies within the magnetosphere. It includes investigation of magnetic disturbances and storms and ionospheric irregularities resulting from particle precipitation and varying electron densities.

In accomplishing its programs, the Division observes and monitors the important parameters in near-earth space with instrumentation carried by satellites such as the Air Force small scientific satellites, the Navy SOLRAD HI, and on NASA satellites. Observations and measurements are made also from a dedicated, heavily instrumented KC-135 which functions as an airborne ionospheric observatory. The flying observatory is used in a program of ionospheric mapping and in the study of ionospheric disturbances both in the arctic and in the equatorial regions.

To complement the satellite-and aircraft-borne observations, the Division maintains a number of ground-based observational sites such as the solar radio observing site at Sagamore Hill, Massachusetts, the ionospheric observatory at Goose Bay, Labrador, its network of magnetic disturbance monitors across the northern United States and its solar research branch at the NSF-operated Sacramento Peak Observatory.

SOLAR RESEARCH

A complete understanding of naturally occurring disturbances in the magnetosphere and the ionosphere requires an understanding of the solar contribution to such disturbances. The Air Force is concerned with the degrading effects on its communication and surveillance systems which result from interaction of those systems with a dynamic space environment. However, the occurrence of the magnetic storms or proton showers which cause these disturbances cannot be predicted without a knowledge of the solar activity which causes them.

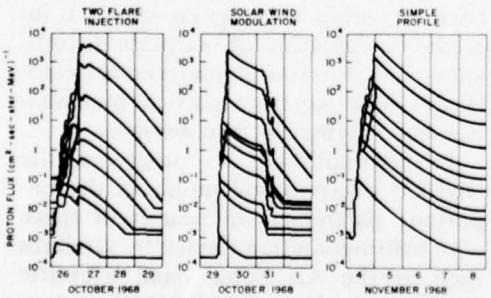

Examples of the predicted output for several energy channels showing the differences between the profiles generated for various flares. The profile on the right is a relatively simple time-intensity profile. The center figure illustrates the effects of solar wind modulation on predicted particle fluxes at the earth as indicated by the sudden decrease on all energy channels. The figure on the left illustrates the predicted flux from a two flare injection, separated by approximately 23 hours.

Systems operators need forecasts or predictions of the onset of these disturbances with adequate warning time to take appropriate action to compensate for the effects of the disturbances. To develop this capability, the Air Force has maintained a solar research program for more than 25 years. At the Air Force Geophysics Laboratory, this program has included studies of particle emission from the sun, of electromagnetic emissions such as X-radiation, ultraviolet, visible, and radio frequency radiation, and observation of physical changes on the surface of the sun.

That portion of the solar research program which deals with solar physics and with optical observations of phenomena related to solar activity such as sunspots and flares is conducted by the Solar Research Branch of the Space Physics Division. This branch is located at the Sacramento Peak Observatory in New Mexico. That facility, now owned and managed by the National Science Foundation, makes available to the Solar Research Branch all its excellent observing telescopes and other instruments as well as its computer.

The research program of the Solar Research Branch is concerned with the physics of the sun. To achieve its ultimate goal of being able to predict the solar activity which will result in the particle emissions of concern to the Air Force, it is necessary to investigate the underlying causes for the development of solar activity such as sunspots and flares. Such research involves not only observations of physical changes on the visible surface of the sun, but also involves a study of the basic physics of the sun. It is concerned with the transfer of energy, particularly from the body of the sun to the corona, with convection, with the morphology of sunspots, and with the magnetohydrodynamics of the sun. Coronal holes are presently being investigated. These are regions of low density in the solar corona

which were first discovered with X-ray detectors on Skylab. The appearance and location of coronal holes have been correlated with the occurrence of geomagnetic activity in the earth's magnetosphere. The Solar Research Branch has devised techniques for observing coronal holes from the ground, and is active in studying the relationship between coronal holes and geomagnetic activity.

Another responsibility of the Solar Research Branch is to support the Air Weather Service in its efforts to monitor and forecast the occurrence of geophysically significant solar flares. The Solar Optical Observing Network system (SOON) was developed at the Sacramento Peak Observatory by Air Force scientists for the Air Weather Service and is now being installed at several Air Force sites. The system consists of a sophisticated 10-inch evacuated telescope with associated filters, spectrograph and magnetograph for observations of solar emissions in the visible spectrum. The Solar Research Branch is working closely with Air Weather Service personnel to establish criteria for observing solar activity, to determine what observable phenomena can be utilized as precursors of solar flares, and to provide scientific and technical guidance as needed.

SOLAR PARTICLE PHENOMENA

During periods of high solar activity, a greatly enhanced charged particle population propagates from the sun through the interplanetary medium. The solar energetic particles emitted from the sun on interplanetary magnetic field lines leading from the sun to the vicinity of the earth will travel through the earth's magnetosphere and impinge on the polar ionosphere. Solar particle events have a deleterious effect not only on polar communication systems but also on satellite sensors that are irradiated by solar particle fluxes.

To understand and thus be able to minimize the effects of these solar particle influxes on Air Force systems, AFGL conducts modeling studies, an experimental program and theoretical investigations. The modeling studies range from numerical statistical descriptions of the available data to phenomenological models that incorporate physical processes to generate a predicted time/intensity profile of the particle fluxes. The *in situ* experimental program began with measurements of solar particles and has culminated in real-time monitoring of solar particle intensities. The theoretical investigations involve studies of particle acceleration mechanisms on the sun, in the interplanetary medium and in the vicinity of the earth.

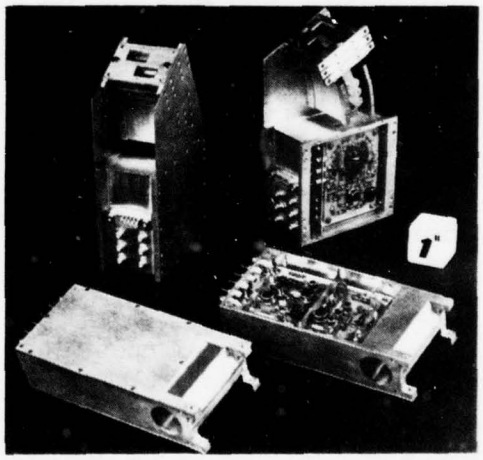

Spaceflight components of the Rapid Scan Particle Detectors. Electrostatic Analyzers (upper) will analyze medium energy particles, while solid state detectors (lower) will analyze high energy particles. A total of 12 sensors will be assembled in one package to make the Rapid Scan Particle Detector.

Modeling Studies: To delineate the solar parameters associated with geophysically significant solar particle events, a catalog was prepared using available satellite and ground-based data. Summaries of this extensive data compilation were included in the *Catalog of Solar Particle*

Events, 1955-1969. For each event, onset time, time of maximum intensity, magnitude and duration are listed together with a set of descriptive notes. In addition, the book contains data on solar optical, radio, and X-ray phenomena associated with particle events.

As part of the on-going development of prediction schemes for solar proton fluxes, a second generation solar particle event model was prepared for the Air Weather Service. This model can be used in conjunction with real-time solar optical and solar radio data available from the Solar Electromagnetic Observing Network, and X-ray and proton measurements available at the Space Environment Support Facility. The computer program predicts a time/intensity proton flux profile for as many as 15 different energy intervals. The program can be run in several modes including a prediction mode when only the solar flare position and electromagnetic emission characteristics (X-ray or radio output) are known, and an update mode that permits initial predictions to be updated when more definitive input parameters or real-time solar proton data have been acquired. The program can also handle several different solar proton events simultaneously. This is often necessary during solar active periods when the particle flux from a new solar proton event may be detected at the earth before the flux from a previous event has decayed. In addition to generating a predicted time/intensity flux profile for selected channels of particle data from the satellites being monitored, the program generates a predicted polar cap absorption profile for both daytime and nighttime conditions, allowing direct comparison with riometer data available from observing locations in the Arctic. The prediction program can utilize real-time solar wind data to better define the propagation conditions existing between the sun and the earth at the time of the solar proton event.

Special versions of this program prepared at AFGL on the CDC 6600 computer were designed to be directly compatible with the Air Force Global Weather Central Univac 1108 computer system and the Real Time Operating System. This program satisfies the Air Weather Service need for an improved solar proton prediction model to be used as a forecast aid for the AFGWC Space Environment Support Facility. In addition to being used by the Air Force, the National Oceanic and Atmospheric Administration Space Disturbance Laboratory is using a specialized version of this program in their forecast center. This program utilizes the X-ray data available to the NOAA Space Environment Support Center from the SMS/GEOS satellites with the proton energy intervals adjusted to match the energy channels from the Solar Proton Measuring Experiment on the SMS/GEOS satellites and the NOAA satellites.

Computer software to process and analyze electron and proton data from USAF synchronous orbit satellites has also been prepared to support the Air Weather Service. One computer program examines electron and proton data on receipt by AFGWC to determine if environmental anomalies or solar proton events have occurred. Another program processes the available data at scheduled intervals, senses when the particle radiation is being modulated by geomagnetic substorms near the satellite, and produces summaries of environmental conditions. The AWS Space Environment Support Facility supplies the output of these programs to its operational customers.

Completed calculations have determined a world grid of vertically incident proton cutoff rigidity values, so that charged particle access from space through the earth's magnetic field to the earth's atmosphere can be determined. Cutoff rigidity is defined as the lowest momentum to charge ratio which a par-

ticle can have and still arrive at a specific point on the earth's surface from a specified direction. In the vertical direction the cutoff rigidity has a value of 13 to 18 GV at the magnetic equator and is theoretically zero at the magnetic poles.

The general equation of particle motion in a magnetic field does not have a solution in closed form even in a simple dipole field. Detailed and extensive numerical calculations of cosmic-ray trajectories in a mathematical model of the earth's magnetic field are required to determine which rigidities are allowed

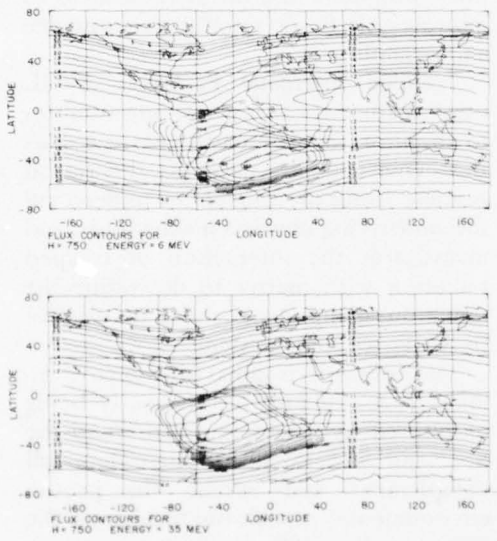

Proton flux distributions in the South Atlantic Anomaly for a height of 750 km. The number of protons at energies of 6 and 35 MeV are indicated. Also shown are the magnetic field shells, listed according to the altitude (in earth radii) at which the shell crosses the magnetic equator.

at a specific geographical location. For these calculations the International Geomagnetic Reference Field representation for a 1965 and a 1975 Epoch were used to evaluate the magnitude of secular changes. The resulting cutoff values are believed to be the most accurate available during quiescent conditions for low and mid latitudes. Comparisons with measurements from balloon-borne detectors show quite good agreement between these theoretical values and the experimentally derived values. While these results are standard for low and mid latitudes, they are not applicable to the polar regions since the magnetospheric effects are not included in the internal geomagnetic field model used.

Experimental Measurements and Results: Observations of solar particle fluxes outside the magnetosphere are made by using instrumentation on the SOLRAD 11 satellites. In a cooperative program between the Navy and the Air Force, the SOLRAD 11A and 11B satellites were successfully launched on March 15, 1976. These satellites were placed in a 20 earth radii circular-equatorial orbit, and then separated until they reached their final configuration of 180 degrees apart in July 1976. Each satellite carries an identical set of experiments to measure continuous electromagnetic, X-ray, ultraviolet, and particle emission from the sun; the solar wind; stellar and earth-aurora X-ray emission; and the visible and infrared emission of the earth's albedo. This pair of satellites can monitor solar electromagnetic and particle emission continuously in real time to furnish warnings of solar outbursts that will degrade the performance of ionospheric-dependent operational systems. In addition, the data obtained will provide an expanded data base from solar minimum to solar maximum that will be used to improve prediction techniques.

Space Physics Division personnel prepared and delivered instrumentation for the SOLRAD 11 satellites to monitor the solar particle fluxes. The proton-alpha telescope detects 1 to 100 MeV protons and 10 to 100 MeV alpha particles in eight energy ranges. The low energy proton spectrometer measures protons between 150 keV and 6 MeV in 12 energy ranges. The particle data provided by these instruments on the SOLRAD 11

satellites should fulfill the operational requirements for monitoring the near-earth solar particle environment.

With the launch of the SOLRAD 11 satellites, tracking of the extremely successful OV5-6 will be discontinued. The OV5-6 satellite has been providing data since 1969. In the past two years, data from the proton-alpha telescope on this satellite were used to establish an improved relationship between solar flare proton fluxes and riometer absorption. Separate calculations were made for the day and night coefficients and the results were shown to be consistent with observations. These relationships were incorporated in the proton prediction model provided to the Air Weather Service as described previously.

These same data have also added to our knowledge of the processes of solar production, storage and interplanetary propagation. A comparison of the results of Lanzerotti and MacLennan obtained during solar maximum (1967-1969) with the OV5-6 results obtained during the declining phase of the solar cycle (1969-1972) showed similar values for the relative alpha particle/proton abundance.

A separate analysis of OV5-6 and S72-1 solar protons events was also made. The energy to be expected from temporary storage near the sun was compared with that from interplanetary diffusion processes. The observed results clearly favor storage in the vicinity of the sun.

Theoretical Studies: A recent puzzle of solar physics was the observation of an enhancement of helium-3 isotopes over deuterium. According to the current theory approximately equal numbers should be produced. A detailed Monte-Carlo calculation utilizing the latest cross-section measurements showed that protons mirroring just below the solar atmosphere will produce excess helium-3 along the field line emanating from the solar surface.

MAGNETOSPHERIC PHENOMENA

The earth's magnetic field traps charged particles to form the inner and outer Van Allen radiation belts. These high-intensity particle flux zones pose severe radiation hazards to both operational systems and man. The solar wind and the interplanetary magnetic field impinge on the earth's magnetic field to produce magnetic storms and substorms. Intense electric currents flowing in the ionosphere and changes in charged particle densities in the ionosphere disrupt satellite communications. AFGL conducts programs in both of these areas to improve Air Force satellite performance and reliability.

Trapped Energetic Particles: AFGL uses instruments on low-altitude satellites to monitor the near-earth energetic particle environment, develops theoretical particle transport models to understand the underlying physical mechanisms, and investigates the interaction of trapped radiation with matter to determine the radiation components most destructive to Air Force space systems.

The energetic trapped proton environment (0.1-100 MeV) is presently being monitored by instruments on board the S3-2 and S3-3 satellites. These data will complement and extend the proton environmental models obtained from the S72-1 satellite. They will also be correlated with measurements by identical instruments on board SOLRAD 11 to determine how particles enter the trapped regions. The particle identifier instrument on Air Force satellite S72-1 detected alpha particles at 750 km altitude, in the earth's radiation belt. The peak in the 18 to 70 MeV per nucleon trapped alpha particle flux was located at a level in the magnetosphere where the field lines cross the magnetic equator at 1.8-2. 8 radii, as opposed to a level of 1.4 earth radii for the field lines where the peak high energy proton flux is found. The reason for this

difference in location is not fully understood although the alpha particles are probably of solar origin while the high energy protons probably come from

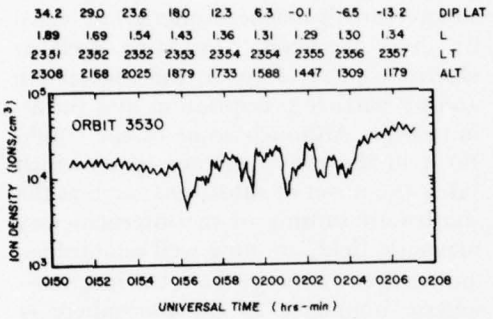

The ion density measured on a typical pass over the magnetic equator by the ISIS-1 satellite, showing the lack of symmetry of an irregularity that crosses the magnetic equator.

cosmic ray stars as neutrons, decaying into protons in the earth's magnetosphere. The number of trapped alpha particles decreases as the fifth power of the energy increases, becoming almost undetectable in the 47-70 MeV per nucleon energy interval. This measurement demonstrated that sources of high energy trapped particles other than cosmic ray albedo neutron decay must exist. Other processes must be included in any final theory of the earth's radiation belt.

Recent dosage calculations have shown that the 2-10 MeV trapped electron flux has a decisive impact on the lifetime of space systems. Because the Air Force will need to know more about this radiation, improved instrumentation is being developed. It will include a magnetic spectrometer using solid-state detectors which will give position as well as energy of the particles.

An AFGL emulsion package carried on the Apollo-Soyuz space mission measured the intensity of trapped protons in the South Atlantic Anomaly. Maps of the trapped proton fluxes in that portion of the earth's inner trapped radiation belt known as the South Atlantic Anomaly are required to determine how much radiation Air Force satellite systems such as DMSP will have to withstand when they fly through this region. Discovery of the physical mechanism responsible for incident trapped proton radiation damage in a thin sensitive layer was made by examining the light flash data reported on Skylab 4.

The Skylab 4 astronauts reported observing intense bursts of light flash activity during the 5 to 10 minutes when their spacecraft passed through the South Atlantic Anomaly. Members of the Space Physics Division showed that the nuclear interactions that produce star patterns in emulsions, occurring in and near the retina of the observer, would cause flashes at a rate consistent with the accepted flux values for the South Atlantic Anomaly and laboratory data on particle-induced visual sensations in humans. Because the retina is analogous to a sensitive thin-film layer, nuclear interactions are expected to be an important cause of radiation degradation of electronic circuits in the South Atlantic Anomaly.

J/3 DMSP Instrument: The Space Physics Division has designed, built, and calibrated an electron spectrometer designated J/3 for SAMSO which is to be flown aboard the Defense Meteorological Satellite Program (DMSP) satellites. This spectrometer consists of two electrostatic analyzers, and will measure the spectrum of precipitating electrons from 50 eV to 20 keV. The DMSP low altitude (200 km) polar orbiting satellite passes through the precipitating electrons that are responsible for the aurora. The data from the J/3 instrument will determine the location of the boundaries of the auroral oval and will be used to correlate electron fluxes with auroral observations.

During the design and construction of the instrument, a computer program was written to trace the particle orbits from the entrance slits to the detectors in an

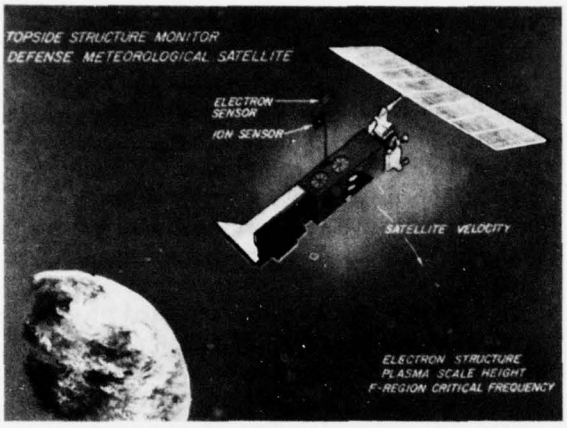

The DMSP Satellite with the sensors installed.

effort to define the instrumental response and detection efficiencies as accurately as possible. Final calibration of the instrument was performed using an electron test source. Comparison of the theoretical design response of the instrument with the actual electron source measurements indicates that this spectrometer has a better calibration accuracy than has been previously available. These electron spectral measurements will be utilized by the Space Physics Division for correlative studies of electron precipitation with substorm phenomena at synchronous altitudes along the same magnetic field line, and also by the Air Weather Service in predicting the total electron content of the ionosphere.

Further research on the precipitating electron fluxes will be undertaken by flying a modified J/3 package on board the forthcoming P78-1 satellite. The goal of this experiment is to measure the pitch angle distribution of precipitating auroral particles. These data are necessary to understand the acceleration of precipitating particles along the magnetic field lines.

Magnetospheric-Ionospheric Coupling: Magnetic substorms at high latitudes, long associated with communications and surveillance disruptions, are usually accompanied by a marked increase in auroral activity and intense ionospheric currents (the auroral electrojet) which can be on the order of a million amperes. The energy source for these magnetic disturbances originates in the sun, and is transported to the earth's magnetospheric boundary by the solar wind, dissipating itself as electric current flow in the ionosphere and by particle precipitation into the atmosphere. Although some of the conditions in the interplanetary space which favor the onset of substorms, such as the southward turning of the interplanetary magnetic field, are now well established, the transfer of energy from the magnetospheric boundary to the ionosphere is still not fully understood. Because there is not sufficient energy of convective motion in the polar ionosphere itself to produce such current intensity, the substorm current system is now considered to be driven by a potential deep in the tail of the magnetosphere which is transferred to the auroral oval ionosphere by the highly conducting paths along the lines of force of the geomagnetic field. Thus, these magnetic-field-aligned currents represent an effective coupling mechanism between the inner and outer magnetosphere. However, the coupling parameter responsible for triggering the substorm disturbance is still not known. In this three-dimensional current model, downward and upward field-aligned currents (line or sheet currents) are connected across the auroral oval ionosphere by the electrojet. Line currents to the east and west of the electrojet imply its being a Pedersen current, while sheet currents to the north and south of the auroral band would be consistent with the electrojet as a Hall current.

A composite experiment measuring magnetic and electric field variations and particle fluxes associated with magnetic disturbances was carried on Air Force satellite S3-2. The satellite has an altitude range from 240 to 1500 km and has an orbital period of 102 minutes. The

electric field experiment is discussed elsewhere in this report. Electron fluxes are measured in 32 discrete energy channels from 80 eV to 17 keV with a planar parallel plate electrostatic analyzer (ESA). This range includes electrons responsible for the aurora as well as those considered to be the current carriers feeding the electrojet. The axis of the instrument is perpendicular to the vehicle spin axis. Since the spin axis is normal to the orbital plane, the ESA samples electrons while scanning through all possible pitch angles once every 20 seconds. Also, the field-aligned currents are detected indirectly by measuring the magnetic field that they create. This is normal to the much larger ambient geomagnetic field in the sub-polar region, and an accurate vector measurement is required for its definition. To accomplish this, a triaxial fluxgate magnetometer is used in conjunction with an automatic ranging current source. This latter incrementally biases out the major portion of the background magnetic field in 128 discrete steps for each axis, thus allowing measurements of high resolution without limiting dynamic range. The sensor of the magnetometer is mounted on a boom which extends 20 feet out from the spacecraft. In this way spurious magnetic fields from the satellite are reduced to a tolerable level, less than 10 gammas, and a fixed relationship is maintained between sensor and spacecraft coordinates.

Since the satellite was launched, there have been four major magnetic storms (i. e. Kp $>$ 7), and a number of other active periods. In February and March 1976, when the spacecraft location was favorable, coordinated measurements were made with the Chatanika Radar facility. This will allow for a direct comparison of *in situ* measurements with such ionospheric parameters as electron density, current intensity, and electric field which are inferred from radar echoes at the ground station. Correlation of DMSP photos of the position and intensity of auroral arcs with electron precipitation and current systems in the auroral oval regions is presently being studied. Satellite data acquired over the northern auroral zone during storms and intense substorms will be used to evaluate the index of activity values developed from the AFGL Magnetometer Network data. In addition, data have been acquired during the special periods of the International Magnetospheric Study of 1976, particularly when two or more deep space probes are in interesting regions simultaneously, e.g., crossing the magnetopause boundary or passing through the neutral sheet of the magnetospheric tail.

Preliminary analyses have been made for several magnetically active periods. Electron spectra and magnetic field component variations have been compared. Discontinuities in the east-west magnetic field component have been observed as high as 1150 gammas during extremely disturbed periods (K_p = 7+), indicating field aligned current densities on the order of 8×10^{-6} amperes per square meter at the most intense intervals. Integrated over one degree of latitude and an assumed 1000 km in east-west linear extent, this intensity equals a current of nearly a million amperes. This upward flowing current occurred at the poleward edge of the Northern Hemisphere auroral oval at approximately 2000 magnetic local time (MLT), and was accompanied by intense fluxes of 2 to 11 keV precipitating electrons. The peak of the electron spectra shifted from 5-6 keV to 9-10 keV in the middle of this upward current region. These spectra are typical of those associated with the production of aurora during substorms. In general, the field aligned currents move equatorward with increasing magnetic activity (higher values of K_p), consistent with

the motion of the boundaries of the auroral oval.

AEROSPACE MAGNETIC MONITORING

The ability to specify magnetic activity levels in real time and to predict such activity hours in advance is urgently needed to support various Air Force agencies including AFSATCOM, SAC, NORAD and AFGWC. Other users would include SAMSO, ARPA and the various groups engaged in fuel and mineral surveys. A program for specification and prediction requires a system for the collection of magnetic activity data, its transmission to a central station and the means for near real-time operation on the data. This is being done by the AFGL magnetic monitoring network.

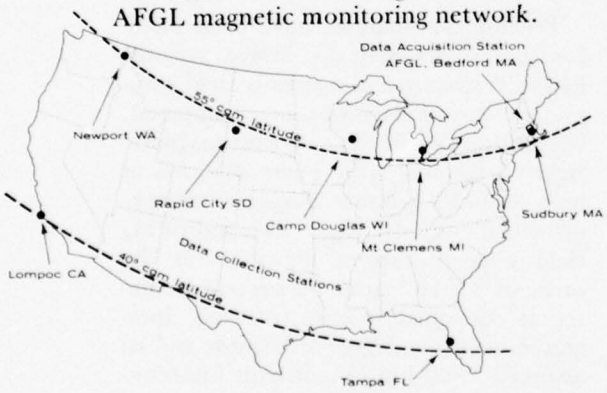

Geographical locations of the stations in the AFGL Magnetometer Network.

AFGL's network of magnetometer stations which extends across the continental United States monitors the earth's magnetic field continuously. Each instrumented data collection station (DCS) operates continuously and automatically, unattended except for routine maintenance. Data from each station are returned in real time on commercial voice-grade communication circuits to a single data acquisition station (DAS) located at Hanscom AFB, Massachusetts. The DAS processes, reduces, and displays the data in real time, and stores processed data in a permanent file for subsequent analysis. All the facilities are dedicated to the program, so essentially uninterrupted operation over an extended time period is possible.

The magnetometer network has several important features. The order of the stations and the rapid sampling rate allow measurement of the strength, direction and rate of change of both strength and direction of the earth's magnetic field. Identical instruments in each station produce directly comparable data. The ability of the stations to operate without interruption for several years allows continuous monitoring of the magnetic field. The automatic real-time processing, storage, reduction, and display of the combined data will allow operational units to make use of the information. Finally, the network can be expanded or operated in conjunction with networks established by other organizations.

The first five stations instrumented for the program are spaced across the northern United States at about 55 degrees N corrected geomagnetic latitude. Two subsequent stations will span the southern United States at about 40 degrees N corrected geomagnetic latitude. The principal instruments at each DCS are triaxial fluxgate and searchcoil magnetometers. The sites are provided with electrical power, a voice-grade communications line for data transmission, and telephone service.

The data-conditioning circuitry at each DCS accepts instrument data and converts them to a signal which can be transmitted by the data communications link (DCL). This process includes sampling of output data, converting to digital form, ordering into a standard frame format, coding for error-rate improvement, and outputting as a serial bit stream. A microprocessor with a stored program controls all of these functions.

Data from each DCS are collected during a ten-second sampling interval and sent as a data frame during a subsequent one-second transmission interval assigned to that DCS. The fluxgate magnetometer is sampled once per second and the searchcoil magnetometer is sampled every 0.2 second.

The DAS has two principal functions: network control and data processing. Network control is accomplished through the generation of a network-control signal which is transmitted continuously on the outlink of the DCL. The line allows simultaneous transmission in both directions, an outlink and an inlink. The inlink is used for data return, time-shared by all of the DCS's, each of which transmits a frame of digitized data in a programmed sequence. The outlink is used to carry the same network-control signal to all of the DCS's. Each DCS responds according to instructions contained in the signal, which synchronizes the taking of data samples by the scientific instruments and the transmission of these data at the proper time. Data processing includes: 1) reception and recording of data for permanent file, 2) making real-time and daily presentations, and 3) handling data for retrospective studies.

Signals produced by the AFGL magnetometer network, three components of the vector magnetic field and its time rate of change at five observing stations, will be regularly subjected to many forms of analysis.

To accomplish this analysis many of the required computer programs were written during the reporting period 1974-1976. The programs prepared were: routine processing of network data; Kp and A_p absolute and conditional probabilities program; and a program to find the frequency distribution of 45 years of K_p and A_p data and find conditional probabilities of A_p (K_p) tomorrow (or up to seven days in the future) given A_p (K_p) today.

Superposed epoch software, to obtain probabilities of given magnetic activity following a certain "key" day such as the day of passage of an interplanetary sector boundary; the Complete Maximum Entropy Program, which finds the power spectrum given a set of data equally spaced in an independent variable (usually time); a non-linear maximum entropy power spectrum package, and the dimensional representation of dynamic power spectra showing power spectra as a function of time were also prepared.

ELECTRICAL PROCESSES RESEARCH

The low energy environmental plasma and electric fields in the ionosphere-plasmasphere-magnetosphere system are important to Air Force satellite systems in three ways. First, small and large-scale variations of ionospheric electron densities degrade electromagnetic propagation at all frequencies. Second, the interaction of the plasma with a satellite modulates the vehicle charge which can cause malfunction of special sensors. Finally, electric fields, especially at high latitudes, produce plasma motions which perturb the ambient plasma flow and contribute to the production of neutral winds.

The research effort includes studies of the low energy plasma in the 0 to 200 eV range and of ionospheric electric fields. Rockets and satellites are used to carry experiments to regions of interest.

Main Plasma Trough: The main ionosphere electron density trough is the region where thermal plasma density depletions are consistently observed at mid latitudes in the night-side ionosphere. It marks the boundary between latitude regions of the ionosphere caused by different primary sources. Little known fea-

tures of the main trough, derived from data taken during more than three years from sensors on ISIS-I and INJUN V, have been studied. The dayside trough was examined and the width, depth, equatorial gradient and poleward gradient were determined as a function of local time and season, for planetary indexes of 3 or less.

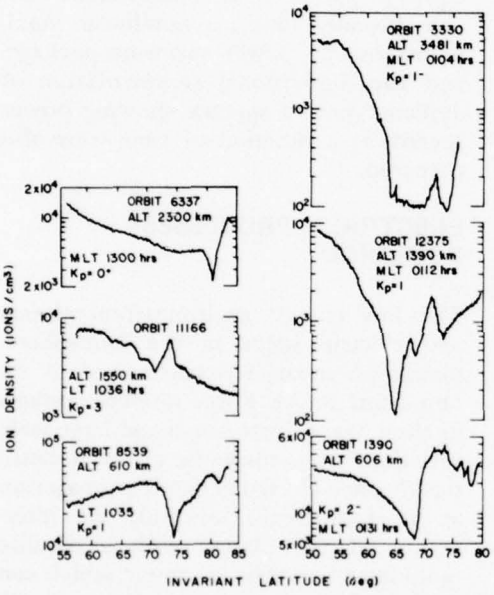

Examples of daytime and nighttime troughs. The deepening of the trough at night, and the change in latitude with magnetic activity, are evident.

The trough is not just a nighttime phenomenon, but exists at all local times. It is consistently found at the equatorial edge of the particle precipitation zone, but cannot be viewed simply as the demarcation between two regions formed from different primary ionization sources. The width, amplitude, and gradient at both the equatorward and poleward walls vary significantly with local time and season. Maximum values are observed on winter nights. Solar radiation is a major contributor to the trough structure at all local times and seasons, except winter nights.

Low Latitude Ionospheric Irregularities: Data from the spherical electrostatic analyzer on the polar orbiting ISIS-I satellite have been used to investigate thermal charged particle irregularities at low latitudes. ISIS-I was launched into a polar orbit with an apogee of 3526 km, a perigee of 525 km and an inclination of 88.5 degrees on January 30, 1969. Data from more than 3000 orbits in the topside ionosphere during the first year of operation have been examined over the latitude range -45 degrees to +45 degrees.

The data from ISIS-I show that 70 percent of equatorial irregularities occur at altitudes below 1200 km. Less than 20 percent actually cross the dip equator. In both Northern and Southern Hemispheres, irregularities occur most often at 10-12 degrees dip latitude, and between 0 and 20 degrees in width. A power spectral analysis has shown that the power decreases approximately with the square of the frequency. No systematic variation in this relationship is found inside or outside the irregularity region. The outer scale size increases consistently inside the irregularity region, typically between 30 and 60 percent. The integrated spectral power over the scale size range 1 to 10 km is highly variable in the irregularity region, and is usually greater than in the surrounding regions. These results in the topside ionosphere are qualitatively in good agreement with observations from ground-based measurements of equatorial scintillations near the peak of the F region and with observations of equatorial irregularities using data from the OGO-6 satellite. The latitude, longitude, and local time dependencies are similar in all observations. From ISIS-I data it is now seen that these irregularities can extend beyond 2000 km in altitude. Irregularities occur most often along the magnetic field lines which cross the magnetic equator at a height of 1.2 earth radii. No irregularities occur on

magnetic lines with heights greater than 1.6 earth radii at the magnetic equator. There is no indication of equatorial symmetry for these irregularities. Where simultaneous data exist for both hemispheres, there is no conjugate mapping along field lines.

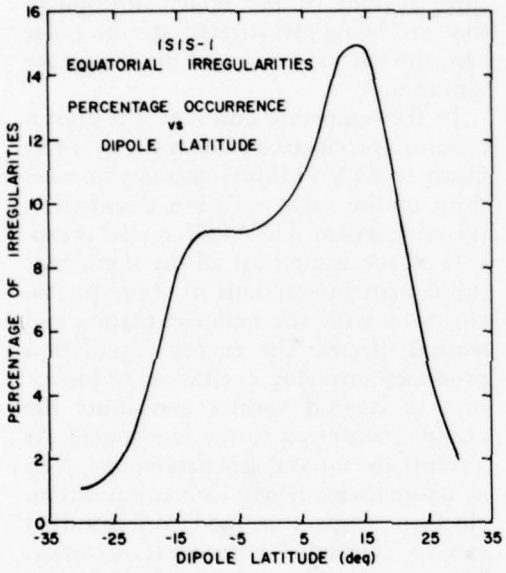

Percentage of irregularities plotted against magnetic latitude, showing the differences between the Northern and Southern Hemisphere averages.

The thin screen approximation can no longer be considered adequate to interpret equatorial scintillations from these irregularities. The observations of this study indicate that their extent is so large that multiple scattering theory must be used.

Inverted V Precipitation Events: The ion and electron densities observed by the AFGL-designed spherical Langmuir probes aboard the polar orbiting Injun 5 satellite have been used to investigate the nighttime ionosphere at altitudes between 2000 and 2500 km in the polar cap, auroral zone and plasma trough. While the satellite is in darkness it is possible to measure the temperature and density of the tenuous polar cap plasma. Between 100 and 300 electrons per cubic centimeter at electron temperatures between 1700 and 2500 K were observed at these altitudes with the higher values appearing during magnetically disturbed periods. A flux of hyperthermal electrons observed in this region has been identified with the plasma observed by the Apollo subsatellites in the high latitude lobes of the geomagnetic tail at lunar distance. Auroral zone Langmuir probe observations have been compared with simultaneous measurements by the University of Iowa LEPEDEA (Low Energy Proton/Electron Differential Energy Analyzer). New observations during this investigation include the observation of proton fluxes in inverted V structures, observation of ambient plasma density enhancements near inverted V structures, and vehicle potential modulation of as much as 40 volts negative as the satellite passed through inverted V precipitation. Inverted V's are narrow regions within the auroral zone where abrupt increases in precipitating electron energies and intensities are observed. The first observation suggests that inverted V's result from field aligned plasma flow rather than simple electrostatic acceleration. At this time it is not possible to determine whether density enhancements associated with inverted V's result from field aligned return currents or from changes of local scale heights due to ionospheric heating by precipitating electrons. The observations of vehicle potential modulation provide a unique set of measurements for the verification of spacecraft charging models. A further result of this study was the development of a magnetospheric model following the suggestion that the distant plasma sheet is bound by a slow mode wave emanating from the merging region, rather than by magnetic field lines. It was shown that many properties of inverted V structures result quite naturally if the earthward flow of plasma is

obstructed by magnetic bottles in the neutral sheet. Equatorward of the auroral zone, the low density plasma of the trough was found to be several times hotter than in the immediate vicinity. It was shown that photoelectrons from the sunlit conjugate ionosphere provide a heating mechanism adequate to explain the temperature enhancements in the trough.

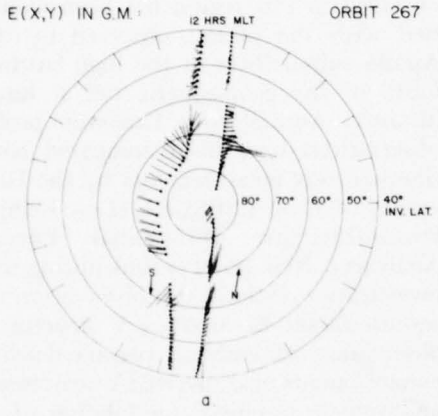

a

Above, a polar plot of the electric field, measured by the satellite on successive polar passes over the North (on the right) and the South (on the left) Poles. The satellite position is shown as a dot. A line is drawn from each dot in the direction of the electric field, with its length proportional to the field strength. The circles show constant invariant latitude. The satellite track is not a straight line because the magnetic pole is displaced from the geographic pole. Magnetic local time advances counterclockwise from midday, at the top. The map below was generated from this plot, by computing the convective drift velocity from the electric field and a knowledge of the earth's magnetic field.

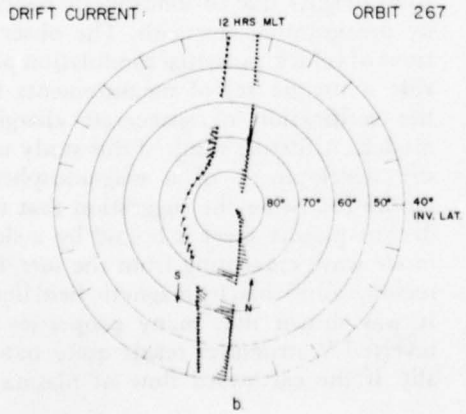

b

Electron Transport-Topside Ionosphere: An analytical model has been constructed to account for the electron transport in the topside ionosphere. The three regions of the upper atmosphere that are being investigated are the polar cap, the auroral zone, and the temperate latitudes.

In the temperate latitudes, the photoelectrons produced by soft X-rays (~14A) down to EUV (1100A) account for one-third of the solar radiation absorbed in the atmosphere. The AFGL model is capable of accounting for all the significant subsequent interactions of those photoelectrons with the ambient plasma and *neutral* species. The energy degradation processes involving excitation or ionization of neutral species contribute the energy transferred to the ionosphere. As a result the ionospheric parameters, such as plasma scale height, ion composition, electron temperature and concentration can be calculated with great accuracy. The model is also capable of calculating the transport of photoelectrons from the sunlit side to the magnetically conjugate dark side ionosphere.

Ionospheric Plasma Monitor: The development of a topside ionospheric plasma monitor for the Defense Meteorological Satellite Program (DMSP) Office at the Space and Missile Systems Organization and the Air Weather Service is underway. The instrument will be flown on three Block 5D DMSP satellites to make *in-situ* measurements of topside plasma scale height, small-scale ionization irregularities and F-region critical frequencies.

Considerable progress has been made on flight instrument development testing and calibration. The first flight unit is complete with 1000 hours of thermal life testing. It will be flown on a satellite

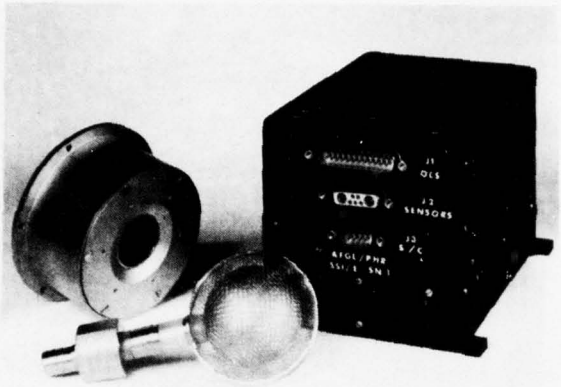

The sensor and electronics package for the DMSP Topside Ionospheric Plasma Monitor.

to be launched in the fourth quarter of calendar year 1976. Computer programs are being developed at AFGL to process flight data on the Global Weather Central UNIVAC 1110 computer. This has necessitated the development of UNIVAC simulation programs on the AFGL CDC 6600 computer. Software routines are also being prepared for the calculation of electron and ion density and temperature, average ion mass and satellite potential from the sensor output. Mapping the plasma density, temperature and average ion mass on a global scale at constant height in the topside ionosphere will provide important data for the study of the dynamics of the upper atmosphere.

The plasma scale height results will be utilized directly as inputs to AWS ionospheric prediction programs. The irregularity measurements can identify the mid-latitude electron trough which will be used to determine whether low-, mid- or high-latitude prediction programs should be used to provide propagation conditions to operating commands. The satellite data from these instruments will extend the capability of the Air Force to provide global information on several ionospheric parameters of importance to communications, surveillance, and detection systems.

SCATHA – Thermal Plasma Analyzer: The Spacecraft Charging Satellite Thermal Plasma Analyzer now under development will measure the direction and magnitude of the plasma bulk motion, the density and temperature of the plasma "bath," in which the satellite is immersed and investigate spacecraft-plasma interaction mechanisms by measuring fluctuations in vehicle potential and charging and discharge currents to the satellite due to environmental factors such as solar illumination, satellite motion, plasma temperature, density and motion variations during quiet and disturbed conditions. It will also study these properties under controlled conditions when the spacecraft potential is varied by means of an electron emitter. These constitute some of the prime measurements required to understand and solve the problem of spacecraft charging at high altitudes.

The Thermal Plasma Analyzer consists of three gridded sensors. Two sensors are

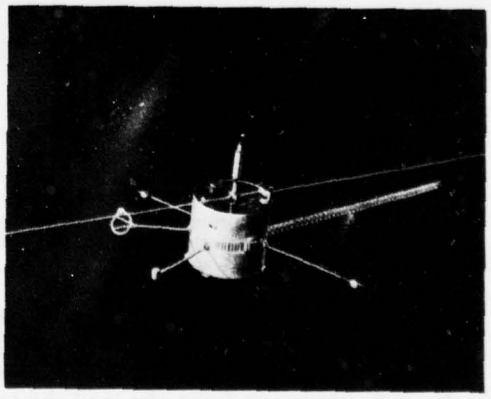

The SCATHA satellite will be a fully instrumented research satellite to investigate the scientific and engineering aspects of spacecraft charging and relate cause and effect in spacecraft charging.

mounted on a space-vehicle-provided boom 3 meters from the nearest space vehicle body-mounted components. The other sensor is body mounted on a conducting surface (the conducting end of the space vehicle). One boom and the surface mounted sensors are parallel to each other and parallel to the space vehicle spin axis. A second boom sensor is perpendicular to the spin axis. The experiment will measure, by retarding potential analysis, the environmental electron and ion densities in the range one particle per 10 cubic centimeters to 10,000 particles per cubic centimeter, and particle energies in the range 0.1 to 100 eV.

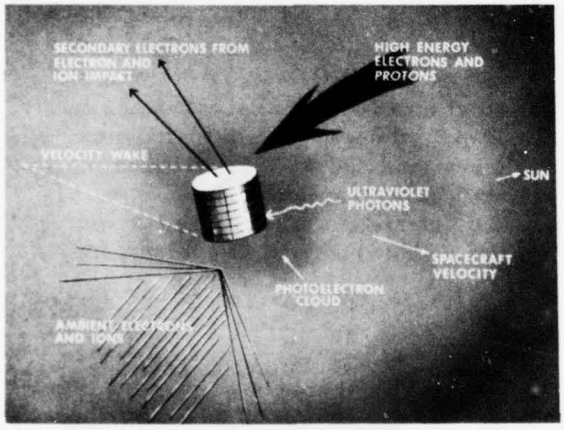

Factors influencing spacecraft charging: Approximately in the order of decreasing importance at synchronous orbit are high energy electrons and ions, ambient electrons and ions, photoelectrons produced by sunlight, secondary electrons from electron and ion impact, and wake effects due to the spacecraft motion through the medium.

A conical wall is mounted in front of the aperture of the SCATHA thermal plasma sensor. The conical wall shades the collecting area from the sunlight to minimize the photoelectron emission from the instrument. Because of the walls shading the probe an analysis of current characteristics was necessary to calibrate

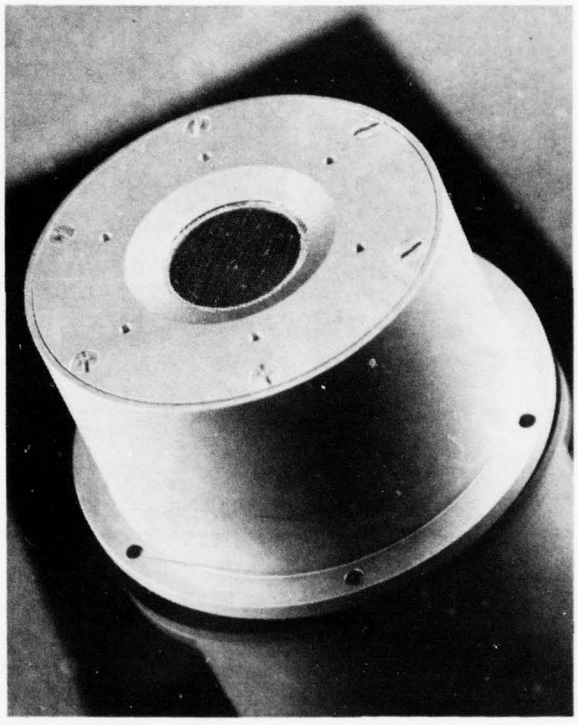

A gridded probe similar to those that will analyze the low energy plasma at synchronous orbit as part of the Thermal Plasma Analyzer.

the probe and aid in subsequent interpretation of the current characteristics. A theoretical calculation of the current flow to the grid in the presence of the shading walls has been completed and the appropriate shielding factors, involving the length of the walls, their tilt with respect to the normal to the collector surface and the collector radius have been found and analyzed.

Electric Field Rocket Studies: Dipole electric field and plasma measurements were made aboard two rocket flights from Fort Churchill, Canada, as part of Project AEOLUS. This mission, consisting of rocket and ground-based measurements, was to investigate effects produced

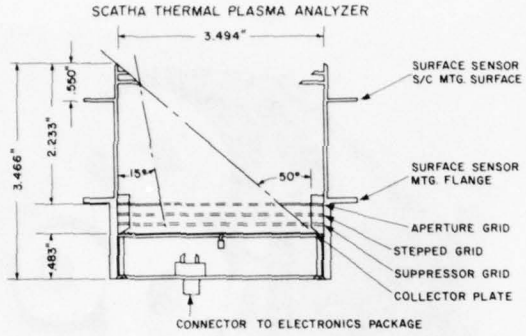

A sketch of the surface and boom mounted instruments for the SCATHA Thermal Plasma Analyzer.

in the ionospheric E-region by auroral disturbances. In addition to the ambient electric fields, neutral and ion composition, neutral winds, neutral density and temperature, and ground-based magnetic fields were measured.

The magnetic field measurements were used to give the approximate position and current density of the auroral electrojet. The rocket measurements were then assessed, and compared to flights performed (as part of the series) in the absence of the electrojet, to determine electrojet effects on ion layering, plasma and neutral motion and associated electric fields.

The large southerly component measured at 115 km on the ascent (30 to 40 mV/m) indicates an easterly convective drift velocity which, at E-region altitudes, corresponds to an East-to-West current flow in the vicinity of the vehicle. The gradual rise and fall of the easterly component, peaking at 35 mV/m at apogee together with the dip to -27 mV/m in the northerly component indicate a constant large-scale field above 180 km of some 50 mV/m directed southeasterly. This agrees in magnitude and direction with a barium release performed from another rocket. These results provide new understanding of E- and F-region current flow at high latitudes.

Electric Field Satellite Studies: A dipole electric field instrument was flown aboard an Air Force polar orbiting satellite launched in 1975. This instrument made the first three-axis measurement of electric fields on a satellite and also was the first attempt to deploy 60-foot long flexible booms to support two of the measurement dipoles, the third axis being on 18-foot long rigid booms deployed parallel to the vehicle spin axis. Two hundred orbits of data have been acquired. Emphasis has been placed on analyzing data at high latitudes and correlating them with other experiments on the spacecraft measuring bulk plasma flow, plasma density and temperature, energetic particles, magnetic field and ion composition.

Incoherent backscatter radar measurements from Chatanika, Arecibo, Jicamarca, and Millstone Hill have been scheduled in conjunction with satellite passes. Battelle Institute also performed Stable Auroral Red (SAR) arc observations in coordination. The measurements were used to build up maps of electric field as a function of time and invariant latitude. From the first maps and a knowledge of the earth's magnetic field, a second set of maps, showing the convective drift velocity, has been built up. The maps show a general anti-sunward drift poleward of the auroral zone in the evening sector and a somewhat indeterminate drift on the morning side of the polar cap. There is a definite reversal of the flow at the equatorward edge of the auroral zone (70 degrees latitude) in the midnight region, but no clear change on the day side.

Such maps, when built up for other local times and classified with varying magnetic activity and altitude range, will give important new insights into plasma circulation in the auroral regions and polar cap in the magnetosphere, and circulating currents in the ionosphere.

Plasma Bulk Motion: Instruments have been designed and constructed for the direct measurement of the bulk or drift motion of thermal energy plasma at ionospheric and exospheric altitudes by polar orbiting Air Force satellites. They are based on improved versions of the ion attitude sensors flown on the Gemini X and XII manned spacecraft. The new instrumentation consisting of an array of planar ion sensors utilizes the spin of the spacecraft to determine the direction of plasma flow relative to the spacecraft. At high latitudes, and about 45 degrees geographic, the bulk motion gives a direct measure of the energy transfer into and out of the ionosphere as well as of the injection or removal of ionization in the auroral and polar regions. These two phenomena cause irregularities, small-scale variation and gradients observed at high latitudes. The effect is to severely degrade the propagation of radio and radar signals over the horizon. The irregularities and gradients reflect or deviate HF electromagnetic ray paths. These measurements will also contribute to the understanding of the formation and maintenance of the auroral and polar ionosphere.

The first of the plasma flow instruments was launched December 1975 into a polar orbit and is working successfully indicating horizontal and vertical plasma flows up to several km/second. The ion sensor array incorporates a new ion sensor design with a greatly reduced sensitivity to sunlight enabling measurements to be made down to plasma densities of approximately 100 particles per cubic centimeter.

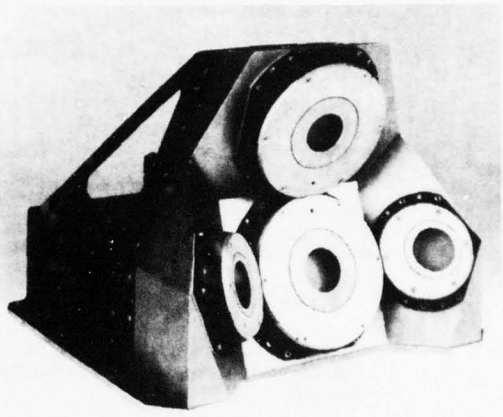

The Bulk Plasma Flow sensor.

IONOSPHERIC DYNAMICS

Two regions of the global ionosphere routinely exhibit a disturbed character: the high latitude ionosphere, poleward of approximately 55 degrees corrected geomagnetic latitude and the equatorial ionosphere, equatorward of approximately 20 degrees geomagnetic latitude.

These regions are characterized by the routine occurrence of ionospheric irregularities, strong horizontal electron density gradients, and rapid changes in the horizontal and vertical electron density distributions. These phenomena arise from a variety of sources, such as ionospheric currents, ionospheric and magnetospheric electric fields, neutral air motion and energetic particle precipitation high latitudes.

The disturbed ionospheric regions affect radio wave propagation over a large part of the radio frequency (rf) spectrum, from Very Low Frequencies (3 to 30 kHz) to Super High Frequencies (3 to 30 GHz). Many Department of Defense communications and surveillance systems operate in or through these disturbed regions.

The Space Physics Division uses a unique tool in the investigation of the disturbed ionosphere and its impact on Air Force systems: an NKC-135 jet aircraft, the Airborne Ionospheric Laboratory, instrumented for auroral and ionospheric research. The instrumentation

consists of sophisticated ionospheric sounders, receivers, covering a large part of the radio wave spectrum, photometers, spectrometers, all-sky cameras and a new all-sky photometer. This combination of experiments is the basis for many studies that describe in detail the environment and the environmental effects on Air Force systems.

The optical response of the atmosphere to the particle precipitation at high latitudes is the aurora. The understanding of the coupling of ionospheric, magnetospheric and auroral phenomena has progressed considerably over the last decades and auroral measurements by the Airborne Ionospheric Observatory have been instrumental in achieving this increased understanding of the high-latitude ionosphere and its impact on Air Force systems. These optical auroral studies are also of significance to the problems encountered by satellite-borne optical sensors.

To enhance the results from the limited number of airborne studies, continuous observations of the high-latitude ionosphere are conducted at the Goose Bay Ionospheric Observatory. These observations are used to develop remote sensing techniques to provide a routine input into the Air Weather Service Space Environment Support System and to permit the classification of specific airborne measurements with respect to the general behavior of the ionosphere.

Continuous Aurora and Auroral E Layer: The analysis of simultaneous optical, photometric and ionospheric measurements in the noon sector of the auroral oval in darkness, made by AFGL's Flying Ionospheric Observatory, resulted in the discovery that well defined auroral-ionospheric regions occur in oval-aligned belts in a definite latitudinal order. Discrete auroras, defining the auroral oval, are associated with a layer of ionospheric sporadic E (E_s) and are co-located with an F-layer irregularity zone (FLIZ); equatorward follows a band of uniform, structureless glow—the continuous aurora—associated with the auroral E layer (E_a); and more equatorward, the particle-produced ionospheric D layer.

In the night sector these three auroral ionospheric regions also exist but frequently overlap.

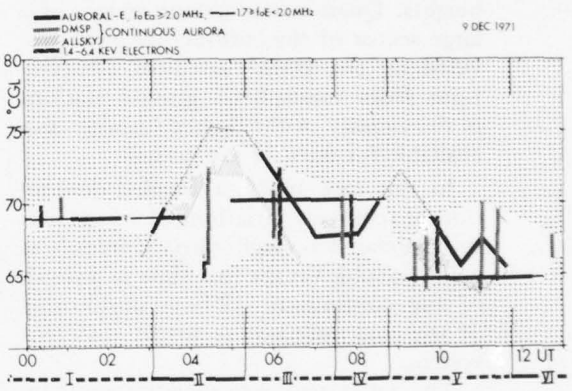

The time history of the latitudinal extent and location of the continuous aurora in the midnight sector measured by ionization, by optical emissions and by particle precipitation. The clear (unshaded) band includes the totality of the measurements: Thin dotted line indicates the aircraft's flight track, heavy solid lines along the flight track indicate when the airborne ionospheric sounder observed overhead auroral E. Horizontal bars show the presence of auroral E at ground stations within a four-hour local time period, centered at corrected geomagnetic local midnight. The latitudinal extent of 1. 4-6. 4 ke V electrons (ISIS 2) and the continuous aurora (DMSP) are shown in two different line patterns—as vertical bars at the time of the satellites' respective orbits. Continuous aurora, observed from aircraft, is indicated by hatched areas.

To understand the interrelation between auroras and the ionosphere in the night sector better, the AFGL Airborne Ionospheric Observatory conducted a number of flights at constant magnetic midnight, collecting rapid sequence ionospheric, photometric and optical data. For one particular case study a flight was coordinated with the ISIS-2 and DMSP

polar orbiting satellites so that the aircraft's flight track was intercepted several times by ISIS-2 and DMSP orbits, resulting in simultaneous aircraft and satellite measurements at each satellite pass. ISIS-2 is instrumented with particle detectors to measure precipitating electrons and protons responsible for auroral emissions and for ionization at D-, E- and F-region heights. Quasi-instantaneous images of a large sector of the auroral oval were provided by the DMSP satellites. Observations from ionospheric ground stations in the vicinity of the flight path were also available for most of the period.

In this case study, a detailed description of temporal variations of aurora and the associated ionospheric parameters was made possible for the first time as a result of the continuous, 12-hour monitoring of the oval midnight sector by different systems.

The rapid sequence measurements by the aircraft permitted detailed monitoring of the drastic changes in auroral brightness and structure, the substorm related changes in width of the auroral belt and the contraction and expansion of the oval diameter, which occurred within the 101-minute intervals between two consecutive DMSP orbits. The analysis revealed that the belt of continuous aurora participates in the rapid movements characteristic of the substorm-related changes observed in the discrete aurora. It had been previously assumed that substorms have little effect on the continuous aurora.

The observations, by different systems, of the continuous aurora, auroral E-layer and 1.4-6.4 keV electrons made in the midnight sector of the oval during a 12-hour period on December 9, 1971, show large variations in the width and location of the continuous aurora and E layer.

The understanding of the close association of auroral forms and ionospheric structures (derived from the coordinated measurements) contributed to the assembling of the "Defense Meterorological Satellite Program Auroral-Ionospheric Interpretation Guide." This guide may be used to interpret auroral features, visible in the DMSP images, in terms of associated ionospheric features and can be applied to interpret the various stages of auroral displays, from extremely quiet magnetic condition to the different phases of auroral substorms.

Auroral Case Studies: The comprehensive investigation of ionospheric and magnetospheric phenomena in the midnight local time sector has resulted in a detailed description of several important ionospheric features in addition to the continuous (E-layer) aurora. These features include discrete auroras in the oval and polar cap, auroral absorption, the F-layer irregularity zone (FLIZ), the polar electrojet, and particle precipitation zones. The conclusions drawn are the results of analysis of simultaneous ground-based, airborne and satellite measurements of interdependent geophysical parameters, which overcome many of the limits on time and space resolution of analyses made from a single type of measurement.

The study revealed the existence of distinct auroral states or sustained periods of a single pattern of auroral/ionospheric behavior. The lifetimes of these states range from two to three hours with transitions between states occurring within a few minutes. The auroral substorm with associated magnetic disturbances and regions of intense auroral particle precipitation constitutes one of these auroral states. Of equal importance are sustained periods of continuous aurora (and auroral E layer), periods of mixed discrete and continuous aurora and periods during which discrete auroras undergo repeated activations. These auroral states, which presumably reflect magnetospheric states, could be recognized because AFGL's Airborne Ionospheric Laboratory could fly in the midnight sector of the oval for periods up to ten hours, which was long

compared with the lifetimes of these states, carrying instruments with sufficient time resolution to detect transitions between states. A type of auroral substorm associated with oscillations of

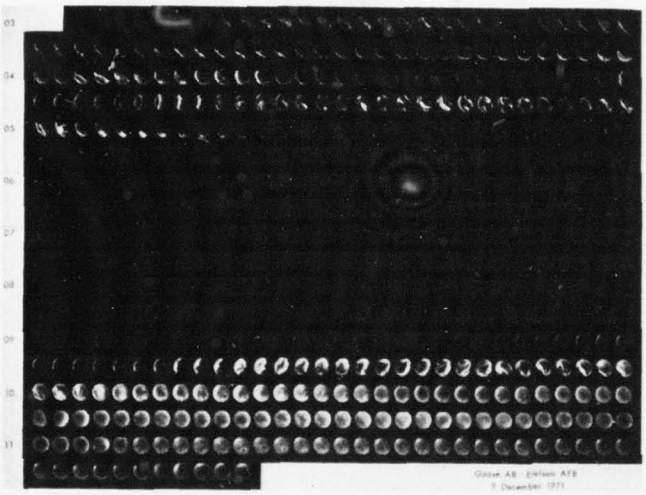

Montage of all-sky camera photographs recorded at one-minute intervals near midnight during a single flight of the AFGL Airborne Ionospheric Laboratory. Each horizontal strip represents one half hour of data with UT time indicated on the left. The lower five strips display the complete photographic record of an auroral substorm while the upper four strips are characteristic of auroral activations of shorter duration.

the earth's bow shock measured by a Vela satellite and characterized by bright, active auroras in the midnight sector, but by a spatially limited auroral electrojet was also observed. The existence of a limited number of identifiable states is significant to studies which attempt to predict future auroral/ionospheric conditions.

Optical Mapping of the Ionosphere: A new program has been undertaken for remote, optical sensing of ionospheric input parameters. Important ionospheric phenomena such as the continuous aurora (and auroral E layer), the main F-region trough, the F-layer irregularity zone and their effect on trans-ionospheric radio propagation and Over-the-Horizon (OTH) Backscatter radar performance will be investigated.

Auroral Activations: The probability of occurrence and lifetimes of active, extensive auroras were investigated.

Defense Meteorological Satellite Program (DMSP) auroral images and AFGL Airborne Ionospheric Laboratory all-sky camera photographs, taken at one-minute intervals on 12 flights at constant local midnight, comprised the data base. The analysis of these two sets of data indicates the occurrence frequency of active aurora to be about 25 percent of the time overall, increasing to about 50 percent under magnetic storm conditions.

The all-sky camera photographs are arranged into a montage which presents about ten hours of auroral observations and dramatically illustrates the extreme variability of the aurora in structure, duration, brightness, extent and location. These data have made it possible to describe the durations of auroral activations which fall into well defined lifetimes of about 15, 35 and 120 minutes. The latter, classically associated with the term auroral substorm, occurs about 6 percent of the time.

GOOSE BAY IONOSPHERIC OBSERVATORY

The disturbances and strong electron density gradients associated with the auroral ionosphere affect high-frequency communications and over-the-horizon backscatter systems. The location of the equatorward boundary of the auroral ionosphere, the poleward F-layer trough wall and the auroral activity to the north of it, are important parameters for the specification of the propagation environment. All of these can change rapidly. Information on these environmental conditions allows warning of possible communications and surveillance system out-

ages. Counteractions or data corrections, based on proper knowledge of the environment, can be initiated by system operators.

Backscatter and vertical soundings from a suitable location allow determination of the location of this boundary and the degree of auroral activity poleward of it. AFGL's Goose Bay Ionospheric Observatory, located at 65 degrees corrected geomagnetic latitude is in a favorable position to monitor the poleward trough wall and auroral activity. Backscatter soundings, made from this location for several years, show the approach of a front of ionospheric irregularities from the north in the afternoon and evening hours. This region of irregularities is associated with the auroral oval and other important regimes of the high-latitude ionosphere and can be used to determine the diameter of the oval and the degree of auroral disturbance.

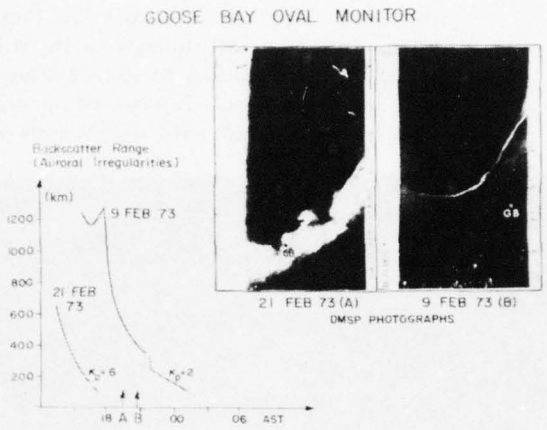

Comparison of Goose Bay backscatter data under average and disturbed magnetic conditions. DMSP auroral images taken at times indicated by arrows show location of Goose Bay and of aurora.

On the quiet day, backscatter echoes were observed around 1800 local time at a range of about 1200 km and arrived over the station around midnight. On the disturbed day, backscatter echoes were observed at 1330 local time at a range of 650 km, and arrived over the station as early as 1800 hours. Extrapolation of oval conditions from time of occurrence and range of backscatter echoes can be made three to six hours prior to the arrival of aurora at Goose Bay. A statistical analysis of backscatter echoes shows that time of occurrence and arrival at the station are well ordered by Kp (averaged over the noon-to-midnight hours). For Kp = 0 to 3 backscatter fronts associated with the approaching oval are clearly identifiable and can be used for the prediction of the location of the poleward trough wall.

Under more disturbed conditions ($Kp \geq 3+$), discrete ionization fronts are less likely to be observed and the appearance of a particle produced E-layer after 1700 hours local time is a regular phenomenon.

Besides the location of the trough wall, users of HF also want information on auroral activity. The strong fluxes of auroral particles that precipitate in substorms result in enhancements of sporadic E and auroral absorption. Both ionospheric phenomena strongly affect HF propagation. Using sporadic E and enhanced absorption as indicators for auroral activity allows the conditions of the auroral oval to be monitored, in real time, if required. Since auroral activity generally occurs over extended local time sectors of the oval, a single measurement can be extrapolated to larger portions of the oval. The refinement of the detection criteria and the correlation of the observed backscatter to a distinct oval size will make the station an important real-time oval monitor.

The Air Weather Service has recognized the importance of the Goose Bay Ionospheric Observatory and has made it part

of its Space Environment Support System (SESS). Since 1974 a steady stream of real-time geophysical data, including ionospheric sounder data, riometer, magnetometer, total electron content, and UHF/VHF scintillation measurements, have been transmitted to Global Weather Central for use in its prediction and monitor service. The importance of Goose Bay will increase, especially during the 414L Over-the-Horizon Radar Systems Performance Tests. During the one-year test period, real-time data available to operators at the Maine test site will allow the assessment of ionospheric conditions in the most disturbed sector of the OTH coverage.

Geomonitor and Geomonitor Display: Significant progress has been made towards real-time automatic monitoring of the auroral oval and ionospheric substorms. The principal research tool used to study the ionosphere has traditionally been the ionosonde which detects radio pulses reflected from ionized layers of the upper atmosphere. The data output of the ionosonde is normally in the form of a photograph or a cathode ray tube presentation, which must be processed and then manually analyzed by a trained observer. AFGL has participated in the development of digital ionosondes which produce ionograms in digital form suitable for hard copy printout, recording on magnetic tape, and computer processing. More recently, computer programs have been developed for the automatic transformation of digital magnetic tape records of ionograms into so-called "characteristics." These characteristics show the variation with time of the vertical height or backscatter range of ionospheric structures and the frequency range of echoes returned from the F-layer, the E layer and sporadic E. The real-time ionospheric data which has been automatically transformed and compressed is in a form suitable for transfer from the AFGL Goose Bay Ionospheric Observatory in the auroral zone to AFGL where techniques for the evaluation and application of real-time data are being developed.

Sporadic E and enhanced absorption can be used to determine oval diameter and auroral activity. These parameters and their temporal variations are easily observable in the "characteristics" presentation. Thresholds indicating the onset of disturbances can be determined and permit the issue of event reports without tedious data evaluation. A concept of combining a suitable presentation of ionospheric characteristics with a display of the more conventional high-latitude disturbance indicators such as magnetometer and riometer measurements has been developed as the basis for a remote, real-time "Auroral Oval and Ionospheric Substorm Monitor."

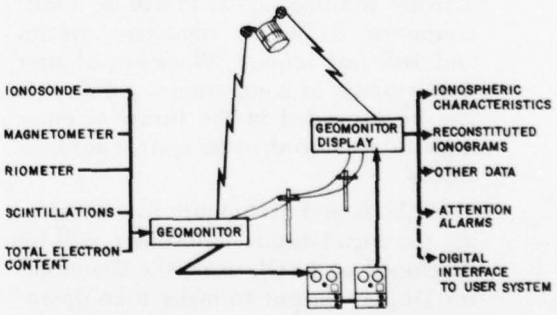

Conceptual layout of the Auroral Oval and Ionospheric Substorm Monitor System.

Hardware to provide for such a monitor system, consisting of a Geomonitor at Goose Bay and a Geomonitor Display system at AFGL is under construction. Data from the ionosonde and the other measurement systems will be digitized and assembled into data messages by the Geomonitor. In real-time operation, the data messages would be transferred by

telephone land line or satellite relay to the user site. During initial checkout, the data will be recorded and then played back into the Geomonitor Display. The data messages will be processed by the Geomonitor Display and displayed.

Ionospheric characteristics will be printed out to provide a hard copy time history of normal diurnal variations and of ionospheric disturbances. Ionograms will be reconstituted on a plasma display device. The reconstituted ionogram has the same format as the original ionogram and shows the shapes and heights of the E and F layers. The reconstituted ionograms assist in the interpretation of the most recent characteristics. A separate printer will display the other geophysical parameter data values.

The Geomonitor Display System will test the data for disturbances such as magnetic bays, riometer absorption or sporadic E events and automatically activate warning lights. It will be a self-contained dedicated hardware system and will not require allocation of user data storage or computing capability. It can be expanded in the future to enter digital data into the user system automatically.

Methods and techniques for monitoring the high-latitude ionosphere will be developed at AFGL using the Geomonitor Display output to make it an operational tool at sites, as for example an OTH radar site, where knowledge about the condition of the auroral ionosphere is required for proper systems management.

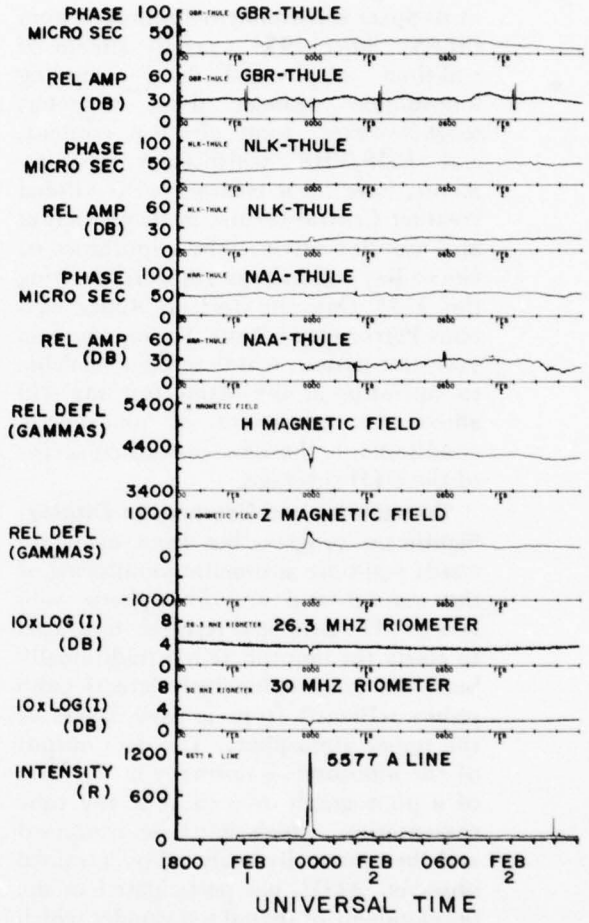

An energetic particle event as observed by ground-based VLF, magnetometer, riometer and photometer systems in the central polar cap at the AFGL Geopole Observatory, Thule, Greenland.

Polar Atmospheric Research: The central polar cap upper atmospheric program was terminated in June 1976 with the closing of the AFGL Geopole Observatory at Thule, Greenland. The Observatory had been in operation 19 years since it was set up for IGY studies. The most recent studies, carried out at the observatory, involved energetic particle events in the central polar cap. The term energetic particle event refers to a period of time, usually less than one hour duration, in which one or more of the riometers shows some absorption. During these times the other sensors usually record disturbances: one or more of the VLF

receivers may show significant absorption, the X(H), Y, and Z-magnetometer data may undergo fluctuations exceeding 250 gamma, and the 5577 angstrom line intensity may exceed 1000 Rayleighs. These events may be preceded or followed by periods of one to two-hour durations during which the VLF, magnetometer, and 5577 angstrom data may show significant disturbances. Those events which are accompanied by significant magnetic field fluctuations are also commonly known as magnetic substorms.

5577 Angstrom Night Airglow in the Central Polar Cap: The 5577 angstrom night airglow emission was measured in the central polar cap by ground-based photometric systems at Thule Air Base, Greenland, during the winters of 1972-1973 and 1974-1975 and at Thule-Qanaq, Greenland, during the winter of 1973-1974. Eighteen energetic particle events occurred at Thule during this period. The 5577 angstrom night airglow emission behaved very differently in the polar cap than at mid and low latitudes. No diurnal variation greater than 5 percent exists in the data. Large amplitude variations in 5577 angstrom daily average emission intensities do occur with changes up to a factor of approximately 8 over periods ranging from 4 to 19 days. These long-term airglow variations have a horizontal scale size of at least 100 km. This fact is supported by a correlation coefficient of 0.94 between daily average 5577 angstrom airglow intensities observed at Thule Air Base and Thule-Qanaq. An interplanetary magnetic field sector related behavior is evident in the daily average intensities which shows an increase of intensity in a + sector and decrease of intensity in a – sector. (A positive interplanetary magnetic field sector is predominantly away from the sun and a negative sector is predominantly toward the sun.) No significant correlation was found between the 5577 angstrom daily average intensities and Zurich sunspot number R_Z, although a positive trend was evident from observing season to observing season. Correlations between the 5577 angstrom daily average intensities and planetary magnetic indices Kp and Ap were inconclusive due to sector related effects.

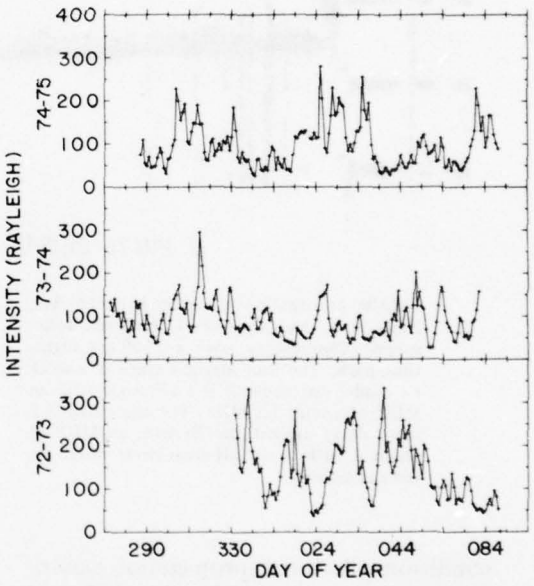

Daily average 5577Å airglow intensities as observed by a two-channel photometer system at the AFGL Geopole Observatory in Thule, Greenland, during the 1972-73, 1973-74 and 1974-75 winter seasons.

High Frequency Radio Wave Propagation in the F-Layer Trough: One of the problems of the Over-the-Horizon (OTH) Backscatter radar systems results from large range and azimuth errors caused by ionospheric refraction. This problem is most serious near the equatorward boundary of the auroral oval. Previous modeling and 3-D ray tracing had indicated that off-great-circle modes, with azimuth errors of up to 14 degrees and associated ground distance errors of up to 400 km, were possible under routinely occurring

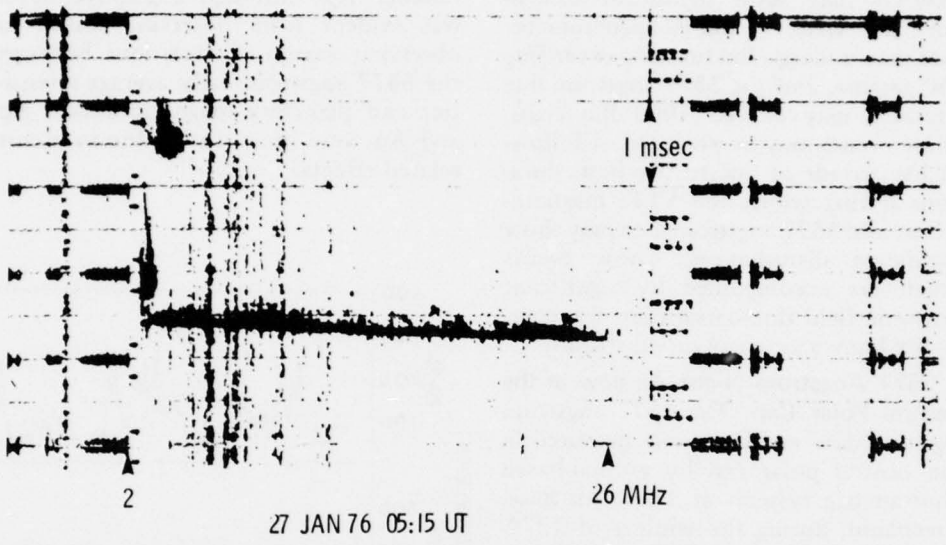

FM/CW propagation ionogram between Ava, New York, and the AFGL Airborne Ionospheric Observatory over a 1500-km nighttime path. The long straight trace is a weak Es mode; just above it is a 1F mode with an MUF of about 3.2 MHz. The trace with a 2 msec delay against the Es with an MUF of about 5 MHz is an off-great-circle mode via the auroral oval.

conditions. Airborne propagation experiments carried out jointly by AFGL and RADC have shown that these modes persist for extended periods.

The estimated locations of the reflection regions of the off-great-circle modes indicate that quiet conditions prevailed throughout the three hours during which the Airborne Ionospheric Laboratory observed this mode on January 27, 1976. The understanding of the behavior of these signals, together with the location of the oval edge, may make it possible to correct the azimuth errors or to identify these signals as strongly affected by errors.

Trans-Auroral Oval High Frequency Radio Wave Propagation: Trans-Auroral Oval Stepped High Frequency (HF) radio propagation experiments were carried out between the Goose Bay Ionospheric Observatory and the Airborne Ionospheric Laboratory flying meridional legs to the north of Goose Bay. Results show that the spatial relation of the propagation path midpoint to the equatorward or poleward boundary of the oval affects propagation parameters such as the Maximum and Minimum Observed Frequencies (MOF and LOF) and the structure of propagating modes. Changes in these parameters seem to be sensitive indicators of the boundary crossing of the midpoint, and an increase in auroral activity.

Systematic changes which cannot simply be explained by the relation of the path midpoint to the auroral oval suggest the existence of oval-aligned ionospheric structures which affect HF propagation. Further investigation should

reveal the relation of these ionospheric features to the oval.

Airborne VHF Scintillation Measurements in the Arctic: For the first time airborne scintillation measurements combined with the assessment of ionospheric and auroral conditions were conducted to investigate in detail the relation of scintillations to the aurora. Satellite transmissions at 250 MHz were received during eight flights in April and September 1975 on board the AFGL Airborne Ionospheric Observatory. The flight track permitted investigation of the occurrence of scintillations in the F-layer trough, the auroral oval and the Polar Cap. Generally, scintillations of appreciable amplitude (approximately 2 dB) were observed only in the northern half of the auroral oval, where auroral forms are generally not embedded in continuous aurora, and in the polar cap just to the north of the oval. Here, scintillations were observed whenever polar cap aurora was observed or

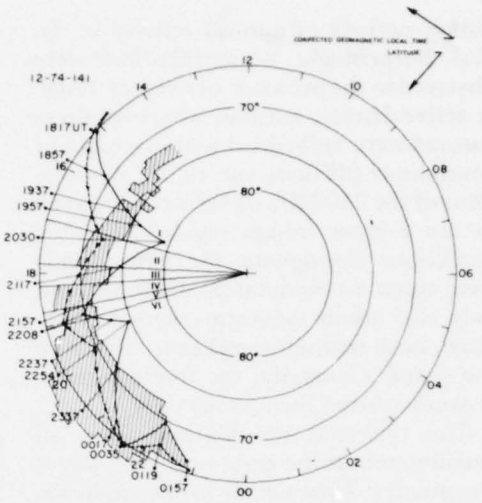

Geometry of propagation conditions with respect to instantaneous oval location for May 21 and May 22, 1974 oblique propagation experiment. Shown are the flight track (solid line), track of midpoint (dashed curve) and location of Goose Bay (individual dots). Superimposed is the instantaneous oval derived from 15-minute Q values. During flight, Sections I, III and V, the midpoint was south, and during Sections II, IV and VI, the midpoint was within the auroral oval.

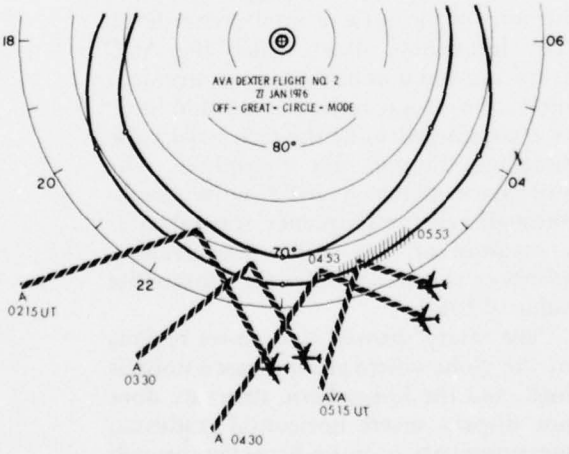

The location of the transmitter site (Ava, New York) and the aircraft in a corrected geomagnetic latitude/time coordinate system. Superimposed is a Q=1 oval, determined from aircraft backscatter observations between 01 00 and 02 20 Corrected Geomagnetic Time. The heavy striped lines show the paths and reflection points of selected off-great-circle modes observed during a three-hour period on January 27, 1976.

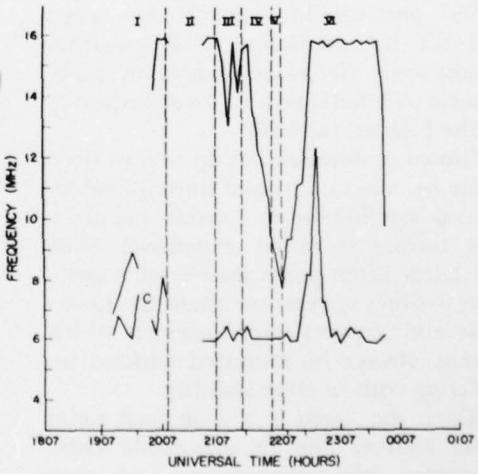

The frequency range, as a function of time, over which a 1 hop E mode was observed at the aircraft. Sections I to IV correspond to the specific propagation situations shown in the figure above.

during periods of auroral activity in the oval. Surprisingly, no scintillations were observed in the presence of even extremely active discrete auroras, whenever these auroras were embedded within a band of continuous (diffuse) aurora. No scintillations of the 250 MHz signal were observed in the F-layer trough region. Magnetic conditions throughout the experiments were quiet to moderately disturbed and only two minor substorms were encountered, both without significant effects on the signal. Generally, the findings relate to weak scatter phenomena only.

The observed scintillations were all encountered in the region of the F-Layer Irregularity Zone which in the midnight sector extends across the northern half of the oval and into the adjacent polar cap region. It seems likely that a combination of strong E-region, auroral, and F-region irregularities is responsible for the observed effects on VHF signals.

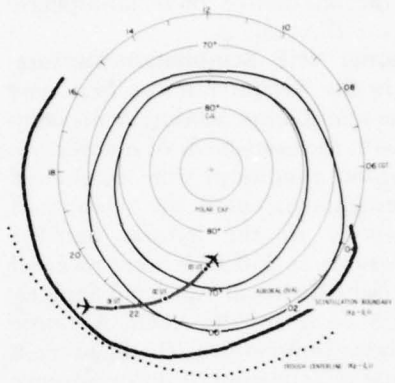

The aircraft flight track for airborne scintillation studies shown in corrected geomagnetic latitude and time. The experiment allows the sampling of scintillation conditions in the trough, the auroral oval and the polar cap.

Passive Topside Monitoring of F Layer Critical Frequency: For range and azimuth corrections required by systems such as the Global Positioning System (GPS) and satellite surveillance radars and for the prediction of propagation conditions, the most important ionospheric parameter is the critical frequency of the F layer, the foF2.

Global monitoring has up to now been made by a net of ground stations and by several satellite-borne topside sounders. The former is rather expensive, while the latter often poses interference problems to other systems on board the spacecraft and requires large antennas which cannot always be mounted without interfering with satellite stability.

Since the earth is a wide-band radio noise source, due to man-made radio frequency (rf) transmissions, and man-made and natural rf noise, a study was made to investigate the possibility of determining foF2 by observing the radio noise penetrating the F layer to satellite heights. Values of foF2 observed on ionograms recorded by the ISIS-2 satellite were compared against the Automatic Gain Control (AGC) voltage, which is a measure of the noise or interference level. The frequency, above which the AGC trace showed a continuous enhancement above the cosmic noise background level, was considered to be the terrestrial noise breaking through the ionosphere. The difference between foF2 noise breakthrough and the frequency was taken as a measure of how well noise measurements can be used to infer the subsatellite value of foF2.

The study showed that above regions of the globe where ground-based noise is high, and the ionospheric structure does not display severe horizontal gradients, measurements of noise breaking through the ionosphere can be used to determine foF2, generally to within 1.0 MHz. Comparison of daytime and nighttime measurements over the ocean showed a considerably smaller difference between foF2 and noise breakthrough at night. It is postulated that this feature is due to multi-hop propagation modes that are at-

tenuated less at night than during the day. A multi-channel HF receiver designed for the measurement of the noise breakthrough will be part of the Block V D DMSP Satellite and Air Weather Service has developed a computer program to determine foF2 by this method in suitable regions.

F-Layer Trough Model: Realistic ray tracing in the region of the main F-layer trough to investigate the effects of the low electron density region and of the strong gradients at its borders on an Over-the-Horizon (OTH) radar has been hampered by the lack of an appropriate model. Initial attempts to use the large data base of topside ionograms collected by the Alouete and ISIS satellites were not very successful due to the large variability in the location of the poleward trough wall. The correlation with Kp was not good enough for ordering the data, especially since the large electron density gradients of the trough wall occur over rather small distances.

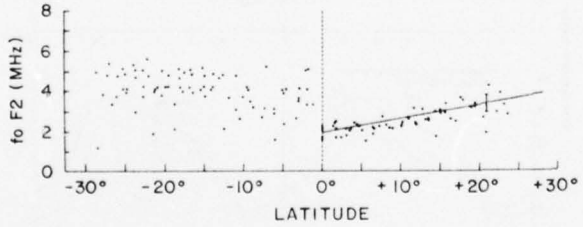

December 9, 1971 ISIS-2 foF2 values plotted vs a reference latitude coordinate system in which 0° corresponds to the trough wall and minus latitude values correspond to the auroral ionosphere, while positive latitude values correspond to the trough ionosphere.

A new data analysis technique was developed, which led to good results. The foF2 values collected during 40 orbits in December 1971 were plotted individually and the transition from the auroral ionosphere to the trough was determined for each path. This permitted the data to be analyzed statistically, without smoothing the gradient to be determined. The study, which was limited to the midnight sector, covered quiet to disturbed magnetic conditions and resulted in a numerical description of the trough wall gradient and the mean trough electron density.

The study shows that the steep electron density gradient that characterizes the poleward wall of the trough is typically 43,000 electrons per cubic centimeter per degree. The wall extends over about 3 degrees of latitude. At the latitude of the base of the poleward trough wall, the electron density is typically 48,000 electrons per cubic centimeter (foF2 = 2.0 MHz). The trough is 4 degrees wide in latitude at 2 MHz—that is, foF2 values remain at or below 2 MHz for about 4 degrees of latitude equatorward from the poleward trough wall. Likewise, the trough is 11 degrees wide at 2.5 MHz and 19 degrees wide at 3.0 MHz.

TRANS-IONOSPHERIC PROPAGATION STUDIES

VHF radio beacon signals from low altitude and synchronous satellites, as well as from radio stars, are used to study the effects of the ionosphere in both producing signal amplitude fluctuations and rotating the plane of polarization of linearly polarized signals. The amplitude fluctuations of the signals are produced by ionospheric irregularities at F-layer heights, particularly at high latitudes and the equator. The Faraday rotation of the plane of polarization is used to study the total electron content of the ionosphere, a parameter of importance in correcting radar range and navigation errors.

Total Electron Content: Measurements of the Total Electron Content (TEC) of the earth's ionosphere are generally made by observing the Faraday rotation of the plane of polarization of linearly polarized VHF radio waves transmitted from geosynchronous satellites. To determine the

total amount of polarization rotation the initial polarization as transmitted from the satellite must be known. Because this is not normally one of the parameters of the satellite measured before launch, AFGL undertook a measurement program to determine the initial polarization from several satellites while in orbit. The technique used was to measure the total polarization rotation of lunar reflected radio waves at a time when the moon passed nearly in back of each satellite. This measurement was made during a winter nighttime when the total rotation was small and changing very slowly. The initial polarization angles of VHF signals appropriate for Faraday rotation measurements from ten different geosynchronous satellites were measured using this technique. Results have been published for use by observers at any station.

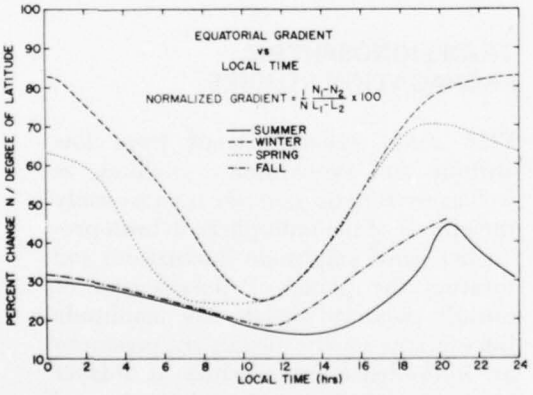

The electron density gradient at the equatorial edge of the trough wall versus local time for the four seasons.

During the launch of the Skylab by NASA on May 14, 1973 an unusually large and rapid decay in the ionospheric TEC was observed. The disturbance appeared as a dramatic "bite-out" of more than 50 percent of the electron content, which lasted for several hours, as compared to the expected TEC curve for that day. A detailed analysis of the F2 region chemistry of the event revealed a devastating loss process due to the discharge of water vapor and unburned hydrogen from the launch rocket. The specific mechanism was the rapid ion-atom interchange reactions between the ionospheric O^+ and the hydrogen and water vapor molecules in the plume, followed by dissociative recombination of the molecular ions. While the launch trajectory was off the East Coast of the United States, effects were seen in TEC observations at Urbana, Illinois; Goose Bay, Labrador and Narssarssuaq, Greenland, in addition to the local station at Hamilton, Massachusetts.

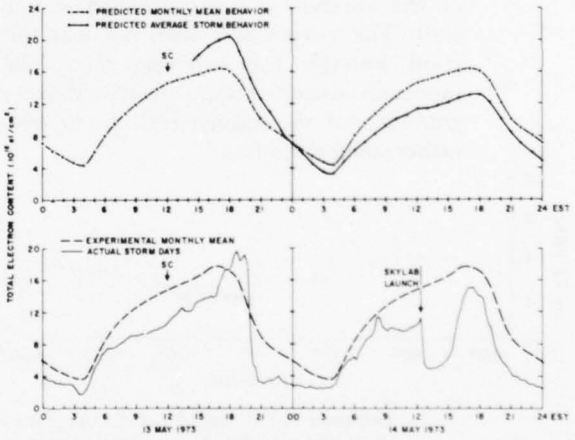

A comparison of the Sagamore Hill predicted monthly mean total electron content and its average storm-time correction for May 1973. The actual experimentally determined monthly mean and the behavior during the geomagnetic storm period May 13 and 14, 1973.

Scintillations of Satellite Signals: Amplitude and phase fluctuations introduced by the ionosphere in signals passing from ground to satellites to ground have become a problem primarily in the equatorial and high latitude regions. With the advent of a series of military and civilian satellites transmitting and receiving at a

variety of frequencies from 136 to 1600 MHz, the phenomenon has received considerable attention. The study of the effects on these signals as a function of time of day, magnetic conditions, latitude and longitude allows operations groups to understand the natural problems they will encounter and allows the engineer to develop second generation systems and equipment to minimize the fading phenomenon.

Recently the AFGL group has been concerned with the effects of the irregularities in the equatorial ionosphere. A belt roughly 20 degrees on each side of the geomagnetic equator displays intense irregularities which produce effects at frequencies as high as 6 GHz even at very high viewing angles. The varieties of equatorial behavior include many facets. Very weak irregularities generated by the equatorial electrojet have recently been found to exist in the pre-noon time period. Very strong irregularities placed in the ionosphere from 200 to 1,000 km have been found to exist when large plumes rise in the equatorial ionosphere. These strong irregularities with deviations of electron density up to half the ambient electron density are responsible for the microwave scintillations and very deep UHF scintillations. Thin weaker irregularities produce the relatively shallow fading at VHF and UHF.

By comparing *in situ* measurements of irregularities from an Orbiting Geophysical Observatory satellite, OGO-6, with ground measurements of scintillations, the seasonal variation of scintillations with longitude is emerging. The first map of this type shows that, in the months of November and December, areas in South America display strong scintillation activity while equatorial regions over India show little activity. This combining of ground measurements of trans-ionospheric transmissions and satellite measurements of irregularities will allow the morphological picture to be developed more fully.

While the equatorial scintillations display only a weak negative correlation with magnetic index, at high latitudes strong magnetic disturbances produce intense scintillations. A model of high-latitude scintillations is being developed using magnetic index, time of day, season and solar flux to determine scintillations. This model utilizes observations over several years from Narssarssuaq, Greenland; Goose Bay, Labrador, and Sagamore Hill, Massachusetts, as its data base. It has been partially completed and will allow forecasters to determine the scintillation level when the magnetic index is forecast. Further work in this area will include developing mathematics for irregularity elongation (along the lines of force of the earth's magnetic field) and for the polar latitudes where there is only a sparse data base.

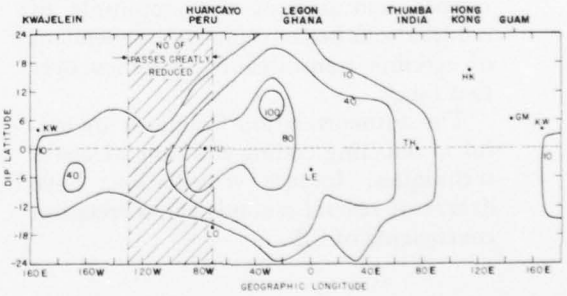

The percentage of scintillations 4.5 dB or greater at 140 MHz between 7:00-11:00 p.m. local time during November and December 1969 and 1970. The map was compiled from scintillation data and OGO-6 observations.

Signal Statistics: Periods of intense scintillations have been analyzed to provide information for evaluation of trans-ionospheric propagation effects on Air Force satellite communication systems operating in the VHF and UHF bands. Using the 40, 137 and 360 MHz signals

from ATS-6, scintillation data from the auroral and equatorial regions have been processed by computer and the amplitude distribution, the rate distribution, the power spectra, and the correlation functions determined. The cumulative amplitude distribution is most useful for determining the required fade margin. The experimental data indicate that the scintillations closely follow the Nakagami m distribution with the Rayleigh distribution being the worst case.

Data on the scintillation rates are used to predict message reliability. When the periods of the fades become less than the message length, the reliability approaches zero. The relationship of scintillation amplitude to the frequency at which the signal fades and recovers has been determined for intense scintillations. Also, based on the measured values of the Nakagami m-parameter, the dependence of scintillations on transmission frequency was measured from the 137 and 360 MHz data. For the most intense scintillations the amplitude of scintillations became almost independent of satellite transmission frequency over that range.

The autocorrelation functions are useful in selecting coding and time diversity techniques. Intense scintillations have delays of several seconds for correlation coefficients of 0.5.

SOLAR RADIO ASTRONOMY RESEARCH

Solar radio investigations of the Trans-Ionospheric Propagation Branch are divided into two general areas. The larger effort uses multi-frequency data collected with patrol type instruments having low angular resolution. Both quiet sun and burst emission components are studied. Less effort is applied to studies using medium to high resolution measurements taken routinely with the Naval Electronics Laboratory Center 60-foot diameter antenna at La Posta, California, and infrequently with the Northeast Radio Observatory Corporation (NEROC) 120-foot diameter Haystack antenna. The research in both areas is strongly oriented toward prediction of geophysical activity after a flare or burst. The research supports the Air Weather Service, the Space and Missile Systems Organization, and operational groups with Air Force commands.

For more than a decade, the 10.7 cm quiet sun radio flux density has been used as one of several inputs into the equation used to predict changes in the orbits of low altitude satellites. For almost twice that time, Laboratory scientists have advocated the use of quiet sun radio flux density data for calibration of telemetry and radar systems. In the past two years, the usefulness of the concept has been recognized to the extent that specifications for new radar systems now include provisions for using quiet sun data for various system checks. This is possible since quiet sun measurements over a wide range of frequencies from meter to millimeter wavelengths now have an absolute accuracy of about 95 percent and a day-to-day consistency as high as 97 percent.

Multi-frequency observations at nine discrete frequencies between 200 and 35,000 MHz yield spectral data on solar disturbances which provide information on physical mechanisms taking place on the sun. Because appearances of phenomena repeat, they can be signatures of either simultaneous or related geophysical events. The signatures which relate to catastrophic events are of special interest. Work on developing and improving radio prediction and warning criteria is of a continuing nature.

Recently, a survey of bursts having the now well known U-shape signature of proton activity was completed for the years 1966 - June 1976. Of 81 radio outbursts with the U-shape signature, at least 79 had confirmed proton association. For the remaining two, proton emission was probable. This means that the U-shape radio burst signature can reliably predict proton activity without "false alarms." This proton activity, however, is not necessarily observed as a polar cap absorption or other geophysical event because both the interplanetary magnetic field lines (IMF) between sun and earth and the transport of protons from the flare or burst site to the sun-earth field line "bundle" play significant roles. Although the majority of radio outbursts having the U-shape signature are followed by geophysical phenomena, other signatures are required to determine which proton emission events will produce an earth-recorded or near-earth geophysical event.

It seems clear that while proton-producing outbursts originate from all solar disk longitudes, a recent AFGL study of large solar outbursts showed that there are preferred Carrington longitudes for proton flares.

Although east limb solar events have produced outstanding geophysical activity, more of the important geophysical events originate in the western solar hemisphere, with generally faster onset. In Sunspot Cycle Number 20, 90 percent of the ground level events originated from solar western hemisphere locations even though the preferred 150-180 degree Carrington longitude interval did not emit any particles resulting in ground level events. Efforts are being made to determine if the radio bursts of the proton events also contain a radio signature of some condition in the solar proton flare producing region which will suggest whether or not the event will ultimately be observed as a geophysical event at the earth. The clue may be in the use of long wavelength radio burst data to indicate the direction of open field lines in the active region for the escape of energetic particles toward or away from the IMF "bundle."

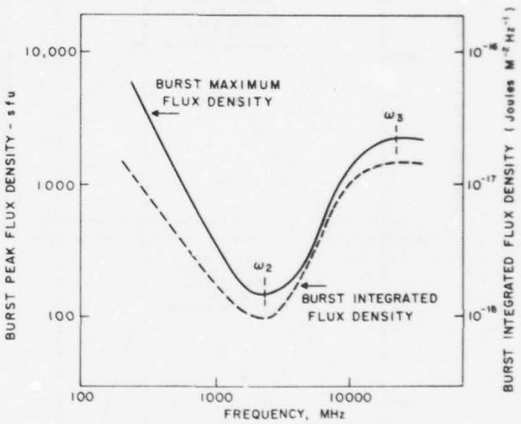

Peak and integrated flux density spectra of the solar outburst of August 21, 1975 near 1520 Universal Time, from Sagamore Hill Observatory data.

Greater utilization of the burst flux density U-shape spectrum than merely the yes-no prediction of forthcoming proton activity has been sought. A number of useful spectral signatures have been found. For example, the frequency at which the power from the burst peaks is indicative in a rough way of the magnetic field intensity in the flare/burst region. The slope in the frequency range above this frequency is indicative of the energy distribution of the radiating electrons. Models have been generated and are now being compared with actual data. A relatively slow decrease with frequency above the frequency of maximum power indicates extremely high energy in the burst region.

AD-A067 252 AIR FORCE GEOPHYSICS LAB HANSCOM AFB MASS F/G 14/2
REPORT ON RESEARCH AT AFGL JULY 1974-JUNE 1976.(U)
JUN 77 J F DEMPSEY
UNCLASSIFIED AFGL-TR-77-0137 NL

2 OF 3
ADA
067252

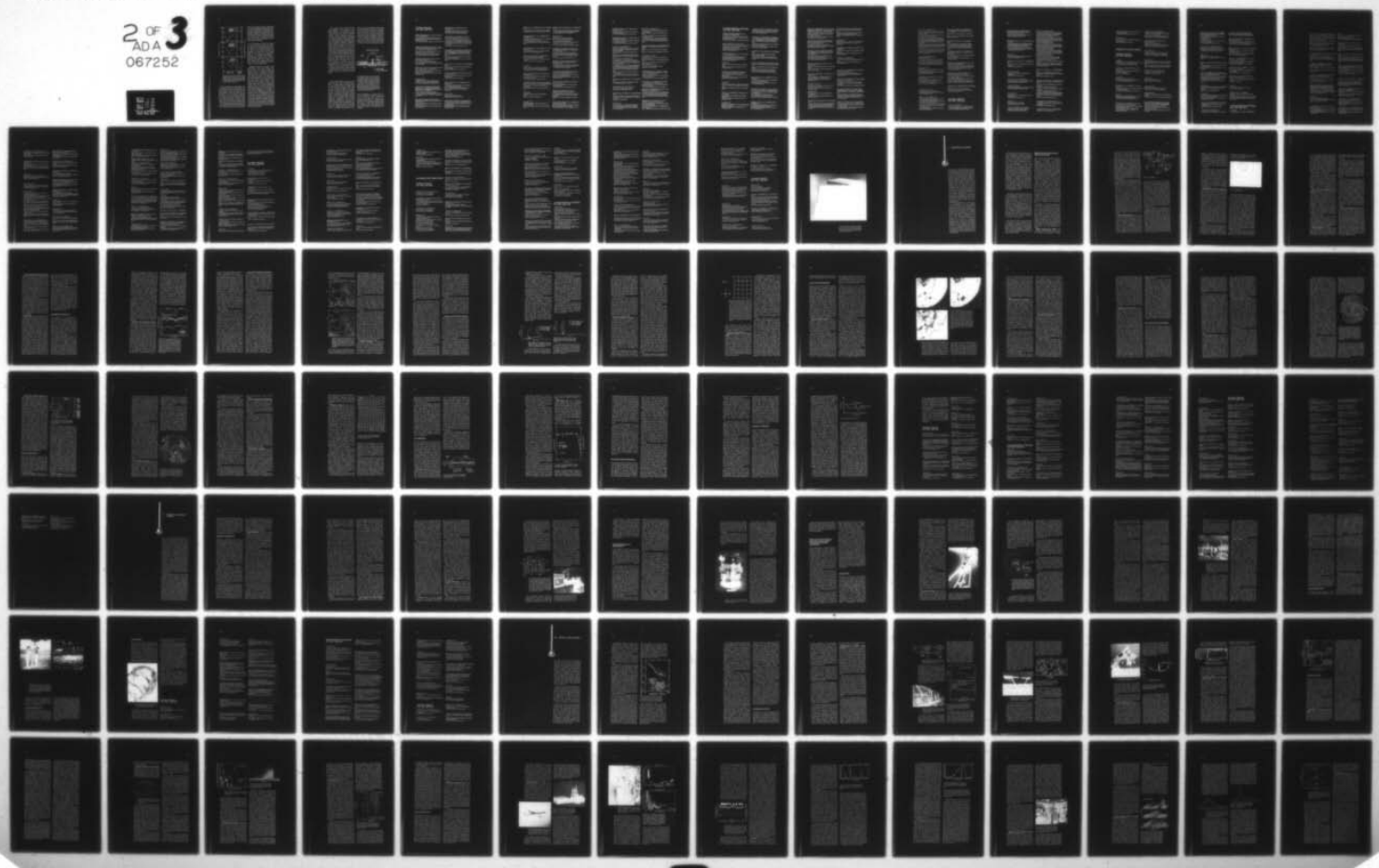

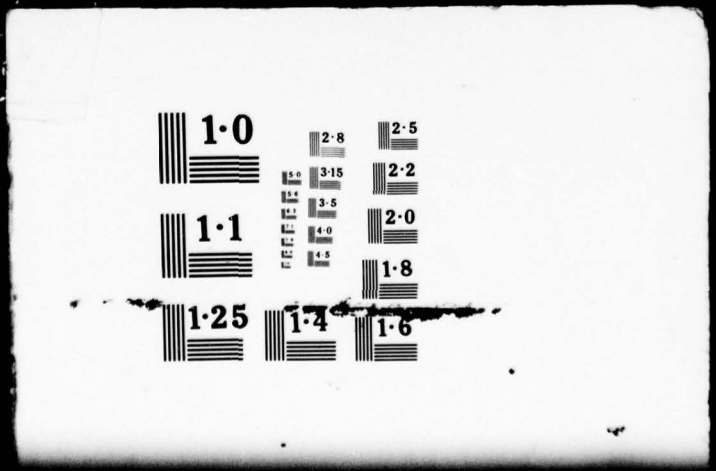

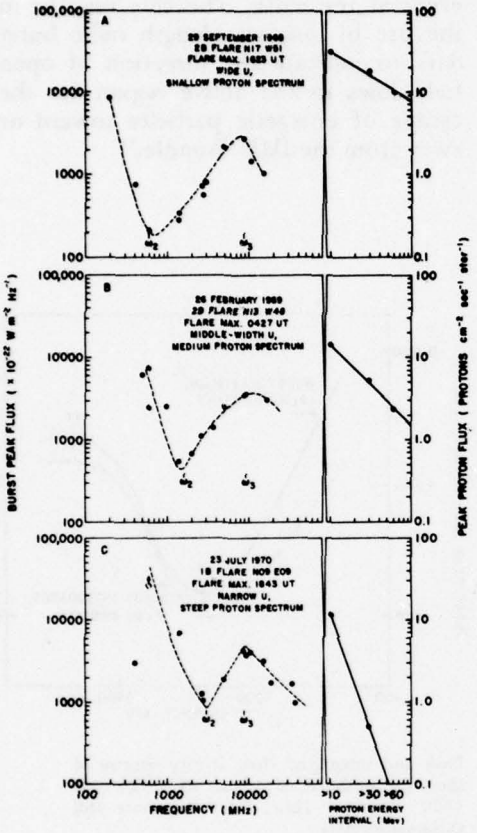

Observed solar radio burst spectra with the associated proton spectra. Note that a large interval between ω_3 and ω_2 is correlated with a moderately hard proton spectrum while a small ω_3/ω_2 ratio is correlated with a steep or soft proton spectrum.

This investigation is one possible way to determine the proton energies in the source. Both protons and electrons can be measured in space. Neither can be measured at the sun. The best that can be done is to infer electron densities from radio and hard X-ray spectral data. An attempt can then be made to describe the acceleration processes which would cause the electron distribution.

The decimeter dip frequency region is fairly well defined in the data. The slope of the burst spectrum in the interval between the minimum power frequency and the maximum power frequency may be used to speculate on the radiation absorption mechanism, assuming gyro-synchrotron emission as the microwave emission process. However, the determination of how the burst is actually attenuated must await better information on the burst region parameters.

An investigation carried out during the past few years showed that there is a useful correlation between the proton flux over a specified interval and the width of the interval between the frequency at which the burst energy peaks and the frequency at which the energy is a minimum. Specifically, a large frequency ratio denotes a hard or relatively flat spectrum in the 10 to more than 60 MeV range while a small ratio of the two frequencies denotes a steep or soft proton spectrum.

Statistical studies were made of the correlation of burst spectral data with proton flux at various energies for about 25 events. The results of the study indicate that it is possible to predict, from radio data alone, the slope of the proton flux maxima or even the ratio of more than 10 MeV to more than 30 MeV protons or more than 10 MeV to more than 60 MeV protons. Earlier work showed that radio burst integrated flux density data can provide quantitative prediction data on the flux of protons with energies greater than 10 MeV or on Polar Cap Absorption at 30 MHz in decibels. By combining predictions of the proton flux with energies of 10 MeV or greater with the frequencies of minimum and maximum power signatures, it should be possible to predict the entire proton spectrum from radio data alone. To improve on this prediction reliability, radio burst integrated flux density for all proton events of sunspot cycle number 20 is being reviewed.

The Radio Solar Telescope Network (RSTN) is a continuing concern. High-resolution radio studies of solar active regions were continued using the NEROC 120-foot Haystack radio telescope at 3.8-cm wavelength. Techniques are being sought that will provide long-term advance warning of eruptive events that can disrupt terrestrial ionospheric and atmospheric conditions. Results of power spectral analysis of the 3.8-cm signals reveal periodicities in the polarized emission from the region prior to a flare event. The most prominent period is 23 seconds. No significant periodicities occur in the pre-flare brightness temperatures, however. Only one observation of an active region erupting with a proton flare was obtained in real time on the Haystack radio telescope. This event, which occurred on August 21, 1975, was surprising in that the brightness temperature of the region was decreasing towards a very low value and there were no unusual polarization variations when it suddenly erupted and caused a 0.7 dB riometer polar cap absorption (PCA) event.

The low level of solar activity over the past two years made conditions favorable for a radio search for coronal holes on the solar disk. Since coronal holes are the sources of high speed wind streams that are thought to be responsible for terrestrial recurrent magnetic storms, a detection and study of these holes at transition level heights (3.8 cm emission level) could provide a valuable input to a magnetic storm forecast capability. Measurements on the Haystack radio telescope in September of 1975 revealed an area in which the radiation was depressed about 8 percent below the background sun level, indicating a possible coronal hole. It was later found to be associated with a large quiescent filament system. To explain the observations a model was developed where a coronal cavity, which normally surrounds arch prominences, could provide the necessary depression value if it had a density one-half the surrounding coronal value. Another depression observed at the same time had a value 6 percent less than the background sun.

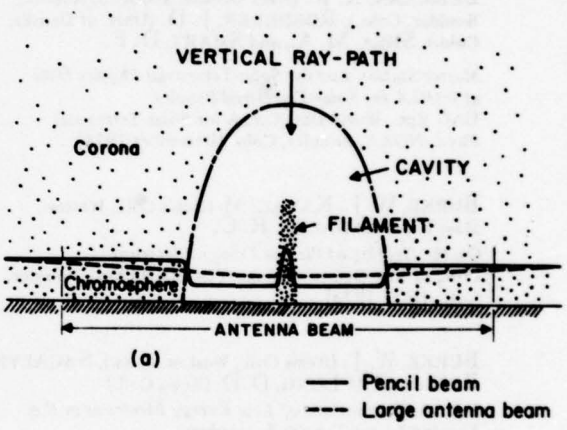

A radio depression area on the sun at 3.8 cm wavelength. First thought to be a coronal hole, it is actually a result of a coronal cavity which surrounds the filament and has a density of one half the normal coronal value. The dashed line shows the levels measured by a large antenna beam such as the Haystack 4. 4 arc-minute beam, as it scans across the cavity. With a higher resolution pencil beam, the level shown by the solid line would be measured. The filament would be detected in the cavity which has a deeper depression level.

The unavailability of optical, EUV, or X-ray coronal hole data for this period did not allow the latter region to be positively identified as a coronal hole. Analysis is now being performed on data from other coronal hole searches with the Haystack radio telescope made at times when supportive measurements are available.

JOURNAL ARTICLES
JULY 1974 - JUNE 1976

AHMED, M. (Regis Coll., Weston, Mass.), SAGALYN, R. C., and SMIDDY, M.
The Morphology of Small Scale Thermal Ionization Irregularities at Height Latitudes Deduced from ISIS-I Satellite Measurements
Proc. of Iono. Eft. Symp., Arlington, Va. (January 1975)

BUHMANN, R. W. (Natl. Oceanic and Atm. Admin., Boulder, Colo.), ROEDERER, J. D. (Univ. of Denver, Colo.). SHEA, M. A., and SMART, D. F.
Master Station List for Solar-Terrestrial Physics Data at WDC-A for Solar-Terrestrial Physics
UAG Rpt., World Data Ctr. A for Solar-Terrestrial Phys., NOAA, Boulder, Colo. (December 1974)

BURKE, W. J., KANAL, M. (Regis Coll., Weston, Mass.), and SAGALYN, R. C.
On the Heating of Plasma Trough Electrons
Proc. of Intl. Symp. on Solar Terrestrial Phys., Boulder, Colo. (June 1976)

BURKE, W. J. (Regis Coll., Weston, Mass.), SAGALYN, R. C., and DU LONG, D. D. (Regis Coll.)
Injun 5 Observations of Low Energy Electrons in the Evening Sector Topside Ionosphere
EOS, Proc. of 1976 Spring Ann. Am. Geophys. Union Mtg. (April 1976)

DANDEKAR, B. S.
Simplified Formula for the Determination of the Altitude of an Auroral Arc from a Single Station
J. of Atm. and Terrestrial Phys., Vol. 36 (1974)

DODSON, H. W., HEDEMAN, E. R. (McMath-Hulbert Obsv., Univ. of Mich.), KREPLIN, R. W., MARTRES, M. J., OBRIDKO, V. N., SHEA, M. A., SMART, D. F., and TANAKA, H.
Catalog of Solar Particle Events, 1955-1969
Vol. 49 of Astrophys. and Space Sci. Library, Ed. by Z. Svestka and P. Simon, D. Reidel Pub. Co., Dordrecht, Holl. (1975)

DU LONG, D. D. (Regis Coll., Weston, Mass.), DOUCETTE, J. (Emmanuel Coll., Boston, Mass.), and SAGALYN, R. C.
Small Scale Irregularities at Low Latitudes in the Topside Ionosphere
EOS, Proc. of 1976 Spring Ann. Am. Geophys. Union Mtg. (April 1976)

FOUGERE, P. F., RADOSKI, H. R., and ZAWALICK, E. J.
A Comparison of Power Spectral Estimates and Applications of the Maximum Entropy Method
J. of Geophys. Res., Vol. 80 (February 1975)

FOUGERE, P. F., and RUSSELL, C. T. (Inst. of Geophys. and Planetary Phys., Univ. of Calif.)
Comment on "Interplanetary Magnetic-Sector Structure, 1926-1971" by L. Svalgaard and "Correspondence of Solar Field Sector Direction and Polar Cap Geomagnetic Field Changes for 1965" by W. H. Campbell and S. Matsushita
J. of Geophys. Res., Vol. 80 (25 June 1975)

FOUGERE, P. F., ZAWALICK, E. J., MC CLAY, J. F., RADOSKI, H. R., PAZICH, P. M., KNECHT, D. J., HUTCHINSON, R. O., TSACOYEANES, C. W., and CANTOR, C. (Emmanuel Coll., Boston, Mass.)
Maximum Entropy Spectrum from the AFGL Magnetometer Network: First Results
Trans. of Am. Geophys. Union, Vol. 57, No. 4 (April 1976)

FOUGERE, P. F., ZAWALICK, E. J., and RADOSKI, H. R.
Spontaneous Line Splitting in Maximum Entropy Power Spectrum Analysis
Phys. Earth Planet. Inter., Vol. 12 (1976)

FUKUI, K., and ENGE, W., BEAUJEAN, R. (Institut fur Kernphysik, Kiel, Ger.)
Beryllium Isotopes in Cosmic Radiation Detected with Plastic Detector
Zeitschrift der Physik, Vol. 277 (1976)

GOLD, R. E. (Univ. of N. H.), SHEA, M. A., and SMART, D. F.
A Preliminary Idealized Network of Neutron Monitors for the Study of Solar Modulation
Proc. of 14th Intl. Cosmic Ray Conf., Munich, Ger. (Aug. 1975), 14 CRG, Vol. 4, MG Session and Pioneer Symp.

HALL, W. N.
Mid-Latitude Pulsating Auroras
Planetary Space Sci., Vol. 22 (1974)

KLECKNER, E. W., SMITH, L. L. (Battelle-Northwest Labs., Richland, Wash.), and WILDMAN, P. J. L.
A Reassessment of the Location of SAR Arcs Relative to the Plasmapause
EOS, Proc. of 1974 Fall Am. Geophys. Union Mtg. (December 1974)

KRUKONIS, A. P., SILVERMAN, J., and YANNONI, N. F.
Terephthaldehydene Bis $\Delta^{1,a}$ Malononitrile, $C_{14}H_6H_4$
Crystal Structure Comm., Parma, Italy, Vol. 3 (1974)

LEZNIAK, J. A. (Univ. of N. H.), SMART, D. F., and SHEA, M. A.
The Effect of Ionization Energy Loss on the Calculation of Rigidity Transmittance Functions
Proc. of 14th Intl. Cosmic Ray Conf., Munich, Ger. (Aug. 1975), 14 CRG, Vol. 4, MG Session and Pioneer Symp.

MAHON, H. P. (Univ. of Mass.), SMIDDY, M., and SAGALYN, R. C.
Electric Field Measurements in the Auroral E-Region
Rad. Sci., Vol. 10, No. 3 (March 1975)

MAPLE, E., and FREY, J. H., FISCHER, W. L. (Sci. Resources Fdn., Watertown, Mass.)
Auroral-Oval Micropulsations at a Sub-Auroral-Zone Station
J. of Geophys. Res., Vol. 81 (March 1976)

PAYNE, R.
Specific Adsorption of Sulfate Ions at a Mercury Electrode from Aqueous Sodium Sulfate Solutions
J. of Electroanalyt. Chem., Vol. 60 (April 1975)

PHELPS, A. D. R. (Regis Coll., Weston, Mass.), and SAGALYN, R. C.
Power Spectra of Plasma Density Irregularities in the High Latitude Ionosphere
J. of Geophys. Res., Vol. 81 (February 1976)

PORTER, H. S. (Univ. of Cincinnati, Ohio), SILVERMAN, S., and TUAN, T. F. (Univ. of Cincinnati, Ohio)
On the Behavior of Airglow Under the Influence of Gravity Waves
J. of Geophys. Res., Vol. 79, No. 25 (1 September 1974)

PRASAD, B.
A Classical "MASER" Action in a Hot Uniform Plasma
Phys. of Fluids, Vol. 19 (March 1976)

RADOSKI, H. R.
Coupled Hydromagnetic Modes: Power Spectra of Numerical Solutions
Trans. of Am. Geophys. Union, Vol. 57, No. 4 (April 1976)

RADOSKI, H. R., ZAWALICK, E. J., and FOUGERE, P. F.
The Superiority of Maximum Entropy Power Spectrum Techniques Applied to Geomagnetic Micropulsations
Phys. Earth Planet. Inter., Vol. 12 (1976)

ROTHWELL, P. L.
Weyl Geometry as a Particle Geometry
Phys. Ltrs. A, Vol. 49A (26 August 1974)
The Scalar Field and Weyl Geometry
Il Nuovo Cimento, Vol. 30B, No. 2 (December 1975)
Production of Flare Produced H^2 and He^3
J. of Geophys. Res., Vol. 81, No. 4 (February 1976)

ROTHWELL, P. L., KATZ, L., YATES, G. K., and SELLERS, B., HANSER, F. A. (Panametrics, Inc., Waltham, Mass.)
Interpretation of Flare-Produced Proton Spectra
Proc. of Intl. Symp. on Solar-Terrestrial Phys., Sao Paulo, Brazil, Vol. 1 (Sun and Interplanet. Medium) (1974)
J. of Geophys. Res., Vol. 80 (December 1975)

RUSSELL, C. T. (Inst. of Geophys. and Planetary Phys., Univ. of Calif.), FLEMING, B. K., and FOUGERE, P. F.
On the Sensitivity of Modern Inferences of Interplanetary Magnetic Polarity to Geomagnetic Activity
J. of Geophys. Res., Vol. 80 (1975)

SAGALYN, R. C., DU LONG, D. D. (Regis Coll., Weston, Mass.), and BREDESEN, S. C.
Survey of Small Scale Irregularities at Low and Mid Latitudes in the Topside Ionosphere
EOS, Proc. of 1976 Spring Ann. Am. Geophys. Union Mtg. (April 1976)

SAGALYN, R. C., and PHELPS, A. D. R. (The Univ. of Oxford, Eng.)
Plasma Density Irregularities in the High Latitude Topside Ionosphere
J. of Geophys. Res., Vol. 81 (February 1976)

SAGALYN, R. C., PHELPS, A. D. R., and AHMED, M. (Regis Coll., Weston, Mass.)
In Situ Measurements of the Structure and Spectral Characteristics of Small Scale F Region Ionospheric Irregularities
Proc. of Iono. Eff. Symp., Arlington, Va. (January 1975)

SAGALYN, R. C., SMIDDY, M., and AHMED, M. (Regis Coll., Weston, Mass.)
High-Latitude Irregularities in the Top Side Ionosphere Based on ISIS I Thermal Ion Probe Data
J. of Geophys. Res., Vol. 79, No. 28 (October 1974)

SELLERS, B. (Panametrics, Inc., Waltham, Mass.), and KELLEY, J. G.
Magnetic Field and Atmospheric Density Effects on PCA Event Ionization
J. of Atm. and Terrestrial Phys. (February 1975)

SELLERS, B. (Panametrics, Inc., Waltham, Mass.), and STROSCIO, M. A., 1ST LT.
Rocket-Measured Effective Recombination Coefficients in the Disturbed D Region
J. of Geophys. Res., Vol. 80, No. 16 (1 June 1975)

SHEA, M. A., and SMART, D. F.
Solar Particle and Related Interplanetary Observations During the Campaign for Integrated Observations of Solar Flares (CINOF)
Proc. of Intl. Symp. on Solar-Terrestrial Phys., Vol. 1 (1974)
The Evaluation of Cutoff Rigidities and Reentrant Albedo Calculations for Palestine, Dallas and Midland, Texas
J. of Geophys. Res., Vol. 80 (April 1975)
The Application of the International Geomagnetic Reference Field to Cosmic-Ray Trajectory Calculations
Proc. of Am. Geophys. Union Mtg., Colo. Springs, Colo., Vol. 56 (August 1975)
A Comparison of Vertical Cosmic-Ray Cutoff Rigidities as Calculated with Different Geomagnetic Field Models; A Five by Fifteen Degree World Grid of Calculated Cosmic-Ray Vertical Cut-Off Rigidities for 1965 and 1975;
Variations of the Calculated Cosmic-Ray Equator Over a 20-Year Interval
Proc. of 14th Intl. Cosmic Ray Conf., Munich, Ger. (Aug. 1975), 14 CRG, Vol. 4, MG Session and Pioneer Symp.

SILVERMAN, J., KRUKONIS, A. P., and YANNONI, N. F.
2-Dicyanomethyleneindane-1, 3-Dione, $C_{12}H_4N_2O_2$
Crystal Structure Comm., Vol. 3 (1974)

SILVERMAN, S. M., and MULLEN, E. G.
Sky Brightness During Eclipses: A Review
Appl. Opt., Vol. 14 (December 1975)

SILVERMAN, J., YANNONI, N. F., and KRUKONIS, A. P.
The Crystal Structures of 9-Dicyanomethylene-fluorene Derivatives IV. 9-Dicyanomethylene-2, 4, 5, 7-Tetranitrofluorene
Acta Cryst., Vol. B30 (1974)

SMART, D. F.
Geomagnetic Effects: A Rapporteur Paper Prepared for the 14th International Cosmic Ray Conference
Proc. of 14th Intl. Cosmic Ray Conf., Munich, Ger., Vol. 11 (Aug. 1975)

SMART, D. F., and SHEA, M. A.
A Technique for Evaluating Mathematical Models of the Magnetosphere
Proc. of Intl. Symp. on Solar-Terrestrial Phys., Vol. 2 (1974)
Cosmic-Ray Penumbral Effects for Selected Balloon Launching Locations;
An Analysis of Trajectory-Derived Penumbral Widths
Proc. of 14th Intl. Cosmic Ray Conf., Munich, Ger. (Aug. 1975), 14 CRG, Vol. 4, MG Session and Pioneer Symp.

SMART, D. F., SHEA, M. A., and DODSON, H. W., HEDEMAN, E. R. (McMath-Hulbert Obsv., Univ. of Mich.)
Distribution of Proton Producing Flares Around the Sun
Space Res. XVI, Akademie-Verlag, Berlin, Ger. (1976)

STROSCIO, M. A., 1ST LT.
Improved Vertex Contribution to the Decay Rate of Orthopositronium
Phys. Ltrs. A (Amsterdam, The Netherlands/November 1974)
Double Vertex Contribution to the Decay Rate of Orthopositronium
Phys. Ltrs. A, Vol. 50A (1975)
Positronium: A Review of the Calculations
Atomic Phys., Vol. 6 (1975)

STROSCIO, M. A., 1ST LT., KATZ, L., YATES, G. K., and SELLERS, B., HANSER, F. A. (Panametrics, Inc., Waltham, Mass.)
Abundances of Solar Cosmic Ray Protons and Alpha Particles for 1969-1972
J. of Geophys. Res., Vol. 81, No. 1 (January 1975)

VANCOUR, R. P., and SELLERS, B., HANSER, F. A. (Panametrics, Inc., Waltham, Mass.)
Bremsstrahlung Effects in Auroral Electron Precipitation Event Absorption
J. of Atm. and Terrestrial Phys., Vol. 38 (1976)

WEBBER, W. R., LEZNIAK, J. A. (Univ. of N. H.), SHEA, M. A., and SMART, D. F.
Geomagnetic Cut-Offs at 1.7 and 2.6 GV-Transmission Functions and Isotopic Analysis of Cosmic Ray Nuclei
Proc. of 14th Intl. Cosmic Ray Conf., Munich, Ger. (Aug. 1975), 14 CRG, Vol. 4, MG Session and Pioneer Symp.

WILDMAN, P. J. L., SAGALYN, R. C., and AHMED, M. (Regis Coll., Weston, Mass.)
Structure and Morphology of the Main Plasma Trough in the Topside Ionosphere
EOS, Proc. of 1976 Spring Ann. Am. Geophys. Union Mtg. (April 1976);
Proc. of COSPAR Satellite Beacon Gp. Symp. (June 1976)

PAPERS PRESENTED AT MEETINGS JULY 1974 - JUNE 1976

AHMED, M. (Regis Coll., Weston, Mass.), and SAGALYN, R. C., SMIDDY, M.

The Morphology of Small Scale Thermal Ionization Irregularities at Height Latitudes Deduced from ISIS-I Satellite Measurements
Iono. Eff. Symp., Arlington, Va. (20-22 January 1975)

BURKE, W. J. (Regis Coll., Weston, Mass.), SAGALYN, R. C., and DU LONG, D. D. (Regis Coll.)

Injun 5 Observations of Low Energy Electrons in the Evening Sector Topside Ionosphere
1976 Spring Ann. Mtg. of the Am. Geophys. Union, Wash., D. C. (12-16 April 1976)

DRYER, M. (Natl. Oceanic and Atm. Adm., Boulder, Colo.), and SHEA, M. A.

Cooperation with the SCOSTEP Project: Study of Traveling Interplanetary Phenomena (STIP)
Solar Flare Build-Up Study, Falmouth, Cape Cod, Mass. (8-11 September 1975)

DUBS, C. W.

Correlation of Ecliptic IMF with Polar Geomagnetic Field
56th Ann. Am. Geophys. Union Mtg., Wash., D. C. (16-20 June 1975)

DU LONG, D. D., DOUCETTE, J. (Emmanuel Coll., Boston, Mass.), and SAGALYN, R. C.

Small-Scale Irregularities at Low Latitudes in the Topside Ionosphere
1976 Spring Ann. Mtg. of the Am. Geophys. Union, Wash., D. C. (12-16 April 1976)

FILZ, R. C.

Evidence for an Energy and L Value, Selective Decrease in 12 to 48 MeV Inner Zone Trapped Protons in April 1973
Am. Phys. Soc. Spring Mtg., Wash., D. C. (26-29 April 1976)

FILZ, R. C., and HOLEMAN, E. (Emmanuel Coll., Boston, Mass.)

Low Altitude Inner Zone Trapped Proton Angular Distributions
56th Ann. Am. Geophys. Union Mtg., Wash., D. C. (16-20 June 1975)

FOUGERE, P. F.

Spontaneous Line Splitting of Short Signals in Maximum Entropy Power Spectra
56th Ann. Am. Geophys. Union Mtg., Wash., D. C. (16-20 June 1975)

A Solution to the Problem of Spontaneous Line Splitting in Maximum Entropy Power Spectrum Analysis
1975 Fall Am. Geophys. Union Mtg., San Francisco, Calif. (8-12 December 1975)

FOUGERE, P. F., ZAWALICK, E. J., MC CLAY, J. F., RADOSKI, H. R., PAZICH, P. M., KNECHT, D. J., HUTCHINSON, R. O., TSACOYEANES, C. W., and CANTOR, C. (Emmanuel Coll., Boston, Mass.)

Maximum Entropy Spectrum from the AFGL Magnetometer Network: First Results
1976 Spring Ann. Mtg. of the Am. Geophys. Union, Wash., D. C. (12-16 April 1976)

FOUGERE, P. F., ZAWALICK, E. J., and RADOSKI, H. R.

Spontaneous Line Splitting in Maximum Entropy Power Spectrum Analysis
16th Gen. Asbly. of the Intl. Union of Geod. and Geophys. (IUGG), Grenoble, Fr. (25 August-6 September 1975)

FUKUI, K., and BEAUJEAN, R., ENGE, W. (Institut fuer Reine und Angewandte Kernphysik, Univ. of Kiel, Ger.)

Low Energy Beryllium Isotopes Detected with Plastic Detector
Symp. on Meas. and Interpretation of the Isotopic Composition of Solar and Galactic Cosmic Rays, Univ. of N. H., Durham, N. H. (9-11 October 1974)

GOLD, R. E. (Univ. of N. H.), SHEA, M. A., and SMART, D. F.

A Preliminary Idealized Network of Neutron Monitors for the Study of Solar Modulation
14th Intl. Cosmic Ray Conf., Munich, Fed. Rep. of Ger. (15-29 August 1975)

KLECKNER, E. W., SMITH, L. L. (Battelle-Northwest Labs., Richland, Wash.), and WILDMAN, P. J. L.

A Reassessment of the Location of SAR-Arcs Relative to the Plasmapause
Am. Geophys. Union 1974 Fall Ann. Mtg., San Francisco, Calif. (12-17 December 1974)
21st Pacific Northwest Regional Mtg., Richland, Wash.

LEZNIAK, J. A. (Univ. of N. H.), SMART, D. F., and SHEA, M. A.

The Effect of Ionization Energy Loss on the Calculation of Rigidity Transmittance Functions
14th Intl. Cosmic Ray Conf., Munich, Fed. Rep. of Ger. (15-29 August 1975)

LEZNIAK, J. A., WEBBER, W. R. (Univ. of N. H.), SMART, D. F., SHEA, M. A., and SAWYER, D. M. JR. (Programming Methods, Inc., Silver Spring, Md.)
The Effect of Ionization Energy Loss on the Cutoff Rigidities Appropriate for Cosmic-Ray Nuclei Observations at Balloon Altitudes
Am. Geophys. Union 1974 Fall Ann. Mtg., San Francisco, Calif. (12-17 December 1974)

MC NULTY, P. J., PEASE, V. P., BOND, V. P. (Clarkson Coll. of Technol., Potsdam, N. Y.), FILZ, R. C., and ROTHWELL, P. L.
Particle Induced Visual Phenomena in Space
19th Plenary Mtg. of Comm. on Space Res. (COSPAR), Philadelphia, Pa. (8-18 June 1976)

NOLTE, J. T. (Am. Sci. & Engrg., Inc., Cambridge, Mass.), SMART, D. F., and GOLD, R. E. (Univ. of N. H.), ROELOF, E. C. (The Johns Hopkins Univ., Silver Spring, Md.)
Examination of Superimposed Solar Proton Event Spectra and Anisotropy Measurements
Am. Geophys. Union 1974 Fall Ann. Mtg., San Francisco, Calif. (12-17 December 1974)

PAVEL, A. L., COHEN, H. A., KATZ, L., and SAGALYN, R. C.
Active Spacecraft Charging Experiments on the SCATHA Satellite
Symp. on Active Exper. in Space Plasmas, Boulder, Colo. (3-5 June 1976)

PAVEL, A. L., ROTHWELL, P. L., RUBIN, A. G., and KATZ, L.
Computer Simulation of Trapped Trajectories and Velocity Distributions in a Satellite Sheath
56th Ann. Am. Geophys. Union Mtg., Wash., D. C. (16-20 June 1975)

PAZICH, P. M., 1ST LT.
Simultaneous Observations of the Interplanetary Magnetic Field by Two Satellites
56th Ann. Am. Geophys. Union Mtg., Wash., D. C. (16-20 June 1975)

RADOSKI, H. R.
Hydromagnetic Waves: Temporal Development of Coupled Models
56th Ann. Am. Geophys. Union Mtg., Wash., D. C. (16-20 June 1975)

RADOSKI, H. R., ZAWALICK, E. J., and FOUGERE, P. F.
The Superiority of Maximum Entropy Power Spectrum Techniques Applied to Geomagnetic Micropulsations
16th Gen. Asbly. of the Intl. Union of Geod. and Geophys. (IUGG), Grenoble, Fr. (25 August-6 September 1975)

RAO, Y. V. (Dublin Inst. for Adv. Studies, Dublin, Ire.), FUKUI, K., and YOUNG, P. S. (Miss. State Univ.)
Multiple Coulomb Scattering Parameters in Emulsions Exposed to High Energy Heavy Ion Beams
Am. Phys. Soc. Spring Mtg., Wash., D. C. (26-29 April 1976)

ROTHWELL, P. L.
Spacecraft Charging – Simulation of the Plasma Sheath
IEMCAP Course, Syracuse Univ., Syracuse, N. Y. (June 1976)

ROTHWELL, P. L., RUBIN, A. G., PAVEL, A. L., and KATZ, L.
Simulation of the Plasma Sheath Surrounding a Charged Spacecraft
56th Ann. Am. Geophys. Union Mtg., Wash., D. C. (16-20 June 1975)

RUBIN, A. G., and FILZ, R. C.
Geomagnetically Trapped Alpha Particles from 18-47 MeV
56th Ann. Am. Geophys. Union Mtg., Wash., D. C. (16-20 June 1975)

SAGALYN, R. C., and BURKE, W. J., KANAL, M. (Regis Coll., Weston, Mass.)
On the Heating of Plasma Trough Electrons
Intl Symp. on Solar Terrestrial Phys., Boulder, Colo. (8-18 June 1976)

SAGALYN, R. C., PHELPS, A. D. R., and AHMED, M. (Regis Coll., Weston, Mass.)
In-Situ Measurements of the Structure and Spectral Characteristics of Small Scale F Region Ionospheric Irregularities
Iono. Eff. Symp., Arlington, Va. (20-22 January 1975)

SELLERS, B., HANSER, F. A., MOREL, P. R., HUNERWADEL, J. L. (Panametrics, Inc., Waltham, Mass.), and PAVEL, A. L., KATZ, L., ROTHWELL, P. L.
Design and Calibration of a High Time Resolution Spectrometer for .05 to 500 keV Electrons and Protons
56th Ann. Am. Geophys. Union Mtg., Wash., D. C. (16-20 June 1975)

SHAPLEY, A. H. (Envmt. Data Svc., Natl. Oceanic and Atm. Admin., Boulder, Colo.), and SHEA, M. A.
International Program for Solar-Terrestrial Monitoring and Data Exchange
Am. Geophys. Union 1974 Fall Ann. Mtg., San Francisco, Calif. (12-17 December 1974)

SHEA, M. A., and SMART, D. F.
A Summary of Solar Particle and Related Observations During the Campaign for Integrated Observations of Solar Flares (CINOF)
Am. Geophys. Union 1974 Fall Ann. Mtg., San Francisco, Calif. (12-17 December 1974)
The Application of the International Geomagnetic Reference Field to Cosmic-Ray Trajectory Calculations
Am. Geophys. Union Mtg. (Zmuda Memorial Conf. on Geomag. Field Models), Colo. Springs, Colo. (24-25 March 1975)
A Comparison of Vertical Cosmic-Ray Cutoff Rigidities as Calculated with Different Geomagnetic Field Models Variations of the Calculated Cosmic-Ray Equator Over a 20-Year Interval
A Five by Fifteen Degree World Grid of Calculated Cosmic-Ray Vertical Cutoff Rigidities for 1965 and 1975
14th Intl. Cosmic Ray Conf., Munich, Fed. Rep. of Ger. (15-29 August 1975)

SHEA, M. A., SMART, D. F. and MOOMEY, W. R., 1ST LT.
Cutoff Rigidities and Transmittance Functions for Selected Cosmic-Ray Balloon Measurement Sites
Symp. on Meas. and Interpretation of the Isotopic Composition of Solar and Galactic Cosmic Rays, Univ. of N.H., Durham, N.H. (9-11 October 1974)

SILVERMAN, S. M.
A Brief Overview of the Contributions of Rayleigh to the Study of Airglow and Aurora
1975 Fall Am. Geophys. Union Mtg., San Francisco, Calif. (8-12 December 1975)

SILVERMAN, S. M., and KORFF, D. F. (Regis Coll., Weston, Mass.)
Solar Sector Effects on Near-Earth Atmospheric Electric Fields at Thule, Greenland
Symp. on High Atm. and Space Problems of Atm. Elec., Grenoble, Fr. (30 August 1975)

SMART, D. F. (Inv. Paper)
Geomagnetic Effects on Cosmic Rays
14th Intl. Cosmic Ray Conf., Munich, Fed. Rep. of Ger. (15-29 August 1975)

SMART, D. F., and SHEA, M. A.
Vertical and Angular Cutoff Rigidities for Selected Cosmic-Ray Balloon Measurement Sites
Am. Geophys. Union 1974 Fall Ann. Mtg., San Francisco, Calif. (12-17 December 1974)
An Analysis of Trajectory-Derived Penumbral Widths
Cosmic-Ray Penumbral Effects for Selected Balloon Launching Locations
14th Intl. Cosmic Ray Conf., Munich, Fed. Rep. of Ger. (15-29 August 1975)

SMART, D. F., SHEA, M. A., and DODSON, H. W., HEDEMAN, E. R. (McMath-Hulbert Obsv., Univ. of Mich.)
Distribution of Proton Producing Flares Around the Sun
Comm. on Space Res. (COSPAR) Mtg., Varna, Bulgaria (29 May-7 June 1975)

STROSCIO, M. A., KATZ, L., and GARRETT, H. B.
Time-Dependent Diffusion Coefficient for Charged Particle Distributions in Stochastic Magnetic Fields
1974 Fall Mtg. of New Eng. Section of Am. Phys. Soc., Clark Univ., Worcester, Mass. (25-26 October 1974)

STROSCIO, M. A., KATZ, L., YATES, G. K., and SELLERS, B., HANSER, F. A. (Panametrics, Inc., Waltham, Mass.)
1969 to 1972 Abundances of Solar Cosmic Ray Protons and Alpha Particles
56th Ann. Am. Geophys. Union Mtg., Wash., D. C. (16-20 June 1975)

WEBBER, W. R., LEZNIAK, J. A. (Univ. of N. H.), SHEA, M. A., and SMART, D. F.
Geomagnetic Cut-Offs at 1.7 and 2.6 GV-Transmission Functions and Isotopic Analysis of Cosmic Ray Nuclei
14th Intl. Cosmic Ray Conf., Munich, Fed. Rep. of Ger. (15-29 August 1975)

WILDMAN, P. J. L., SAGALYN, R. C., and AHMED, M. (Regis Coll., Weston, Mass.)
Structure and Morphology of the Main Plasma Trough in the Topside Ionosphere
1976 Spring Ann. Mtg. of the Am. Geophys. Union, Wash., D. C. (12-16 April 1976)
Symp. of the Comm. on Space Res. (COSPAR) Beacon Satellite Gp., Boston Univ., Mass. (1-4 June 1976)

ZAWALICK, E. J., RADOSKI, H. R., and FOUGERE, P. F.
Multiplet Structure in Micropulsation Spectra
1975 Fall Am. Geophys. Union Mtg., San Francisco, Calif. (8-12 December 1975)

TECHNICAL REPORTS JULY 1974 - JUNE 1976

FILZ, R. C., and KATZ, L.
An Analysis of Imperfections in DMSP Photographs Caused by High Energy Solar and Trapped Protons
AFCRL-TR-74-0469 (19 September 1974)

FUKUI, K., and ENGE, W., BEAUJEAN, R., BARTHOLOMA, K. P. (Institut fuer Reine und Angewandte Kernphysik, Kiel, Ger.)
Use and Processing of Plastics as Particle Detectors
AFCRL-TR-75-0223 (22 April 1975)

HOLEMAN, E. (Emmanuel Coll., Boston, Mass.), and FILZ, R. C.
An Analysis of Imperfections in DMSP Photographs Caused by High Energy Solar and Trapped Protons
AFCRL-TR-74-0469 (19 September 1974)
Proton Flux Data Obtained on Air Force Satellite 72-1 Over the Period October 1972 to February 1973
AFCRL-TR-75-0377 (June 1975)

MC CLAY, J. F.
Pc1 and Pc5 Micropulsation Polarization Patterns
AFCRL-TR-75-0307 (May 1975)

MC NULTY, P. J., FILZ, R. C., and ROTHWELL, P. L.
Role of Nuclear Stars in the Light Flashes Observed on Skylab 4
AFGL-TR-76-0151 (May 1976)

PAVEL, A. L., CAPT.
Plasma Heating Through Parametrically Induced Turbulence
AFGL-TR-76-0116 (2 June 1976)

PAVEL, A. L., CAPT., and KATZ, L.
Plasma Environment of a Synchronous Orbit Satellite
AFGL-TR-76-0028 (17 February 1976)

PAZICH, P. M., CAPT.
Conditional Probabilities of the Geomagnetic Index A_p
AFGL-TR-76-0034 (23 February 1976)

RADOSKI, H. R.
Hydromagnetic Waves: Temporal Development of Coupled Modes
AFGL-TR-76-0104 (6 May 1976)

RUBIN, A. G.
Resistivity of Dense Copper Vapor
AFGL-TR-76-0067 (5 April 1976)

RUBIN, A. G., BESSE, A., and COHN, A.
Radiation from Hydrogen-Argon Mixtures
AFCRL-TR-74-0522 (18 October 1974)

SHEA, M. A., and SMART, D. F.
Asymptotic Directions and Vertical Cutoff Rigidities for Selected Cosmic-Ray Stations as Calculated Using the Finch and Leaton Geomagnetic Field Model
AFCRL-TR-75-0177 (1 April 1975)
Tables of Asymptotic Directions and Vertical Cutoff Rigidities for a Five Degree by Fifteen Degree World Grid as Calculated Using the International Geomagnetic Reference Field for Epoch 1975. 0
AFCRL-TR-75-0185 (3 April 1975)
Tables of Asymptotic Directions and Vertical Cutoff Rigidities for a Five Degree by Fifteen Degree World Grid as Calculated Using the International Geomagnetic Reference Field for Epoch 1965.0
AFCRL-TR-75-0381 (17 July 1975)
Asymptotic Directions and Vertical Cutoff Rigidities for Selected Cosmic-Ray Stations as Calculated Using the International Geomagnetic Reference Field Model Appropriate for Epoch 1975.0
AFCRL-TR-75-0247 (5 May 1975)
Editors, *Results Obtained During the Campaign for Integrated Observations of Solar Flares (CINOF)*
AFCRL-TR-75-0437 (13 August 1975)
An Analysis of the Solar Particle Data Obtained During CINOF
Results Obtained During the Campaign for Integrated Observations of Solar Flares (CINOF), AFCRL-TR-75-0437 (13 August 1975)

SHEA, M. A., SMART, D. F., and CARMICHAEL, H.
Summary of Cutoff Rigidities Calculated with the International Geomagnetic Reference Field for Various Epochs
AFGL-TR-76-0115 (26 May 1976)

SHEA, M. A., SMART, D. F., and MC CALL, J. R., GUMM, B. S. (Univ. of Calif., Lawrence Livermore Lab.)
Tables of Vertical Cutoff Rigidities for Epochs 1955 and 1960
AFCRL-TR-74-0550 (4 November 1974)
Tables of Non-Vertical Cutoff Rigidities for 76 Various Locations
AFCRL-TR-75-0008 (30 December 1974)
Tables of Asymptotic Directions and Vertical Cutoff Rigidities for a Five Degree by Fifteen Degree World Grid Using the Finch and Leaton Geomagnetic Field Model
AFCRL-TR-75-0042 (22 January 1975)

SILVERMAN, S. M., and MULLEN, E. G.
Sky Brightness During Eclipses: A Compendium from the Literature
AFCRL-TR-74-0363 (5 August 1974)

STROSCIO, M. A., 1ST LT., and SELLERS, B. (Panametrics, Inc., Waltham, Mass.)

Atmospheric Response Function for the Calculation of Riometer Absorption
AFCRL-TR-74-0472 (27 September 1974)

WILDMAN, P. J. L.
Studies of Low-Energy Plasma Motion: Results and a New Technique
AFGL-TR-76-0168 (25 June 1976)

IONOSPHERIC PHYSICS DIVISION

JOURNAL ARTICLES JULY 1974 - JUNE 1976

AARONS, J.
High Latitude F Layer Irregularities During the Magnetic Storm of October 31-November 1, 1972
J. of Geophys. Res., Vol. 81 (February 1976)

AARONS, J., and MARTIN, E. (Emmanuel Coll., Boston, Mass.)
The Effects of the August 1972 Magnetic Storms on Ionospheric Scintillations
Rad. Sci., Vol. 10 (June 1975)

ALLEN, R. S.
Modeling the Topside of the F Region
Proc. of Iono. Eff. Symp., Wash., D. C. (Jan. 1975), J. W. Goodman, Ed. (Naval Res. Lab.)

BABCOCK, R. R., and PARKER, J. T. (Palehua Obsv., Haw.)
Spectral Characteristics of Solar Radio Bursts Associated with Shortwave Fadeouts
J. of Atm. and Terrestrial Phys., Vol. 37 (1975)

BASU, S.
Universal Time Seasonal Variations of Auroral Zone Magnetic Activity and VHF Scintillations
J. of Geophys. Res., Vol. 80 (December 1975)

CASTELLI, J. P., and CARRIGAN, A. L. (Space Phys. Lab.), KO, H. C. (Ohio State Univ.)
Spectral Association of the 7 August 1972 Solar Radio Burst with Particle Acceleration
Coronal Disturbances, Proc. of IAU Symp. #57, Gordon Newkirk, Jr., Ed., D. Reidel Pub. Co., Dordrecht, Holl. (1974)

CASTELLI, J. P., and GUIDICE, D. A.
Verification of Solar Patrol Calibration at 15.4 GHz
Astrophys. Ltrs., Vol. 16 (1975)
Impact of Current Solar Radio Patrol Observations
Vistas in Astron., Vol. 19 (1976), Pergamon Press

CASTELLI, J. P., GUIDICE, D. A., and KALAGHAN, P. M.
Millimeter Wave Solar Observations
IEEE Trans. on Microwave Theory and Techniques, Vol. MTT-22, No. 12 (December 1974), Pt. II

DANDEKAR, B. S.
Simplified Formula for the Determination of the Altitude of an Auroral Arc from a Single Station
J. of Atm. and Terrestrial Phys., Vol. 36 (1974)

GUIDICE, D. A.
Sagamore Hill Radio Observatory (Observatory Reports)
Bull. of Am. Astronom. Soc., Vol. 7, No. 1 (January 1975)
Sagamore Hill Radio Observatory (Observatory Reports)
Bull. of Am. Astronom. Soc., Vol. 8, No. 11 (1976)

GUIDICE, D. A., and CASTELLI, J. P.
Spectral Distributions in Microwave Bursts
Solar Phys., Vol. 44, No. 1 (1975)

HALL, W. N.
Mid-Latitude Pulsating Aurorae
Planetary Space Sci., Vol. 22 (1974)

KALAGHAN, P. M.
Limb Brightening at Millimeter Wavelengths
Solar Phys., Vol. 39, No. 2 (December 1974)

KLOBUCHAR, J. A.
Polarization of VHF Waves Emitted from Geostationary Satellites
J. of Geophys. Res., Vol. 80, No. 31 (1 November 1975)

LOVELL, R. R., STEVENS, N. J. (NASA Lewis Res. Ctr., Cleveland, Oh.), SCHOBER, W. (SAMSO, Los Angeles, Calif.), PIKE, C. P., and LEHN, W. (AF Mat. Lab., Wright-Patterson AFB, Oh.)
Spacecraft Charging Investigations: A Joint Research and Technology Program
Am. Inst. of Aero. and Astro. Progress Ser., N. Y., Vol. 47 (1976)

MENDILLO, M. (Boston Univ., Mass.) HAWKINS, G. S. (Smithsonian Astrophys. Obsv., Cambridge, Mass.), and KLOBUCHAR, J. A.
A Large-Scale Hole in the Ionosphere Caused by the Launch of Skylab
Sci. (31 January 1975)
A Sudden Vanishing of the Ionospheric F Region Due to the Launch of Skylab
J. of Geophys. Res., Vol. 80 (June 1975)

MENDILLO, M., and KLOBUCHAR, J. A.
Investigations of the Ionospheric F-Region Using Multi-Station Total Electron Content Observations
J. of Geophys. Res., Vol. 80 (February 1975)

PIKE, C. P.
DAPP Satellite Observations of Aurora
EOS, Trans. of Am. Geophys. Union, Vol. 55, No. 6 (1974)

PIKE, C. P., and BUNN, M. H. (SAMSO, Los Angeles, Calif.)
A Correlation Study Relating Spacecraft Anomalies to Environmental Data
Am. Inst. of Aero. and Astro. Progress Ser., N. Y., Vol. 47 (1976)

PIKE, C. P., and MENG, C. I. (Space Sci. Lab., Univ. of Calif., Berkeley), AKASOFU, S. I. (Geophys. Inst., Univ. of Alaska), WHALEN, J. A.
Observed Correlations Between Interplanetary Magnetic Field Variations and the Dynamics of the Auroral Oval and the High-Latitude Ionosphere
J. of Geophys. Res., Vol. 79, No. 34 (7 December 1974)

PRASAD, B.
A Classical "MASER" Action in a Hot Uniform Plasma Enhanced Coherent Raman Emission from Uniform Plasmas
Phys. of Fluids, Vol. 19 (March 1976)

RUSH, C. M.
Limitations of Mapping Techniques to Predicting Total Electron Content at a Distant Point
Proc. of Symp. on Eff. of the Iono. on Space Sys. and Comm. (December 1975)

RUSH, C. M., and EDWARDS, W. R., JR., MAJ.
Sensitivity of HF Circuit Simulations to Electron Density Models
Rad. Sci., Vol. 10, No. 10 (October 1975)

RUSH, C. M., and ELKINS, T. J.
An Assessment of the Magnitude of the F-Region Absorption on HF Radio Waves Using Realistic Electron Density and Collision Frequency Models
The J. of the Intl. Telecomm. Union (August 1975)

RUSH, C. M., and MILLER, D., GIBBS, J. (Arcon Corp., Wakefield, Mass.)
The Relative Daily Variability of foF2 and hmF2 and Their Implication on HF Radio Propagation
Rad. Sci., Vol. 9, No. 8 and 9 (August-September 1974)

SIZOO, A. H. (Boston Coll., Chestnut Hill, Mass.), and WHALEN, J. A.
Lightning and Squall Line Identification from DMSP Satellite Photographs
Proc. of 6th Conf. on Aerosp. and Aero. Met. (AMS), El Paso, Tex. (12-15 November 1974)

SLACK, F. F., and MAJKOWICZ, L. A. (Dept. of Phys., Univ. of Queensland, Aus.)
Further Comments on Quasi-Periodic Scintillations in Radio-Satellite Transmissions
J. of Atm. and Terrestrial Phys., Vol. 38 (1976)

SNYDER, A. L., JR., and AKASOFU, S.-I. (Geophys. Inst., Univ. of Alaska)
Auroral Oval Photographs from the DMSP 8531 and 10533 Satellites
J. of Geophys. Res., Vol. 81, No. 10 (1976)

STRAKA, R. M., and PAPAGIANNIS, M. D., KOGUT, J. A. (Boston Univ.)
Study of a Filament with a Circularly Polarized Beam at 3.8 Cm
Solar Phys., Vol. 45 (1975)

TOMAN, K.
On Wavelike Perturbations in the F Region
Rad. Sci. (February 1976)

WHITNEY, H. E., and AARONS, J.
Amplitude Scintillation Observations and Systems Application
Proc. of AGARD Specialists Mtg. of EM Wave Propagation Panel on Rad. Sys. and the Iono., Athens, Greece (May 1975)

PAPERS PRESENTED AT MEETINGS JULY 1974 - JUNE 1976

AARONS, J.
Global Morphology of Ionospheric Scintillations II

Symp. of the Com. on Space Res. (COSPAR) Beacon Satellite Gp., Moscow, USSR (25-29 November 1974)

High Latitude Morphology of Ionospheric Scintillations
Symp. on Eff. of the Iono. on Space Sys. and Comm., Wash., D. C. (20-22 January 1975)

High Latitude F Layer Irregularities During the Magnetic Storm of Oct. 31-Nov. 1, 1972
1975 Intl. IEEE/AP-S Symp. and USNC/URSI Mtg., Univ. of Ill., Urbana, Ill. (2-5 June 1975)

Equatorial Scintillations: A Review
High Latitude Scintillations During Magnetic Activity
18th Gen. Asbly. of Intl. Union of Rad. Sci. (URSI), Lima, Peru (11-19 August 1975)

AARONS, J., BASU, S., and MARTIN, E. (Emmanuel Coll., Boston, Mass.)
The Stormtime Component of Scintillations
Symp. of the Com. on Space Res. (COSPAR) Beacon Satellite Gp., Boston Univ., Boston, Mass. (1-4 June 1976)

AARONS, J., and HAWKINS, G. S. (U. S. Inf. Agcy., Wash., D. C.), MARTIN, E. (Emmanuel Coll., Boston, Mass.)
The Seasonal Pattern of High Latitude F-Layer Irregularities
1975 USNC/URSI-IEEE Mtg., Boulder, Colo. (20-23 October 1975)

AARONS, J., and ROBERTS, L. W. (Transp. Sys. Ctr., Dept. of Trnsp., Cambridge, Mass.)
Brief Report on Propagation Problems of a Satellite Solar Power System
Mtg. of the Electmg. Propagation Panel (AGARD), Paris, Fr. (21 October 1974)

AARONS, J., WHITNEY, H., MULLEN, J. P., HAWKINS, G. S., and BUSHBY, A., LANAT, J. (Instituto Geophys. del Peru, Lima, Peru), DOS SANTOS LUCENA, L. (UFRAN, Natal, Brazil)
The Nature and Occurrence of Equatorial Scintillation
18th Gen. Asbly. of Intl. Union of Rad. Sci. (URSI), Lima, Peru (11-19 August 1975)

ALLEN, R. S.
Modeling the Topside of the F Region
Symp. on Eff. of the Iono. on Space Sys. and Comm., Wash., D. C. (20-22 January 1975)

BARRON, W. R., and BAKSHI, P. (Boston Coll., Chestnut Hill, Mass.)
Spectral Correlations Between Solar Flare Radio Bursts and Associated Proton Fluxes
1974 USNC/URSI-IEEE Mtg., Boulder, Colo. (14-17 October 1974)

BASU, S.
Magnetically Conjugate Mid-Latitude Irregularity Structures Observed with OGO-6
1976 Spring Ann. Mtg. of the Am. Geophys. Union, Wash., D. C. (12-16 April 1976)

BASU, S. (Emmanuel Coll., Boston, Mass.), and AARONS, J.
Daytime VHF Scintillations at Huancayo and the Equatorial Electrojet
Symp. of the Com. on Space Res. (COSPAR) Beacon Satellite Gp., Boston Univ., Boston, Mass. (1-4 June 1976)

BASU, S., and BASU, S. (Emmanuel Coll., Boston, Mass.)
Correlated Measurements of Scintillations and In-Situ F-Region Irregularities from OGO-6
Symp. of the Com. on Space Res. (COSPAR) Beacon Satellite Gp., Boston Univ., Boston, Mass. (1-4 June 1976)

BIBL, K. (Lowell Technol. Inst. Res. Fdn., Lowell, Mass.), PFISTER, W., REINISCH, B. W. (LTI Res. Fdn.), and SALES, G. S.
Motions in the Upper Atmosphere Using Spectral Data from Spaced Antennas
Conf. on the Upper Atm. (Am. Met. Soc.), Atlanta, Ga. (30 September-4 October 1974)

CASTELLI, J. P., GUIDICE, D. A., and AARONS, J.
Comparison of Morphology and Spectra of August 7, 1972 Outburst at Microwaves and Hard X-Rays
18th Gen. Asbly. of Intl. Union of Rad. Sci., Lima, Peru (11-19 August 1975)

CHACKO, C. C., MENDILLO, M. (Boston Univ., Boston, Mass.), and PIKE, C. P.
A Representation for the Ionospheric Electron Density Trough
1976 Spring Ann. Mtg. of the Am. Geophys. Union, Wash., D. C. (12-16 April 1976)

CHERNOSKY, E. J., and GARRETT, H. B.
Geomagnetic Activity as Related to Day-to-Day Changes in Sunspot Count
56th Ann. Am. Geophys. Union Mtg., Wash., D. C. (16-20 June 1975)

CHERNOSKY, E. J., and KLOBUCHAR, J. A.
Diurnal Rates of Change in TEC Observed from Cape Kennedy-ATS 3
Jt. Satellite Studies Gp. Mtg., No. Andover, Mass. (7-9 June 1976)

CORMIER, R. J., and LORENTZEN, A. H.
Digital Ionospheric Sounding and Subsequent Automatic Processing
Mitre/Bedford Amateur Rad. Club, Bedford, Mass. (5 February 1975)

DU LONG, D. D. (Regis Coll., Weston, Mass.), and ALLEN, R. S.
Specification of Navigation and Radar Errors Caused by the Ionosphere
Symp. of the Com. on Space Res. (COSPAR) Beacon Satellite Gp., Boston Univ., Boston, Mass. (1-4 June 1976)

ELKINS, T. J.
High Frequency Adaptive Communications
Allied Rad. Freq. Agcy. Symp., NATO Hq., Brussels, Belgium (18-21 November 1975)

KALAGHAN, P. M.
Solar Limb Brightening at Millimeter Wavelengths
143rd Mtg. of the Am. Astronom. Soc., Rochester, N. Y. (20-23 August 1974)

KLOBUCHAR, J.
Problems in Ionospheric Time Delay Modeling for Satellite Positioning Systems
AGARD Specialists Mtg. of the Electmg. Wave Propagation Panel, Athens, Greece (26-30 May 1975)
Initial Polarization Transmitted at VHF from Geostationary Satellite Beacons
A Comparison of Total Electron Content as Determined from Group Path Delay and Faraday Measurements
1975 Intl. IEEE/AP-S Symp. and USNC/URSI Mtg., Univ. of Ill., Urbana, Ill. (2-5 June 1975)
Average Behavior of the Ionospheric F-Region at L=4
1976 Spring Ann. Mtg. of the Am. Geophys. Union, Wash., D. C. (12-16 April 1976)
A Review of Ionospheric Time Delay Limitations to Ranging Systems
Symp. of the Com. on Space Res. (COSPAR) Beacon Satellite Gp., Boston Univ., Boston, Mass. (1-4 June 1976)

KLOBUCHAR, J. A., and HAWKINS, G. S.
(Smithsonian Astrophys. Obsv., Cambridge, Mass.)
Seasonal and Diurnal Variations in the Total Electron Content of the Ionosphere at Invariant Latitude 54 Degrees
On the Determination of Mid-Latitude Ionospheric Time Delay from foF2
Symp. on Eff. of the Iono. on Space Sys. and Comm., Wash., D. C. (20-22 January 1975)

KLOBUCHAR, J. A., and HOSSEINIEH, H. H.
(Emmanuel Coll., Boston, Mass.)
Seasonal and Solar Flux Dependence of Mid-Latitude Slab Thickness
1974 USNC/URSI-IEEE Mtg., Boulder, Colo. (14-17 October 1974)

KRUKONIS, A. P., and WHALEN, J. A.
Lifetimes of Bright, Active, Expanded Auroras Near Midnight
1976 Spring Ann. Mtg. of the Am. Geophys. Union, Wash., D. C. (12-16 April 1976)

MARTIN, E. (Emmanuel Coll., Boston, Mass.), and AARONS, J.
F-Layer Scintillations and the Aurora
Symp. on Eff. of the Iono. on Space Sys. and Comm., Wash., D. C. (20-22 January 1975)

MENDILLO, M. (Boston Univ., Boston, Mass.), and HAWKINS, G. S., KLOBUCHAR, J. A.
A Large-Scale "Hole" in the Ionospheric F-Region Caused by the Launch of Skylab
1974 USNC/URSI-IEEE Mtg., Boulder, Colo. (14-17 October 1974)

MENDILLO, M. (Boston Univ., Boston, Mass.), and KLOBUCHAR, J. A.
Seasonal Effects in Ionospheric Storms
COSPAR-URSI Symp. on Beacon Satellite Investigations of the Iono. Structure and ATS-6 Data, Moscow, USSR (24-29 November 1974)

MOORE, J. G.
Airborne Optical Measurements of Dayside Polar Airglow and Aurora
56th Ann. Am. Geophys. Union Mtg., Wash., D. C. (16-20 June 1975)

MULLEN, E. G.
Central Polar Cap (OI) λ 5577 Å Night Airglow
Am. Geophys. Union Fall Mtg., San Francisco, Calif, (8-12 December 1975)

MULLEN, J. P., and AARONS, J.
Scintillations Observed through the Magnetospheric Cleft
Symp. of the Com. on Space Res. (COSPAR) Beacon Satellite Gp., Boston Univ., Boston, Mass. (1-4 June 1976)

MULLEN, J. P., and HAWKINS, G. S.
Daytime Equatorial Scintillations in VHF Trans-Ionospheric Radio Wave Progagation from ATS-3 at Huancayo, Peru

1974 USNC/URSI-IEEE Mtg., Boulder, Colo. (14-17 October 1974)

Equatorial Scintillations at 136 MHz Observed Over Half a Sunspot Cycle
Symp. on Eff. of the Iono. on Space Sys. and Comm., Wash., D. C. (20-22 January 1975)

PAPAGIANNIS, M. D. (Boston Univ., Mass.), STRAKA, R. M., and KOGUT, J. A. (Boston Univ., Mass.)

Analysis of Active Region SFC 158/73
147th Mtg. of Am. Astronom. Soc., Chicago, Ill. (December 1975)

PAPAGIANNIS, M. D., (Boston Univ., Mass.), STRAKA, R. M., KOGUT, J. A., and TYLER, J. E. (Boston Univ., Mass.)

Solar Radio Observations at 3.8 Cm with the 120-Foot Haystack Antenna
Am. Geophys. Union 1974 Fall Ann. Mtg., San Francisco, Calif. (12-17 December 1974)

PFISTER, W., and SALES, G. S.

Spectral Analysis of F-Region "Drift" Measurements in Goose Bay, Labrador
18th Gen. Asbly. of Intl. Union of Rad. Sci. (URSI), Lima, Peru (11-19 August 1975)

PIKE, C. P.

A Correlation Study Relating Spacecraft Anomalies to Environmental Data
56th Ann. Am Geophys. Union Mtg., Wash., D. C. (16-20 June 1975)

PIKE, C. P., DANDEKAR, B. S., and MENG, C. I. (Univ. of Calif.), AKASOFU, S. I. (Univ. of Alaska)

A Correlation Study Relating DMSP Satellite Observations of the Aurora to the Bz Component of the IMF
1976 Spring Ann. Mtg. of the Am. Geophys. Union, Wash., D. C. (12-16 April 1976)

PIKE, C. P., and WHALEN, J. A.

Observations of the Red-Band and Auroras
Am. Geophys. Union 1974 Fall Ann. Mtg., San Francisco, Calif. (12-17 December 1974)

PIKE, C. P., WHALEN, J. A., WAGNER, R. A., WEBER, E. J., and BUCHAU, J.

Studies of DMSP Photographs at AFCRL
16th Gen. Asbly. of the Intl. Union of Geod. and Geophys. (IUGG), Grenoble, Fr. (25 August-6 September 1975)

PITTENGER, E. W., LT. COL.

AFCRL Programs in Trans-Ionospheric Propagation and the Ionospheric Environment
DNA Satellite Link-Eff. Mtg., R&D Assoc., Santa Monica, Calif. (4 June 1975)

RUSH, C. M.

Limitations of Mapping Techniques to Predicting Total Electron Content at a Distant Point
Symp. on Eff. of the Iono. on Space Sys. and Comm., Wash., D. C. (20-22 January 1975)

An Empirical Electron Density Model for Use in Specifying Radio Propagation Conditions
18th Gen. Asbly. of Intl. Union of Rad. Sci. (URSI). Lima, Peru (11-19 August 1975)

RUSH, C. M., and AARONS, J.

High Latitude Phenomena. A Review of U. S. Results Published Between 1972 and 1974
18th Gen. Asbly. of Intl. Union of Rad. Sci., Lima, Peru (11-19 August 1975)

RUSH, C. M., and EDWARDS, W., MAJ.

Sensitivity of the HF Propagation Characteristics to Electron Density Parameters
1974 USNC/URSI-IEEE Mtg., Boulder, Colo. (14-17 October 1974)

SLACK, F. F.

ATS-6 40 and 360 MHz Differential Phase Measurements
Symp. of the Com. on Space Res. (COSPAR) Beacon Satellite Gp., Boston Univ., Boston, Mass. (1-4 June 1976)

STRAKA, R. M.

Polarization Variations in Active Regions at 3.8 Cm
1974 USNC/URSI-IEEE Mtg., Boulder, Colo. (14-17 October 1974)

TOMAN, K.

Spectral Behavior of Ionospheric Waves
1974 USNC/URSI-IEEE Mtg., Boulder, Colo. (14-17 October 1974)

Spectral Analyses of Ionospheric-Doppler Time Series
1975 Intl. IEEE/AP-S Symp. and USNC/URSI Mtg., Univ. of Ill., Urbana, Ill. (2-5 June 1975)

On Wavelike Perturbations in the F Region
18th Gen. Asbly. of Intl. Union of Rad. Sci. (URSI), Lima, Peru (11-19 August 1975)

WAGNER, R. A., WHALEN, J. A., and BUCHAU, J.

Substorm Related Latitudinal Shifts of the Continuous Aurora Observed in the Magnetic Local Midnight Sector
56th Ann. Am. Geophys. Union Mtg., Wash., D. C. (16-20 June 1975)

WEBER, E. J., and MENDE, S. B. (Lockheed Palo Alto Res. Lab., Palo Alto, Calif.), EATHER, R. H. (Phys. Dept., Boston Coll., Mass.)

Observations of August 4, 1972 PCA Event from South Pole Station
1974 Fall Ann. Am. Geophys. Union Mtg., San Francisco, Calif. (12-17 December 1974)

WEBER, E. J., 1ST LT., WHALEN, J. A., and BUCHAU, J.
Coordinated Airborne, Ground Based and Satellite Observations of Auroral Activity in the Midnight Local Time Sector
56th Ann. Am. Geophys. Union Mtg., Wash., D. C. (16-20 June 1975)

WHALEN, J. A., BUCHAU, J., and KRUKONIS, A. P.
Temporal Patterns of Auroral Activity at Midnight
Am. Geophys. Union 1974 Fall Ann. Mtg., San Francisco, Calif. (12-17 December 1974)

WHALEN, J. A., and KRUKONIS, A. P.
Inter-Relations of Oval, Polar Cap and Cleft Auroras in the Noon Sector
56th Ann. Am. Geophys. Union Mtg., Wash., D. C. (16-20 June 1975)

WHALEN, J. A., and WAGNER, R. A.
Characteristics of the Continuous Aurora Inferred from E-Layer Parameters
1976 Spring Ann. Mtg. of the Am. Geophys. Union, Wash., D. C. (12-16 April 1976)

WHITNEY, H. E.
Empirical Descriptors of Ionospheric Scintillations and Their Uses for System Design
1974 USNC/URSI-IEEE Mtg., Boulder, Colo. (14-17 October 1974)
Amplitude and Fade Rate Statistics for Auroral and Equatorial Scintillation
Symp. on Eff. of the Iono. on Space Sys. and Comm., Wash., D. C. (20-22 January 1975)
Amplitude and Rate Characteristics of Intense Scintillations
Symp. of the Com. on Space Res. (COSPAR) Beacon Satellite Gp., Boston Univ., Boston, Mass. (1-4 June 1976)

WHITNEY, H. E., and AARONS, J.
Amplitude Scintillation Observations and Systems Application
AGARD Specialists Mtg. of the EM Wave Propagation Panel on Rad. Sys. and the Iono., Athens, Greece (26-30 May 1975)

WHITNEY, H. E., and CANTOR, C. (Emmanuel Coll., Boston, Mass.)
Amplitude and Fade Rate Statistics for Equatorial and Auroral Scintillations
Symp. on Eff. of the Iono. on Space Sys. and Comm., Wash., D. C. (20-22 January 1975)

WONG, M. S.
Iterative Ray-Tracing Simulation of Minimum Group-Path Traces in Swept-Frequency Backscatter Ionograms
Over-The-Horizon Detection Tech. Rev. Mtg., Patrick AFB, Fla. (25-27 March 1975)

TECHNICAL REPORTS JULY 1974 - JUNE 1976

AARONS, J.
Global Morphology of Ionospheric Scintillations II
AFCRL-TR-75-0135 (11 March 1975)
Equatorial Scintillations: A Review
AFGL-TR-76-0078 (13 April 1976)

ALLEN, R. S., and CONNELLY, J. M., VESPRINI, R. L.
Specification of the Thickness of the Topside of the Ionosphere
AFCRL-TR-75-0529 (6 October 1975)

ANDREOLI, L. J. (SAMSO, El Segundo, Calif.), and PIKE, C. P.
The DMSP Auroral-Ionospheric Interpretation Guide: Introduction
Def. Met. Satellite Program Auroral-Iono. Interpretation Guide, AFCRL-TR-75-0191 (4 April 1975)

BAKSHI, P. (Boston Coll., Chestnut Hill, Mass.), and BARRON, W.
Spectral Correlations Between Solar Flare Radio Bursts and Associated Proton Fluxes, I
AFCRL-TR-74-0508 (October 1974)
Spectral Correlations Between Solar Flare Radio Bursts and Associated Proton Fluxes, II
AFCRL-TR-75-0579 (July 1975)

BASU, S., BASU, S. (Emmanuel Coll., Boston, Mass.), and KHAN, B. K. (Inst. of Rad. Phys. and Elect., Univ. of Calcutta, India)
Model of Equatorial Scintillations from In Situ Measurements
AFGL-TR-76-0080 (13 April 1976)

CASTELLI, J. P., BARRON, W. R., and AARONS, J.
An Atlas of Quiet Sun Radio Frequency Measurements Made at the Sagamore Hill Solar Radio Observatory, 1966-1974
AFCRL-TR-75-0132 (10 March 1975)

CORMIER, R. J., and DIETER, K. (Boston Coll., Chestnut Hill, Mass.)
Automatic Processing of Digital Ionograms
AFCRL-TR-74-0502 (7 October 1974)

DANDEKAR, B. S.
Improving the Global Ionospheric Predictions of f_0F_2
AFGL-TR-76-0124 (10 June 1976)

EDWARDS, W. R., JR., MAJ., RUSH, C. M., and MILLER, D. M. (Arcon Corp., Wakefield, Mass.)
Studies on the Development of an Automated Objective Ionospheric Mapping Technique
AFCRL-TR-75-0124 (5 March 1975)

ELKINS, T. J.
An Analysis of Polar Cap Backscatter Radar Data
AFCRL-TR-74-0457 (16 September 1974)

GAUNT, D. N.
Improvement in Short Wave Fade Detection
AFCRL-TR-75-0262 (8 May 1975)

KLOBUCHAR, J. A.
A First-Order, Worldwide, Ionospheric Time-Delay Algorithm
AFCRL-TR-75-0502 (25 September 1975)

KLOBUCHAR, J. A., and ALLEN, R. S.
Maximum Ionospheric Range Errors for Air Defense Command Radars
AFGL-TR-76-0042 (2 March 1976)

KOSSEY, P. A., and LEWIS, E. A.,
Detection and Classification of Solar X-Ray Flares Using VLF Phase and Amplitude Information
AFCRL-TR-74-0468 (20 September 1974)

LEWIS, E. A., and KOSSEY, P. A.
POWERFLUX I: A Method of Estimating Wave Intensities at Large Distances from Ground-Based Low Frequency Transmitters
AFCRL-TR-75-0338 (16 June 1975)

MENDILLO, M., HAWKINS, G. S., and KLOBUCHAR, J. A.
An Ionospheric Total Electron Content Disturbance Associated with the Launch of NASA's Skylab
AFCRL-TR-74-0342 (29 July 1974)

PFISTER, W., and SALES, G.
Pulse Sounding with Closely Spaced Receivers as a Tool for Measuring Atmospheric Motions and Fine Structure in the Ionosphere. VIII. Application to Aircraft Signals
AFCRL-TR-75-0193 (7 April 1975)

PIKE, C. P.
An Analytical Model of the Main F-Layer Trough
AFGL-TR-76-0098 (4 May 1976)

Editor
Defense Meteorological Satellite Program Auroral-Ionospheric Interpretation Guide
AFCRL-TR-75-0191 (4 April 1975)
Auroral-Ionospheric Variability
Def. Met. Satellite Program Auroral-Iono. Interpretation Guide, AFCRL-TR-75-0191 (4 April 1975)

PIKE, C. P., WAGNER, R. A., and AKASOFU, S.-I. (Geophys. Inst., Univ. of Alaska)
An Ionospheric Substorm Model
Def. Met. Satellite Program Auroral-Iono. Interpretation Guide, AFCRL-TR-75-0191 (4 April 1975)

PRASAD, B., GUIDICE, D. A., and CASTELLI, J. P.
Temporary Decrease in the Normal Solar Radio Intensity Level and Its Association with an Impulsive Burst
AFCRL-TR-75-0331 (13 June 1975)

RASMUSSEN, J. E., LEWIS, E. A., KOSSEY, P. A., and DOS SANTOS, R., MAJ., BAF DE FREITAS, C., MAJ., BAF (Centro Tecnico Aerospacial, Sao Jose dos Campos, S. P., Brazil), KAHLER, R. C., KLEMETTE, W. I. (Barkley and Dexter Labs., Fitchburg, Mass.)
Low Frequency Wave-Reflection Properties of the Equatorial Ionosphere
AFCRL-TR-75-0615 (3 December 1975)

RASMUSSEN, J. E., MC LAIN, R. J., CAPT., and TURTLE, J. P.
VLF/LF Reflectivity of the Polar Ionosphere 19 January - 2 March 1975
AFCRL-TR-76-0045 (22 January 1976)

SILVERMAN, S. M., and MULLEN, E. G.
Sky Brightness During Eclipses: A Compendium from the Literature
AFCRL-TR-74-0363 (5 August 1974)

SLACK, F. J.
ATS-6 40- and 360-MHz Differential Phase Measurements
AFGL-TR-76-0119 (2 June 1976)

WHITNEY, H. E.
Ionospheric Scintillation Effects on VHF-UHF Communication Systems
AFGL-TR-76-0097 (3 May 1976)

WONG, M. S.
Ray-Tracing Simulation of Swept-Frequency Backscatter Ionograms
AFCRL-TR-74-0539 (25 October 1974)
Iterative Ray-Tracing Simulation of Minimum Group-Path Traces in Swept-Frequency Backscatter Ionograms
AFCRL-TR-75-0241 (2 May 1975)

SACRAMENTO PEAK OBSERVATORY

JOURNAL ARTICLES
JULY 1974 - JUNE 1976

ALTROCK, R. C., and CANFIELD, R. C.
Analysis of the Solar Mg I Spectrum
The Astrophys. J., Vol. 194 (1974)

ALTROCK, R. C., and CANNON, C. J. (Institut d'Astrophysique, Paris, Fr.)
The Formation of MgI 4571 A in the Solar Atmosphere V. The Multi-Dimensional Structure of the Photosphere and Low Chromosphere
Solar Phys., Vol. 42 (1975)

ALTROCK, R. C., and MUSMAN, S.
Physical Conditions in Granulation
The Astrophys. J., Vol. 203 (1976)

BECKERS, J. M.
The Next Decade in Observational Solar Research
Highlights of Astron. (1974)
The Maximum Polarization for Resonance Scattering
Solar Phys., Vol. 37 (August 1974)
A Search for Deuterium on the Sun
The Astrophys. J., Vol. 195 (1975)
The Compression of Data Resulting from Photon Counters
Space Sci. Instmn., Vol. 1 (1975)
The Flux of Alfven Waves in Sunspots
The Astrophys. J., Vol. 203 (1976)

BECKERS, J. M., and ARTZNER, G. (Lab. de Phys. Stellaire et Planetaire, CNRS, Fr.)
High Resolution Spectroscopy of the Disk Chromosphere III. Upward Moving Disturbances as Observed in the Ca II K-Line Wings
Solar Phys., Vol. 37 (August 1974)

BECKERS, J. M., DICKSON, L., and JOYCE, R. S.
Observing the Sun with A Fully Tunable Lyot-Ohman Filter
Appl. Opt., Vol. 14, No. 9 (September 1975)

BECKERS, J. M., DICKSON, L., and WOODMAN, D.
Cinematography of Solar Intensity, Velocity, and Magnetic Fields
Opt. Engrg., Vol. 14, No. 1 (January-February 1975)

BECKERS, J. M., and ENGVOLD, O.
A Comparison of Spicules in the H and He II (304 Å) Lines
Solar Phys., Vol. 40 (1975)

BECKERS, J. M., and MILKEY, R. W. (Kitt Peak Natl. Obsv., Tucson, Ariz.)
The Line Response Function of Stellar Atmospheres and the Effective Depth of Line Formation
Solar Phys., Vol. 43 (1975)

CANFIELD, R. C.
A Simplified Method for Calculation of Radiative Energy Loss Due to Spectral Lines
The Astrophys. J., Vol. 194 (1974)

DUNN, R. B., and ZIRKER, J. B. (Univ. of Haw.), BECKERS, J. M.
Properties of the Solar Filigree Structure
Chromospheric Fine Structure – IAU, R. Grant Athay, Ed. (1974)

FISHER, R., and MUSMAN, S.
Detection of Coronal Holes from λ5303 Fe XIV Observations
The Astrophys. J., Vol. 195, No. 3, Pt. 1 (1975)

JOCKERS, K., and ENGVOLD, O. (Univ. of Oslo, Norway)
Prominence Eruption Accompanied by Twist Re-Adjustment
Solar Phys., Vol. 44 (1975)

RUST, D. M.
Observations of Flare-Associated Magnetic Field Changes
High Alt. Obsv. Proc., Flare-Related Mag. Fld. Dyn., Boulder, Colo. (December 1974), D. M. Rust, Co-Ed.

Inference of the Hard X-Ray Source Dimensions in the August 7, 1973 White Light Flare
Proc. of IAU Symp. No. 68, Solar Gamma X and EUV Radn., D. Reidel Pub. Co. (October 1975)

RUST, D. M., and BRIDGES, C. A., III
The Work of the Diode Array: He 10830 Observations of Spicules and Subflares
Solar Phys., Vol. 43 (1975)

RUST, D. M., CANFIELD, R. C., and PRIEST, E. R. (High Alt. Obsv., NCAR, Boulder, Colo.)
A Model for the Solar Flare
High Alt. Obsv. Proc., Flare-Related Mag. Fld. Dyn., Boulder, Colo. (December 1974), D. M. Rust, Co-Ed.

RUST, D. M., and HEGWER, F. (High Alt. Obsv., NCAR, Boulder, Colo.)
Analysis of the August 7, 1972 White Light Flare: Light Curves and Correlation with Hard X-Rays
Solar Phys., Vol. 40 (1975)

RUST, D. M., and MACHADO, M. E.
Analysis of the August 7, 1972 White Light Flare: Its Spectrum and Vertical Structure
Solar Phys., Vol. 38 (1974)

RUST, D. M., and NAKAGAWA, Y. (High Alt. Obsv., NCAR, Boulder, Colo.), NEUPERT, W. M. (NASA Goddard Space Flt. Ctr., Greenbelt, Md.)
EUV Emission, Filament Activation and Magnetic Fields in a Slow Rise Flare
Solar Phys., Vol. 41 (April 1975)

RUST, D. M., and NEUPERT, W. M. (NASA Goddard Space Flight Ctr., Greenbelt, Md.), NAKAGAWA, Y. (High Alt. Obsv., NCAR, Boulder, Colo.)
Evidence for Energy Transport in Magnetically Confined Coronal Enhancements Above Active Regions
High Alt. Obsv. Proc., Flare-Related Mag. Fld. Dyn., Boulder, Colo. (December 1974), D. M. Rust, Co-Ed.

SIMON, G. W., ALTROCK, R. C., NOVEMBER, L. J., WORDEN, S. P., and MILKEY, R. W. (Kitt Peak Natl. Obsv., Tucson, Ariz.)
Heights of Formation of Non-Magnetic Solar Lines Suitable for Velocity Studies
(Res. Note) Solar Phys., Vol. 43 (1975)

SIMON, G. W., SEAGRAVES, P. H., and TOUSEY, R., PURCELL, J. D. (U. S. Naval Res. Lab., Wash., D. C.), NOYES, R. W. (Ctr. for Astrophys., Cambridge, Mass.)
Observed Heights of EUV Lines Formed in the Transition Zone and Corona. II. NRL Rocket Observations
Solar Phys., Vol. 39 (1974)

TSUBAKI, T.
Line Profile Analysis of a Coronal Formation Observed Near a Quiescent Prominence: Intensities, Temperatures and Velocity Fields
Solar Phys., Vol. 43 (1975)

TSUBAKI, T., and ENGVOLD, O. (Univ. of Oslo, Norway)
An Analytical Representation for Photographic Characteristic Curves
AAS Photo-Bull., Issue No. 9, No. 2 (1975)

WAGNER, W. J.
Solar Rotation as Marked by EUV Coronal Holes
Astrophys. J. Ltrs., Vol. 198 (15 June 1975)

WAGNER, W. J., HEASLEY, J. N., and TANDBERG-HANSSEN (High Alt. Obsv., NCAR, Boulder, Colo.)
Study of He I Emission Lines in the Solar Atmosphere III. The Triplet-Singlet Line Intensity Ratios in Solar Prominences
Astron. and Astrophys., Vol. 40 (1975)

WORDEN, S. P.
The Limitations of Astronomical Image Reconstruction
The Obsv. (15 December 1975)
Digital Analysis of Speckle Photographs: The Angular Diameter of Arcturus
Pubs. of Astronom. Soc. of the Pacific, Vol. 88 (1976)
Astronomical Image Reconstruction
Vistas in Astron., Vol. 20 (1976)

PAPERS PRESENTED AT MEETINGS JULY 1974 - JUNE 1976

ALTROCK, R. C.
Physical Conditions in Granulation
Solar Phys. Div. Mtg., Am. Astronom. Soc., Univ. of Colo., Boulder, Colo. (20-22 January 1975)
Research at Sacramento Peak Observatory
Neighborhood Astron. Mtg., Lubbock, Tex. (12 July 1975)
Horizontal Temperature Fluctuations in the Low Solar Photosphere
146th Mtg. of Am. Astronom. Soc., San Diego State Univ., San Diego, Calif. (17-20 August 1975)
Solar Photospheric Velocity Fields
Intl. Colloquium on Phys. of Motions in Stellar Atm., Nice, Fr. (1-5 September 1975)
Convective Flux in the Visible Photosphere
148th Mtg. of Am. Astronom. Soc., Haverford Coll., Haverford, Pa. (21-24 June 1976)

ALTROCK, R. C., and CANNON, C. J. (Univ. of Sydney, Aust.)
The Multi-Dimensional Structure of the Photosphere and Low Chromosphere of the Sun
144th Mtg. of Am. Astronom. Soc., Gainesville, Fla. (10-13 December 1974)

BECKERS, J. M.
Is the Solar Filigree the Site of Strong Photospheric Magnetic Fields?
Solar Phys. Div. Mtg., Am. Astronom. Soc., Univ. of Colo., Boulder, Colo. (20-22 January 1975)
The Flux of Alfven Waves in Sunspots
146th Mtg. of Am. Astronom. Soc., San Diego State Univ., San Diego, Calif. (17-20 August 1975)
Spatially Resolved Motions in the Solar Atmosphere
Intl. Colloq. on Phys. of Motions in Stellar Atm., Nice, Fr. (1-5 September 1975)
Magnetic Fields in the Solar Atmosphere
Intl. Symp. on Solar Terrestrial Phys., Boulder, Colo. (8-18 June 1976)
Solar Rotation and Gravitational Red Shift as Determined from Sunspot Spectra
148th Mtg. of Am. Astronom. Soc., Haverford Coll., Haverford, Pa. (21-24 June 1976)

BRIDGES, C. A., and RUST, D. M. (Am. Sci. & Engrg., Inc., Cambridge, Mass.)
The Work of the Diode Array
Solar Phys. Div., Am. Astronom. Soc., Univ. of Colo., Boulder, Colo. (20-22 January 1975)

CANFIELD, R. C.
Observational Evidence for Unresolved Motions in the Solar Atmosphere
Intl. Colloq. on Phys. of Motions in Stellar Atm., Nice, Fr. (1-5 September 1975)

FISHER, R. R., and CANFIELD, R. C.
Evidence for Magnetic Field Reconnection in the Flare Process. Diode Array Observations of the 18:28 U.T. Flare, 10 August 1975
148th Mtg. of Am. Astronom. Soc., Haverford Coll., Haverford, Pa. (21-24 June 1976)

FISHER, R. R., MUSMAN, S., and SEAGRAVES, P.
Coronal Density Distributions from FeXIV λ5303 Data
Solar Phys. Div. Mtg., Am. Astronom. Soc., Univ. of Colo., Boulder, Colo. (20-22 January 1975)

GOE, G., and KOUTCHMY, S.
Observed Large Scale Solar Intensity Fluctuations Attributed to Terrestrial Atmospheric Acoustic-Gravity Waves
Intl. Symp. on Solar Terrestrial Phys. Boulder, Colo. (8-18 June 1976)

JOCKERS, K.
Reconnection, Caused by Nonexistence of Force-Free Equilibria, as a Mechanism for Solar Flares
Solar Flare Build-Up Study, Falmouth, Cape Cod, Mass. (8-11 September 1975)

JOCKERS, K., and ENGVOLD, O.
Spectral and Slitjaw Observations of an Eruptive and Untwisting Filament
Solar Phys. Div. Mtg. of Am. Astronom. Soc., Univ. of Colo., Boulder, Colo. (20-22 January 1975)

JOCKERS, K., and ROOSEN, R. G. (NASA/Goddard Space Flight Ctr., N.M. Station), CRUIKSHANK, D. P. (Inst. for Astron., Univ. of Haw.)
A Kinematographic Study of the Tail of Comet Kohoutek (1973f)
Intl. Astronom. Union Comsn. 15, Study of Comets, NASA Goddard Space Flt. Ctr., Greenbelt, Md. (28 October - 1 November 1974)

KEIL, S. L.
Photospheric Inhomogeneities: Continuum Fluctuations
148th Mtg. of Am. Astronom. Soc., Haverford Coll., Haverford, Pa. (21-24 June 1976)

MUSMAN, S.
Observations of Solar Convection
Fluid Mech. Div. Mtg. of Am. Phys. Soc., Pasadena, Calif. (25-27 November 1974)
Observations of Velocity and Intensity Fluctuations in Solar Granulation
Solar Phys. Div. Mtg. of Am. Astronom. Soc., Univ. of Colo., Boulder, Colo. (20-22 January 1975)

MUSMAN, S., and NYE, A. H.
Global Solar Oscillations
148th Mtg. of Am. Astronom. Soc., Haverford Coll., Haverford, Pa. (21-24 June 1976)

MUSMAN, S., NYE, A. H., and THOMAS, J. H., (Univ. of Rochester, N. Y.)
Observations of Penumbral Waves in the Photosphere
148th Mtg. of Am. Astronom. Soc., Haverford Coll., Haverford, Pa. (22-25 June 1976)

RUST, D. M.
Observations of Magnetic Field Changes with Flares
Symp. on Flare Related Mag. Field Dyn., Boulder, Colo. (23-25 September 1974)

RUST, D. M., CANFIELD, R. C., and PRIEST, E. R. (High Alt. Obsv., NCAR, Boulder, Colo.)
A Model for the Solar Flare
Symp. on Flare Related Mag. Field Dyn., Boulder, Colo. (23-25 September 1974)

SIMON, G. W., DUNN, R. B., and LA BONTE, B. J. (Calif. Inst. of Technol., Pasadena, Calif.)
A Phenomenological Study of High-Resolution Granulation Photographs
Solar Phys. Div. Mtg. of Am. Astronom. Soc., Univ. of Colo., Boulder, Colo. (20-22 January 1975)

SIMON, G. W., and WORDEN, S. P.
Motions and Flux Dispersal in Supergranules
Intl. Astronom. Union Symp. No. 71 on Basic Mechanisms of Solar Activity, Prague, Czech. (23-30 August 1975)
Velocities Observed in Supergranules
Intl. Colloq. on Phys. of Motions in Stellar Atm., Nice, Fr. (1-5 September 1975)

STENCL, R. E. (Univ. of Mich. Obsv., Ann Arbor, Mich.), and CANFIELD, R. C.
Stellar Emission Lines in the Wings of Calcium H and K
148th Mtg. of Am. Astronom. Soc., Haverford Coll., Haverford, Pa. (21-24 June 1976)

TSUBAKI, T.
Spectrophotometric Study of a Coronal Formation Observed Around a Prominence on 23 March 1974
Solar Phys. Div. Mtg. of Am. Astronom. Soc., Univ. of Colo., Boulder, Colo. (20-22 January 1975)
Coronal Velocity Fields Derived from Line Profile Analysis of Fe XIV λ5303
146th Mtg. of Am. Astronom. Soc., San Diego State Univ., San Diego, Calif. (17-20 August 1975)

WAGNER, W. J.
The Rigid Rotation of Coronal Holes
146th Mtg. of Am. Astronom. Soc., San Diego State Univ., San Diego, Calif. (17-20 August 1975)
Rotational Characteristics of Coronal Holes
Intl. Astronom. Union Symp. No. 71 on Basic Mechanisms of Solar Activity, Prague, Czech. (23-30 August 1975)

WORDEN, S. P.
On the Origin of 2^h 40^m Global Solar Oscillations
148th Mtg. of Am. Astronom. Soc., Haverford Coll., Haverford, Pa. (21-24 June 1976)

WORDEN, S. P., and COLEMAN, G. D.
Mass Loss from Stellar Flares
146th Mtg. of Am. Astronom. Soc., San Diego State Univ., San Diego, Calif. (17-20 August 1975)
Flare Stars and Galactic Winds
147th Mtg. of Am. Astronom. Soc., Chicago, Ill. (7-10 December 1975)

WORDEN, S. P., and HARVEY, J. W., LYNDS, C. R. (Kitt Peak Natl. Obsv., Tucson, Ariz.)
Reconstructed Images of Alpha Orionis Using Stellar Speckle Interferometry
Opt. Soc. of Am., Topical Mtg. on Speckle Phenom. in Opt., Microwaves, and Acoust., Asilomar, Calif. (24-26 February 1976).

WORDEN, S. P., SIMON, G. W., and NOVEMBER, L. J. (JILA, Univ. of Colo.)
The Character of 300-Second Oscillators
146th Mtg. of Am. Astronom. Soc., San Diego State Univ., San Diego, Calif. (17-20 August 1975)

TECHNICAL REPORTS JULY 1974 - JUNE 1976

BECKERS, J. M.
New Views of Sunspots
AFCRL-TR-75-0089 (10 February 1975)
Magnetic Fields in the Solar Atmosphere
AFGL-TR-76-0131 (22 June 1976)

BECKERS, J. M., BRIDGES, C. A., and GILLIAM, L. B.
A High Resolution Spectral Atlas of the Solar Irradiance from 380 to 700 Nanometers. Volume I: Tabular Form
AFGL-TR-76-0126(I) (16 June 1976)
A High Resolution Spectral Atlas of the Solar Irradiance from 380 to 700 Nanometers. Volume II: Graphical Form
AFGL-TR-76-0126 (II) (16 June 1976)

BECKERS, J. M., DICKSON, L., and JOYCE, R. S.
A Fully Tunable Lyot-Ohman Filter
AFCRL-TR-76-0090 (10 February 1975)

DEMASTUS, H. L.
A Twenty-Year Summary of Sacramento Peak Weather - August 1954 Through July 1974
AFGL-TR-76-0096 (3 May 1976)

WORDEN, S. P., 1ST LT.
Astronomical Image Reconstruction
AFCRL-TR-75-0630 (12 December 1975)

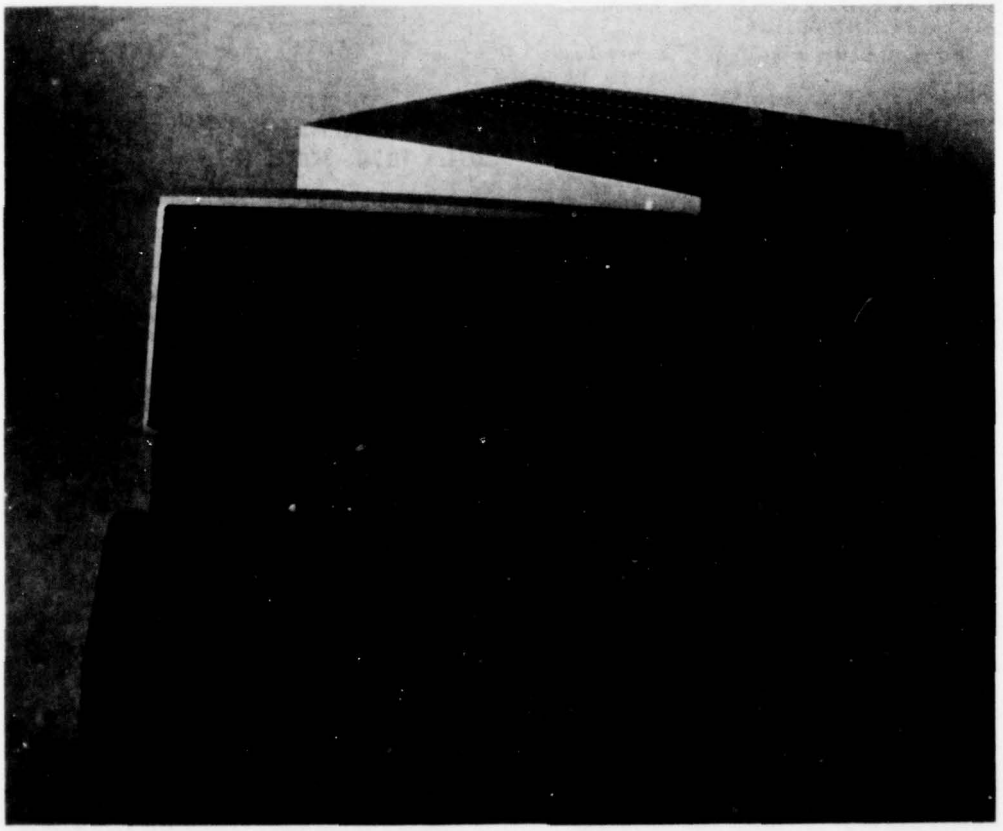

A Data Terminal in the Modular Automated Weather System. The keyboard can be used to call up any of the four pages of data normally displayed by the system, or change the instructions given to the system.

V METEOROLOGY DIVISION

In the years since World War II, many people have used the term "all-weather" to characterize the Air Force of the future. In the three decades since that war, scientists and engineers have made important advances in their attempts to develop Air Force systems in the operation of which weather would not be a limiting factor. But the goal of an all-weather Air Force has not yet been reached. Nor is it likely that it will be reached within the next few years. So it remains for other scientists and engineers to develop a greater understanding of meteorological phenomena and to develop better techniques of measuring, processing, and displaying critical weather elements, forecasting their occurrence and severity and, in some cases, even modifying them.

While these people have made important contributions in these technical areas, Air Force system concepts have continually become more and more sophisticated. Systems whose development seemed far in the future in the 1940's will become operational by the 1980's. However, increases in sophistication very often mean new meteorological constraints and, therefore, new technical problems to be solved by atmospheric physicists and chemists, meteorologists, mathematicians, computer specialists, engineers, and technicians. Consequently, there is a continuing need for a strong Air Force program in research and development. The major responsibility for this program rests with AFGL's Meteorology Division.

During the period covered by this report the program of the Meteorology Division included the following principal efforts: the development of methods of observing and forecasting airfield weather, the modeling of atmospheric circulations, the application of data from meteorological satellites to analysis and forecasting, the development of techniques for the processing and display of weather radar data, and the development and application of climatological techniques for utilization in the design of Air Force systems. The program has also included the development and testing of techniques of warm fog dissipation, methods of identifying the microphysical characteristics of cloud and precipitation particles during hypersonic reentry of ballistic missiles through the atmosphere, and techniques for decreasing the detectability of aircraft through the use of dispensed aerosols.

This report contains brief descriptions of meteorological instrumentation and related equipment. Some of the items are for direct use in in-house research programs whereas other items are primarily for eventual use by the Air Weather Service. Development and testing of the equipment has been performed not only at Hanscom AFB but at two field sites: the Weather Radar Facility at Sudbury, Massachusetts, and the Weather Test Facility at Otis AFB, Massachusetts. The airborne equipment has been tested on a leased aircraft as well as two C-130 aircraft.

The success of the various programs has been due, in large measure, to the fine support received from other components of the Air Force, other Department of Defense agencies, the National Oceanic and Atmospheric Administration, and the National Aeronautics and Space Administration.

OBSERVING AND FORECASTING AIRFIELD WEATHER

For economy and operational effectiveness, the development of automated techniques to replace costly human methods of local weather observation is being emphasized. As part of a continuing program of aviation terminal weather research, the Meteorology Division has undertaken the development of a Modular Automated Weather System (MAWS). The program has progressed rapidly during 1975-1976, with installation of an experimental model of MAWS at Scott AFB, Illinois, scheduled for late fall of 1976. The objective of the field demonstration is to explore in more detail the utility of MAWS for direct support of fixed-base military operations. The modular design of MAWS offers many options in the selection of system components. Sensors and processing and display units may be added or substituted as necessary to satisfy specific local base requirements. The demonstration model employs off-the-shelf commercial sensors as well as automated versions of in-place inventory instruments such as the rotating beam ceilometer and transmissometer.

In addition, the initial components of MAWS serve as a baseline for the evaluation of new candidate sensors for automated observing systems. Inter-comparison tests of new instruments and observing techniques are being carried out at Hanscom AFB and the AFGL Weather Test Facility established at Otis AFB, Massachusetts. Instruments and techniques under development and evaluation include laser systems for the measurement of ceiling, slant visual range, and runway visual range as well as techniques for observing sky cover and obstructions to vision.

MAWS Demonstration Model: The versatility of MAWS results from the use of solid-state microprocessor compo-

nents. Remote and supervisory data sets composed of central processing units, read-write and programmable memory plus suitable control logic are easily adaptable to aviation weather input/output requirements. The microprocessors can be programmed to interface with a wide variety of sensing elements each having different raw data conversion and sampling rate requirements, and measuring in different ranges. Many different kinds of output devices can also be used so that the configuration of the system can be individualized by custom-written software packages to satisfy specific local requirements at each operational location.

In addition to its ability to accept a variety of sensors and peripherals, the MAWS will have several features which greatly extend its reliability in a remote environment. Built-in redundancy is planned for the system. Stand-by modules within the system will periodically test the working hardware. If the hardware is not performing within certain limits, the stand-by hardware will take over the operation and set a flag, thereby alerting the technician to a failure. The software will contain routines for continually editing the data by examining processed variables with respect to prescribed limits and setting an error flag when suspicious data are encountered, indicating a faulty sensor. Finally, short programs residing in the microprocessors perform diagnostic tests of the entire system.

Surface Weather Sensors: Since one of the experimental objectives is to help determine the basic requirements for the number and spacing of airfield observing sites and frequency of observations, the array of weather instruments to be installed as part of the MAWS for demonstration at Scott AFB, Illinois, will be more extensive than any system anticipated to support fixed base operations. At each observing site continuous measurements will be made of wind speed, wind direction, temperature, dewpoint and scatter coefficient (visibility). Three observing sites are to be located adjacent to Runway 15/33, and will be collocated with existing weather instruments near the end points and the mid-point of the runway. In addition, observing sites are located at two levels (25 meters and 50 meters) of an instrumented tower that is offset 600 meters from the touchdown point of Runway 15. The instruments in the demonstration model are the same type as those used successfully in the Hanscom mesoscale network during the past few years.

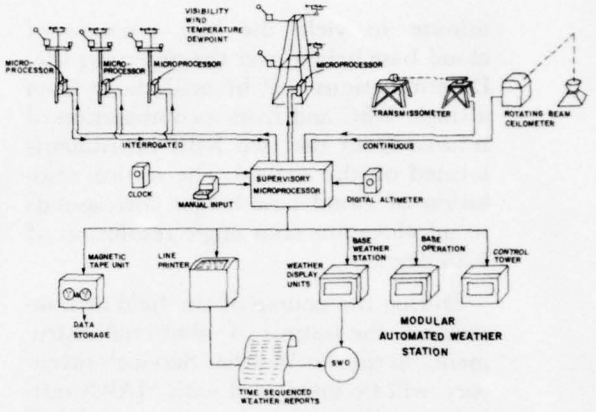

MAWS System Diagram

Fully automated measurements of cloud-base height are obtained from two AN/GMQ-13 Rotating Beam Ceilometers (RBCs) already in place near the approach zones of Runway 13/31. By far the most complex interface problems encountered thus far were associated with the integration of the RBC with MAWS. The processing system successfully establishes a background level from each 90-degree scan of the source lamp, filters out spurious and unwanted returns, identifies primary and secondary peaks representative of cloud structure, and analyzes the sequence of data over the past

minute to yield the best estimate of cloud base height over the observing site. Determinations will be made both from a single RBC and from a combination of returns from the two RBC instruments located on the airfield. The vertical resolution of cloud base height corresponds to an elevation scan angle resolution of 0.25 degree.

During the course of the field demonstration, the output of additional instruments in the Air Weather Service's inventory will be integrated with MAWS output for direct field intercomparison of the performance characteristics of new and conventional instruments. Inventory instruments to be interfaced with the automated system include the AN/GMQ-20 wind set, the AN/TMQ-11 temperature/dewpoint set, and the AN/GMQ-11 transmissometer.

Recording and Display Components: Many devices will be used in the MAWS demonstration model for real-time display and storage of processed weather observations and forecasts. The continuous flow of surface weather information will be archived on magnetic tape in a form suitable for convenient recall for climatological use or for technique development. An on-line printer provides hard-copy output of current weather data. The printer can be programmed to display sequential observations from selected sensor combinations; processed information, such as objective forecasts; or derived quantities in support of "met-watch" advisories and weather warnings. The printout capability will be used during the field demonstration to monitor and intercompare measurements from instruments of different type, spacing, and elevation.

Fresh observations, updated each minute for most elements, are displayed in alphanumeric form on the primary output device. The message format need not be the same for all display units; it may be adjusted to conform to the real-time information requirements of the traffic control center, the operations center, or the staff weather office.

Page from MAWS Display

Each alphanumeric display unit of the demonstration model can display any one of the four pages presently available in the system. The information on the first two pages is updated each minute. It includes ceiling, visibility, temperature, dewpoint, and altimeter setting at the latest observation time, and the observations made 5, 10, 15, and 30 minutes previously. Wind direction, wind speed, and peak wind gusts at the surface and at 25 and 50 meter tower levels are also shown. The display also gives the latest average and the highest and lowest values during the past 10 minutes of visual range for Runway 13, Runway 31, and the 25 and 50 meter tower levels. Also included are the temperature maximum and minimum for the past 24 hours and the relative humidity, sea level pressure, and one-hour pressure change, updated each hour.

The third page displays automated forecasts of runway visual range that are updated each minute as new observa-

tions are acquired and processed. Based on a conditional probability model that was developed and tested for the Hanscom mesoscale forecasting experiments, the forecasts give the probabilities that the visual range will be less than threshold values of 800 meters and 400 meters at selected times up to three hours. Experimental probability forecasts of ceiling will soon be added to MAWS; they will be based on a model similar to the one developed for visual range.

The latest observations of special weather elements that require dissemination as alerts or warnings when critical values are expected or reached are displayed on the fourth page of the display. For the Scott AFB demonstration, these automated "metwatch" parameters are runway cross-wind component, wind chill temperature, and wind gust spread.

New Instrument Development and Evaluation: Surface weather instruments which promise improved accuracy, representativeness, and reliability at reasonable operating costs are still sought. Several observing techniques and instruments having good potential for use in fully automated systems are under development and evaluation at the Air Force Geophysics Laboratory. For rigorous evaluation of instrument performance, a Weather Test Facility has been installed at Otis AFB, Massachusetts, which is located in an area having a relatively high frequency of critically low ceiling and visibility conditions.

Prominent among the new instruments which will be extensively evaluated during the coming year are two lidar systems that have been built as part of the AFGL program to investigate the usefulness of a lidar for determining ceiling and slant visual range (SVR).

Lidar Ceilometer: The transmitter of the lidar ceilometer is an erbium doped glass laser which has an output power level which is corrected and digitized for processing. Peak detection is used to determine the range to the lowest cloud layer and the range to the most significant layer.

Preliminary tests of the lidar ceilometer are being carried out at Hanscom AFB, Massachusetts, prior to installation at the Weather Test Facility. In initial tests the lidar ceilometer ranged to a cloud layer at a height of 5 km; the peak detection technique was used to process the signal and provided excellent results; and the acousto-optical modulator worked well as a Q-switch at the erbium wavelength.

The lidar clearly has excellent potential for automated ceiling measurements. In addition, it can provide significant input into the determination of sky cover and present weather conditions because of its ranging capability and the information contained in its atmospheric return signal. A rain/snow/fog (RSF) condition is determined from the frequency content and the amplitude of the lidar atmospheric return. If the atmospheric return contains no low frequency component, it is assumed that there is no restriction. This system will be evaluated in comparison with other present weather observing techniques at the Weather Test Facility.

Slant Visual Range Lidar: Also under development is an experimental lidar system to measure slant visual range. The system is housed in a mobile van and can be operated from its own generators or from local power. The lidar has an eye-safe frequency-doubled ruby laser and two photomultiplier (PM) detectors. The lidar telescope can be manually oriented to measure at any angle from the vertical to the horizontal. The Slant Visual Range lidar is undergoing tests at Hanscom AFB to evaluate the design concept. Upon successful completion of these tests, the system will be moved to Otis AFB for comparison testing with tower-mounted visibility meters.

Forward Scatter Meter/Tower System: Another system for the determination of Slant Visual Range is also under evaluation at Otis AFB. Measurements with forward scatter visibility meters mounted on a remote tower are used to yield estimates of slant visual range in the approach zone. The efficacy of this approach depends primarily upon the degree of correlation between the vertical structure of atmospheric extinction coefficient as measured at the tower and the effective average extinction coefficient along the actual visual path of the pilot in the approach zone.

Experiments have been undertaken to explore more fully the horizontal and vertical variability of fog structure based upon data gathered by the Weather Test Facility. Preliminary results of the fog variability studies, carried out exclusively during advection fogs at Otis AFB, lend strong support to the scatter meter/tower approach to slant visual range measurements.

Digital Radar: In forecasting precipitation and convective storm activity using weather radar information, the forecaster determines the most recent motion and development of precipitation echo patterns, and predicts the future echo pattern and intensity. He then interprets the predicted intensity in terms of actual weather conditions. Real-time forecast experiments in AFGL's project in mesoscale forecasting have demonstrated that the procedure is very hectic when storms are developing and moving rapidly. Therefore, efforts have been made to simplify the forecast procedure. A series of computer routines was developed. These routines first provide the speed and direction of echo pattern motion from the most recent series of digital radar maps. Next the computer predicts the minute-by-minute radar reflectivity expected over each of a list of locations. Studies relating radar reflectivity to visibility, rainfall rate and wind gusts are then used in converting reflectivity to forecasts of weather conditions. Probability forecasts of severe weather phenomena were successfully made during feasibility tests, based only on digital radar information, using only a few seconds of computer time.

While the radar information gathered over the past three years has not yet been completely processed, we are becoming aware of certain limitations to radar as a forecast tool. The uncertainty in drop-size distribution associated with any given echo results in errors of 40 to 60 percent in specifying visibility and rainfall rate. In shower conditions, when such errors are small compared to the uncertainty of what lies between weather stations, quantitative radar information is very useful. With winter storms and widespread precipitation, the information is of less value.

ATMOSPHERIC MODELING

The atmosphere is a complex fluid system capable of sustaining motions on a whole spectrum of time and space scales from very short, rapidly moving sound waves to ultra-long, quasi-stationary planetary scale waves. There are important nonlinear interactions or feedbacks among many of these differing scale sizes such that changes on one scale affect both longer and shorter scales and, in turn, are affected by them.

Progress in understanding such a large and complex nonlinear system, and therefore improved predictability, largely depends on our ability to formulate valid, but much simpler, analogues (models) of the complete system. Ideally, such models should take into account the important parameters and should be amenable to controlled experimentation. Mathematical models of the atmosphere, based upon the laws of fluid dynamics, meet these requirements and are widely

used in atmospheric prediction. The mathematical model is constructed to incorporate the most relevant physics for the problem at hand. The numerical solution is designed to approximate (and hopefully converge to) the unique analytic solution of the model which would have been obtained, if one existed and it was possible to obtain it. For brevity, this process of model building and numerical solution is called numerical weather prediction (NWP), although the designation NWP is usually applied to a more restricted class of models—those used in routine weather forecasting.

There are, however, some problems with NWP models which cause the time development of the model to diverge from the time development of the real atmosphere and therefore degrade the quality of the prediction. The goal of AFGL's efforts in mathematical modeling is to minimize the sources of model error, which include inadequate representation of relevant physical processes, incomplete description of the initial state of the prognostic parameters, and imperfect representation of differential equations by finite-difference approximations.

Accuracy and Computational Effort: Numerical Weather Prediction requires compromises. The speed and capacity of the computer place severe practical limits on both the physics which can be represented in the model and the scales in time and space which can be explicitly resolved in the numerical solution. Since even the simplest realistic NWP models are nonlinear, the problem of scale resolution is a physical as well as a numerical problem. Indeed, one of the most difficult problems in NWP is the proper treatment of those physical processes which occur in the atmosphere on a scale which is too small or too rapid to be resolved by the space-time network, but which are too important to be ignored. This is the problem of sub-grid scale processes. The numerical errors due to truncation increase with increasing mesh size (that is, the distance between grid points). Furthermore, the greater the mesh size, the more difficult it becomes to represent sub-grid-scale processes such as viscous dissipation in terms of large-scale parameters. However, for a typical model involving three space dimensions and time, halving the mesh length causes a 16-fold increase in computer time. If the computer does not have sufficient capacity, there is a large additional increase in "bookkeeping" time. These strong practical reasons for maintaining a relatively coarse network of solution points have caused us to search for alternative methods of decreasing truncation error and improving accuracy. One such alternative is to increase the order of

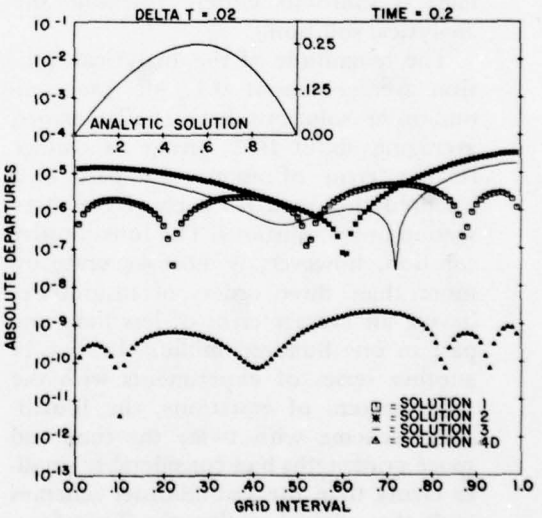

Comparison of four numerical solutions with the exact analytical solution. The analytic solution is in the small plot at the upper left. Because the errors, although small, are important, the main part of the graph shows only the differences between each solution and the analytic solution. Solutions 1, 2, and 3 are second-order numerical solutions and have similar errors. Solution 4 is a fourth-order numerical solution and can be seen to about 1,000 times more accurate than the second-order solutions.

accuracy of the finite-difference approximations to the differential equations.

The effectiveness of a high-order finite-difference approximation to a simple, one-dimensional nonlinear, time dependent advection equation has been demonstrated. This simple system, which possesses many of the features of the more realistic NWP models, has a known analytical solution which makes it an ideal system for experimentation. The accuracy of a fourth-order numerical solution scheme has been compared with three different second-order schemes. The solutions are carried out in a normalized, non-dimensional time-space gridmesh with time intervals of 0.02 and a space mesh length of 0.01, dividing the space domain from 0 to 1. The solutions were compared after an elapsed time of 0.2, or after 10 time steps. All four numerical solutions closely resemble the analytical solution.

The magnitude of the analytical solution averages about 0.1. All three second-order solutions have similar errors, averaging about 10^{-6}, giving an average relative error of about one part in a hundred thousand for each of the three second-order solutions. The fourth-order solution, however, is more accurate by more than three orders of magnitude, having an average error of less than one part in one hundred million. In fact, in another series of experiments with the same system of equations, the fourth-order scheme with twice the time and space gridlengths had considerably smaller errors than the second-order schemes with the original gridlengths. Therefore, at least for this simple system, considerable computational effort can be saved without sacrificing accuracy by using a coarser time-space mesh with a higher order difference approximation. It is likely that the same advantages of the higher order scheme apply to realistic NWP models, especially where most of the error occurs in the larger scale sizes.

Noise and the Treatment of Diffusion: The growth of noise in the real atmosphere is limited by small-scale diffusion and viscous dissipation, which is the final stage in the transfer of kinetic energy from larger to smaller scales. In numerical modeling, this diffusion process which occurs on a microscopic scale in the atmosphere must be represented in the model or parameterized in terms of scale sizes which are many orders of magnitude larger.

This creates the dilemma of noise and sub-grid-scale processes. Errors in the initial data, model inadequacies, improper treatment of both real and artificial boundaries, and inadequate resolution of important components of the system all produce noise in numerical models. If the noise is not controlled in the numerical solution, it will not only produce inaccurate forecasts and limit the time for which forecasts can be made, but may also cause the solution to become unstable and completely meaningless. But no matter how small we make the grid size of the model, we can never expect to treat atmospheric diffusion explicitly. Furthermore, as has already been indicated, time, economics, and machine capacity limit the extent to which grid size can be reduced. The 16-fold increase in computer cost each time we halve the grid distance in three dimensions requires that the physical diffusion which takes place in the real atmosphere be represented parametrically in numerical models. The principal shortcoming of conventional methods of representing diffusion in both operational and general circulation models for numerical weather prediction is that the meteorologically important cyclone-scale waves in the model are damped along with the computationally produced two-grid-interval noise. The resulting predictions are too smooth and fail to forecast newly developing disturbances adequately. Any good model needs a means of represent-

ing viscous dissipation that is very strong for the short wavelength noise and very weak for the larger, meteorologically important waves.

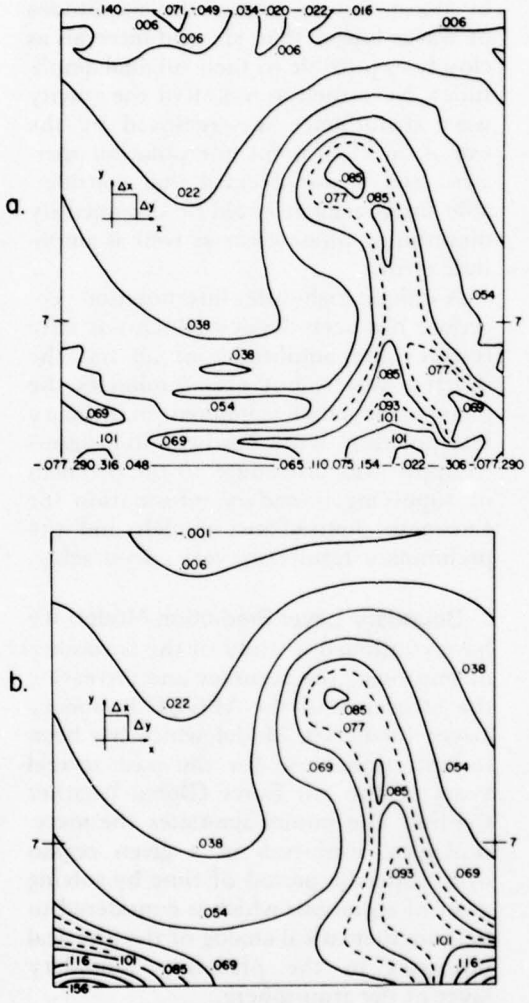

Solutions for the surface temperature field (non-dimensional) after 200 half-hour timesteps of a channel model integration. (a) No Filtering: Large amplitude noise is present, especially at the lateral walls where several individual gridpoint values of temperature are displayed. (b) Filter applied once each timestep.

We have devoted considerable attention to this problem and have devised a digital filter which appears to have just the right properties to control noise, represent atmospheric diffusion, yet not suppress physically meaningful information in the model. The filter is actually a flexible sequence of filters varying from three-point operators in one dimension when applied near boundaries to high-ordered operators in the interior of the grid domain. The filter has now been applied in a variety of numerical models varying from fine-mesh limited area models and channel models with solid walls to large-scale general circulation models.

For a channel model with solid walls, this type of filter can remove large amplitude, short wavelength noise near the boundaries while leaving the interior solution virtually unchanged. The non-dimensional surface temperature field was tested with rigid walls at the top and bottom in a channel periodic in one direction.

Another test of the filter has been run, again in conjunction with a channel model. In this case the walls were isolated; hence they caused no difficulties. An integration was made of an idealized cyclonic storm that produced strong surface frontal zones as the storm matured. In the unfiltered run, energy increasing in the smallest scales caused short wavelength waves to form parallel to the frontal zones and noise to develop within the center of the cyclone. The filtered run maintained the same large-scale growth of the storm and of the frontal zones while removing the unrealistic smaller scale waves and noise, thus modeling atmospheric diffusion processes on a sub-grid scale more realistically.

Fine-Mesh Modeling: The shortest wave that can be resolved in a numerical model has a length of two grid intervals. However, such waves and even those that are four to five times longer are poorly represented in numerical models, partly as a result of truncation and numerical procedures and partly as a consequence

of the fact that the basic observational network is itself rather coarse. Fronts and other phenomena directly associated with clouds and precipitation occur on scale sizes which are poorly handled by large-scale numerical models. This difficulty can be alleviated, if not circumvented, by reducing the grid size. However, as we have already indicated, this approach is very costly in computer time and is impractical for a global or hemispheric model. Nevertheless, over limited areas, this approach is both feasible and appropriate, especially for regions with greater than average observational density.

A new and serious difficulty is introduced in trying to limit the area of solution—namely, the treatment of the artificial, internal, lateral boundaries. For certain relatively simple models the appropriate physical boundary conditions are well understood, and their numerical treatment presents no serious problem. Unfortunately, this is not generally the situation. Therefore, means must be devised to prevent the solution from becoming contaminated by noise. We have devised new types of high-ordered interpolation procedures for handling the boundary problem. We have adopted the customary procedure of carrying out a large-scale solution of the model with a coarse network covering a global or hemispheric domain and using the coarse mesh solution to supply boundary information for the fine-mesh domain. It is in the process of interpolation from the coarse to fine mesh that we make use of our high-ordered interpolators which are based upon the concept of restoring information which is lost in the process of two-point linear interpolation.

In an earlier study, it was shown that a large improvement could be effected in the suppression of gravity-wave noise generated by the artificial boundaries by the simple expedient of using an eight-point interpolation operator rather than the customary two-point linear interpolation operator. The eight-point operator was specifically designed to damp short waves which are heavily contaminated by noise, but to restore the amplitudes of waves longer than six grid intervals as closely as possible to their original amplitudes. Nevertheless, not all of the gravity wave disturbance was removed by the use of the eight-point interpolation operator, and it was decided that considerable improvement could be obtained by diminishing phase error as well as amplitude error.

A unique high-order interpolation procedure has been devised which not only restores the amplitudes of all but the shortest waves, but also minimizes the phase error which is inherent in ordinary interpolation. Work has been in progress to apply this procedure to the problem of supplying boundary information for fine-mesh, limited-area models and the preliminary results are very encouraging.

Boundary Layer Prediction Model: We have continued a study of the feasibility of improving the accuracy and increasing the efficiency of the AFGWC Boundary Layer Prediction Model which has been in operational use for the past several years at the Air Force Global Weather Central. The model simulates the meteorological evolution in a given region over a specific period of time by solving a set of equations which is considered to be a mathematical analog of the physical processes in the planetary boundary layer of the atmosphere.

Accuracy and efficiency have been selected as the two most important attributes of the performance of an operational prediction model. The root-mean-square difference between prediction and observation for the entire set of grid points over the domain of prediction is employed to measure the accuracy of the model. The amount of time required by the central processing unit of the

computing facility is used to measure the efficiency of the model.

By regarding the model as a complex of interlocking logical operations, an incremental improvement procedure has been developed. A particular modification is introduced into the model and parallel computations are carried out both with and without the modification. The statistics of the difference in forecast error between the modified and unmodified models form the basis for determining the utility of the modification. Two examples are given to illustrate the mechanics of the procedure.

The current operational model (designated Model 6) employs a lengthy and rather involved algorithm to compute the value of eddy diffusivity at each of the seven levels in the vertical where predictions are made. Three profiles of the average forecast error for the North American region for a number of real synoptic situations were picked at random over a year. The three profiles relate to the 12-hour forecast prepared at 12Z (called day group), the 12-hour forecast prepared at 00Z (called night group), and the 24-hour forecast prepared at 12Z.

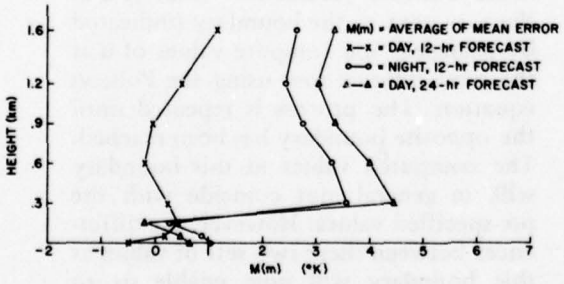

Time average of temperature errors versus height for Model 6. Inadequacy of eddy diffusivity in the model leads to significant errors in the nighttime predictions.

A marked difference was noted in the errors in the 12-hour forecast temperatures between the day and night groups. The night group of the 12-hour forecasts and the day groups of the 24-hour forecasts both need improvement.

Analyses and examination of individual cases led us to focus on the eddy diffusivity as the most likely candidate for improvement. Since there was little indication of what sort of change might lead to an improvement, we took the simplest alternative by assuming that the eddy diffusivity remains constant in the vertical throughout the entire boundary layer, with the value estimated in the surface layer. This change in eddy diffusivity gave rise to improved predictions in the lower part of the boundary layer but produced a degradation in the forecasts for the upper part.

We then moved on to the next level of sophistication by assuming that the eddy diffusivity decreases linearly with height if the whole layer is thermally stable and remains constant if the whole layer is thermally unstable. The result was Model 46.

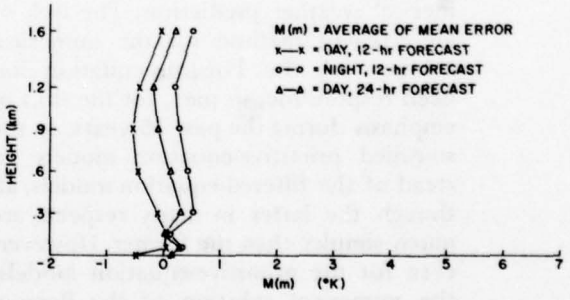

Time average of temperature errors versus height for Model 46. Better modeling of eddy diffusivity has greatly reduced the temperature errors.

It is obvious from comparison of the models that Model 46 is more accurate. It is also more efficient. The treatment of diffusion in Model 46 is not only conceptually but also computationally simpler than in Model 6.

Another set of tests was carried out to determine the most appropriate space-time resolution of the numerical grid of the model. Four models were considered: the basic model with the operational grid spacing (the size of the limited-area fine mesh) and a 30-minute time step; a model with the operational grid spacing and a 60-minute time step; a model with twice the operational grid spacing and a 30-minute time step; and a model with twice the operational grid spacing and a 60-minute time step.

The results have led us to retain the second model for further experiments with more samples while rejecting the third and fourth models as unacceptable. Preliminary results show that the second model yields forecasts with essentially the same accuracy as the basic model but with only half the computational effort. For the immediate future, more synoptic samples will be collected for tests and an effort will be made to improve the prediction of the moisture field.

Efficient Global Model Solution: The Poisson equation plays an important role in problems such as air pollution and numerical weather prediction. The lack of an efficient method for the numerical solution of the Poisson equation has been responsible, in part, for the shift in emphasis during the past 15 years, to the so-called primitive-equation models instead of the filtered-equation models, although the latter in many respects are much simpler than the former. However, even for the primitive-equation models, the numerical solution of the Poisson equation is important in objective analysis and initialization. Since these are required in daily routine operations in the weather services, it is of paramount importance that the procedures be efficient.

We have developed here an efficient algorithm for the solution of a discrete Poisson equation on the surface of a sphere. The algorithm is cast in a global setting in anticipation of the development of global numerical prediction models and also because this is where it has its principal applicability. However, the method is also applicable in limited-area models and in channel models.

The method has been called the shooting method because its principle is similar to that of shelling by artillery. If the exact location of the artillery and the targets are known, we fire the first shots using arbitrary elevation angles. The shots will generally miss the targets. However, knowing the miss distance of each shot from each target, we may then adjust both the location and elevation angle of each battery so that the second shots will land directly on target.

The method is illustrated with a problem in a rectangular domain. The discrete Poisson equation couples the forcing function f at a given point with the values of the unknown u at five points neighboring each other. The forcing function at each of the interior points of the domain indicated by the dotted points and values of u at the boundaries indicated by open circles are known. We want to find values of u which satisfy the Poisson equation in the interior of the domain. In the shooting method, we make arbitrary guesses for values of u at the row next to the boundary (indicated by triangles) and compute values of u at the next interior row using the Poisson equation. The process is repeated until the opposite boundary has been reached. The computed values at this boundary will, in general, not coincide with the pre-specified values. However, the differences between these two sets of values at this boundary will now enable us to compute the correct values at the first interior row. Once the correct values at the first interior row are known, the problem is then solved by shooting once more.

The main advantage of this method is in its efficiency. In the traditional meth-

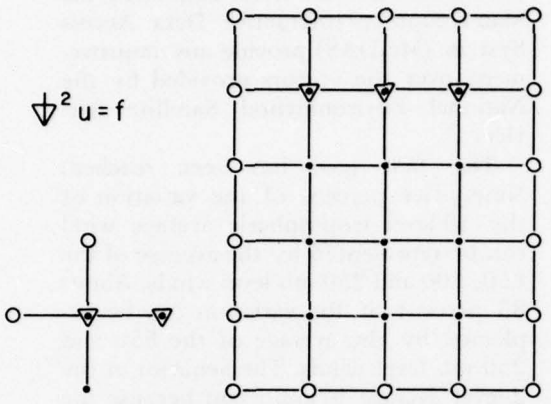

Solving the Poisson Equation by the Shooting Method: The equation relates the value of f, called the forcing function, to the values of the unknown, u. Starting with known values of u at the points indicated by the open circles, the value of u is guessed for the row of interior points in the triangles. Using the assumed values and the equation, we can calculate the value of u at all the points in the interior, and also for the points along the opposite edge for which we already have actual values. The difference between the actual and calculated values along the edge can be used to calculate the correct values at the first interior row. A second set of calculations then gives the correct values at all the interior points.

od of relaxation, a grid of 32 x 32 requires as many as 30 iterations. The work in the shooting method, however, is roughly equivalent to three iterations. The saving in time is significant.

Modeling Stratospheric Environmental Impact: Air Force systems operate through the depth of the atmosphere. Within the troposphere, pollutants from these systems are removed within a time scale of weeks by storms, rainfall and turbulence. Higher up in the stratosphere, however, vertical mixing is greatly reduced compared with the troposphere, and pollutants may remain there for years. Horizontal motion does take place so that the pollutants introduced anywhere may be distributed worldwide after several months.

An important consideration is the effect pollutants will have on the trace constituents naturally present in the stratosphere. While making up only a very small fraction of the atmosphere, trace constituents such as ozone influence the radiation balance of the earth-atmosphere system while blocking lethal ultraviolet radiation which would otherwise reach the earth's surface. Thus the possibility exists that Air Force operations may modify the stratospheric gaseous or aerosol composition sufficiently to affect the photochemical and radiation balance of the stratosphere, which in turn could have a significant impact upon the worldwide climate. Since any large-scale atmospheric changes are expected to be slow and subtle, the most effective approach to this problem is through controlled experimentation with mathematical models of the atmosphere which can simulate the present atmospheric behavior as well as the consequences of perturbed stratospheric conditions.

Our goal is the development of a time-dependent, three-dimensional model of the atmosphere which incorporates spherical geometry and which includes all of the important physical processes, the major gaseous and aerosol constituents, and the principal topographic features of the underlying surface. The basic framework for the model, consisting of the equations of motion with appropriate boundary conditions, has been developed and programmed for testing. Initial integrations, using simplified flow patterns, are proceeding to determine the adequacy of the finite-difference approximations being used and the minimum required grid-mesh spacing. The model has been integrated out to 60 days, with satisfactory results. A filtering procedure designed to damp the poorly resolved, shorter scales of motion while leaving the meteorologically significant motions intact, has been

tested successfully using a three-dimensional channel model of the atmosphere.

SATELLITE METEOROLOGY

Imagery from meteorological satellites has continued to expand in quantity, detail, and diversity. The analysis and utilization of this imagery to solve Air Force problems require techniques to process the vast quantity of data, extract pertinent information, and utilize independent information from diverse images. The extraction of meteorological intelligence from satellite sounders is in its infancy. The limitations imposed by clouds and water vapor are severe. In addition, there are problems associated with the accuracy of measurement and with interpretation. Efforts to overcome these limitations require initiatives to isolate the specific sources of instrument and analysis noise, and the design of new sounders which utilize additional and independent atmospheric radiations.

Tropical Cyclone Studies: The use of imagery to improve the forecasting of tropical cyclones has been approached from two directions. One is to use the imagery to extract quantitative information for inclusion in numerical prediction models and the other uses the large-scale cloud distribution directly.

The first approach is based on the assumption that cloud displacements in successive geosynchronous satellite pictures are representative of the wind velocity at the level of the clouds and that these cloud-derived winds can be utilized in a dynamic model. The SANBAR model is a barotropic model which utilizes a mean tropospheric wind based on the average of 10 winds between 100 and 1000 mb. The goals of this study are to determine, first, how well a 1-, 2-, or 3-point average can represent the 10-point mean; second, the effect on the forecast of using cloud displacements, and third, if cloud vectors derived by the Man-computer Interactive Data Access System (McIDAS) provide any improvement over the vectors provided by the National Environmental Satellite Service.

The first goal has been reached. Ninety-five percent of the variation of the 10-level tropospheric average wind can be represented by the average of the 850, 500 and 250 mb level winds. About 85 percent of the variation can be explained by the average of the 850 and 250 mb level winds. The behavior of the 2-level average is important because the probability of seeing low or high clouds is much greater than that of seeing middle clouds. The second goal is now being investigated with 1975 data on Atlantic hurricanes. The study was attempted with 1974 data, but the storms that year were of a type that were particularly unsuited for the SANBAR model and the results of the analysis were inconclusive. The second and third goals are expected to be satisfied late in 1977.

The second approach, one of examining the distributions for clues to typhoon motion utilized the McIDAS at AFGL. Programs were developed which allowed the computation and display of the average cloud field over a large area in relation to the center of the storm. This technique, called "compositing," is a powerful tool that has often been used in analysis of fields that are easily defined quantitatively such as pressure or temperature. The capability of computing and displaying the differences in the cloud fields associated with different types of storms was also developed. Compositing has the advantage of reinforcing significant features and muting the random details of a data field.

The following illustrations show an example of one of the more significant results achieved using the NOAA archive tapes of scan-radiometer visible data. Figure a is the composite brightness of four

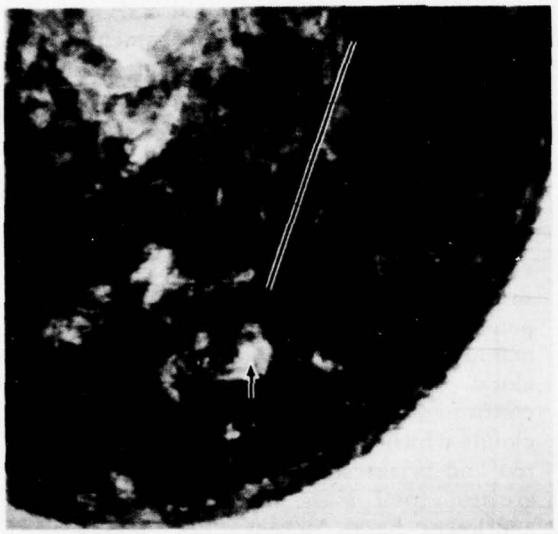

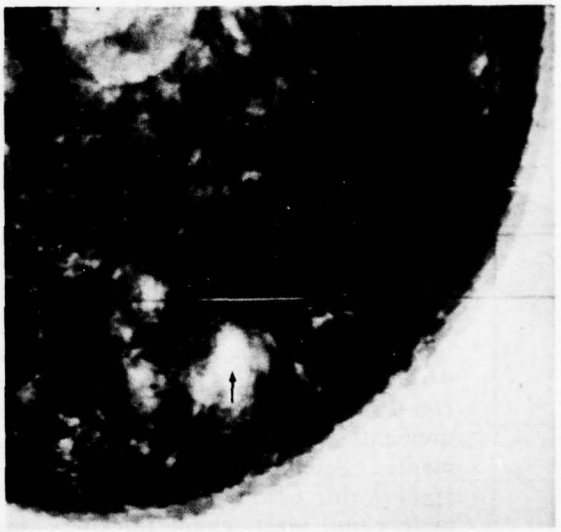

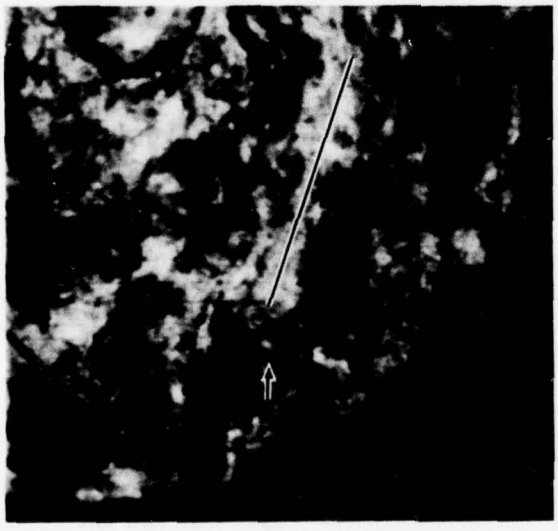

(a) The composite brightness of four storms that moved in a general westerly direction in the next 24 hours. The arrow indicates the center of the storms. (b) The composite brightness of four storms that moved in a general northwesterly direction in the next 24 hours. The arrow indicates the center of the storms. (c) The difference between pictures (a) and (b). The center of all eight storms is gray, since the area was bright in both pictures. The bright band with the line through it was bright in (a) and dark in (b). This band was also associated with westerly moving storms located both to the east and west of this area.

storms located in the box bounded by 15 and 20 degrees N, and 120 and 125 degrees E which moved in a westerly direction during the next 24 hours. Figure b is the composite brightness for four storms in the same area which moved in a northwesterly direction. Figure c is the difference between the two. Bright locations in figure c were bright in figure a and dark in figure b. Those locations which were dark in figure a and bright in figure b show up dark while those locations which were bright or dark in both pictures show up gray. Thus the center of the typhoons indicated by the arrow in figure c is gray since both figures a

and b were bright there. The significant feature to note is the long bright cloud band leading away from the center toward the northeast. It represents an area that was bright for westerly and dark for northwesterly moving storms in that 5-degree box. What gives it significance is that this band is also observed associated with westerly moving storms in locations to the east and west. This work will continue using an expanded data sample as well as investigating the features of the cloud field as revealed in the infrared display.

Cloud Properties from Satellites: Radiation data from satellites have been compared with simultaneous cloud measurements with aircraft-borne instruments. Satellite meteorologists have applied this unique set of data to estimate cloud mass, cloud thickness, and ceiling height from satellites. The methods developed may also be used to improve the detection of heavy weather over data-sparse regions and to verify forecasts of clouds and rain based on numerical prediction models. The methods have the further advantage of bypassing formidable calculations of cloud radiative properties observable by satellites for ice clouds with highly irregular particle shape, size, and number concentration.

The weather satellite instrument simultaneously detects visible and infrared radiation. The visible radiation is reflected sunlight at 0.5 to 0.7 micron. Since the spacecraft are sun-synchronous polar-orbiting satellites, simultaneous visible and infrared measurements are available over the globe once per day. The visible measurements are normalized to standard viewing geometry. This is the only correction which must be applied to standard data archives before using the methods to estimate cloud properties and derive climatologies.

A series of simultaneous measurements of clouds by satellites and aircraft began in January 1974. Forty-five flights have been made to date. At the time of the satellite overpass an aircraft equipped with cloud physics instrumentation descended in a spiral. Aircraft data were used to measure cloud mass as a function of altitude. Regression techniques were then used to estimate cloud mass as a function of altitude. Regression techniques were then used to estimate cloud mass and thickness from the corresponding satellite data. Relationships between ceiling height and cloud parameters were developed in a similar manner using surface observations as cloud truth height. The observations confirmed a simple physical hypothesis: clouds which appear coldest in the infrared and brightest in the visible have the greatest total mass, vertical thickness and lowest bases. Moreover, the observations provide a quantitative basis for estimates of cloud properties from satellites.

Snow-Cloud Discrimination: The main objective of this study was to evaluate the usefulness of the data from the S192 Multispectral Scanner aboard SkyLab in Snow-Cloud Discrimination. The spectral range covered by the scanner was from 0.4 to 2.35 microns and 10.2 to 12.5 microns. This experiment package on SkyLab provided an opportunity to examine the reflectance characteristics of snow and clouds in the spectral range from the visible to the near infrared. Films for 17 SkyLab passes were received and analyzed at AFGL along with some digital tape data.

Analysis of pairs of SkyLab imagery, one set in the visible spectrum and one set in the near infrared, shows marked differences in the characteristic reflectances of snow, water clouds and ice clouds in the two bands. In the visible spectrum, all three scenes have high values of reflectance and appear white. The reflectances of these three scenes in the near infrared (SkyLab Band II, 1.55 to 1.75 microns) range from high (water

clouds) to medium (ice clouds) to very low or black (snow). These differences, which are reflected in the ratios of the reflectance in the visible spectrum (SkyLab Band 6, 0.68 to 0.76 micron) to that in the near infrared (SkyLab Band II, 1.55 to 1.75 microns), appear to provide a method for discriminating between snow cover, ice clouds, and water clouds. The mean snow ratio between the reflectance in the visible and the near infrared was 53.66 ± 24.4 and the mean cloud ratio was 5.47 ± 0.8. Based on the analysis of the SkyLab data, the ideal band pass for snow/cloud discrimination would start at 1.5 microns and extend to a wavelength no longer than necessary to provide sufficient energy on the detector.

Application of Microwaves: AFGL research has shown that it is possible to infer atmospheric structure from measurements of microwave energy emitted, absorbed, and scattered by the atmosphere, and that such measurements would have some advantages over those presently in use. Currently, infrared sensors are used to infer atmospheric structure. In the infrared spectrum, most cloud systems are opaque. This physical property of clouds limits the useful data a satellite can collect. On the other hand, most cloud systems are transparent to microwaves, allowing atmospheric soundings in both clear and cloudy areas. The strong microwave absorption spectra of water vapor at 22 GHz and 183 GHz (1.36 cm and 0.16 cm wavelengths respectively) and of oxygen at 60 GHz and 118 GHz (0.5 cm and 0.25 cm wavelengths respectively) are used to determine the atmospheric structure. Water vapor profiles are inferred from measurements of the water vapor spectrum and temperature profiles from the oxygen spectrum. The oxygen spectrum at 60 GHz will be used in the microwave temperature sounder (SSM/T), advanced by AFGL, which is to be flown onboard the Defense Meteorological Satellite System (DMSS) satellite.

Because the microwaves penetrate clouds in varying degrees from full transparency for ice clouds to total opacity for heavy rain clouds, the microwave region possesses a unique property for probing cloud structure. Analysis has indicated that when the 118 GHz and 60 GHz regions are used simultaneously, cloud liquid water content can be measured. A contractor is currently building a 118 GHz radiometer to verify this hypothesis. The "windows" between the absorption spectra stated above and the frequency range below 22 GHz may be utilized to determine earth surface condition and areas of precipitation over land. A microwave imager will allow determination of ice/sea boundaries, sea surface temperature, sea state and surface winds over oceans and potentially the ability to differentiate rain areas over land. AFGL has advocated a multi-channel mechanically scanned microwave imager to be flown onboard the DMSS.

WEATHER RADAR TECHNIQUES

The Meteorology Division's program in weather radar investigations falls into two areas. As part of an overall effort to define the size distribution and phase of all hydrometeors affecting supersonic SAMSO test missiles, one area of investigation concerns both the prediction and measurement of the liquid water content of the precipitation encountered along the trajectory of these vehicles. A more general description of this work is given elsewhere in this chapter under the title of the Weather Erosion Programs. In the second area of investigation, studies are aimed at developing improved weather radar and data processing techniques and instrumentation that will enable the operational detection of meteorologically significant features of storms and

the prediction of their motion and development to be made in a timely and accurate manner. Here the concern is with the identification and forecasting of severe weather hazards which are a threat to both people and aircraft on the ground and to flying aircraft. Among these hazards are tornadoes, hurricanes, windstorms, hail, turbulence, and heavy snow.

In recent years, most of the research has been conducted at three locations. At the AFGL Weather Radar Facility in Sudbury, Massachusetts, state-of-the-art processing and display equipments together with three radars of differing wavelengths are used to investigate both widespread and convective precipitation systems. The investigations focus on the techniques and instrumentation for measuring, processing, displaying, and automatically interpreting ground-based weather radar information. At two other locations, weather radar investigations are centered around the needs of the Weather Erosion Programs. High-power, high-sensitivity radars at both the NASA Wallops Flight Center at Wallops Island, Virginia, and the Kwajalein Missile Range at Roi Namur, Marshall Islands, are utilized in these investigations together with instrumentation similar to that found at Sudbury, but modified to meet the needs of the two erosion programs.

Critical Success Index: In response to an Air Weather Service request for a comprehensive analysis of Doppler and conventional radar as an operational tool for identifying and predicting hazardous weather, a critical review of all current techniques and earlier research results amenable to quantification was conducted. A decision tool called the Critical Success Index was developed as a means of evaluating the relative merits of the various techniques. The index is found by dividing the number of successful identifications by the sum of the successes and errors of both kinds, that is, false alarms and failures to predict. Application of this index to all available reports of the results of these radar techniques revealed a clear superiority of Doppler methods for the detection of tornadoes and other damaging wind storms and non-Doppler methods for the detection of large hail. As a result of this study, the Air Weather Service has included the requirement for a Doppler capability in its plans for the forthcoming Advanced Weather Radar.

Real-Time Analysis of Wind: The coarse but definitive warnings of tornadoes and other severe wind disturbances in convective storms provided by the Plan Shear Indicator display encouraged the development of real-time digital methods for the quantitative determination of the velocity structure within these storm systems. During the previous reporting period, Laboratory and contractor scientists, working in association, developed a revolutionary Doppler processing scheme, called the pulse-pair technique, which enabled the calculation of Doppler spectral moments at approximately 10,000 times the speed of the fastest Fourier transform technique. The instrument was installed in the Porcupine Doppler radar.

The pulse-pair processor computes the mean and spectral width, or variance, of velocity spectrum directly, performing relatively simple operations on the complex Doppler time series. The processor has a speed comparable to the Plan Shear Indicator, but gives a digital velocity mean output as well as variance, and for this reason can feed a variety of display systems as well as yield an output suitable for computer processing. The pulse-pair technique offered, for the first time, the possibility of digital parameterization of the velocity fields for efficient and reliable objective identification and short-term forecasting of severely destructive storms.

Another development reported on previously was the color display. It overcame the problem of variation of the strength of return with range, and the inability of the operator to discriminate many shades of gray. It contours the video signal output of the weather radar and integrator according to a desired, predetermined scheme, and stores the resulting data as one of 16 color-coded levels in four independent image-oriented memories, each of which refreshes one raster-scan color television monitor. The operator can easily recognize the 16 color-coded levels of signal intensity. The system can store indefinitely, update or erase any of the four stored images independently. With appropriate antenna scanning, it can generate a constant altitude PPI display for each of four selectable altitudes, as well as the more usual RHI and PPI displays. The Pulse-Pair Processor and Color Display have resulted in a quantum increase in the information that is available in real time concerning the structure of the wind field as measured by Doppler radar. The patterns of velocity information are often quite complex. However, comparisons of rawinsonde and Doppler velocity information for periods when the winds are uniform at a given altitude have shown that even the most complex patterns can be interpreted in real time on the basis of combinations of simpler structures.

We have represented features which actually appeared in a color display in black and white. In the color display each of the rings has its own color. The point in the center of the pattern is the location of a Doppler radar which has just scanned through an extensive precipitation cloud at a low elevation angle. The greater the distance of a point in the pattern from the radar position, the greater its altitude. The lines are isolines of the radial component of the wind. All along the railroad track, the radial component is zero. When we combine the information from the railroad track and the distribution of colors, we can determine the direction and speed of the wind at any point in the pattern. In the case shown, the wind at point A (close to the radar and at a low altitude) is from the southeast while the wind at point B (further from the radar and at a higher altitude) is from the south. This pattern

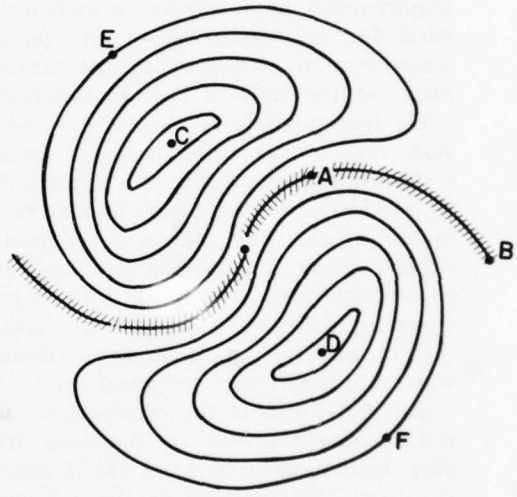

A black and white representation of features which actually appeared in a color display of the structure of the wind field in an area of widespread precipitation as measured by Doppler radar. The Doppler radar was located in the center of the display. Each ring indicated a particular value of the radial component of the wind, and was in the color chosen to indicate that value. The crossed line "railroad track" indicated a zero radial wind component.

then shows a wind veering with height. As one moves from the radar to point C or point D, the magnitude of the radial wind component increases with altitude, whereas from C to E and D to F the wind decreases with altitude. This technique, effective in stratified precipitation, is now being extended to severe convective storms.

Liquid Water Content Analyzer: The color display system has been successfully used during the past three years of the Weather Erosion Program to define the radar reflectivity structure of the atmosphere during all SAMSO launch activities at Wallops Island. The system has continued to provide the SAMSO Launch Director with a quantitative visual description of meteorological conditions throughout the test. SAMSO's test requirements demonstrate an increasing need for knowledge about the liquid water content structure of the atmosphere at the time of launch. However, while it is possible to make the conversion from radar reflectivity to liquid water content manually, it is impossible to provide more than coarse manual estimates in real time. Therefore, a liquid water content analyzer was developed to automatically determine the reflectivity along an arbitrary trajectory. It makes the conversion from reflectivity to liquid water content using empirical relationships, and presents the resultant liquid water content profile on the same display system used to brief the Launch Director. This analyzer has been found to be an extremely useful adjunct to the weather radar instrumentation, and its capability has recently been expanded to provide real-time predictions of erosion and erosion-related phenomena.

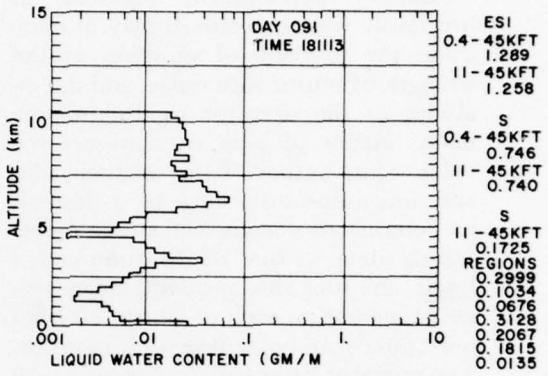

A typical display of the liquid water content profile predicted for a scan of the SPANDAR radar at Wallops Island, Virginia, at 1811Z on 31 August 1976.

DESIGN CLIMATOLOGY

Military materiel must have year-round world-wide endurance capability and operational utility. Overdesign could be costly, yet ineffective, but underdesign could cause failure and loss of life. Climatological studies, therefore, have been continued to improve our knowledge of the risks to Air Force equipment design and operational planning caused by weather extremes.

Climatic Extremes: Department of Defense Military Standard 210, Climatic Extremes for Military Equipment, is the document used by the three Services to specify climatic design criteria for equipment destined for world-wide usage. AFGL has technical responsibility for keeping this document up to date. A revised standard was accepted by DOD and published in December 1973. This exceptionally valuable document for use in designing equipment is intended for world-wide usage. However, if the design criteria contained in this document are used for equipment which will be used in only one location, that is, the tropics, costly over-design may result. To eliminate this problem, an effort has been started to prepare 1-, 5-, and 10-percent global mappings of extremes of weather elements. Such presentations will permit designers to choose design criteria based on the intended deployment area. Temperatures equalled or exceeded 1, 5, and 10 percent of the time during the hottest and coldest months have been mapped for the Northern Hemisphere. They are now being mapped for the Southern Hemisphere. The next element planned for study is the instantaneous precipitation rate.

Wind Variability: Surface wind variability is an important consideration in

the design and operation of many Air Force systems. For example, accurate estimation of the wind speed range and gustiness is extremely important during the take-off and landing operation of VSTOL aircraft and helicopters. A technique was developed for estimating these parameters for given time intervals, during periods of strong winds, from the mean wind speed. The results of this study are now being used by the Air Weather Service to provide guidance to forecasters supporting helicopter operations. The National Weather Service has also adopted the technique for use in its automated wind forecasts.

Wind information is required for the targeting of ballistic missiles. If observations and conventional short-range forecasts are unavailable, climatology provides the best estimate of upper air winds. Computer-generated winds based on theoretical models of the wind field provide the present backup climatology. A comparison between computer-generated winds and a climatology based on four to eight years of daily actually observed winds was made at approximately 400 stations in the Northern Hemisphere. The altitudes ranged from 5,000 to 80,000 feet. This comparison indicates that there are some large differences between the two sets of winds. Therefore, it was concluded that a climatology based on more than four years of daily observed winds is generally superior to computer-generated climatic winds based on the models presently used.

Line-of-Sight Climatology: Many current and proposed Air Force systems use optical, infrared, and laser sensors for their detection, lock-on, and tracking components. Because many of these components cannot operate through heavy haze or clouds, there is an increased need for information on the probability of haze- or cloud-free lines of sight. Two efforts have been conducted to determine how often haze or clouds would limit operations: an aircraft in-flight observation program and the development of a cloud-free line-of-sight (CFLOS) model based on observed cloud-cover statistics.

The collection of more than 275,000 in-flight line-of-sight observations from aircraft to the earth's surface, the horizon and to the sky over much of the Northern Hemisphere was analyzed and prepared for publication. Probabilities of clear, cloud-free or haze-free lines of sight from aircraft at various flight altitudes have been determined and are being readied for publication. This information will be valuable to designers and operators of many electro-optical systems coming into or already in the inventory. The utility and optimum deployment of these weapon systems can

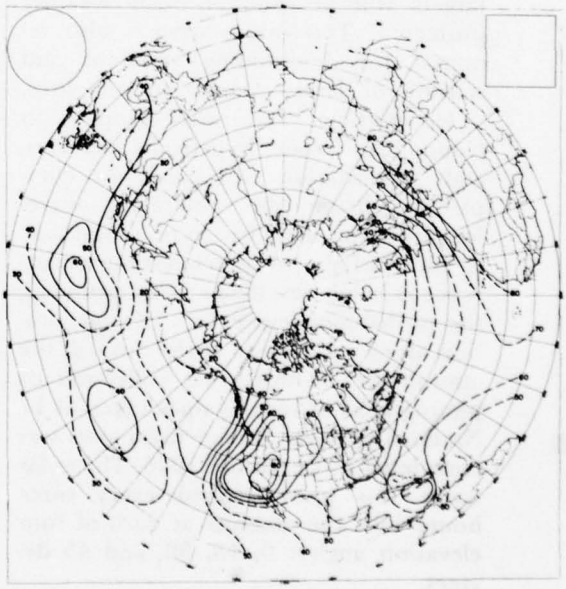

Probabilities of a cloud-free line-of-sight between an aircraft at altitude and the earth's surface. The solid lines indicate a high degree of confidence in the analysis while the dashed lines indicate less confidence because the analysis is based on a smaller number of observations.

be estimated from a knowledge of clear and cloud-free line-of-sight statistics.

A program to collect in-flight line-of-sight observations at altitudes under 10,000 feet over western Europe is presently under way. These observations are taken primarily by Army helicopter units.

A model for estimating CFLOS probabilities has been developed by correlating cloud-cover observations with whole-sky photographs. This model, which provides CFLOS probabilities through the atmosphere for any desired elevation angle based on cloud-cover statistics for a given location, was used to produce an atlas of CFLOS probabilities for Germany. Similar atlases for the U.S.S.R. and the U.S.A. are being developed. Efforts are also being made to model joint probabilities of CFLOS in order to estimate the probability that two or more targets will be simultaneously weather protected. This information is also required for determining locations and spacing of laser communications sites.

Ice particles and water droplets in clouds can erode hypersonic vehicles, and precipitation can partly or completely absorb the millimeter wavelengths often used for communications. A climatology of precipitation occurrence is being developed for determining the probability and extent of precipitation along various ray paths through the atmosphere. A three-year collection of photographs of radar scopes taken at 17 National Weather Service radar sites was completed in December 1975. The radar scope was photographed every three hours with the antenna at each of four elevation angles: 0, 15, 30, and 45 degrees.

These photographs will be used to develop a climatology of the slant range thickness of precipitation echoes. These data will provide probabilities of precipitation interference along ray paths from the surface, between two altitudes, and from any altitude out to space or to the ground.

Standard and Reference Atmospheres: The *U. S. Standard Atmosphere, 1976* has been completed. It is a major revision of the *U. S. Standard Atmosphere, 1962*, and includes the AFGL 50- to 90-km revision. The same revision was adopted by the International Standards Organization (ISO) for the ISO Standard Atmosphere.

As part of a continuing investigation of the distribution and variability of atmospheric properties up to 120 km, the *U. S. Standard Atmosphere Supplements, 1966* are also being revised and expanded in scope. Monthly models for each 15 degrees of latitude from equator to pole are being developed for altitudes up to 90 km. Specialized winter models are also being constructed to describe warm and cold stratospheric and mesospheric conditions typical of arctic and subarctic regions. Consequently, these reference atmospheres will provide the horizontal and vertical distributions of thermodynamic properties of the atmosphere that would be encountered by aerospace vehicles. Mean monthly models from the surface to 90 km have been completed for the equator, 15, 30, and 45 degrees north latitude.

Multi-Predictor Probability: A model of conditional probability developed previously has been extended to give the probability that the phenomenon predicted will exceed a threshold value, subject to specific values of two or more predictors. In the formula for calculating the probability, the conditional probability is replaced by the normalized distribution for the varying quantity. This value is shown to be given by a sum of terms, where each term is the value of one predictor, transformed into a normalized distribution and multiplied by its partial regression coefficient.

A test of this model on regular three-hour observations of precipitation re-

vealed strong evidence of the validity of the probability estimates, and also demonstrated that the model can yield very good estimates of the conditional probability with as many as seven predictors.

Coverage of Areas: Meteorological observations are generally taken at a specific geographical location and at a single instant of time. It is often important to know how representative these observations are of the weather in the surrounding area. When a storm passes, what fraction of a city or state will receive rainfall? What is the probability that a satellite camera will have a clear view of at least 80 percent of a city? These and similar questions have led to the general investigation by a statistical modeling of areal coverage. The study did not attempt to describe, or map, actually occurring details of weather phenomena, but did estimate the probability of events occurring with specific areas or fractions of areas. The effort was centered on maximum or minimum values of a meteorological element in a given area or the highest minimum, or lowest maximum, in a given fraction of the area. Archived data were used, not as comprehensive climatology in themselves, but as a guide to modeling.

The problem, at the outset, was to devise a procedure that would produce a simulated horizontal synoptic field probabilistically without recourse to physical laws or dynamics. Once such a Monte Carlo procedure was adopted, it was repeated many times to produce a large set of synoptic situations, comprising a sample that could be surveyed for spatial correlation or association of events. The collection of information so obtained constitutes the model. It has a parameter (r) termed scale distance and defined as the distance over which the correlation coefficient is 0.99.

An illustration of the results of the Monte Carlo sampling process is the calculation of the probability of an event occurring in one tenth of an area of known size when its single-point probability is known. If an event, such as rain, is known to occur at a rain gauge with a frequency of 2 percent at any hour of the day, then the probability of its single-point non-occurrence is 98 percent.

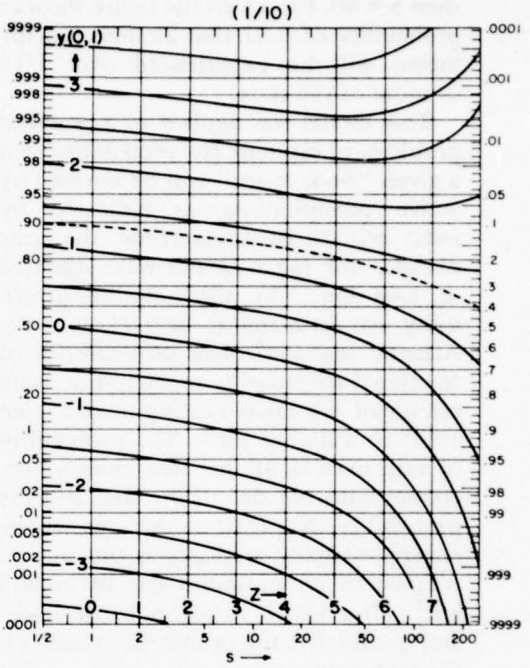

Probability Estimates of the highest minimum in 1/10 of the area (S^2), given the single-point probability (ordinate scale.)

From the point 0.98 on the left-hand scale of the figure used to calculate the probability, we follow a curve of constant probability across the figure to the value of the area ratio of interest. (The value, $S = \sqrt{A/r}$, where A is the area of interest, and r is the distance for which the correlation is 0.99.) If the area is the size of the state of Massachusetts (A = 21,358 km^2) and the scale distance for one-hour of July rainfall is r = 3.61 km,

then S = 40, for which the figure shows a probability of 0.07 that 24-hour precipitation will be experienced over 1/10 or more of the state.

This model was applied to a practical problem, to estimate the probability that a given "floor space" will be covered by active precipitation, as indicated by radar echoes. In summertime, the scale distance for radar echoes was estimated at 1.48 km. The single-station probability was estimated to be 0.04 along the Atlantic seaboard. The probabilities of fractional coverage by precipitation were estimated for areas ranging in size from 1500 to 100,000 km^2. The probability of rain over ¼ of the area or more decreases with the size of the area. But the probability that 1/10 of the area will be covered actually increases as the area increases, to an optimum size of 50,000 km^2, after which it begins to decrease, and eventually, the probability reaches 0 for a very large area.

FOG DISPERSAL

Since the beginning of scheduled flying, fog has hampered airport operations. In the Air Force, where schedules must often be met whatever the weather, fog can seriously compromise operations. In recognition of this fact, the Air Force has a vigorous program to develop and use fog dispersal technology. AFGL has studied techniques for operational fog dispersal for several years. Recent attention has been focused on the development of an operational warm fog dispersal system using ground based heat sources. A smaller effort was mounted to explore the feasibility of using compressed air for supercooled fog dispersal.

Warm Fog: A modern Warm Fog Dispersal System (WFDS) using momentum-driven heat sources has been designed. The system has two principal components: the combustors and the controls. The combustors are located along both sides of the approach and rollout portions of the runway. The clearing produced will allow landings to be safely completed under Category I aviation conditions. This means that the visibility will be raised to 800 meters (1/2 mile) to a depth of 60 meters (200 feet). In the interest of safety, the clearing depth in the Warm Fog Dispersal System will be 75 meters (250 feet) at the start of the approach zone and taper down to 15 meters (50 feet), 300 meters (1500 feet) downrunway of the nominal touchdown point of the runway. The clearing depth will remain 15 meters (50 feet) until the end of the runway or until some convenient exit taxiway. The clearing will be 150 meters (500 feet) wide at the start of the approach zone and taper down to 60 meters (200 feet) near the touchdown point.

Theoretical calculations, verified by empirical testing of subscale WFDS combustors, both performed over the past two years at AFGL, show that of the order of 10^{10} cal of heat/minute are required to disperse the fog over the volume necessary to support Air Force operations. The heat must be evenly dispersed to insure an even clearing over the intended target volume. Numerical modeling of heat plumes combined with field

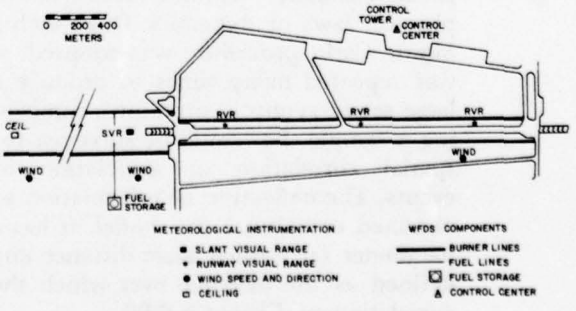

Schematic representation of a modern Warm Fog Dispersal System using momentum-driven heat sources.

observations performed on scales between 1/6 and 1/12 of full scale have provided design specifications for the WFDS combustors. Different amounts of heat and thrust are required for combustors near the approach, touchdown, and rollout areas of the runway.

The theoretical and empirical investigations performed to develop the combustor specifications also showed that the location, intensity, and depth of the heat plume all critically depend upon wind. It is for this reason that the second major component of the Warm Fog Dispersal System, the control system, is so important. Wind and visibility systems will be installed near the approach and rollout portions of the Warm Fog Dispersal System to monitor changes in these critical meteorological parameters.

In the approach zone, indirect probing devices will be used because observations will be needed to a depth of up to 75 meters (250 feet) in an area where towers cannot be erected. Acoustic and laser doppler wind sensors are being tested for use as the wind monitoring devices. Laser devices to determine slant visual range (SVR) and/or laser ceilometers will be tested to monitor the clearing produced by the Warm Fog Dispersal System in the approach zone. In the rollout region of the runway, conventional runway visual range (RVR) and wind instrumentation will be used.

All of the meteorological information will be transmitted to a control point. There, computer directed commands will be issued to the combustors to modulate heat and thrust in response to changes in wind and/or visibility.

The combustors for the Warm Fog Dispersal System will be developed in FY-1977. Limited portions of the WFDS will be tested at a heavily instrumented, off-runway site in FY-1978. Full scale operational demonstration tests of the WFDS are planned to start in October 1979. The program is being managed by the Air Force Civil Engineering Center, with technical support provided by AFGL.

Supercooled Fog: The Air Weather Service (AWS) has been conducting supercooled fog dispersal operations in Alaska and Washington for several years. At first the clearing agent was dry ice dispensed from the air. Recently it has become liquid propane spray dispensed from the ground. With the increasing cost and possible decreasing availability of propane, it became appropriate to investigate other methods of dispersing supercooled fog.

Another method calls for the substitution of compressed air for propane. When the compressed air is vented through a suitable supersonic nozzle, the adiabatic expansion of the air upon its exit cools the fog-laden air to the point where many ice crystals are produced by

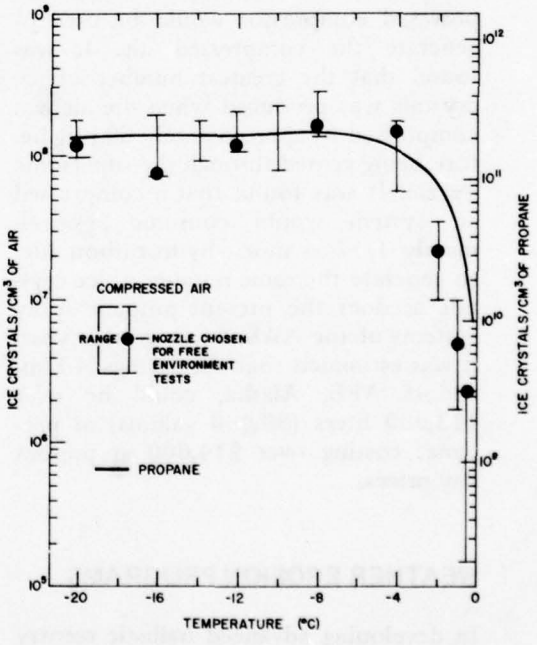

Ice crystal concentrations produced by compressed air and propane under controlled environment conditions.

homogeneous nucleation. These ice crystals react with the fog in the same way as do those produced by the propane dispensed in the successful AWS operations.

The number of ice crystals produced by compressed air and propane during controlled environment tests conducted at the U. S. Army Cold Regions Research and Engineering Laboratory were compared. These results were verified in a limited number of free environment tests conducted on Elk Mountain in Wyoming. The adiabatic expansion of 1000 cm^3 of previously compressed air produces the same number of ice crystals as does the evaporation of 1 cm^3 propane.

In an operational adaptation of the compressed air technique, a gasoline powered compressor would be used to generate the compressed air. It was found that the greatest number of ice crystals was produced when the air was compressed to approximately 60 psig before being vented through the supersonic nozzle. It was found that a compressed air system would consume approximately 1/17 as much hydrocarbon fuel to generate the same number of ice crystals as does the present propane spray systems of the AWS. In an average year, it was estimated that the savings at Elmendorf AFB, Alaska, could be over 113,000 liters (30,000 gallons) of propane, costing over $14,000 at present day prices.

WEATHER EROSION PROGRAMS

In developing advanced ballistic reentry systems, the design engineer must know how candidate materials erode when they traverse clouds or precipitation during hypersonic reentry through the atmosphere, for this process can affect the accuracy and even the survivability of a reentry vehicle. Likewise, in predicting the combat performance to be expected of a reentry system, the operations analyst must know the frequency and severity of erosion weather in potential target areas. On both of these questions the Meteorology Division has continued during the past two years to support the Air Force's Space and Missile Systems Organization (SAMSO).

Field tests of erosion are conducted at both NASA's Wallops Island range in Virginia and at the Kwajalein Missile Range in the southwest Pacific. In such tests the role of AFGL scientists is to document the weather actually encountered by the test vehicle. This is accomplished through coordinated measurements made with an ultrasensitive ground-based radar and from aircraft specially instrumented with cloud microphysical sensors. The basic methodology was developed more than five years ago expressly for the erosion tests. Since then, instrumentation and procedures have been continually upgraded in the interest of enhancing the accuracy and utility of the meteorological data, not only for documentation after the test, but also as a real-time input to launch decisions.

The mass density of cloud or precipitation particles (hydrometeors) is the foremost weather parameter in the erosion equation. The current standard device for measuring this is a particle spectrometer which counts and sizes the particles individually. The sizing is actually done in terms of the maximum width of a horizontal shadow of the particle or, by a more advanced version of the spectrometer, in terms of the full two-dimensional shadow. While the relation between these measures and the mass of the particle is straightforward for a spherical particle, it is far from simple for snowflakes and other forms of solid particles. Consequently, in order to use the particle spectrometer to infer mass, AFGL has had to undertake extensive fundamental studies of the relationship

between the geometry and the mass of all forms of solid hydrometeors.

Even so, the mass measurements made with the particle spectrometer are at best indirect and dependent on statistical relationships. Therefore, it has long been a goal of the Weather Erosion Program to develop a device capable of sensing hydrometeor water content directly. Experimental versions of two sensors, operating on quite different principles, are currently being flown. Although test results are most encouraging, neither device has yet been certified for routine use.

In order that current weather conditions can be assessed in real time for the guidance of the SAMSO test director in deciding when to launch his test vehicle, the data systems aboard C-130E and Learjet 36 aircraft feed into onboard computers, the data from which provide hydrometeor water content and other critical weather parameters for immediate relay to the ground.

For the same reason, computers have also been incorporated in the radar data systems. In consequence, at both ranges the current distribution of water content and the expected test results can be evaluated instantly for any proposed test trajectory. Further details of the Liquid Water Content Analyzer developed by AFGL for use at Wallops Island are included under Weather Radar Techniques.

AFGL is concerned not only with test weather but also with target weather. It has painstakingly synthesized the sequence of erosion weather for an entire year at locations representative of potential target areas. These data are now in use by SAMSO and other agencies as a test bed for systems assessment.

Special methods are needed for generating such climatologies because hydrometeor water content is not a weather parameter that is routinely observed and archived by the operational weather services. The meteorological satellite is a particularly promising tool for circumventing this obstacle. AFGL scientists have devised methods whereby erosion indices, such as the Environmental Severity Index, can be estimated from metsat data alone and mapped over virtually the entire globe. Results of the pilot application of this so-called Satellite-Correlation Technique so impressed DDR&E that a whole year of daily maps is now in production for potential target areas and for each of four erosion indices. While the technique is being used in this instance for climatological purposes, it could be easily adapted to real-time employment in the forecasting mode if there were a need.

AEROSOL TECHNIQUES

Aerosol techniques have been used by AFGL to increase the survivability of aerospace vehicles. To accomplish this, a dual approach has been employed. First, methods were developed to uniformly dispense aerosols in the vicinity of the vehicle to improve survivability. Then measurements were made on the decrease of vehicle detectability through the use of the dispensed aerosols.

While aerosols can be dispensed in a number of ways, only two were considered where uniform flow was a consideration. The first was as a suspension of the solid in a freon vehicle which could be injected as a liquid. When this method was employed, the freon was dispensed through a nozzle at a uniform rate, and if the particles were well suspended in the liquid, a uniform suspension of aerosol could be achieved when the freon evaporated in the atmosphere. This method proved effective and as much as 20 percent of the solid could be suspended in the freon when the appropriate emulsifying agents were used. Since our basic aerosol dispensing system was designed for airborne use, the freon suspension dispensing system was not

considered to be the best possible solution to the problem because of the range penalties incurred by the aircraft in carrying the 80 percent by weight of freon needed to dispense the aerosol.

Since one of our objectives was to carry the maximum weight of aerosol with a minimum range penalty, a large part of our effort was then concentrated on dispensing a solid powder through pipes and nozzles at uniform flow rates. When particles are decreased in size, the surface area per unit mass increases and the associated surface forces in the powder also tend to increase. Since we were interested in uniformly dispensing submicrometer non-uniform particles, the agglomeration problem that had to be overcome was considerable. Deagglomerating agents with extremely small diameters, uniform charge, and spherical shape were developed to fluidize the aerosols. These deagglomerating agents promoted fluidization of the aerosols through two mechanisms. They first penetrated the interstices of the aerosols and because of their spherical shape acted as a lubricant in preventing the irregular surfaces from clumping together. The other mechanism in the fluidization of the aerosol was due to the uniform negative charge on the deagglomerating agent. This placed a negative charge on all aerosol particles and separated the particles electrostatically. With proper deagglomeration and the selection of optimum tubing design and nozzle diameter, aerosols could be dispensed uniformly at flow rates as low as one ounce per second. The limiting factor in aerosol dispensing was the ratio of particle diameter to nozzle diameter. For any particle diameter, when this ratio approached 0.006, clogging of the nozzle occurred.

The aerosol flow techniques were developed concurrently with measurements on the survivability of vehicles through the use of these aerosols. Previous flight test data showed the feasibility of aero-

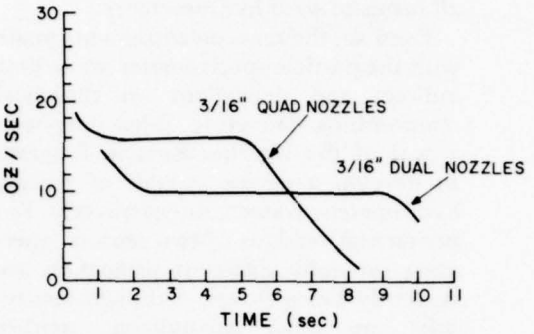

Uniform aerosol flow through a nozzle

sol techniques in increasing aircraft survivability. The first aerosol dispensers used in these tests were crude models, in which a decaying pressure system was used and the aerosol flow as a function of time was exponential. The flow rate started out extremely high initially when the aerosol was first released from a pressurized tank and then dropped off rapidly as the pressure decreased. Because of the extremely high flow rates and non-uniform flow it was impossible to obtain any quantitative data. In order to obtain the quantitative data necessary for the evaluation of our aerosol technique, a turbojet engine was placed in a test cell at Pease AFB, New Hampshire. Measuring equipment was set up in a van behind the engine so that the aerosol effects could be measured. The variables introduced in these tests were aerosol composition, aerosol size, and aerosol flow rate. Because of our newly developed dispensing techniques, the flow rates were kept low enough to preclude saturation of the measuring instruments. A series of measurements was made with the aerosols and the results of the initial tests were used to further improve the aerosols and injection techniques. A preliminary analysis of the collected data showed that aerosol techniques are effective in increasing aircraft survivability.

A fifteen-fold improvement was made in aerosol effectiveness between the initial and final tests. Because of this improvement, the weights of aerosol necessary for vehicle survivability are quite small and do not impose any great penalty on the using aircraft.

The results of this study have been turned over to Air Force Avionics Laboratory for further development. It is planned to fly the system under simulated combat conditions for further evaluation and to run a trade-off study against more conventional survivability techniques.

JOURNAL ARTICLES JULY 1974 - JUNE 1976

BROUSAIDES, F. J.
The Radiosonde Hygristor and Low Relative Humidity
Bull. of Am. Met. Soc., Vol. 56, No. 2 (February 1975)

FINGER, F. G., GELMAN, M. E. (Natl. Met. Ctr., NOAA, Wash., D. C.), SCHMIDLIN, F. J. (NOAA, Wallops Island, Va.), LEVITON, R., and KENNEDY, B. W. (U.S. Army Atm. Sci. Lab., White Sands Missile Range, N. M.)
Compatibility of Meteorological Rocketsonde Data as Indicated by International Comparison Tests
J. of Atm. Sci. (September 1975)

HARDY, K. R., and HOOKE, W. H. (Wave Prop. Lab., NOAA, Boulder, Colo.)
Further Study of the Atmospheric Gravity Waves Over the Eastern Seaboard on March 18, 1969
J. of Appl. Met., Vol. 14, No. 1 (February 1975)

HAUGEN, D. A., KAIMAL, J. C., and READINGS, C. J., RAYMENT, R. (Met. Res. Unit, RAF Cardington, Eng.)
A Comparison of Balloon-Borne and Tower-Mounted Instrumentation for Probing the Atmospheric Boundary Layer
J. of Appl. Met., Vol. 14, No. 4 (June 1975)

KAIMAL, J. C.
Sensors and Techniques for Direct Measurement of Turbulent Fluxes and Profiles in the Atmospheric Surface Layer
Atm. Technol., No. 7 (Fall 1975)

KUNKEL, B. A., SILVERMAN, B. A., and WEINSTEIN, A. I.
An Evaluation of Some Thermal Fog Dispersal Experiments
J. of Appl. Met., Vol. 13, No. 6 (September 1974)

LYNCH, R. A.
Shearing Stress Meter
J. of Appl. Met., Vol. 13, No. 5 (August 1974)

METCALF, J. I.
Gravity Waves in a Low-Level Inversion
J. of Atm. Sci., Vol. 32, No. 2 (February 1975)
Micro-Structure of Radar Echo Layers in the Clear Atmosphere
J. of Atm. Sci., Vol. 32, No. 2 (February 1975)

MUDRICK, S. E.
On the Use of a Scale-Dependent Filter in Channel Model Integrations
J. of Comp. Phys., Vol. 20, No. 1 (January 1976)

MUENCH, H. S.
The Use of Digital Radar Data in Severe Weather Forecasting
Bull. of Am. Met. Soc., Vol. 57 (March 1976)

RAO, K. S., WYNGAARD, J. C., and COTE, O. R.
Local Advection of Momentum, Heat and Moisture in Micrometeorology
Boundary-Layer Met., Vol. 7, No. 3 (November 1974)

READINGS, C. J. (Met. Res. Unit, RAF, Cardington, Eng.), HAUGEN, D. A., and KAIMAL, J. C.
The 1973 Minnesota Atmospheric Boundary Layer Experiment
Wea., Vol. 29, No. 8 (August 1974)

SHAPIRO, R.
The Variance Spectrum of Monthly Mean Central England Temperatures
Qtr. J. of Royal Met. Soc., Vol. 101, No. 429 (July 1975)
Linear Filtering in Numerical Integration
Math. of Comp., Vol. 29, No. 132 (October 1975)
Solar Magnetic Sector Structure and Terrestrial Atmospheric Vorticity
J. of Atm. Sci., Vol. 33, No. 5 (May 1976)

WEINSTEIN, A. I.
Projected Utilization of Warm Fog Dispersal Systems at Several Major Airports
J. of Appl. Met., Vol. 13, No. 7 (July 1974)

WYNGAARD, J. C.
Progress in Research on Boundary Layers and Atmospheric Turbulence
Rev. of Geophys. and Space Phys., Vol. 13, No. 3 (July 1975)

WYNGAARD, J. C., and ARYA, S. P. S. (Univ. of Wash.)
Effect of Baroclinicity on Wind Profiles and the Geostrophic Drag Law for the Convective Planetary Boundary Layer
J. of Atm. Sci., Vol. 32, No. 4 (April 1975)

WYNGAARD, J. C., and COTE, O. R.
The Evolution of a Convective Planetary Boundary Layer—A Higher-Order-Closure Model Study
Boundary-Layer Met., Vol. 7, No. 3 (November 1974)

WYNGAARD, J. C., COTE, O. R., and RAO, K. S.
Modeling the Atmospheric Boundary Layer
(Inv. Paper) Adv. in Geophys., Vol. 18A (November 1974)

YANG, C.-H.
A Controlled Experiment with One-Dimensional Interpolation
J. Appl. Met., Vol. 13, No. 6 (September 1974)

PAPERS PRESENTED AT MEETINGS JULY 1974 - JUNE 1976

BARAD, M. L.
AFCRL Program in Mesometeorology
Mtg. of U. S. Army Eur. Meso-Met. Adv. Panel, Garmisch-Partenkirchen, Fed. Rep. of Ger. (1-3 October 1975)

BARNES, A. A., NELSON, L. D., and METCALF, J. I., 1ST LT.
Weather Documentation at Kwajalein Missile Range
6th Conf. on Aerosp. and Aero. Met., El Paso, Tex. (12-14 November 1974)

BUNTING, J. T., and CONOVER, J. H.
The Inference of Cloud Water Content from Satellite and Other Measurements
2nd Conf. on Atm. Radn., Arlington, Va. (29-31 October 1975)
Progress on Derivation of Cloud Water Content for Satellites
6th Conf. on Aerosp. and Aero. Met., El Paso, Tex. (12-14 November 1974)

CHISHOLM, D. A.
An Analysis of the Time and Space Characteristics of Terminal Weather Parameters and Their Relationship to Mesoscale Weather Prediction Models
1st Am. Met. Soc. Conf. on Regional and Mesoscale Modeling, Analys. and Prediction, Las Vegas, Nev. (6-9 May 1975)
Mesoscale Observation and Forecasting at AFCRL
Conf. on East Coast Winter Storms, Am. Met. Soc. Hq., Boston, Mass. (6-7 August 1975)

CHISHOLM, D. A., HERING, W. S., and MUENCH, H. S.
Airport Visibility: Its Observation, Variability, and Prediction
6th Conf. on Aerosp. and Aero. Met., El Paso, Tex. (12-14 November 1974)

CONOVER, J. H.
Forecasting Research Flights into Winter Storms
Conf. on East Coast Winter Storms, Am. Met. Soc. Hq., Boston, Mass. (6-7 August 1975)

COTE, O. R., and WYNGAARD, J. C.
Modeling Turbulent Diffusion of Pollution in the Atmospheric Layer
Symp. on Atm. Diffusion and Air Pollution (Am. Met. Soc.), Santa Barbara, Calif. (9-13 September 1974)

DONALDSON, R. J.
History of a Tornado Vortex Traced by Plan Shear Indicator
16th Radar Met. Conf., Houston, Tex. (21-23 April 1975)
Advantages of Doppler Radar for Meteorological Applications
Met. Svc. and Supporting Res. Interdept. Com. for Appl. Met. Res., NOAA, Rockville, Md. (3 June 1975)

DONALDSON, R. J. DYER, R. M., and KRAUS, M. J.
An Objective Evaluation of Techniques for Predicting Severe Weather Events
9th Conf. on Severe Local Storms, Norman, Okla. (21-23 October 1975)

DYER, R. M.
A Relation Between Reflectivity and Mean Fall Speed in Hail
16th Radar Met. Conf., Houston, Tex. (21-23 April 1975)

FALCONE, V. J., JR., and CARNEVALE, R. F.
Atmospheric Temperature Inferring from Passive Radiometry
6th Conf. on Aerosp. and Aero. Met., El Paso, Tex. (12-14 November 1974)

FITZGERALD, D. R.
Electrical Structure of Large Overwater Shower Clouds
5th Intl. Conf. on Atm. Elec., Garmisch-Partenkirchen, Ger. (2-7 September 1974)

GLOVER, K. M., and JAGODNIK, A. J., NOVICK, L. R. (Raytheon Co., Wayland, Mass.)
A Weather Radar Scan Converter/Color Display
16th Radar Met. Conf., Houston, Tex. (21-23 April 1975)

GROGINSKY, H. L., NOVICK, L. R., (Raytheon Co., Wayland, Mass.) and GLOVER, K. M.
Spectral Mean and Variance Estimation Via Pulse Pair Processing
16th Radar Met. Conf., Houston, Tex. (21- 23 April 1975)

HAUGEN, D. A., and KAIMAL, J. C.
Measurement of the Temperature Structure Parameter with an Acoustic Echo Sounder
16th Conf. on Radar Met., Houston, Tex. (21-23 April 1975)

HAUGEN, D. A., KAIMAL, J. C., and READINGS, C. J. (Met. Res Unit, Bedford, Eng.)
An Experimental Study of the Planetary Boundary Layer
55th Ann. Mtg. of the Am. Met. Soc., Denver, Colo. (20-23 January 1975)

HAUGEN, D. A., KAIMAL, J. C. and READINGS, C. J., MARKS, A. J. (Met. Res. Unit, Bedford, Eng.)
The Minnesota 1973 Atmospheric Boundary Layer Experiment
8th AFCRL Sci. Balloon Symp., Hyannis, Mass. (30 September -3 October 1974)

KAIMAL, J. C., and HAUGEN, D. A.
Evaluation of an Acoustic Doppler Radar for Measuring Winds in the Lower Atmosphere
16th Conf. on Radar Met., Houston, Tex. (21-23 April 1975)

KLEIN, M. M., and KUNKEL, B. A.
Interaction of a Buoyant Turbulent Jet with a Co-Flowing Air Stream
27th Ann. Mtg. of the Div. of Fluid Dyn., Calif. Inst. of Technol., Pasadena, Calif. (25-27 November 1974)
Similarity and Scaling for a Heated Turbulent Buoyant Planar Jet in the Presence of a Co-Flowing Air Stream
Am. Phys. Soc., Div. of Fluid Dyn., 28th Ann. Mtg., Univ. of Md., College Pk., Md. (24-26 November 1975)

KUNKEL, B. A.
Optimization of a Thermal Fog Dispersal System
4th Conf. on Wea. Mod., Ft. Lauderdale, Fla. (18-21 November 1974)

LEE, J. T. (Natl. Severe Storms Lab., Stillwater, Okla.), and KRAUS, M. J.
Plan Shear Indicator and Aircraft Measurements of Thunderstorm Turbulence: Experimental Results
16th Radar Met. Conf., Houston, Tex. (21-23 April 1975)

LEVITON, R., and KENNEDY, B. W. (U. S. Army Atm. Sci. Lab., White Sands Missile Range, N. M.)
International Comparison of Meteorological Rocket Sensors
Conf. on the Upper Atm. (Am. Met. Soc.), Atlanta, Ga. (30 September - 4 October 1974)

METCALF, J. I., 1ST LT., BARNES, A. A., JR., and NELSON, L. D.
Water Content and Reflectivity Measurement by "Chirp" Radar
16th Radar Met. Conf., Houston, Tex. (21-23 April 1975)

MOROZ, E. Y., and TRAVERS, G. A.
Lidar Programs at AFCRL for Measurement of Cloud Height and Slant Visual Range
7th Intl. Laser Radar Conf., Stanford Res. Inst., Menlo Pk., Calif. (4-7 November 1975)

MOROZ, E. Y., and VIEZEE, W. (Stanford Res. Inst., Menlo Pk., Calif.)
Experimental Evaluation of the Lidar Technique for Determining Slant Visual Range
1974 Intl. Laser Radar Conf. (6th Conf. on Laser Atm. Studies), Sendai, Jap. (3-6 September 1974)

MUENCH, H. S.
Objective Forecasting from Digital Radar Presentations
The 6th Natl. Conf. on Wea. Forecasting and Analys., Am. Met. Soc., Albany, N. Y. (10-14 May 1976)

POCS, K.
An Overview of the Loki-Dart Meteorological Rocket Sounding System
4th Latvian Conf. of Sci. and Technol., McGill Univ., Montreal, Que., Can. (31 July - 2 August 1976)

SHAPIRO, R.
Climate Dynamics and the General Circulation of the Atmosphere
Sigma Xi Sp. Lecture, Boston Univ., Boston, Mass. (22 March 1976)

SILVERMAN, B. A.
Air Force Thermal Fog Dispersal System for Airports
4th Conf. on Wea. Mod., Ft. Lauderdale, Fla. (18-21 November 1974)

VALOVCIN, F. R.
Direct Application of VTPR Data
6th Conf. on Aerosp. and Aero. Met., El Paso, Tex. (12-14 November 1974)

WEINSTEIN, A. I.
Projected Utilization of Warm Fog Dispersal at Major Airports
6th Conf. on Aerosp. and Aero. Met., El Paso, Tex. (12-14 November 1974)
Air Pollution and Warm Fog Dispersal
4th Conf. on Wea. Mod., Ft. Lauderdale, Fla. (18-21 November 1974)
AFCRL Fog Program
3rd Ann. Conf. on the Phys. of Marine Fogs, Naval Elect. Lab. Ctr., San Diego, Calif. (7-8 January 1975)
R&D Efforts at AFCRL Related to Fog
4th Ann. Marine Fog Investigation (MFI) Conf., Lab. of Atm. Phys., Desert Res. Inst., Reno, Nev. (6-7 January 1976)
The Air Force Geophysics Laboratory (AFGL) Weather Test Facility
Ann. Army-Natl. Guard Safety Conf., Otis AFB, Mass. (16 May 1976)

WEINSTEIN, A. I., and KUNKEL, B. A.
Fog Dispersal - Modern Implementation of Proven Concepts
Intersoc. Conf. and Exposition on Transp., Los Angeles, Calif. (18-23 July 1976)

WEINSTEIN, A. I., KUNKEL, B. A., and KLEIN, M. M.
A Modern Thermal Fog Dispersal System for Airports
Intl. Symp. on Wea. Mod., Grenoble, Fr. (5 September 1975)

WYNGAARD, J. C.
Optical Turbulence Parameters in the Planetary Boundary Layer: Some Theory and Observations
Opt. Propagation Through Turbulence Mtg., Univ. of Colo., Boulder, Colo. (8-13 July 1974)

WYNGAARD, J. C., and ARYA, S. P. S. (Univ. of Wash.)
Effect of Baroclinicity on Wind Profiles and the Geostrophic Drag Law for the Convective Planetary Boundary Layer
Am. Geophys. Union 1974 Fall Ann. Mtg., San Francisco, Calif. (12-17 December 1974)

WYNGAARD, J. C., and COTE, O. R.
A Planetary Boundary Layer Model
Symp. on Atm. Diffusion and Air Pollution (Am. Met. Soc.), Santa Barbara, Calif. (9-13 September 1974)

TECHNICAL REPORTS
JULY 1974 - JUNE 1976

BARNES, A. A., JR., and METCALF, J. I., CAPT.
ALCOR High Altitude Weather Scans. AFCRL/A.N.T. Report No. 1
AFCRL-TR-75-0645 (31 December 1975)

BARNES, A. A. JR., METCALF, J. I., 1ST LT., and NELSON, L. D.
Aircraft and Weather Data Analysis for PVM-5. AFCRL/Minuteman Report No. 1
AFCRL-TR-74-0627 (23 December 1974)

BARNES, A. A., JR., NELSON, L. D., and METCALF, J. I., 1ST LT.
Weather Documentation at Kwajalein Missile Range
AFCRL-TR-74-0430 (12 September 1974)

BERKOFSKY, L.
A Numerical Forecasting Model for Operational Use in the Tropics
AFCRL-TR-74-0398 (16 August 1974)

BERTHEL, R. O.
A Climatology of Selected Storms for Wallops Island, Virginia, 1971-1975
AFGL-TR-76-0118 (2 June 1976)

BOUCHER, R. J.
Evaluation of Clear Air Turbulence Detection by Ground-Based Radars, Special Rawinsondes, and Aircraft, 1967-1971
AFCRL-TR-74-0489 (1 October 1974)

BUNTING, J. T., and CONOVER, J. H.
The Use of Satellite Data to Map Excessive Cloud Mass
AFCRL-TR-76-0004 (6 January 1976)

CHISHOLM, D. A.
Objective Prediction of Mesoscale Variations of Sensor Equivalent Visibility During Advective Situations
AFGL-TR-76-0132 (23 June 1976)

CHISHOLM, D. A., and JACOBS, L. P.
An Evaluation of Scattering-Type Visibility Instruments
AFCRL-TR-75-0411 (31 July 1975)

CHURCH, J. F., LT. COL., POCS, K. K., and SPATOLA, A. A.
The Continuous Aluminum-Foil Hydrometeor Sampler; Design, Operation, Data Analysis Procedures, and Operating Instructions
AFCRL-TR-75-0370 (11 July 1975)

CONOVER, J. H.
Specification of Current and Future Cloud Amounts and Ceilings from Satellite Data
AFCRL-TR-75-0626 (9 December 1975)

DONALDSON, R. J., JR., DYER, R. M., and KRAUS, M. J.
Operational Benefits of Meteorological Doppler Radar
AFCRL-TR-75-0103 (21 February 1975)

FITZGERALD, D. R.
Electrical Structure of Large Overwater Shower Clouds
AFCRL-TR-74-0390 (19 August 1974)
Experimental Studies of Thunderstorm Electrification
AFGL-TR-76-0128 (22 June 1976)

HAUGEN, D. A., KAIMAL, J. C., and READINGS, C. J., MARKS, A. J. (Met. Res. Unit, RAF, Cardington, Bedford, Eng.)
The Minnesota 1973 Atmospheric Boundary Layer Experiment
Proc., 8th AFCRL Sci. Balloon Symp., 30 Sept. to 3 Oct. 1974, AFCRL-TR-74-0393 (21 August 1974)

IZUMI, Y., and CAUGHEY, J. S. (Met. Res. Unit, RAF Cardington, Bedford, Eng.)
Minnesota 1973 Atmospheric Boundary Layer Experiment Data Report
AFCRL-TR-76-0038 (21 January 1976)

KLEIN, M. M., and KUNKEL, B. A.
Interaction of a Buoyant Turbulent Planar Jet with a Co-flowing Wind
AFCRL-TR-75-0368 (10 July 1975)
Interaction of a Buoyant Turbulent Round Jet with a Co-flowing Wind
AFCRL-TR-75-0581 (11 November 1975)

METCALF, J. I., CAPT., BARNES, A. A., JR., and KRAUS, M. J.
Final Report of PVM-4 and PVM-3 Weather Documentation. AFCRL/Minuteman Report No. 2
AFCRL-TR-75-0097 (19 February 1975)
Final Report of STM-8W Weather Documentation. AFCRL/Minuteman Report No. 3
AFCRL-TR-75-0207 (11 April 1975)
Final Report of PVM-5 Weather Documentation. AFCRL/Minuteman Report No. 4
AFCRL-TR-75-0302 (28 May 1975)

METCALF, J. I., CAPT., KRAUS, M. J., and BARNES, A. A., JR.
Final Report of OT-45, PVM-8, and RVTO Weather Documentation. AFCRL/Minuteman Report No. 5
AFCRL-TR-75-0388 (23 July 1975)
Final Report of PVM-6 and PVM-7 Weather Documentation. AFCRL/Minuteman Report No. 6
AFCRL-TR-75-0481 (11 September 1975)

MOROZ, E. Y., and TRAVERS, G. A.
Measurement of Cloud Height
AFCRL-TR-75-0306 (29 May 1975)

MORRISSEY, J. F., and WEISS, B. D.
Dropsonde Wind Measurements Using Omega/Loran Tracking
AFCRL-TR-75-0096 (19 February 1975)

MUDRICK, S.
On the Use of a Scale-Dependent Filter in Channel Model Integrations
AFCRL-TR-75-0214 (16 April 1975)

PEIRCE, R. M., LENHARD, R. W., and WEISS, B. D.
Comparison Study of Models Used to Prescribe Hydrometeor Water Content Values. Part I: Preliminary Results
AFCRL-TR-75-0470 (5 September 1975)

PLANK, V. G.
Liquid-Water-Content and Hydrometeor Size Distribution Information for the SAMS Missile Flights of the 1971-72 Season at Wallops Island, Virginia. AFCRL/SAMS Report No. 3
AFCRL-TR-74-0296 (2 July 1974)

PLANK, V. G., and SPATOLA, A. A.
Observations of the Natural Dissipation of Appalachian Valley Fog
AFGL-TR-76-0100 (3 May 1976)

SHAPIRO, R.
Comparison of Strategies in Numerical Integration of a Nonlinear Advection Equation
AFCRL-TR-75-0212 (15 April 1975)

TAHNK, W. R., CAPT.
Objective Prediction of Fine-Scale Variations in Radiation Fog Intensity
AFCRL-TR-75-0269 (12 May 1975)

WEINSTEIN, A. I.
Projected Interruptions in Airport Runway Operations Due to Fog
AFCRL-TR-75-0198 (8 April 1975)

WEINSTEIN, A. I., and HICKS, J. R. (Corps of Engrs., U. S. Army Cold Reg. Res. and Engrg. Lab., Hanover, N. H.)
Compressed Air for Supercooled Fog Dispersal
AFCRL-TR-75-0561 (22 October 1975)

YANG, C. H.
A Proposed Procedure for Diagnosis and Improvement of Dynamical Prediction Models
AFGL-TR-76-0079 (13 April 1976)

YEE, S. Y. K.
An N-Level Quasi-Geostrophic Model Suitable for Operational Use
AFCRL-TR-74-0525 (22 October 1974)
The Use of a Balance Equation Model in Numerical Weather Prediction
AFCRL-TR-75-0424 (August 1975)
A Shooting Method for the Solution of a Discrete Poisson Equation on the Surface of a Sphere
AFGL-TR-76-0035 (23 February 1976)

VI TERRESTRIAL SCIENCES DIVISION

The Terrestrial Sciences Division conducts research in geodesy, gravity, seismology, and geology. Activities cover a wide range of efforts on the earth's surface, subsurface and near atmosphere supporting the deployment, operation, and delivery of Air Force weapons. These efforts involve the collection and interpretation of geophysical data, the application of mathematical models to actual physical phenomena, and the development and testing of new instrumentation for experimental studies. Division scientists conduct field expeditions that are sometimes worldwide in extent to collect data. They conduct experimental studies in the laboratory, in the field, and aboard aircraft or satellite vehicles. The Division maintains close working relations with many organizations within the government and the civilian sector.

The reporting period saw an increasing sophistication and sensitivity in Air Force systems. This necessitated advanced research on terrestrial effects constraining their use. A high priority was assigned to earth motion effects on inertial guidance systems. The increased emphasis included both natural and man-made motion effects, and both current and proposed missile systems. Geodetic and gravimetric programs consisting of both theoretical studies and hardware development provided more accurate descriptions of the size and shape of the earth, located positions on the earth's surface to greater accuracies, and better defined the earth's

gravity potential. Seismological and geological efforts became strongly oriented to better understanding seismic wave interaction with structures, the deformation of the earth's crust at long periods, and the specific effects of such phenomena on various weapon systems. At the end of this reporting period, work related to nuclear test detection and geological siting was phased out.

GEODESY AND GRAVITY

Geodesy is concerned with the size, shape, and mass distribution of the earth. Accurate geodetic information is a necessary foundation for accurate determination of position, distance, and direction for launch sites, tracking sensors, and targets. The geodetic and gravimetric parameters for the earth and geodetic information for positioning not only form the structural framework for mapping, charting, and navigational aids, but are also direct data inputs for missile inertial guidance systems. Current geodetic information is inadequate to meet the requirements of future USAF weapon systems.

The Division maintains continuing research and development programs in geometric geodesy and in physical geodesy (or gravity). These programs are directed towards improving both fundamental knowledge of earth size, shape, and mass parameters, and also techniques for determining position, distance, and direction on the earth's surface and in terrestrial and inertial three-dimensional coordinate systems.

Continuing cooperation and participation by AFGL is required in the National Geodetic Satellite Program, together with the Defense Mapping Agency, the Army, the Navy, the National Aeronautics and Space Administration, the National Oceanic and Atmospheric Administration, the U. S. Geological Survey, other civilian agencies and academic observatories. The Terrestrial Sciences Division also participates with the International Gravity Commission in the development of a world-wide gravity reference network. A world-wide system of earth-tide profiles is being established in cooperation with the International Center for Earth Tides, Brussels, Belgium.

Satellite Altimetry: A geodetic satellite has been specially instrumented to make altitude measurements over oceans. The radar altimeter readings from this satellite can be used to determine the shape of the ocean's surface, thereby having applications in geodesy, geophysics and oceanography. The only satellite with an on-board altimeter specially designed for this purpose is GEOS-3, which was launched in April 1975.

If the earth were all water, right to its center, mean sea level would be a spheroid of revolution. However, the earth is largely solid and supports density variations in continental areas and under oceans. These density variations cause mean sea level to vary by scores of meters from its reference spheroid. The equipotential surface, which is the extension of mean sea level throughout the earth, is called the geoid. The undulations of this geoid from the reference spheroid are related to the earth's gravity field, and the relationship has been a principal topic of investigation by physical geodesists, who have devised means for determining the spheroid-geoid separations from gravimetric measurements. Now, satellite altimetry can be used to measure the shape of the geoid, or an oceanic portion of it, so we can calculate the earth's gravity field from spheroid-geoid separations.

The GEOS-3 radar altimeter is designed to measure the satellite's distance above sea level to a fraction of a meter. If the satellite's orbit can be independently established from the ground, or from satellite-to-satellite tracking to about 1 meter accuracy, the determination of the shape of the mean sea level is a straight-

forward procedure. However, standard global tracking nets cannot achieve 1-meter orbital accuracies, so the high precision requires denser nets, satellite-to-satellite tracking, or other advanced schemes.

At AFGL, the approach to satellite altimetry has been to assume that ground tracking is only good enough to achieve orbital accuracies of about 20 meters; this is easy and routine. If we knew the position and momentum of the satellite at any epoch, and integrated the satellite motion over a short arc (less than one quarter of a revolution), we could recover the position of the satellite to within about 1 meter over the entire arc. Although the position and momentum of the satellite on the short arc are not known with adequate precision, by comparing altitudes from a number of independent, interlocking short arcs, we have available data to refine our knowledge of position and momentum and improve our ability to determine the short arcs. Where two short arcs cross, the difference in measured altitudes to sea level is the vertical distance between the two arcs. The vertical inter-orbit ties provide a rather tight interlocking net of arcs, particularly in the very important vertical direction. Subtracting the altimeter measurements from this net gives, finally, the shape of the ocean surface.

In practice, the oceanic geoid is determined from the satellite altimeter measurements in one simultaneous least squares reduction. Both the shape of the geoid and weakly constrained position and momentum values are estimated simultaneously, defining hundreds of independent, interlocking short arcs. Patterned characteristics of the normal equations make such a massive solution possible. The AFGL program for Short Arc Reduction of Radar Altimetry is called SARRA.

Altimetry observations over two portions of the Indian Ocean and one portion of the North Atlantic have been processed with the SARRA computer program. The results confirm that highly accurate reference orbits are not required for SARRA reductions. Plots of residuals after the adjustment showed that the noise of the altimeter measurements in recovering the Indian Ocean and a portion of the North Atlantic geoid range from 1.0 to 1.5 meters. Also, the recovered geoid of the interior portion of each area generally agreed with information about the geoid derived from other sources.

Once the oceanic geoid is established by satellite altimetry, AFGL will combine this information with other existing physical geodesy material to determine the gravity field of the earth. The most obvious and effective supplementary observations are gravity measurements. Such observations are most available and most accurate over land—precisely where satellite altimetry is not useful. Another source of information is predetermined geocentric coordinates of any satellite stations that are located on a leveling net tied to mean sea level.

The utilization of radar altimetry by itself, and in combination with existing gravity material is also being examined by developing equations that relate surface density values to geoid undulations and gravity anomalies.

Present levels of observational accuracy make satellite altimetry much more sensitive to the shape of the earth than gravimetry; a 1-meter rms anomaly height over an area of 1 square degree tells much more about the shape of the earth than the same square with a 3 milligal rms gravity anomaly. (One milligal equals 10^{-3} cm/sec^2 or about one-millionth of the earth's surface gravity.) Because this relative information content applies to the description of the earth's gravity field as well, satellite altimetry will make significant contributions to gravity mapping.

Laser Ranging and Radio Interferometry: Highly accurate distance measure-

ments of the moon and high artificial satellites, made by earth-based laser ranging telescopes, and accurate angular measurements by radio interferometers may soon produce significant advances in geodesy and geodynamics. Measurements accurate to a few centimeters are expected during the next three years, which will allow us to measure solid-earth tides and continental drift, as well as to improve our knowledge of variations in the earth's rotation rate and polar motion.

AFGL participated in the NASA Lunar Laser Ranging Experiments. Since 1970, more thean 1700 range measurements have been made between the McDonald Observatory in Texas and four of the retroreflectors placed on the moon by the Apollo and Soviet space missions. AFGL scientists have analyzed these data using the Planetary Ephemeris Program, a large software package developed under contract by AFGL and other DOD agencies. The data analysis has significantly improved our knowledge of the lunar orbit and physical libration, the coordinates of the McDonald Observatory, the principal term in the earth's gravity field, and day-to-day variations in the earth's rotation rate. AFGL's analysis of lunar ranging data also produced the first verification of the Principle of Equivalence for massive bodies, the cornerstone of Einstein's General Theory of Relativity. This significant scientific achievement was reported in both academic and popular publications. The AFGL lunar laser telescope, operated in Arizona between 1968 and 1972, has been refurbished by Australian geodesists and is now in operation near Canberra. Laser ranges from a southern hemisphere observatory will allow analyses of the lunar data to make separate determinations of variations in the earth's rotation and movement of the pole.

Complementing the lunar ranging experiment is an extensive NASA-DOD program for laser ranging to earth satellites. The launch of the high-altitude, high mass density Laser Geodetic Satellite (LAGEOS) in 1976 has provided a target whose orbit is relatively free from the effects of atmospheric drag and small-scale variations in the earth's gravity field, allowing range measurements for geodesy accurate to 5 to 10 centimeters. Data from LAGEOS observations should be available within the next two years and will be analyzed at AFGL.

A third advanced technique which has been used for geodetic measurements is very-long-baseline interferometry (VLBI). VLBI determines the three-dimensional position of one radio telescope relative to another using observations of distant radio sources such as quasars. AFGL is supporting the development of a very accurate VLBI system. Geodetic positions have been determined within one meter over continental distances and a few centimeters over a distance of several kilometers by analyses of data already obtained. Variations in earth rotation have also been determined from VLBI data.

Many geodetic parameters, such as the coordinates of observing stations and the earth's instantaneous pole of rotation, can be determined most efficiently by combining several types of data during analyses. The Planetary Ephemeris Program will be used at AFGL to perform simultaneous least squares solutions for a large number of parameters, using lunar laser ranging, satellite laser ranging, and VLBI data.

Absolute Gravimetry: AFGL has developed a new second generation absolute gravity measuring system. The method used for measurement is to drop one reflector of a two-beam Michelson interferometer and determine the distance fallen in known time intervals by direct measurements of interference fringes.

The first generation AFGL instrument was designed for an accuracy of better than ± 0.05 milligal. It was transported

to eight different sites, and, after one to two weeks total setup, operate, and take down time, determined absolute gravity values to within its design accuracy at most sites. The apparatus required about 20 containers for shipment, with a total weight of about 2,500 pounds.

The new AFGL instrument was designed to decrease the time required to obtain an absolute value of gravity while retaining a precision at least as good as the first generation instrument. Observation time has been reduced to about two or three days and the total weight has been reduced to at most 800 pounds. Radical changes in the mechanical design, state-of-the-art electronics and computing equipment have made the weight reduction possible.

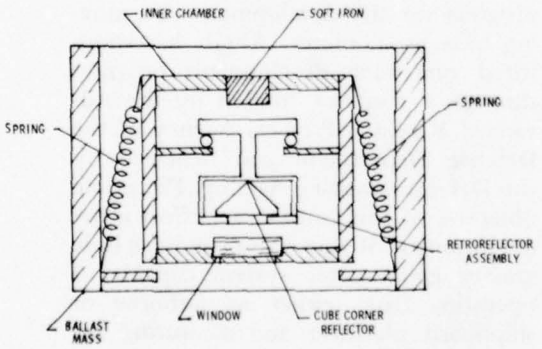

The free-falling chamber containing the cube corner reflector in the second-generation absolute gravity measuring instrument. The inner-and-outer-chamber design permits operation in a moderate vacuum rather than an ultra-high vacuum. The retroreflector then moves only very little with respect to the inner chamber and air resistance forces are minimized. The springs are released at the same time as the outer chamber, pulling the inner chamber down from the retroreflector.

The mechanical design focused on eliminating the need for an ultra-high vacuum. This removes the weight (approximately 100 pounds) of the high vacuum pump and cuts the time of observation by at least one full day. A much wider range of materials can be used in the vacuum chamber, thereby simplifying its operation.

This need for a high vacuum was eliminated by enclosing the freely falling reflector in a small evacuated chamber which falls along with the reflector. They both fall in a larger vacuum chamber, but since the air which comes into contact with the falling object is falling with the acceleration of gravity, air resistance cannot affect the measurement. Although the mechanism required for separating the reflector from the small chamber during the fall is somewhat elaborate, it is very reliable and has withstood countless cycles of operation.

The electronics system makes digital time measurements between a large number (about 750) of interference fringes and thus allows for extensive averaging of seismic effects as well as theoretically giving an independent measurement of the gravity gradient. The digital data are processed between each drop by an on-line minicomputer.

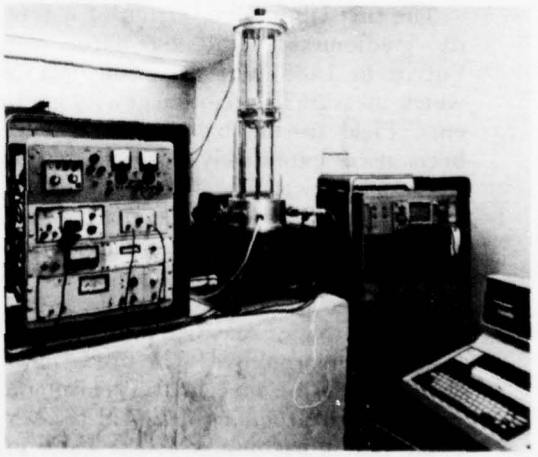

Second generation laser interferometer gravity system: The three transportable electronics racks each weigh about 150 pounds and can be handled by two persons. The other components will have suitable shipping cases also.

The system is being thoroughly checked out in the laboratory before it is taken to remote sites. The drop-to-drop scatter in the data has been as small as ± 0.08 mgal and the reproducibility of average measured values has been better than 0.1 milligal. The electronics and computation subsystems have been shown to allow an absolute accuracy of 0.001 milligal, so that the effects which will limit the accuracy lie in the mechanical subsystem.

MOVING BASE GRAVITY GRADIOMETER

If the gradients of the terrestrial gravity field could be measured from a moving platform with sufficient accuracy, a powerful tool for the solution of a number of problems involving gravity would exist. This gravity gradient is the spatial rate of change of the gravity vector. The unit used to describe it is the Eotvos unit (EU). One EU = 10^{-9} sec^{-2} = 1 mgal/10 km.

The first laboratory version of a gravity gradiometer, built by Baron von Eotvos in 1888, was a torsion balance which measured horizontal gravity gradients. Field torsion balances have since been used extensively for exploration by geophysicists who found the instruments valuable for detecting density variations within the earth. A major drawback to this type of instrumentation is the slowness of operation and the instrument's extreme sensitivity to its surrounding environment. The urgent need to better define the gravity field of the earth led to programs designed to overcome the shortcomings of the basic instruments such as the torsion balance. One such program was the moving base gravity gradiometer.

We now have the prospect of measuring all the components of the gravity gradient from a moving base. The concept of an airborne gravity gradiometer is especially attractive for geodesists and geophysicists who need high resolution gravity data over extensive areas in short periods of time. Airborne gravimeters have been limited in their success because aircraft accelerations cannot be directly discriminated from gravity accelerations, and complex data filtering techniques are required. A properly designed moving base gravity gradiometer would not detect linear aircraft accelerations and so would be free from this important limitation of airborne gravimetry. On the other hand, gradiometers are very sensitive to rotation; but aircraft rotations can be detected by inertial instrumentation and compensated for in real time.

Currently, several programs are in progress for the development of a moving base gradiometer. AFGL has sponsored one such development program through a contract funded by the Advanced Research Projects Agency of the Defense Department and managed by the Defense Mapping Agency. The prime objective of this contractual effort is the development of a prototype moving base gravity gradiometer system capable of operating from either an airborne or shipboard platform and measuring the gravity gradient to an accuracy of 1 EU over a 10-second integration time period.

The AFGL effort currently under contract calls for design and fabrication of a basic sensor. This sensor structure consists of two mass-loaded arms, pivoted freely at right angles about a common axis and connected by a stiff torsion spring. In operation, the sensor is rotated about its torsional axis at exactly half its torsional resonance frequency. Most alternating torques caused by external accelerations coupling through an imperfect mechanical system are at the spin frequency and therefore can only weakly excite the torsional resonant mode. The

gravity gradient field, however, induces alternating torques at twice the spin frequency that are preferentially "amplified" by the mechanical resonance. The alternating torques are converted into measured AC voltages by piezoelectric transducers.

The phase and amplitude of the rotating gravity gradiometer sensor provide measurements of two elements of the gravity gradient. Three sensors, operating about mutually perpendicular axes, are required to measure the complete gravity gradient.

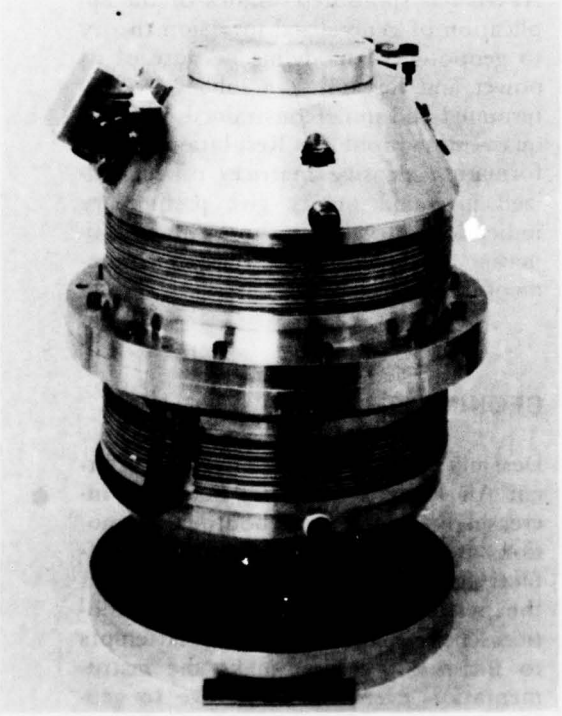

The first prototype of the Moving Base Rotating Gravity Gradiometer built under contract for AFGL.

The design of the rotating gravity gradiometer requires a consideration of all possible error sources, and methods for their elimination or compensation must be designed or developed. A state-of-the-art Vibration Isolation Alignment and Leveling System (VIALS) for support on a moving base platform is also required. Tests of the suitability of the rotating gravity gradiometer for operating on a moving base will be performed in laboratory simulators to define the VIALS requirements and the real-time compensation techniques to be used. Subsequently, the VIALS and the compensation package will be built and integrated with the sensors. Tests of the entire system will then be performed on laboratory simulators and, finally, in actual airborne/shipboard operations.

To date, two prototype rotating gravity gradiometers have been fabricated. The second sensor incorporates all design changes brought about through one year of laboratory testing and modification of unit number one. Dramatic improvements in test data resulted from continuous laboratory testing of the first prototype. In April 1975, using ordinary ball bearings, the instrument produced a 300 EU output in a 10-second integration time in a vertical orientation. By January 1976, using a specially designed bearing, this output level was reduced to 5 EU. Comparable results were also obtained with the instrument placed in a horizontal orientation. This came about through solution of what at times seemed almost insurmountable problems. Many advances in a variety of fields beyond the then known state-of-the-art have resulted from this development effort. Extensive work still is needed before the entire system will be ready for operational deployment, but the high risk factor initially assigned to this effort has been greatly reduced.

When the rotating gravity gradiometer fulfills its promised sensitivity, it will be of enormous value in the detailed mapping of the earth's gravity field and will contribute significantly to inertial navigation and guidance.

MODELS OF EARTH'S GRAVITY FIELD AND APPLICATION OF ADVANCED ADJUSTMENT TECHNIQUES

Gravity gradiometry, satellite altimetry, ground-to-satellite tracking, satellite-to-satellite tracking, and conventional gravimetry provide an immense amount of information concerning the geopotential at different levels. The data are not uniformly distributed over the earth, and contain errors, sometimes even gross errors. AFGL has pursued various techniques for combining these inhomogeneous, occasionally sparse, noisy and inconsistent data from physical geodesy into uniform parametric representations of the geopotential.

Geopotential models are developed of regional and of global extent. The simplest approach is that of the standard linear least squares method which solves for an arbitrarily chosen set of parameters (for instance, the coefficients of a truncated spherical harmonic expansion) from a collection of measurements whose relative weights are assigned. Except for weighting, however, such a solution does not take into account the properties of the measurements and the geopotential.

One extended least squares method which considers the covariances of measurements and the geopotential in solving for the model parameters is known as the collocation method. AFGL has extensively developed the collocation method for combining various kinds of physical geodesy data into regional and global geopotential models. Conceptually, and generally in practice, collocation model solutions are superior to conventional least squares solutions.

Except when a problem is ill-posed so that a set of model parameters must be revised to effect a solution, least squares and collocation solutions provide no measure of the efficiency of a model. In general, a better fit of a particular set of measurements can be made by revising the model without increasing the number of parameters. Generalized inversion theory, which has been extensively developed for geophysical modeling, provides a means for accomplishing this. AFGL has sponsored studies of the application of generalized inversion theory to geopotential modeling because of its power and flexibility in solving overdetermined and underconstrained linear or quasi-linear problems. Resolution and information density matrices of generalized inversion theory give preliminary indications of value in choosing and estimating parameters and selecting measurement data.

GEOKINETICS

Designers and operators of many different Air Force systems are becoming increasingly concerned about earth motions and their effects. Earth motion effects (geokinetics) can adversely affect the performance of high-precision, motion-sensitive instrumentation. Attempts to increase precision make the instrumentation even more sensitive to geokinetic effects. Inertial guidance instrumentation is a typical example. Each generation of gyros or accelerometers developed for use in guidance systems exceeds the sensitivity of the previous generation by an order of magnitude or greater. Unfortunately, this enhance-

ment in performance also increases the potential for errors caused by the motion environment in which the instrument must operate.

In other instances, the structural response of a facility to motion inputs may be the principal concern. If the facility must provide a relatively stable motion environment for the instrumentation or operational system housed in it, then the natural vibration frequencies of the structure must be well outside the bandwidth of significant input motions to prevent amplification of motion amplitudes. Laboratories for testing and calibration of precision instruments, missile silos, and radar installations may all experience earth motion problems.

The apparent solution to problems caused by earth motion effects is to develop more effective isolation or compensation techniques. However, complete knowledge of the characteristics of the motion environment and the manner in which this environment interacts with system or facility performance is needed to do this. The objective of the geokinetic research and exploratory development conducted by the Terrestrial Sciences Division is to develop this knowledge and provide it to system designers and engineers.

The major effort in geokinetics during this reporting period was the measurement and characterization of the motion environment of Minuteman silos and the identification of errors in guidance system performance caused by the motion environment. Two special studies were also performed, at the request of other Air Force agencies which required assistance in analyzing motion-related problems.

Silo Motion Studies: In 1974, a Minuteman test silo at Hill AFB, Utah, was instrumented with a number of motion sensors and a motion measuring system to characterize the motion environment of the silo and to identify those motions which introduced alignment and performance errors into the guidance system. The study included two separate parts: a seismic experiment and an alignment experiment. For the seismic experiment, seismometers were placed at a number of locations both inside and outside of the silo. Inside the silo, sensors were placed at the base of the silo, on the missile suspension system, and on a wafer located just above the inertial guidance system. The seismic experiment was concerned principally with motions with periods less than one minute.

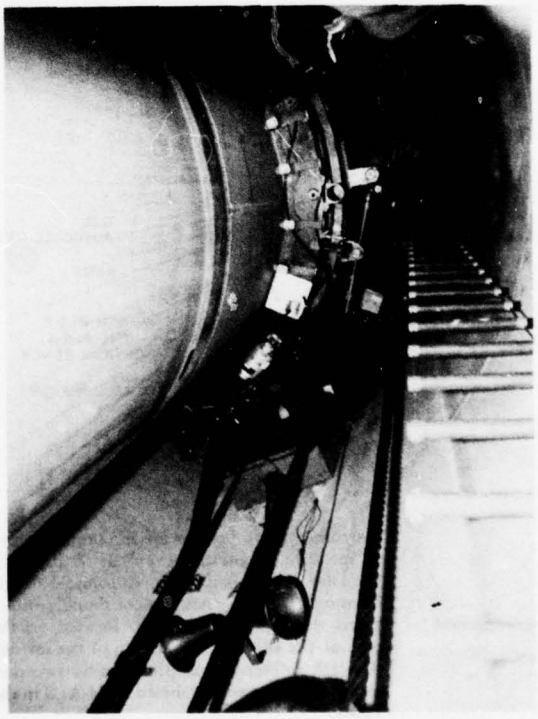

In the silo motion study, seismometers were placed on the missile suspension system, as is shown here, as well as on the missile in the vicinity of the guidance system. Both long and short period seismometers were used to measure motions of the missile.

In the alignment experiment, tiltmeters were used to measure long-term tilts of the silo and the missile, and elaborate instrumentation was used to measure azimuthal rotations. An automatic angle measuring system continually compared the alignment of mirrors mounted on the silo wall and missile skin with the azimuth indicated by a reference system. The reference system used consisted of two portable gyrocompasses (Azimuth Laying Sets) which provided updated estimates of a north reference at periodic intervals. Tilt and tilt rate errors were then removed from the azimuth estimates to add greater precision to the measurements.

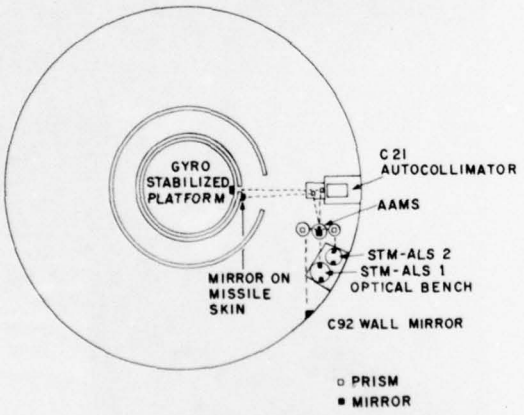

Instrumentation used in the silo motion study to measure long-term azimuthal rotations of the silo and missile. An Automatic Angle Measuring System (AAMS) continually monitored the motion of mirrors located on the wall of the silo and on the skin of the missile. A north reference was provided by two portable gyrocompasses, labeled STM-ALS in the figure.

A complete definition of the motion environment of a silo requires the specification of those features of the observed motion that are significant to hardware performance. One of the first steps in the definition is to separate the motions into rotational and translational components. The wavelengths of the important motions are quite large compared to the dimensions of the silo, and the frequencies are lower than the resonant frequencies of the silo. For this reason, only three linear and three rotational components are needed to specify the motion field fully.

Next, the statistical class of the motions must be established. The vertical motions observed at the base of the silo exhibit the attributes of a normal, or Gaussian, distribution. The vertical motions observed on the missile, however, show a Rayleigh distribution, reflecting the fact that the suspension system is a linear, time invariant, lightly damped system.

A principal difference between the silo motions and the missile motions is that silo motions are predominantly linear, while the missile motions show a strong rotational component. Missile rotations are a source of concern since they cause much larger errors than linear motions.

Power Spectral Densities (PSD's) were computed for silo and missile motions during both quiet and disturbed conditions. In quiet conditions, missile motions are largely uncorrelated with silo inputs; rather they reflect the response characteristics of the missile suspension system. The resonant frequencies of the suspension system cause the missile motions to be greater than the ground motions at these frequencies. Following large seismic events, the ground motions will become the primary cause of missile motions. However, the response characteristics of the suspension system will continue to influence the motion spectra. The suspension system response does not remain linear at higher motion levels

since it has a number of frictional elements that tend to release at modest loads.

During quiet conditions, the missile motion peaks at frequencies of 0.33-0.39 Hertz, 1.17-1.25 Hertz, and 4.7-5.2 Hertz. The first two are peaks in the horizontal motion spectra, while the third is a strongly amplified vertical motion. The first two are specified resonant frequencies for the suspension system while the third is not.

One objective of the alignment experiment was to measure the long-term rotations of the silo and missile. These motions are of interest because changes in the azimuth references used in aligning the Minuteman Missile Guidance Set (MGS) have a direct effect upon guidance system accuracy. The azimuth references are either the C-21 autocollimator attached to the silo wall, or the roll gimbal notch, attached to the missile. Thus, motions of the azimuth references are directly related to motions of the silo and missile.

During a 22-day period from October 30 through November 21, 1974 continual azimuth measurements were made on the silo wall and missile silo mirrors at approximately 34-minute intervals. During most of this time, there were no unusual motion-producing activities within or near the silo. This was taken as the "quiet" period of the silo and missile data histories. An anomalous motion period, caused by a ground loading event, spans the last two days of the data history. A 65,000 pound vehicle, parked about 75 feet from the silo, produced the surface loading which resulted in relatively large rotations of the silo and missile during the two-day period.

The azimuthal data from the silo and missile were examined for drift and spectral characteristics. The drifts were examined by computing slopes, since the data exhibited apparent trends, and the motions could be described as functions of time. Power spectral densities were computed to analyze the azimuthal data.

The data show that the silo rotated counterclockwise during the measurement period, but not at a constant rate. The slope of the silo data varies considerably over the history but most markedly during the surface loading event. The slope computed for the missile skin mirror is quite small during the quiet period and in the opposite direction from the slope determined for the silo wall mirror. This implies that for very long period motions, there was no strong coupling between the missile and silo.

The power spectral density (PSD) of the silo motions shows two strong peaks in the spectrum at the diurnal (24-hour) and half-diurnal (12-hour) periods. There is also considerable power at periods of 5.4 and 4.4 hours. For the missile skin mirror PSD, the long period bands (12.2 hours and longer) contain most of the power. The diurnal and half-diurnal periods are also prominent in the missile PSD.

Because one result from the Hill AFB study was the finding that activities at or near the silo can load the surface to the point that the silo will experience discernible tilts, tilt measurements were also made in several Wing IV silos at Whiteman AFB, Missouri. Tiltmeters were installed in the silos on the optical bench prior to the removal of the Missile Guidance Set and were left in place until well after activity ceased to determine if the silo, after tilting, returned to its original position. A secondary purpose of the tilt measurements was to examine the tilt environment in which the Azimuth Laying Set must operate to obtain azimuth estimates for realigning the Missile Guidance Set after replacement. A third objective of the study was to ascertain whether the long-term motions of unstable silos are primarily steady or episodic. If episodic, these abrupt azimuth shifts might be traced to mainten-

ance procedures or meteorological phenomena.

The tilt measurements performed at Wing IV showed that silo tilts there are considerably less than those observed earlier at Hill AFB, indicating that the silos tested at Wing IV are much more stable than the test silo at Hill AFB.

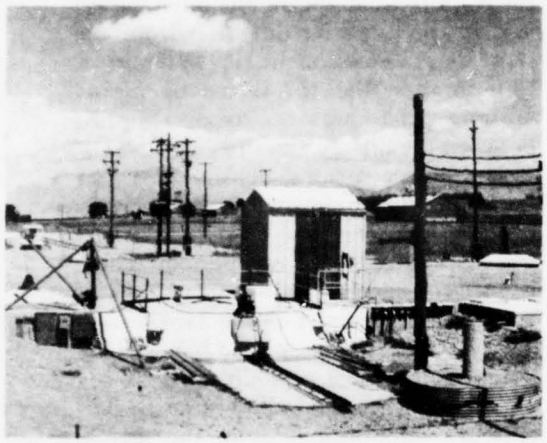

Minuteman test silo at Hill AFB, Utah, where silo motion study was conducted in 1974. Seismometers, tiltmeters, and other motion measuring devices were placed in the silo to characterize the motion environment of the silo and missile and to determine the effects of earth motions on guidance system alignment and performance.

Finally, a theoretical program has been started to support the Minuteman silo motion measurements. It includes analytical and numerical modeling of the response of the silo to seismic inputs. In pursuit of the analytic approach, formal solutions to the three-dimensional problem of wave scattering and diffraction due to an impulsive acoustic point source in a fluid half-space, in which a semi-infinite vertical soft cylinder is embedded, were obtained in integral form. To follow the numerical approach, a three-dimensional finite element formulation, based on variational principles for axially symmetrical problems of elastic wave scattering and diffraction due to an axially symmetrical source, was completed. It will be used to solve problems such as the seismic response of a finite vertical cylindrical cavity with an open end on the surface of a half-space. The finite element method was chosen because it offers greater flexibility than the finite difference method in dealing with irregular geometries, non-uniform meshes and boundary conditions.

Special Studies: The Terrestrial Sciences Division conducted two special ground motion studies for other Air Force agencies to determine whether motions generated by explosive sources should be of concern to radar facilities. The first study was concerned with ground motion caused by explosive charges used in excavating limestone from a quarry in southern Florida. The blasts affected a Ground Control Intercept (GCI) radar facility at Richmond AFS, Florida. In recent years, the quarry activities had moved as close as 1200 feet to the facility. In addition to concern over the effects that the blasting may have on the critical alignment of the search radar and the height finder, there was concern over the structural integrity of the buildings. Therefore, the Aerospace Defense Command (ADC) requested that AFGL measure ground motions to determine whether the quarrying company was exceeding the blasting code established by Dade County, Florida. The code specifies the restraints to explosive generated motions in terms of both amplitude and particle velocity. The measurements taken were specified in these terms.

To measure the ground motions from the quarry blasts, a special Seismic Activity Monitor (SAM) system was constructed. Although specially designed to collect seismic data, it can be used for other applications by modifying the amplifiers for the intended usage. The SAM system is a self-contained auto-

matic digital system. It stores the most recently collected data and updates it. Whenever the magnitude of the activity exceeds a threshold level, the SAM system is activated to record the data held in temporary storage on magnetic tape, and continues to record data for a preselected time after the activity drops below the threshold again. The data stream includes both seismic data and time. The SAM will accept up to 16 channels of analog data in this manner. For the Richmond AFS study, only six channels were used.

During five months at the Richmond site, the SAM system recorded 120 quarry blasts. Although there was visual evidence of structural damage to the facility before the study began, none of the 120 events recorded could be classified as having exceeded the blasting code.

In the second special study, seismic and acoustic instrumentation was deployed at the site chosen for the construction of a phased array radar at Camp Edwards, Massachusetts. The radar, called PAVE PAWS, is being constructed for the Electronic Systems Division (ESD) to provide early warning of sea-launched ballistic missiles. The study, requested by ESD, measured the motion levels generated by the firing of large artillery shells. ESD requested the study because the site is adjacent to an Army National Guard artillery range, and it was feared that firings might degrade the accuracy of the radar.

Data from both 105 and 155 mm howitzer firings were recorded in the study. The study concluded that neither the seismic nor the acoustic energy generated by the firings would be critical to the design specifications of the facility.

CRATERING STUDIES

An explosion which produces a crater also causes extensive permanent deformation in the geological material surrounding the crater. The geometry of this zone of plastic deformation depends on how the energy released by the explosion is coupled into the ground. The energy coupling, in turn, depends on the type of explosive, its depth of burial, and the physical properties of the surrounding terrain. Knowledge of the extent of the subsurface deformation zone is required for efficient design and deployment of surface-mobile weapon systems.

A series of small-scale explosion cratering experiments has been conducted in granular sand materials at Fort Devens, Massachusetts. In these experiments, the geometry of the subsurface deformation zone has been inferred from direct measurements of penetration resistance of the sand before and after cratering, and from surface measurements of changes in the electrical resistivity of the sand due to cratering. Analysis of the experimental data indicates that penetrometer measurement of ground strength is the more reliable method of determining subsurface deformation. These small-scale experiments also suggest that the area of the deformed zone underneath the visible crater does not change with the depth of the burst. The region of appreciable reduction of ground strength was confined to twice the radius of the crater rim crest.

Terrestrial Thermal Sources: A study of volcanic eruption clouds as indicators of the amount of thermal energy in the source was made. Cloud height was found to be directly related to the rate at which volcanic ash is erupted. This ash production rate presumably increases as heat emission increases.

The models used to describe hot gas plumes produced by industrial facilities can also be used to describe the clouds produced by major explosive eruptions. Such models indicate that eruption

Penetrometer measurements of ground strength before and after an explosive cratering event have been used to determine the extent of permanent subsurface deformation produced in sandy media. This information can be used in designing and developing Land-Mobile Weapons Systems.

clouds which succeed in penetrating the tropopause come from eruptions that produce more than a thousand tons of ash per second and more than 4 million megawatts of thermal energy.

SITING METHODOLOGY

Rapid, accurate, and cost effective methods are needed to determine the local geological conditions at a wide variety of candidate sites, so that appropriate sites for deployment of land mobile weapons systems can be selected. Surface soil properties, local depth to bedrock, and local depth to water table are all important. Satellite imagery can be used to make the preliminary identification of favorable areas. Research within the Terrestrial Sciences Division was directed toward developing criteria for preliminary site selection from satellite photography. An experimental program was also developed which sought to assess the efficiency of electrical surveys and induced polarization surveys in characterizing the subsurface geology of large areas.

SOIL BLOWOFF

Since the first atomic explosion, dust lofting has been observed during many above-surface nuclear weapons tests. Apparently, the thermal radiation is so intense, out to several fireball radii, that dust particles are explosively ejected ("popcorned") from the ground to the air. By absorbing thermal energy, the dust particles create a layer near the ground consisting of heated air, dust, gas, and vapors ejected from the surface. This layer transmits shock waves more rapidly than air, leading to the formation of a "precursor" wave in advance of the main shock wave. This phenomenon causes large departures from the response calculated to occur when a blast wave interacts with the ideal surfaces presently assumed in the nuclear weapons effects codes.

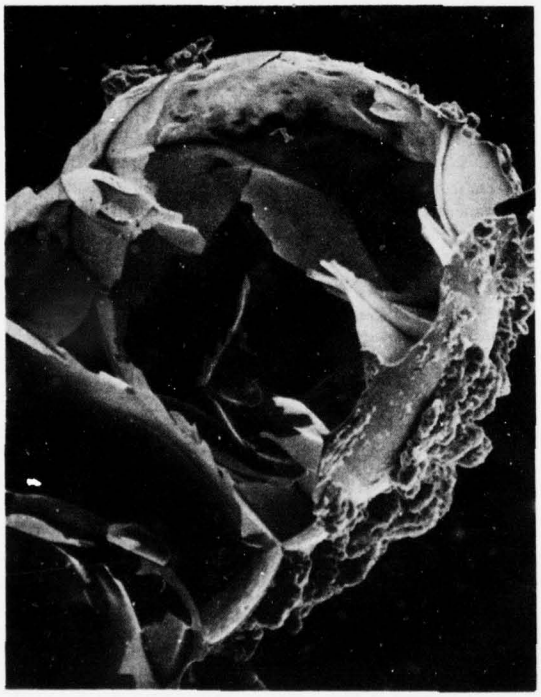

Hollow glass sphere (0.2 mm diameter) formed by melting of soil in solar furnace.

In addition to modifying shock propagation, the dust layer, which may extend hundreds of meters above the surface, alters peak pressures, force directions, and dynamic pressures predicted by ideal blast-wave theory, drastically affecting the response of target structures. Furthermore, the dust loading of the air may influence radar propagation and the ablation of reentry vehicles.

The fundamental mechanism of soil blowoff at high levels of thermal radiation is unknown, but is presumed to be the release of the pore moisture in soils or structural water contained in hydrous minerals, particularly from the clay minerals in soils.

The objective of this study is to clarify the physical mechanism of thermal blowoff in soils. This is being accomplished by examining the reaction products of soils exposed to high energy thermal pulses generated in the White Sands Solar Furnace. Various soils and other test materials irradiated in this solar furnace are now being studied.

JOURNAL ARTICLES JULY 1974 - JUNE 1976

CRONIN, J. F., ET AL.
Ultraviolet Photography
Manual of Remote Sensing (Am. Soc. of Photogram.), Vol. 1, Chap. 2 (1975)

ECKHARDT, D. H.
Discussion on "On the Phase Constraint of the Magnetotelluric Impedance"
Geophys., Vol. 40, No. 6 (December 1975)

GIESE, R. F., JR.
Electrostatic Energy of Columbite/Ixiolite
Nature, Vol. 256, No. 5512 (July 1975)
The Location of Hydrogen in YOOH
Acta Crystallographica, Vol. 1331, Pt. 7 (July 1975)

HEAD, J. W. (Brown Univ., Providence, R. I.), and SETTLE, M.
Rim Profile Studies of Lunar Craters: Morphology and Variability
EOS, Trans. Am. Geophys. Union, Vol. 56, No. 12 (December 1974)

HEAD, J. W. (Brown Univ., Providence, R.I.), SETTLE, M., and STEIN, R. (Brown Univ., Providence, R. I.), and HUNT, M. S.
Volume of Material Ejected from Major Lunar Basins: Implications for the Depth of Excavation
Lunar Sci. VI (1 March 1975), The Lunar Sci. Inst., Houston, Tex.
Volume of Material Ejected from Major Lunar Basins and Implications for the Depth of Excavation of Lunar Samples
Proc. of 6th Lunar Sci. Conf., NASA, Vol. 3 (December 1975)
Automatic Astronomic Positioning System
The Federation, Vol. 1, No. 2 (November 1975)

HUNT, M. S., and HERRING, J. C., MAJ. (Def. Mapping School., Wash., D.C.), GILBERT, P. F. (Geodetic Survey Sq., Aerosp. Ctr., Warren AFB, Wyo.)
Applications for the Automated Astronomic Positioning System (AAPS)
Proc. of Comsn. 5; Survey Instm. and Methods, XIVth Intl. Cong. of Surveyors, Intl. Fedn. of Surveyors, 7-16 Sep. 1974, Wash., D.C.

MC GETCHIN, T. R. (Los Alamos Sci. Lab., N. M.). and SETTLE, M.
Cinder Cone Separation Distances: Implications for the Depth of Formation of Gabbroic Xenoliths
EOS, Trans. Am. Geophys. Union, Vol. 56, No. 12 (December 1975)

ROONEY, T. P., RIECKER, R. E., and GAVASCI, A. T. (Lamont-Doherty Geol. Obsv., Columbia Univ., N. Y.)
Hornblende Deformation Features
Geol., Vol. 3, No. 7 (July 1975)

SETTLE, M.
Translation and Distribution of Explosion Crater Ejecta: Implications for Impact Cratering
EOS, Trans. of Am. Geophys. Union, Vol. 56, No. 6 (June 1975)

SETTLE, M., and HEAD, J. W. (Brown Univ., Providence, R. I.)
Excavation Depths of Basin-Sized Impacts: Evidence from Lunar Crater Morphometry
EOS, Trans. of Am. Geophys. Union, Vol. 56, No. 12 (December 1975)
Excavation Depths of Large Lunar Impacts: Shallow or Deep?
Interdisciplinary Studies of the Imbrium Consortium, Smithsonian Astrophys. Obsv., Cambridge, Mass. (March 1976)
Impact Cratering: Models of the Growing Crater Cavity
EOS, Trans. of Am. Geophys. Union, Vol. 57 (April 1976)

SETTLE, M., and HEAD, J. W. (Brown Univ., Providence, R. I.), MC GETCHIN, T. R. (Los Alamos Sci. Lab., N. M.)
Ejecta from Large Craters on the Moon: Discussion
Earth and Planetary Sci. Ltrs., Vol. 23 (August 1974)

SETTLE, M., and NEEDLEMAN, S.
Deformation in Granular Earth Media Produced by Explosive Cratering: Implications for Impact Cratering
EOS, Trans. Am. Geophys. Union, Vol. 56, No. 12 (December 1974)

SHAPIRO, I. I., COUNSELMAN, C. C., III (Mass. Inst. of Technol.) and KING, R. W., CAPT.
Verification of the Principle of Equivalence for Massive Bodies
Phys. Rev. Ltrs., Vol. 36, No. 11 (15 March 1976)

WILLIAMS, J. G. (Jet Propulsion Lab., Pasadena, Calif.), ET AL., ECKHARDT, D. H.
New Test of the Equivalence Principle from Lunar Laser Ranging
Phys. Rev. Ltrs., Vol. 36, No. 11 (15 March 1976)

WIRTANEN, T. E.
Field Results with an Automated Reticle Geodetic Theodolite
Proc. XIV Fedn. Intl. des Geometres Cong., Wash., D.C. (September 1974)

PAPERS PRESENTED AT MEETINGS JULY 1974 - JUNE 1976

BLIAMPTIS, E. E.

A Square Array for Geoelectric Measurements
Sec. Wkshp. on EM Induction in the Earth, Carleton Univ., Ottawa, Can. (22-28 August 1974)

Mutliple Utilization of Solar Energy System (MUSES)
Am. Phys. Soc. New Eng. Sec. Mtg., No. Dartmouth, Mass. (9-10 April 1976)

A Large Scale System for Effective Utilization of Incident Solar Radiation
New Eng. Solar Energy Assoc. Mtg., Univ. of Mass., Amherst, Mass. (24-25 June 1976)

ECKHARDT, D. H.

Lunar Libration Theory
8th GEOP Res. Conf.: Lunar Dyn. and Selenodesy, Ohio State Univ., Columbus, Oh. (10-11 October 1974)

Cassini's Laws
Rad. Phys. Sem., Dept. of Earth and Planetary Sci., Mass. Inst. of Technol., Cambridge, Mass. (6 October 1975)

HAMMOND, J. A.

Absolute Gravity Measurements
Colloq., Dept. of Geod. Sci., Ohio State Univ., Columbus, Ohio (23 May 1975)

HAMMOND, J. A., and FALLER, J. E. (Jt. Inst. for Lab. Astrophys., Boulder, Colo.)

A New Portable Absolute Gravity Instrument
7th Mtg. of the Intl. Gravity Comsn., Paris, Fr. (2-7 September 1974)

HEAD, J. W. (Brown Univ., Providence, R. I.), and SETTLE, M.

Rim Profile Studies of Lunar Craters: Morphology and Variability
Am. Geophys. Union 1974 Fall Ann. Mtg., San Franisco, Calif. (12-17 December 1974)

HEAD, J. W. (Brown Univ., Providence, R. I.), SETTLE, M., and STEIN, R. (Brown Univ., Providence, R. I.)

Volume of Material Ejected from Major Lunar Basins: Implications for the Depth of Excavation
6th Lunar Sci. Conf., Johnson Space Ctr., Houston, Tex. (17-21 March 1975)

HUNT, M. S., and HERRING, J. C., MAJ. (Def. Mapping Sch., Wash., D.C.), GILBERT, P. (DMA Aerosp. Ctr./Geod. Survey Sq., Warren AFB, Wyo.)

Applications for the Automated Astronomic Positioning System (AAPS)
14th Cong., Fedn. Internationale de Geometres (FIG), Wash., D. C. (6-16 September 1974)

KING, R. W., 1ST LT., and COUNSELMAN, C. C. III, SHAPIRO, I. I. (Mass Inst. of Technol.)

Data Reduction Techniques for Cycle-Counting VLBI Systems
1974 USNC/URSI-IEEE Mtg., Univ. of Colo., Boulder, Colo. (14-17 October 1974)

Lunar Moment-of-Inertia Ratios, Third-Degree Gravity Harmonics, and Apollo Landing-Site Coordinates: VLBI Results
Am. Geophys. Union 1975 Fall Ann. Mtg., San Francisco, Calif. (8-12 December 1975)

Lunar Dynamics and Selenodesy: Results from Analysis of VLBI and Laser Data
IUGG-COSPAR-IAU Symp. on Sci. Appl. of Lunar Laser Ranging, Austin, Tex. (8-10 June 1976)

KING, R. W., 1ST LT., CLARK, T. A. (NASA Goddard Space Flight Ctr., Greenbelt, Md.), COUNSELMAN, C. C. (Mass. Inst. of Technol.), KNIGHT, C. A. (Haystack Obsv., Tyngsboro, Mass.), ROBERTSON, D. S., and SHAPIRO, I. I. (Mass. Inst. of Technol.)

Universal Time: Lunar Ranging Results and Comparisons with VLBI and Classical Determinations
IUGG-COSPAR-IAU Symp. on Sci. Appl. of Lunar Laser Ranging, Austin, Tex. (8-10 June 1976)

KING, R. W., 1ST LT., and COUNSELMAN, C. C., III, SHAPIRO, I. I. HINTEREGGER, H. F. (Mass. Inst. of Technol.), RYAN, J. W. (NASA Goddard Space Flight Ctr., Greenbelt, Md.)

Selenodetic Control Using Differential VLBI Observations of ALSEPS
8th Geod./Solid-Earth and Ocean Phys. (GEOP) Res. Conf.: Lunar Dyn. and Selenodesy, Ohio State Univ., Columbus, Ohio (10-11 October 1974)

KING, R. W., 1ST LT., and SHAPIRO, I. I., COUNSELMAN, C. C., III (Mass. Inst. of Technol.)

Verification of the Principle of Equivalence for Massive Bodies
Am. Astronom. Soc. Mtg., Pasadena, Calif. (11-12 December 1975); Symp. on the Sci. Appl. of Lunar Laser Ranging, Univ. of Tex., Austin, Tex. (8-10 June 1976)

Lunar Moment-of-Inertia Ratios, Third Degree Gravity Harmonics, and Apollo Landing Site Coordinates: VLBI Results
Symp. on Sci. Appl. of Lunar Laser Ranging, Univ. of Tex., Austin, Tex. (8-10 June 1976)

Mc GETCHIN, T. R. (Los Alamos Sci. Lab., N. M.), and SETTLE, M.
Cinder Cone Separation Distances: Implications for the Depth of Formation of Gabbroic Xenoliths
Am. Geophys. Union Ann. Fall Mtg., San Francisco, Calif. (8-12 December 1975)

SETTLE, M.
Translation and Distribution of Explosion Crater Ejecta: Implications for Impact Cratering
56th Ann. Am. Geophys. Union Mtg., Wash., D. C. (16-20 June 1975)

SETTLE, M., and HEAD, J. W. (Brown Univ., Providence, R.I.)
Excavation Depths of Basin-Sized Impacts: Evidence from Lunar Crater Morphometry
Am. Geophys. Union Ann. Fall Mtg., San Francisco, Calif. (8-12 December 1975)
The Role of Rim Slumping in the Modification of Lunar Crater Morphometry
7th Lunar Sci. Conf., The Lunar Sci. Inst., Johnson Space Ctr., Houston, Tex. (15-19 March 1976)
Impact Cratering: Models of the Growing Crater Cavity
1976 Spring Ann. Mtg. of the Am. Geophys. Union, Wash., D. C. (12-16 April 1976)

SETTLE, M., and NEEDLEMAN, S.
Deformation in Granular Earth Media Produced by Explosive Cratering: Implications for Impact Cratering
Am. Geophys. Union 1974 Fall Ann. Mtg., San Francisco, Calif. (12-17 December 1974)

WIRTANEN, T. E.
Field Results with an Automated Reticle Geodetic Theodolite
XIV Fedn. Internationale des Geometres Cong., Wash., D. C. (6-16 September 1974)

TECHNICAL REPORTS JULY 1974 - JUNE 1976

BLIAMPTIS, E. E., and THOMSON, K. C.
Geophysical Methods in Terrestrial Material Property Determinations
AFCRL-TR-75-0393 (23 July 1975)

CROWLEY, F. A., and OSSING, H. A.
On Motion Environment
AFGL-TR-76-0152 (June 1976)

GIESE, R. F., JR.
A Computer Program for Plotting Coordinaton Polyhedra in Ionic Crystals - DRWMIN
AFCRL-TR-75-0234 (24 April 1975)
Crystal Structure of Ideal, Ordered One-Layer Micas
AFCRL-TR-75-0438 (13 August 1975)
Crystal Structures of Ideal, Ordered Two-Layer Micas
AFCRL-TR-75-0471 (5 September 1975)

GIESE, R. F., JR., and DENTAN, C. M. (State Univ. of New York, Buffalo, N. Y.)
Application of Principal Components Analysis to the Study of Silicate Crystal Structures
AFCRL-TR-75-0372 (14 July 1975)

HADGIGEORGE, G., and BROWN, D. C., TROTTER, J. E. (DBA Sys., Inc., Melbourne, Fla.)
Computer Simulations of the Recovery of Geoidal Undulations Over the North Atlantic by the Short Arc Reduction of Satellite Altimetry
AFCRL-TR-75-0282 (19 May 1975)

HADGIGEORGE, G., WIRTANEN, T. E., ILIFF, R. L., ECKHARDT, D. H., and BROWN, D., TROTTER, J. (DBA Sys., Inc., Melbourne, Fla.), RAPP, R. (Ohio State Univ.)
AFCRL Contributions to the National Geodetic Satellite Program (NGSP)
AFCRL-TR-74-0217 (2 May 1974)

HUNT, M. S.
An Evaluation of AAPS Acceptance Performance
AFCRL-TR-75-0068 (3 February 1975)
Star Catalogues and Their Significance to Geodesy of the 1980's
AFGL-TR-76-0015 (5 February 1976)

ILIFF, R. L.
Light Shutter for Laser Applications
AFGL-TR-76-0059 (17 March 1976)

OSSING, H. A., and CROWLEY, F. A.
Richmond Air Force Station Strong Motion Study - Preliminary Report
AFCRL-TR-75-0576 (7 November 1975)

ROONEY, T. P., RIECKER, R. E., and GAVASCI, A. T. (Lamont-Doherty Geol. Obsv., Columbia Univ., N. Y.)
Mechanical Twinning in Experimentally and Naturally Deformed Hornblende
AFCRL-TR-74-0361 (1 August 1974)

VII OPTICAL PHYSICS DIVISION

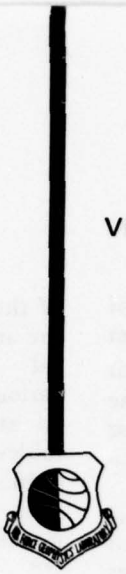

The Optical Physics Division conducts research on the sources, transmission, and detection of optical and infrared radiation and their interaction with the aerospace environment. Field measurements, laboratory studies, theoretical studies, and analyses are conducted to determine and understand the optical and infrared properties of the environment including the atmosphere and celestial sky. These determine how well the atmosphere transmits radiant energy and also how much energy the atmosphere radiates, both under natural and perturbed conditions.

Any optical or infrared detection, surveillance, reconnaissance, or weapon system that operates in or above the atmosphere must look through the atmosphere or look against a background of either atmosphere or sky. Therefore, the optical properties of the environment, especially the atmosphere, must be known, as well as how they will enhance or limit the operation of these systems.

Using data and results from field measurements of these optical/IR properties of the environment and related laboratory and theoretical studies, our goal is to develop "tools" that can be used directly for the design and operation of Air Force systems. These tools include various models such as the LOWTRAN atmospheric transmission and HITRAN laser transmission computer codes, the AFGL IR Star Atlas and the LWIR Earth Limb model.

The Division's effort on the sources of optical/infrared radiation ranges from measurements of atmospheric and stellar emission, missile and aircraft plume signatures to research into molecular physics and molecular interactions, optical and spectroscopic techniques.

The portion of the electromagnetic spectrum studied extends in wavelength from 2,000 angstroms in the ultraviolet to 1 millimeter where the far infrared blends into the microwave radio spectrum.

The research in the Division is divided into studies of: the visible and near visible properties of the atmosphere, where aerosol and molecular scattering is the predominant mechanism of attenuation; the infrared properties of the lower atmosphere where thermal equilibrium usually prevails; the optical and infrared properties of the upper atmosphere (including auroras and airglow) where individual molecular interactions must be considered; the infrared properties of exoatmospheric sources—stars, nebulae, zodiacal dust; measurements of the radiation from man-made sources such as missile or aircraft plumes; and development of improved techniques for spectroscopic measurements.

A major area of investigation by the Division concerns atmospheric attenuation or transmission of radiation by the atmosphere, including laser beams. Atmospheric molecules absorb optical and infrared radiation selectively at discrete wavelengths. Extensive computer programs have been developed which make use of the vast collection of spectroscopic data for molecules (AFGL Atmospheric Absorption Line Parameters Compilation) and which permit the calculation of this transmission, particularly for laser beams (HITRAN). The well known LOWTRAN atmospheric transmission computer code has been adopted and used widely for determining the low resolution (approximately 20 wave numbers) transmission of the atmosphere for any path through the atmosphere for a wide range of tactical weapon delivery problems under various meteorological conditions. Detailed atmospheric absorption curves and tables for laser transmission have been published. The application of these codes to the emission and transmission of plume radiation has been underway.

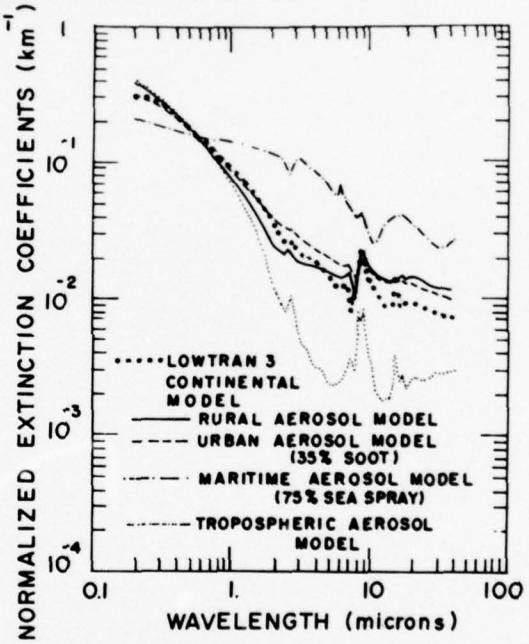

Computed extinction coefficients for several aerosol models as a function of wavelength. To make comparison easier, the models have been normalized so that in each, the visibility is 23 km at a wavelength of 0.55 micrometers.

The measurement and use of atmospheric transmission and emission also provides a method for remotely sensing atmospheric composition (including the effect of addition of contaminants, for example, from missile or jet engine exhausts) and meteorological conditions such as temperature, humidity and ozone content. The transmission codes have been extensively applied to the design and improvement of remote atmospheric sensing sensors on the Air Force meteorological satellites.

Scattering by aerosols and molecules in the atmosphere also contributes both to attenuation and to reduction in the contrast of a target seen through the atmosphere. Extensive measurements from the Division's C-130 Flying Laboratory and balloons have been made to determine the geographic, seasonal and altitude variations, as well as the optical properties of these aerosols and the effect of the underlying terrain, water surface or snow cover. The results of these measurements have been applied to several target acquisition and detection problems. As one extension of these measurements, an extensive international program of measurements is being carried out in Europe.

Similarly, the emission of the atmosphere, insofar as it creates a disturbing or masking background against which a target must be located, is also a major concern of the Division efforts. Such emissions represent interfering background noise superimposed on the optical/IR target signals that a surveillance system may be trying to detect. The emission of the lower atmosphere can be calculated from computer programs similar to those discussed previously. However, the emission from the upper atmosphere (above about 70 km) requires a much more detailed knowledge of the interactions and collisions among the individual molecules, many of which will be in excited states with excess energy. The amount and wavelength of the radiation resulting from this nonequilibrium chemistry, and the effects of disturbances by protons and electrons as would occur during an aurora or a nuclear burst are also being studied. Therefore, a sizable laboratory and theoretical research program is conducted to study the physics and chemistry of the atmosphere, particularly those molecular interactions which lead to infrared emission, as well as an extensive measurement program. This has included both the use of the Division's NKC-135 optical/infrared flying laboratory, and rockets, particularly in Alaska, where the infrared emission of the aurora is studied in the Infrared Chemistry Experiments for the Coordinated Auroral Program (ICECAP). A computer program (called OPTIR) has been developed to predict and compute the optical and IR emission of the upper atmosphere, primarily for disturbed conditions. Such background emission, particularly during disturbed conditions such as auroras, could seriously impair the operation of a surveillance, detection, tracking, or terminal guidance system.

A satellite or rocket-borne infrared system looking away from the atmosphere will still see the celestial sky as a background. Consequently, the Division is carrying out a rocket program to map the celestial sky as well as zodiacal emission in the infrared. Also, measurements of missile and aircraft plumes are being obtained from rockets and aircraft.

An inseparable part of these measurements and studies is the development and use of more sensitive advanced cryogenically cooled infrared sensors and spectrometers by the Division. Such a technique to which the Division has made significant contributions is multiplex spectroscopy, where all wavelengths entering the spectrometer-interferometer are analyzed simultaneously. The most recent development has been time-resolved spectroscopy which permits the spectral measurement of chemical reactions with millisecond time resolution.

ATMOSPHERIC OPTICS

The objective of the Atmospheric Optics program is to develop techniques for evaluating and predicting the effects of atmospheric scattering and absorption of light on the performance of optical systems looking through the earth's atmosphere. Air molecules and aerosol or haze

particles suspended in the atmosphere scatter and absorb light. These attenuation processes occur throughout the visible and infrared spectrum and they are more or less pronounced depending on aerosol and molecule type and the wavelength of the light. The goal of this program is an understanding of the effects of atmospheric optical properties on the performance of various Air Force systems and the capability of predicting these atmospheric optical properties for conditions under which these Air Force systems must operate.

At present, one of the least known parameters in the atmospheric attenuation process is the optical effect of aerosol particles. It is little known because the composition of natural aerosols is so complex and the variation in aerosol distributions in the atmosphere with changing meteorological and geographical conditions is enormous.

The Atmospheric Optics program is therefore directed primarily at studies of aerosol optical properties and their effect on optical propagation. Experiments are conducted to determine the optical properties, in particular the refractive index, of aerosol particles of various types. Ground and airborne measurements are made to determine the spatial and temporal variability of aerosol concentrations, size distribution and composition together with measurements of the transmission and scattering effects.

From these experimental data models have been developed which, together with the appropriate data for molecular absorption and scattering, allow one to calculate the atmospheric transmission or scattering at any given wavelength, either for lasers (HITRAN) or for broadband optical systems (LOWTRAN). These models also can be used as inputs into more complex radiation transfer codes which include multiple scattering processes and which are needed to compute such quantities as sky radiance backgrounds or contrast attenuation.

Measurements of Aerosol Optical Properties: To determine the correlations between the atmospheric optical properties and the general meteorological conditions such as air mass and vertical structure, a coordinated measurement program has been established in Europe with several other countries to conduct routine measurements at several locations of such quantities as visible and IR transmission, illumination, path radiance, and scattering intensity, along with aerosol distribution measurements and other meteorological parameters. Surface measurements of these parameters are supplemented by airbone measurements from AFGL's atmospheric optics C-130 Flying Laboratory.

Measurements will be conducted over a two-year period to derive an atmospheric optics climatology for the European environment and to study the variability of seeing and transmission conditions with changes in weather conditions. Very specialized instrumentation is required to measure the optical effects of aerosols. Several unique instruments have been developed under the Atmospheric Optics program for the measurement of Optical Atmospheric QUantities in Europe (OPAQUE).

One of the quantities which is very little known at present is the intensity of infrared radiation scattered from aerosols. The angular dependence of scattered light in the infrared can be efficiently measured by viewing a collimated laser beam from the side at different angles. An experiment has been installed in a trailer, in which a CO_2 laser beam is projected outside the trailer. The scattered intensity is measured by a cooled HgCdTe detector scanning along the laser beam as a function of the scattering angle between 10 degrees (forward scattering) and 170 degrees (backscattering). The scattered light energy per unit path length and

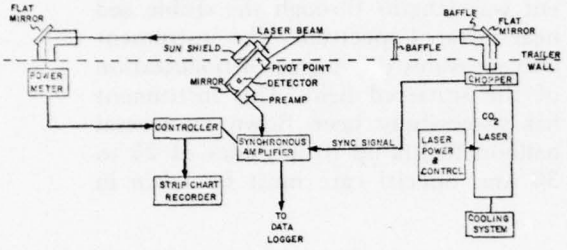

Schematic Block Diagram of the CO_2-Laser Scattering Nephelometer, which measures the angular dependence of scattering.

steradian is about 10^{-8} to 10^{-10} times the intensity of the incident laser beam. Although this is a very small percentage (comparable signals in the visible would be approximately one to two orders of magnitude higher), such signals can still be detected. The importance of these measurements is that the variation in the scattering properties can be determined for different types of aerosols and under various weather conditions.

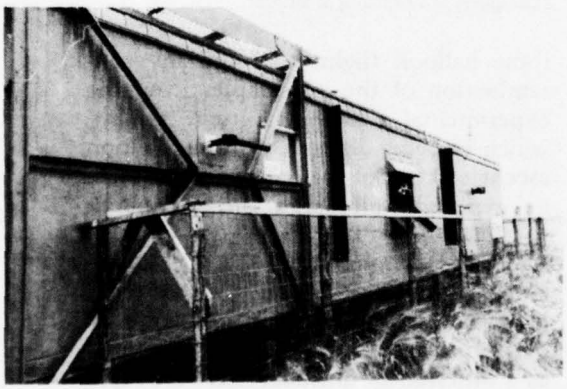

The laser nephelometer installed in its trailer. The laser beam travels between the two tubes. The detector, on its turntable, is visible in the center of the trailer.

Scattering of light in the atmosphere does not occur only from artificial light beams such as lasers; every air volume is illuminated by natural light from the sun, the sky, or at night from the moon. This light is scattered into various directions, some of it into the field of view of any system looking through the atmosphere. This so-called "path radiance" is responsible for the washout of contrast between object scene elements. A knowledge of the dependence of this "path radiance" on atmospheric conditions, illumination, look angles, etc., is therefore very important in the evaluation of the performance of optical systems. In order to measure this quantity directly as a function of all these variables, an instrument

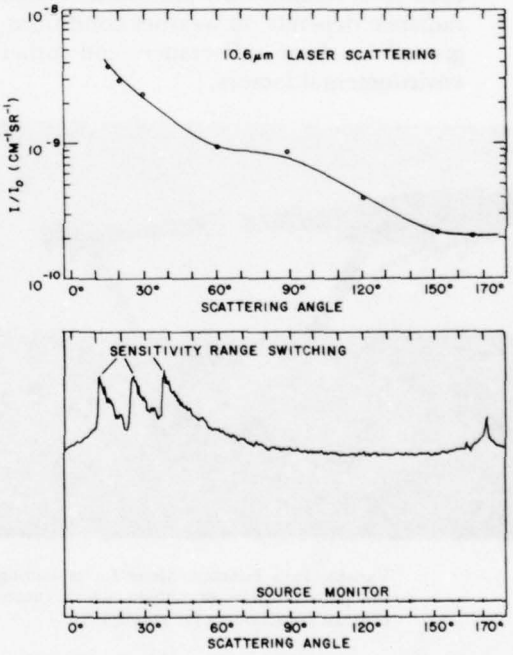

An example of a scattering measurement. The lower curves are the actual records of the scattered signal and the laser source stability; the top curve is the derived absolute scattering function.

was developed under contract, It consists of a high sensitivity photometer which looks into a black hole. The airgap between these two components is illuminated by ambient light, and the scattered light in the direction of the photometer as seen against the black hole as back-

ground is identical to the path radiance for the short path element between the two arms of the instrument. The instrument can rotate around a vertical axis, permitting the measurement of the path radiance as a function of sun-observer angle geometry. If this incremental path radiance is summed over a finite path length one can easily calculate from it the amount of contrast reduction which would occur along a given atmospheric path assuming a constant path radiance along the path. This so-called variable path function meter is presently being used to determine how atmospheric path radiance depends on weather conditions, ground surface reflectance and other environmental factors.

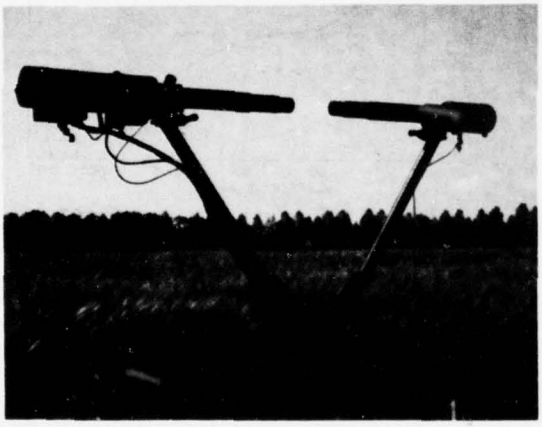

Variable Path Function Meter for measuring the path radiance or airlight which causes contrast reduction by the atmosphere.

Because of the nonuniform distribution of aerosol particles with altitude it is particularly important to develop techniques for *in situ* measurements of the atmospheric optical parameters as a function of altitude. A balloon-borne instrument was developed which can measure various scattering properties of the atmosphere up to altitudes of 30 km or more. A high intensity light source illuminates a sample volume of ambient air. Five radiometers pointed at this air volume measure the intensity of scattered light in five different directions at four different wavelengths through the visible and near infrared spectrum. The instrument also measures the degree of polarization of the scattered light. This instrument has successfully been flown on several balloon flights up to altitudes of 25 to 30 km. Special care must be taken in

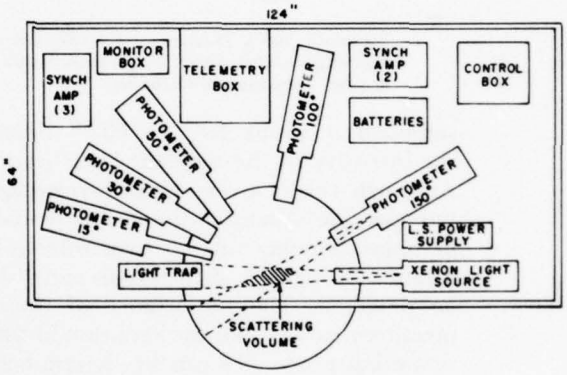

Schematic block diagram of the balloon-borne nephelometer. It is used to measure the angular scattering properties of the atmosphere as a function of altitude.

these balloon flights to avoid any contamination of the air samples from the experimental equipment itself. Ballast, which is being dispensed during balloon ascent to control the balloon flight must be expelled well below the instrument gondola.

As an example, on one of the balloon flights where the intensity of scattered light into 15 degrees forward angle at 0.475 micrometer wavelength is measured as a function of altitude, there is a rapid decrease of haze scattering above the surface layer after launch and a more or less stable haze layer up to 6-7 km. A rapid decrease of larger aerosols above that altitude accounts for the rapid decrease of signal up to 13 km altitude. A sharp peak in the scattered light around 25 km altitude was caused by a rare occurrence of a nacreous cloud on the lee side of the

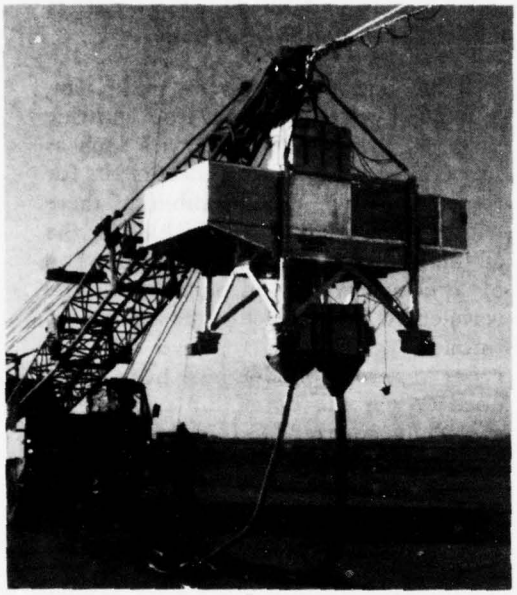

The gondola carrying the nephelometer, ready for launch of the balloon.

San Andres Mountains in New Mexico, where this balloon flight took place. A comparison between the ascent and descent portion of this balloon flight shows the reproducibility of the major atmospheric optical characteristics in the experiment.

It requires carefully planned experiments such as this to obtain the basic atmospheric optical quantities needed to predict the propagation of optical radiation through the atmosphere.

Aircraft Measurement Program: The Air Force tactical/operational regime requires a thorough understanding of the atmospheric optical properties from the surface to 10 km. To provide the data on which to base sophisticated prediction models, aircraft measurements of all parameters affecting the atmospheric contrast transmittance, which determines an optical system's capability to identify a specified target, have been and are being taken by an instrumented C-130A Hercules Flying Atmospheric Optics Laboratory. These data include scattering coefficients, sky and terrain radiances, path radiances and aerosol size distributions. Data analysis and summaries are presented in report form and are used in applying modern technology to solving target acquisition/identification problems involving optical systems.

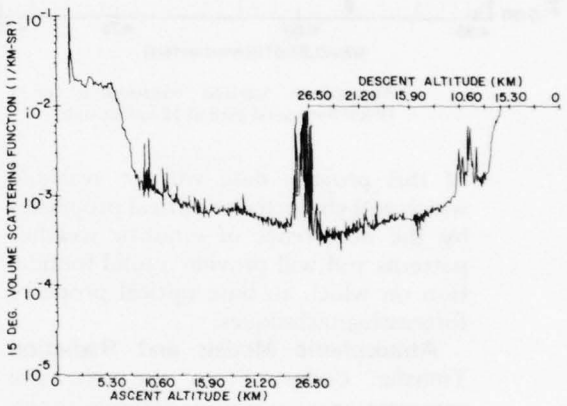

An example of the measured scattering intensity at 0.475 micrometer wavelength at a 15-degree scattering angle as a function of altitude in ascent and descent.

In 1974 the Atmospheric Optics Flying Laboratory participated in joint Army-Navy-Air Force efforts to determine instrumentation and data reduction methods for measuring and documenting both apparent and inherent contrast of scene objects. Most recently, an extensive effort has been made to provide a more extensive documentation of the seasonal characterization of atmospheric optical properties in Europe, under both maritime and continental influences. The aircraft data are taken on tracks approximately 50 km long at specific levels from 300 to 6000 meters above ground level. The tracks are chosen to include ground stations participating in the data gathering effort. This program will continue for

two years with data gathering deployments scheduled for two-month periods spread over all four seasons. By the end

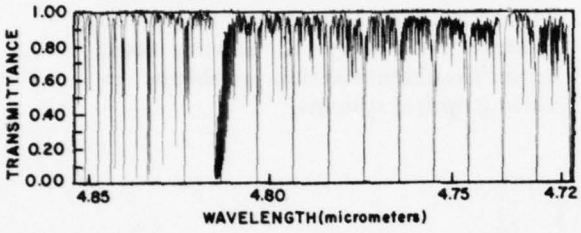

Atmospheric infrared transmission for a 10-km horizontal path at 12-km altitude.

of this project, data will be available which will characterize optical properties by the occurrence of synoptic weather patterns and will provide a solid foundation on which to base optical property forecasting techniques.

Atmospheric Models and Radiation Transfer Codes: From the extensive measurements on various aerosol properties as well as atmospheric optical parameters and from consolidation of the results from other research activities throughout the world, it was possible to derive a number of atmospheric aerosol models and their optical properties, which can be considered reasonably representative for certain environmental situations.

Such models have been developed for the boundary layer near the earth's surface, the upper troposphere and the stratosphere up to 100 km altitude. For the boundary layer below 2 km, ten models have been defined which describe rural, urban and maritime environments for several surface visibilities. For the upper troposphere and the stratosphere, models for the spring-summer and fall-winter seasons have been derived. Models of the stratosphere can be defined which describe different conditions of volcanic dust injection into the upper atmosphere. The number density, the size distribution, and the aerosol particle refractive index have been defined for these various models as a function of altitude.

If these aerosol properties are known, it is possible to calculate, from existing theories, the optical properties such as scattering and absorption coefficients for these aerosol models. Combining these with the corresponding quantities for the air molecules allows the full description of atmospheric optical parameters. The wavelength dependence of the aerosol extinction coefficients for five different types of aerosol models have been developed. When the extinction coefficients are all normalized at 0.55 micrometer wavelength, there are large differences between the extinction by the various aerosol types in the infrared region, up to a factor of 20 in some regions. Some of the features, such as the high values for the maritime aerosol model are explained by the high percentage of larger aerosols in the size distribution for this type. Other features such as a peak around 9-10 micrometers are caused by abnormalities in the aerosol refractive index at these wavelengths. The major conclusion from these model calculations is that although the visibility may be the same, different types of aerosol models will cause quite different attenuation conditions in the infrared and to some extent also in the ultraviolet. These differences between various aerosol types also are quite noticeable in the amount of contrast reduction which may occur. Such conclusions strengthen the need for more detailed field measurements and for the development of efficient and accurate computer programs to perform such calculations for real-time situations.

However, since in most practical situations it will not normally be possible to obtain detailed measurements of the existing aerosol distributions or properties, it is necessary to develop efficient empirical correlations between aerosol models and standard meteorological conditions.

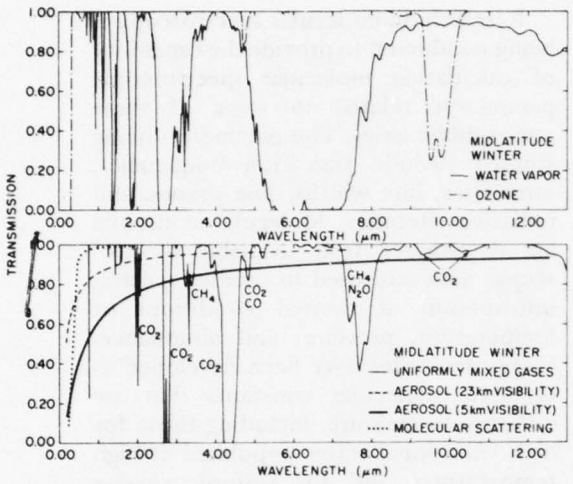

Atmospheric transmission along a vertical path from sea level to space.

INFRARED PHYSICS

The infrared physics program includes research on, and measurements of, the mechanisms of attenuation, absorption, transmission, and emission of infrared radiation in the aerospace environment. This includes infrared background emitted by the atmosphere and celestial sky. It also includes the attenuation by the atmosphere of the infrared radiation from natural sources, natural or man-made disturbances, or targets such as missile or aircraft plumes.

The results of these efforts, in addition to the data measured directly, are models and computer codes which allow the prediction of this infrared emission and transmission for any situation. Also, improved spectroscopic measurement techniques are being developed.

Atmospheric Transmittance-Radiance Models: Models for predicting the transmittance and radiation properties of the atmosphere have been developed for both high and low spectral resolution applications. Two basically different transmittance models have been developed.

The low-resolution (20 wave number spectral resolution) model covers the spectral range from 0.25 to 28.5 micrometers and accounts for both molecular and aerosol attenuation for a wide range of atmospheric paths. A graphical representation of the model is described in *Optical Properties of the Atmosphere, Third Edition* (AFCRL-72-0497), and a computer version is given in *Atmospheric Transmittance from 0.25 to 28.5 Micrometers: Computer Code LOWTRAN 3B* AFGL-TR-76-0258). The latter computer program contains three boundary layer aerosol models and one model for the free atmosphere, six standard geographical atmospheric models (tropical, midlatitude summer, midlatitude winter, subarctic summer, subarctic winter and the 1962 U. S. Standard Atmosphere) for altitudes from 0-100 km, and a capability for the user to insert additional (nonstandard) atmospheric conditions. Recent additions included in the LOWTRAN 3B model modify the water vapor continuum in the 4- and 10-micrometer window regions, provide an option for using additional boundary layer aerosol models (for example, maritime, urban, rural) and include a tropospheric model for use above the boundary layer (that is, above 2 km altitude). This model has been widely used for making broadband atmospheric transmittance estimates. A new version of the computer code has been adapted to predict atmospheric and earth thermal backgrounds.

The second atmospheric transmittance model, HITRAN, uses the summation of the individual molecular absorption line profiles of the various atmospheric gases to determine the monochromatic transmittance at each wavelength. This method is known as a "line-by-line calculation" and can be used to determine the transmittance of the atmosphere at any given spectral resolution by averaging over the required spectral interval. This is the only approach capable of computing very high

resolution spectra for the transmittance of laser beams through the atmosphere. This approach may also be used to predict atmospheric propagation characteristics for spectral resolution up to the 20 wavenumber capability of LOWTRAN.

A frequently asked question is: "What laser frequencies are attenuated the least by the atmosphere?" This question has been answered for carbon monoxide, hydrogen fluoride, deuterium fluoride and carbon dioxide laser systems in a summary report on laser transmittance (AFCRL-TR-74-0003). In addition to addressing the problem of laser propagation of these specific laser systems, the summary report provides synthetic spectra for the entire spectral region from 0.76 micrometer to 31.25 micrometers, thereby allowing a quick estimate of atmospheric attenuation for laser propagation throughout this entire portion of the infrared. The compilation of atmospheric absorption lines used as a basis for much of our work is described in the *AFCRL Atmospheric Absorption Line Parameters Compilation* (AFCRL-73-0096). Since the publication of this report in early 1973, we have made available over 200 copies of these data on magnetic tape. Detailed information on over 135,000 spectral lines in the spectral region from 0.68 micrometer to the microwave region are contained on this tape. Atmospheric species included in the compilation are: H_2O, CO_2, O_3, N_2O, CO, CH_4, and O_2.

Current efforts involve improving the data base, both by correcting existing data and adding new material. New material to be added includes weak absorption features of the major atmospheric absorbing gases. Absorption parameters for trace atmospheric and pollutant gases will compose a separate tape. Additional gases on which some work is currently in progress include NO, NO_2, HNO_3, NH_3, OH, HCl, HF, and SO_2.

Research on molecular spectroscopy is being conducted to provide the capability of calculating molecular spectroscopic parameters related to some of these atmospheric gases. The parameters being studied include transition frequencies, intensities, line widths, line shapes, and radiative lifetimes. Molecular constants are determined from available spectroscopic data and used to predict spectral information at desired conditions of temperature, pressure, and abundance. Computer codes have been developed to calculate molecular constants that are difficult to measure, including those for high vibrational states populated at high temperatures and for isotopic species that are significant in weak absorption regions of the atmospheric spectrum.

During the past two years, a great deal of the modeling effort has been in direct response to specific application requirements. The development of the LOWTRAN 3 code was spurred by such requirements. Both HITRAN and LOWTRAN have been applied to a wide variety of laser and broadband tactical design and system application problems.

Another application of the transmittance modeling activity is the problem of the satellite remote sensing of meteorological variables. The Line Parameters Compilation has been used as a data base for such calculations to determine the spectral channels most suitable for use in satellite sensor design. In addition, transmittance calculations performed with these models are being used in the development of software packages for the reduction of satellite-measured radiances in terms of the three dimensional structure of temperature and moisture.

The Line Parameters Compilation has also been applied to the understanding of the signature of a hot gas (for example, the exhaust plume of an aircraft) as viewed through a colder intervening atmosphere. In conjunction with aircraft-borne measurement programs, these calcula-

tions allow us to investigate the altitude and range dependence of exhaust plume emission signatures.

Infrared Background Measurements: The Air Force needs to detect infrared emitting targets at the greatest possible range. If these targets are viewed against background radiance, knowledge of this radiation is necessary to permit discrimination of the target from the background.

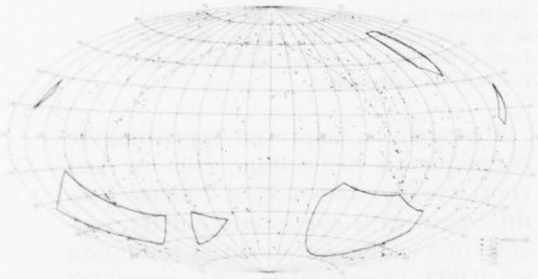

Infrared stellar sources observed at a wavelength of 11 micrometers using a rocket-borne telescope. The dotted line delineates the galactic plane.

The scope of the problem is determined by the coverage and sensitivity requirements of the space surveillance program. The first requirement is a specification of the celestial background at projected sensitivity levels. These levels are now sufficiently low so that we must be concerned not only with stars but, in addition, take into account the effects of zodiacal radiation – that is, thermal emission from particles distributed about the ecliptic plane caused by the absorption of solar radiation. The additional requirement to observe low-altitude satellites means that we must determine the lower limit set by the earth's upper atmospheric limb radiance.

The Division has conducted a series of experiments to obtain infrared survey data on the celestial background with state-of-the-art cryogenically cooled sensors flown on rocket probes. The thrust of the program has been threefold: to obtain the most complete sky coverage possible with as high a sensitivity as compatible with the need to cover a large area on each flight; to generate from these data a background map; and to apply these data to the model to statistically extend the empirical data base to faint irradiance levels.

To date about 79 percent of the sky has been surveyed at an effective wavelength of 4.2 micrometers, 90 percent at 11 micrometers, 87 percent at 20 micrometers and 36 percent at 27 micrometers. The Northern Hemisphere data have been published in the *AFCRL Infrared Sky Survey, Volume I, Catalog of Observations at 4, 11, and 20 Microns* (AFCRL-TR-75-0373). A new catalog (AFGL-TR-76-0208) which includes Southern Hemisphere data is now available.

Present plans are to develop instrumentation to be flown on an ARIES compatible payload which gimbals the cryogenic sensor. Each flight will survey approximately 35 percent of the sky at effective wavelengths of 11, 20 and 28 micrometers. The optics will permit scanning to -55 degrees in declination from White Sands Missile Range with no degradation in sensitivity, permitting coverage of the important area south of the galactic center.

Preliminary data for the earth limb and zodiacal radiances were obtained August 3, 1976 from a rocket probe launched at White Sands Missile Range, New Mexico. The experiment took advantage of the excellent out-of-field-of-view rejection characteristics of the sensor. The combined experiment obtained data of the earth's atmosphere as well as zodiacal data particularly at angles close to the sun.

Parallel efforts to develop computer codes which model the infrared radiance from the upper atmosphere have been under way for the past five years. The model incorporates photochemical and

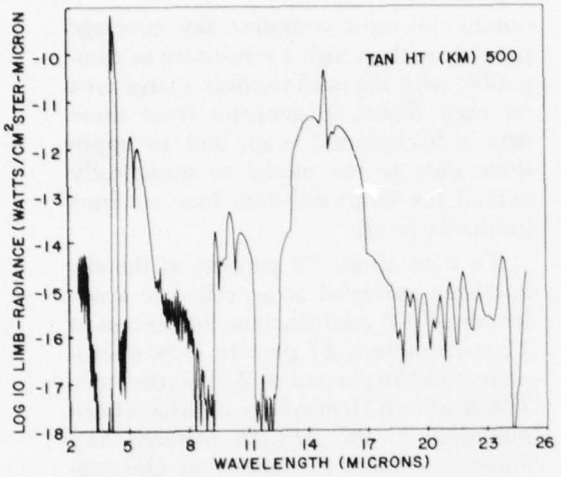

Infrared limb radiance from the high-altitude radiance model. Data refer to a 500-km tangent height.

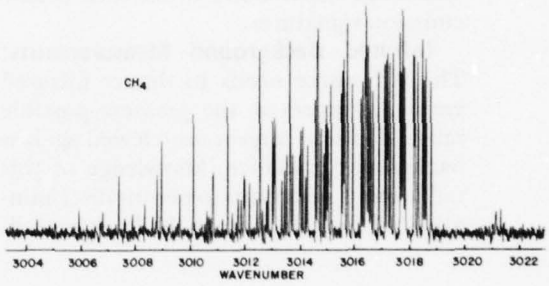

The absorption spectrum of methane measured in the laboratory with the 2-meter path difference interferometer. The spectral resolution is 0.006 wavenumber.

thermal emission mechanisms for the major infrared active molecular species. Radiance profiles can be generated in the 5 to 25 micrometer region up to 500 km altitude. The presently available model is an updated version of the results reported in AFCRL-TR-74-0606.

The zodiacal light represents the limiting background for observations made in deep space. The present program envisions experimental flights to provide the basis for a complete model of the zodiacal light. The cryogenic sensors for carrying out these measurements are being designed and constructed at AFGL.

Multiplex/High-Throughput Spectroscopy: Detailed knowledge of the spectral characteristics of background radiation and of atmospheric emission and absorption are required to design high sensitivity military sensors for optimum performance. Concurrently, research on techniques to enhance the sensitivity of sensors must be performed. Multiplex/high-throughput techniques can yield the required detailed spectral information and at the same time be used to develop more sensitive sensors.

Research on improved spectrometric techniques is being done in-house and contractually. In-house, a 2-meter path difference cat's eye interferometer, capable of yielding an apodized resolution of 0.005 wavenumber, was assembled and has yielded high-resolution spectra of methane, carbon dioxide, and water absorptance. These data will be used to update the transmission computer codes. Since the 2-meter interferometer has a built-in calibration consisting of a frequency-stabilized helium-neon laser, it yields high-confidence data. This instrument will also be used to determine the efficiency of background suppression techniques being pursued at AFGL based on a double-beaming technique in Fourier spectroscopy developed at AFGL.

An advanced state-of-the-art 0.1 wavenumber cryogenic cat's eye interferometer is being developed for stratospheric background emission studies. Once its performance is demonstrated by balloon-borne measurements, this instrument will serve as a prototype for use in systems and measurement programs requiring high-sensitivity, high-resolution performance.

A singly encoded Hadamard spectrometer capable of yielding a multiplex advantage of about 256 was assembled and tested. The unique feature of this

instrument is that it is the first Hadamard spectrometer employing an exit mask with curved slots, thereby increasing the throughput (when compared to a "straight slot" Hadamard spectrometer) nearly an order of magnitude. The curvature of the slots in the exit mask was calculated by incorporating the aberration properties of the optical components as well as the dispersive property of the grating.

Remote Sounding: The first meteorological satellites were designed to transmit cloud pictures. It was soon realized that the atmospheric emission in the thermal infrared region of the spectrum was related to the temperature of the atmosphere, so that remote passive temperature sensing was possible. This possibility follows from the relation between the atmospheric emission in the thermal infrared region of the spectrum and the vertical atmospheric temperature field. Vertical temperature inferencing became operational in 1970 with the orbiting of the Vertical Temperature Profile Radiometer (VTPR) sounder aboard a NASA-NOAA meteorological satellite. Similar data observed by the Defense Meteorological Satellite Program (DMSP) became generally available in 1974. Later versions of these vertical sounding systems also contain spectral channels intended to sound the vertical distribution of water vapor, a parameter of substantial interest to the Air Force.

Work in the Division has been concentrated in two areas: 1) The transmittance modeling described above has been applied to the development of new design concepts and data analysis schemes for the remote sounding of the vertical distributions of temperature and water vapor in the infrared and microwave regions of the spectrum. Modifications to existing infrared sensors have been proposed and constructed and these modified sensors will be flown on future Defense Meteorological Satellites. A study of water vapor and 15-micron carbon dioxide transmittances is under way to aid in the understanding and interpretation of discrepancies found in comparisons of satellite measured and computed atmospheric radiance distributions. 2) The ultimate utilization of the satellite measured radiances in the thermal infrared requires an inversion procedure, a mathematical device whereby either the vertical distribution of temperature (or water vapor) or the vertical distribution of the sources and sinks of radiation in the atmosphere are derived from a spectral scan of the upwelling radiance. This information is then fed into dynamical models of atmospheric motion as a key element of weather forecasting on various scales.

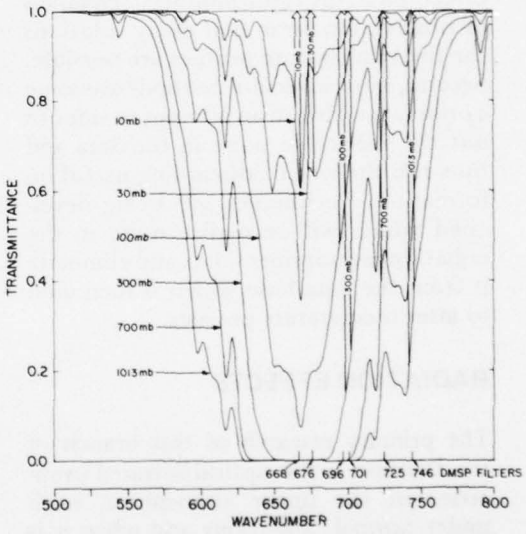

Satellite temperature sounding using the 15-micrometer band. Arrows indicate the approximate atmospheric levels from which the radiation at the frequencies of the DMSP channels is emitted to space.

Using such a spectral scan to determine the temperature (or moisture) at each level in the atmosphere has proved to be very difficult. All levels of the atmosphere contribute at each particular frequency, so that the radiance sensed by the satellite is a mixture of thermal information from all levels. Probing different frequen-

cies merely weights radiation according to height, depending on the transmittance of the atmosphere.

Mathematically, the radiation is expressible as an integral transform of the temperature-related Planck intensity summed over the atmosphere. Typically, the radiances are observed over six to eight different frequency channels. The vertical temperature distribution is then recoverable as an inverse transform of the radiance profile, hence, the name inversion given to this particular inference problem. The heart of the problem is that the vertical temperature distribution is deduced from intensity differences between neighboring frequency channels, a second order effect. First, the finite number of channels of observation mean that many solutions for the temperature profiles are possible. Second, most inversion methods use some *a priori* algorithm in an attempt to smooth out the inevitable noise in the data and thus run the risk of discarding useful information. Techniques are being developed which will recognize noise in the radiation measurement data and eliminate it from the data base which is then used to infer temperature profiles.

RADIATION EFFECTS

The primary research of this branch of the Division is the optical/infrared properties of the upper atmosphere, both under normal conditions and when it is disturbed by auroras or nuclear detonations. At the altitudes considered, thermal equilibrium usually does not exist, and it is necessary to consider the collisions or interactions of individual pairs or triads of molecules, one or more of which may be an excited state (that is, with excess internal energy). Extensive laboratory and theoretical studies, as well as rocket and aircraft measurements of upper atmospheric optical/infrared phenomena are carried out. The results of these laboratory studies and aircraft measurements also apply to missile or jet engine plume infrared radiation, which have also been measured. The goal of the research is to generate both directly measured data and also models and computer codes which permit the prediction of the optical/infrared emission of the upper atmosphere, particularly under disturbed conditions. Such data and codes are particularly applicable to surveillance and detection systems operating in space or near space.

Optical/Infrared Code (OPTIR): OPTIR is a computer code and modeling effort which describes the optical/infrared characteristics of natural and high energy sources in the atmosphere. The code is particularly designed to model nuclear detonations in the atmosphere and predict their effects on optical/infrared systems. Modular sub-elements of the OPTIR code have been adapted for specific radiation and energy deposition applications, such as low-altitude burst signatures (TACTIR), auroral deposition and radiative characteristics (OPTAUR), and observations by surveillance systems (SAMPLR).

A model for the production and decay of a condensation cloud following a low-altitude burst in a moist atmosphere has been developed and coupled with a model of the time-dependent radiative transport through the cloud. For radiative transmission in non-disturbed atmospheres the AFGL LOWTRAN 3 model has been included as an overlay in OPTIR. The atmospheric heave model has been expanded to incorporate the effects of ultraviolet radiation and has been coupled to the OPTIR code to permit the description of a second burst in the modified atmosphere following a first burst. The Jensen-Cain model of the geomagnetic field has been included in OPTIR which provides the capability of locating the debris conjugate regions of a high-altitude burst and the declination and inclination angles of the field.

The OPTIR capability has been used effectively in programs to determine nuclear effects on optical/infrared systems. The potential concerns to optical/infrared systems arising from nuclear bursts have been cataloged. Correlations of visible/infrared data obtained in Project ICECAP have been utilized in a determination of the time-space structural characteristics of auroral infrared radiation for optical/infrared systems.

Aircraft Program: The AFGL Flying Infrared Laboratory is an NKC-135 aircraft, modified to provide 55 viewing ports behind which selected radiometers, interferometer-spectrometers, and spatial mappers are operated as primary data collection systems. The aircraft measurement program has pioneered in the acquisition of infrared sky background emission levels against which current and future Air Force systems must operate.

The AFGL Optical/Infrared Flying Laboratory, an NKC-135 modified extensively for infrared research, provides access to environmental measurements over a wide variety of geographic and meteorological conditions.

The airborne program capitalizes on the cost-effective world-wide deployment capability of the reliable jet tanker, and provides the infrared research scientist a laboratory environment above most obscuring clouds and absorbing atmospheric constituents. Geographic and seasonal variations in specific phenomena can be readily studied from this platform. These activities are closely coordinated with rocket probe and balloon-borne measurements, and are planned to test specific theoretical modeling based on laboratory simulation results.

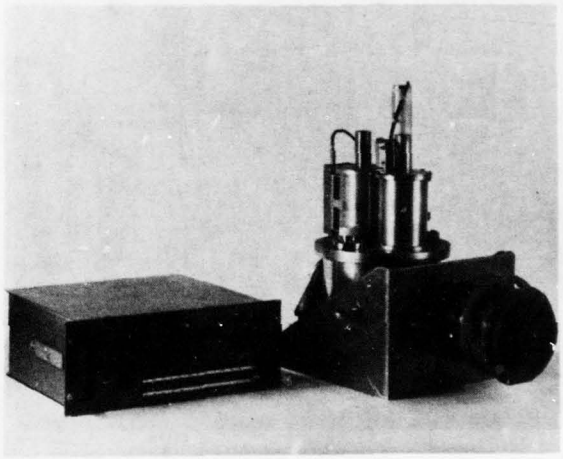

AFGL prototype Michelson interferometer operated at liquid nitrogen temperatures designed for aircraft deployment. This instrument is now capable of producing infrared spectra with one wavenumber resolution.

The instrumentation is developed to be interchangeable between the airborne laboratory and close-in ground stations to insure the quality and reliability of each measurement. An extensive controlled calibration and coordinated data reduction effort continuously monitors each instrument's performance and enhances data analysis. Both absolute measured irradiance and absolute source radiance spectral data plots of field measurements are provided; absolute infrared spatial data isoradiance arrays are available to assist in the analysis effort.

An extensive data base of atmospheric transmission and infrared background measurements has resulted from the target/background missions on which the

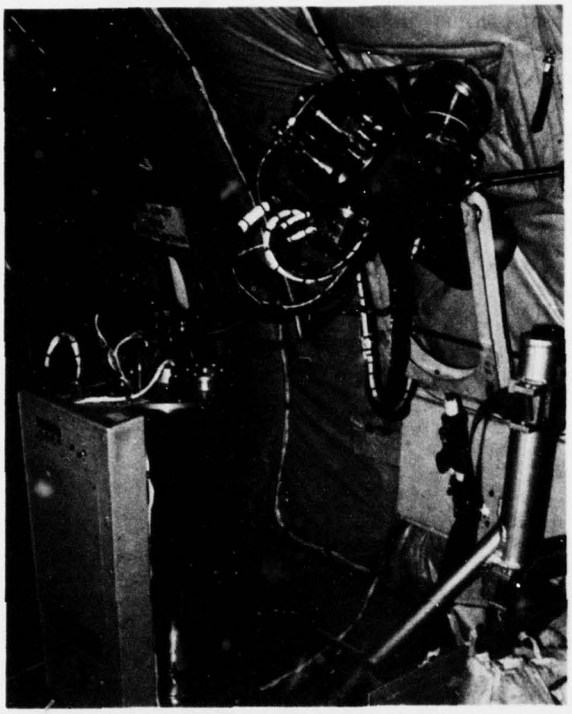

Flight test configuration of prototype interferometer installed on the Infrared/Optical Flying Laboratory to measure the upper atmosphere emissions through a liquid nitrogen-cooled window.

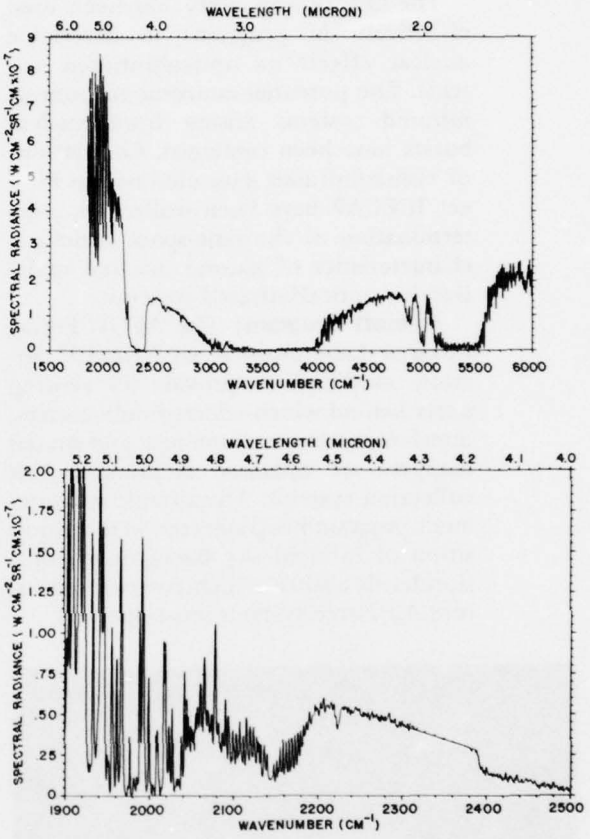

Indicative of the difference in background measurements is this daytime comparison of the desert spectra observed between 1.7 and 5.5 micrometers (resolution 4 wavenumbers) from 29,000 feet altitude at a 45-degree depression angle and the clear sky spectra observed between 4.0 and 5.3 micrometers (resolution 1 wavenumber) from 15,000 feet altitude at an 8-degree elevation angle.

interferometer-spectrometers were used. The variety of instruments and information display techniques allows maximum utilization of the data from each mission. Airborne measurements of atmospheric spectral transmission are an integral part of each measurement profile and provide the data for the AFGL LOWTRAN-3 and HITRAN transmission/emission codes to predict the infrared signature as viewed from a more complicated geometry or from space. This is accomplished with the Type V interferometer-spectrometer measurements which have a resolution of 1 wavenumber over the spectral range 2-5.5 micrometers. The specific source or background of interest, as viewed through the intervening atmosphere, is monitored at selected infrared wavelengths by the several spatial mappers, and when correlated with the visible aiming camera record, becomes the basis for spatial "footprint" analysis. However, the experimenter determines the selection of the wavelengths to be covered, the sensitivities required, the specific instruments and modifications thereto, and the mission profile best suited to acquire the data.

The aircraft missions obtain data necessary to Air Force and DOD evaluation and development programs. A typical result from this field data is taken from the March 1975 airborne participation in the ICECAP auroral measurements. Flying at 35,000 feet, the flying laboratory carried three radiometers to monitor the intensity of the 0.39-micrometer N_2^+ first negative band, the 1.70-micrometer OH Meinel band, and the 2.83-micrometer combined radiation from the NO fundamental vibration-rotation bands, OH Meinel band and water vapor thermal emission. These measurements were made possible by use of the unique cryogenic-cooled optical chopper operated external to the aircraft skin – the same system which obtained the first zenith mid-SWIR atmospheric emission spectra reported in 1974 in *Applied Optics* and the last *Report on Research.* Correlative enhance-

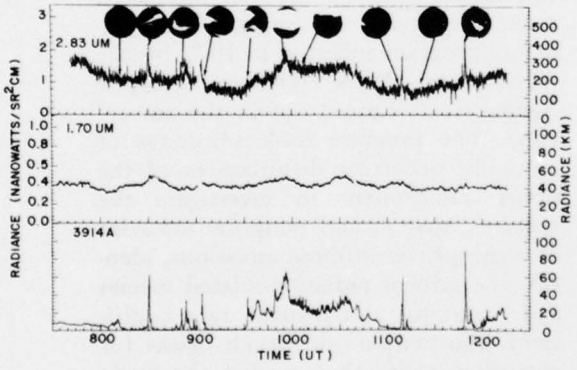

Measurements made on March 10, 1975 from 35,000 feet over Alaska of night aurora zenith emissions. First overtone of OH compared with fundamental OH and NO, and N_2^+ first negative band during auroral activity recorded in all-sky camera sequence – Flying Infrared Laboratory ICECAP data.

ments between 0.39-micrometer and 2.83-micrometer signals were observed during bright visible auroral activity in the winter zenith sky over Alaska, while the 1.70-micrometer measurement indicated that the OH radiation remained quiescent. The observations have been interpreted as the first measurement from an aircraft of vibrationally excited NO molecules in the aurorally enhanced upper atmosphere. The whole story of auroral infrared chemistry and the resulting infrared signatures is being pursued by continuing coordinated measurements.

Prototype cryogenic interferometer/radiometer development continues toward the next generation of fully cold systems viewing through frost-free windows cooled to liquid nitrogen temperatures. Software development for data reduction and handling has progressed significantly. A great deal of emphasis is being placed on this important and demanding task. Each of the basic measurement tools (interferometric spectrometers, multi-channel radiometers and spatially scanning radiometers) requires unique analysis tools and techniques for proper data reduction and analysis. For the interferometers, a very high resolution Fourier Analyzer is necessary, and a specially modified commercial system is used. With this tool, special software and hardware have been created in-house for data previewing, co-adding, Fourier analysis, calibration, digital recording display and plotting. For spatial radiometric analysis, a special purpose minicomputer system has been acquired capable of interfacing to a high-resolution intensity-modulation display and CRT-graphic display system. With the in-house software programs and procedures being developed, a capability is being achieved to produce spatial images yielding quantitative spatial infrared intensity distribution. The goal of the data analysis effort is to turn the measurements made from the aircraft into meaningful data that directly satisfy Air Force mission requirements.

ICECAP: On April 1, 1976 the first altitude profile of emission spectra of atmospheric species O_3 (9.6 micrometers), CO_2 (15 and 4.3 micrometers)

and NO (5.6 micrometers) at 2 wavenumber resolution were obtained from a rocketborne cryogenic HIgh-Resolution Interferometer-Spectrometer (HIRIS) experiment. The Sergeant rocket, launched at Poker Flat, Alaska, carried the 900-pound payload to an apogee of 126 km. The payload penetrated an aurora on rocket ascent and descent that had been predosed by intense auroral breakup minutes before. A total of 150 spectral scans were obtained between cover opening at 88 km on upleg and closing at 62 km on the downleg. The instrument was parachuted to earth and successfully recovered in excellent condition.

The HIRIS instrument is a Michelson interferometer which scans the spectral region from 455 to 2500 wavenumbers (4 to 22 micrometers) and produces a double-sided interferogram every 1.36 seconds. The interferometer consists of a base, slide assembly, fixed and moving mirrors, all made of hardened A-2 steel for homogeneous thermal response. The entire optical system including detector, collecting optics, interferometer cube and baffles is operated at approximately 10 degrees K through cooling with supercritical helium. This method of operation provides conditions of low background radiation for the arsenic doped silicon detector. The reduced flight spectra show the instrument yielded better than the expected 2 wavenumber resolution.

At approximately 90 km, after vehicle/payload separation, clamshell nosecone ejection and cover opening, the payload went into a pitch maneuver resulting in an instrument field-of-view which scanned vertically, through the earth limb and down at the earth at a rate of 10.5 degrees per second. The payload made six complete revolutions during the 150 spatial scans obtained. During each revolution, approximately 12 spectra above the horizon, two spectra of the earth limb and 12 spectra of the earth itself were taken. These data are being reduced and

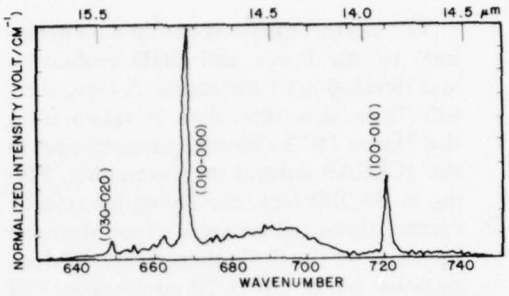

Vertical viewing high resolution spectrum of carbon dioxide bands at 76 km during the downleg trajectory of the HIRIS rocket flight.

analysis will yield significant new results. With the launch of the HIRIS rocket in April 1976, the field measurements portion of ICECAP (Infrared Chemistry Experiments for the Coordinated Auroral Program) was brought to a successful conclusion. ICECAP was an integrated rocket, aircraft, and ground measurements program initiated in 1972 by the AFGL and DNA (Defense Nuclear Agency) and carried out in the auroral zone. The program took advantage of naturally occurring disturbances of the upper atmosphere to investigate the spectral, spatial, and temporal behavior of atmospheric infrared emissions, identify the critical radiation-related species and reactions, and provide rate coefficient information and bench marks for computer codes that predict the background radiances. These studies, utilizing the extraordinary data base achieved by the experimental investigations, will continue for several years although new, immediately useful and significant results have already been published. The development of state-of-the-art sensitive cryogenic (nitrogen and helium cooled) spectral instruments for ground, aircraft and particularly rocket-borne investigations of the upper atmosphere was a particularly important facet of this program.

A total of 24 rockets were launched in the years 1972 through 1976. Some of these made cryogenic radiometric measurements of infrared bands and were fired in predetermined sequence for auroral dynamic and night/day studies using small single- or two-stage rockets. Other rockets were launched with cryogenic spectrometers for first-of-a-kind measurements of auroral infrared emissions. Finally, there were four rockets that were launched in successive years that carried multiple experimental payloads for the simultaneous measurement of the energy spectra of the bombarding auroral particles, the composition, ionization, temperature and electric fields of the disturbed medium, and the visible and infrared emissions. Up to 25 separate experiments were flown on these large multi-staged rockets with supporting ground optical and radar measurements. These data establish the bench marks for the auroral and nuclear computer codes such as OPTIR and ARTIC. In addition the AFGL Flying Infrared Laboratory flew many supporting and independent missions in this program. A special series of reports called HAES (High Altitude Effects Simulation) Reports has been instituted to provide a mechanism for dissemination of the tremendous amount of data accumulated, and over 100 reports have been published to date.

Significant progress has been made in the understanding and modeling of the upper atmospheric infrared emissions. Calculations of the CO_2 15-micrometer radiance from sea level to 150 km are in reasonable agreement with the measurements. The same high altitude radiance model, however, predicts the 9.6-micrometer ozone radiation to be about a factor of 5 less than the observations from 70 to 100 km. It is not known whether the accepted ozone concentrations are too low or whether the model is in error. There is less confidence in the O_3 mixing ratios than for CO_2. As reported previously, this program obtained the first auroral enhancements of 2.8 and 5.3-micrometer emission from nitric oxide, and 4.3-micrometer emission from carbon dioxide.

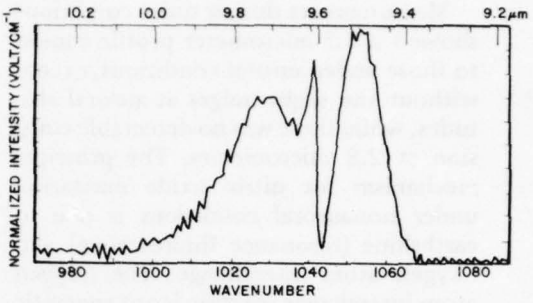

Vertical viewing high resolution spectrum of ozone at 9.6 micrometers at 76 km during the downleg trajectory of the HIRIS rocket flight.

Analysis indicates that the observed temporal and spatial behavior of the 4.3-micrometer auroral radiation can be explained by a mechanism involving vibrational excitation of nitrogen by direct electron impact, followed by a collisional resonance vibrational transfer to excite carbon dioxide, followed by emission by the carbon dioxide at 4.3 micrometers. This mechanism is complicated by repeated transfers of the vibrational energy back and forth between nitrogen and carbon dioxide, and by repeated absorption and emission by the carbon dioxide, which is optically thick enough below 90 km to ensure that the 4.3-micrometer radiation will be absorbed and re-emitted many times as it escapes from the atmosphere. The data requires from 3 up to 18 vibrational quanta or excited nitrogen molecules produced per ionization event. Another significant result caused by the absorption and re-emission of all of the radiation is that the time response for the auroral 4.3-micrometer emission is of the order of 5 to 10 minutes after the electron deposition.

Measurements during quiet conditions showed a 5.3-micrometer profile similar to those under auroral conditions, except without the slight bulges at auroral altitudes, while there was no detectable emission at 2.8 micrometers. The principal mechanism for nitric oxide excitation under nonauroral conditions is due to earthshine (resonance fluorescence) and oxygen atom interchange. The oxygen atom interchange reaction is not energetic enough to excite vibrational levels above the first, and at the collision-limited densities above 100 km, most of the ambient nitric oxide is in the ground state; consequently, both mechanisms raise nonexcited nitric oxide only to the first vibrational level. Consequently, there is a high altitude emission layer of 5.3-micrometer radiation which peaks at about 130-140 km. Russian observers in a limb viewing mode aboard Salyut 4 recently reported observing these emissions at higher altitudes (150-200 km).

Aurora produces nitric oxide which is excited to high vibrational levels and thus results in overtone emission at 2.8 micrometers as well as 5.3-micrometer radiation. This is because the nitric oxide excitation occurs during the formation process when nitrogen atoms (produced primarily by ion recombination) react with oxygen molecules and the reactions have excess energy (exothermic). A portion of this excess energy is used in forming NO at high vibrational levels. This molecular emission is referred to as a chemiluminescent reaction. Thus, auroral emissions at 2.8 micrometers are a direct way to observe the formation of NO.

Laboratory Cold Infrared Chemiluminescent Experiments: The laboratory has built and is now operating a new unique facility to study, in a controlled laboratory environment, specific chemical interactions which are important sources of atmospheric infrared radiation that could compromise the performance of defense systems. Prediction and assessment of background radiance perturbations resulting from natural and artificial disturbances requires a determination of the efficiency with which reactions produce excited molecules and the magnitudes of processes which allow radiation of the excitation energy and its redistribution or degradation. The long radiative lifetimes of vibrational infrared transitions make it necessary to operate experimentally at pressures low enough to simulate upper atmospheric densities and still not suffer the penalty of spurious laboratory effects such as wall collisions.

These conditions have been achieved uniquely by the new facility, called COCHISE (COld CHemiexcited Infrared Simulation Experiments). The entire experiment is conducted inside a cavity held at 20 degrees K by a closed-cycle helium gas refrigeration system. Part of the refrigeration capacity is also used to provide a cryopumping capability within a closely temperature-controlled reaction chamber inside the 20 degrees K cavity which serves effectively as a wall-less reaction volume within which chemical interac-

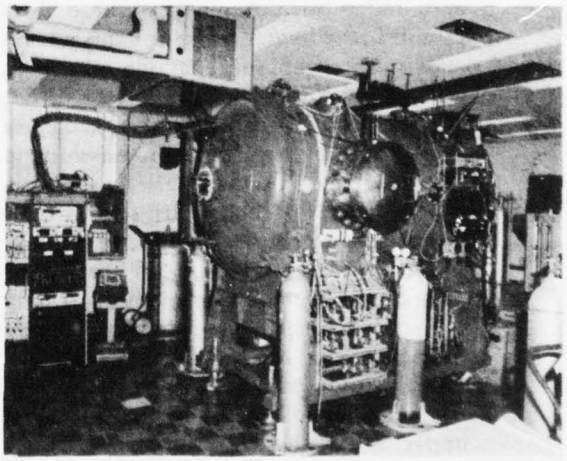

A general view of the COCHISE facility showing the main vacuum chamber in foreground. The control electronics at the left and a portion of the closed cycle helium refrigerator in the background to the right.

tions are initiated. An infrared scanning monochromator stationed behind a window in another portion of the 20 degrees K environment observes the resulting radiation. Since the effects of thermal background radiations on the infrared instrument have been completely eliminated in this way, upwards of five orders of magnitude improvement in detectivity over room temperature operation have been achieved, and are required to observe the low radiation density in the millitorr pressure range reaction cell.

In initial applications, chemistry has been initiated by mixing the products of a microwave discharge with unactivated target gases; with contact times of a few milliseconds the radiation observed is representative of the initial undisturbed product molecule vibrational distribution. Further development is under way to add ultraviolet and tunable laser diagnostics for ionic and non-radiating species which will allow the laboratory to make a unified approach to problems requiring detailed study. Upon completion of the present analysis task the facility will be used to provide a complete account of the infrared radiation emitted by vibrationally excited ozone molecules formed in oxygen atom recombination.

Infrared Radiation from Air Excited by Electron Deposition: Electron excitation and subsequent energy transfer processes by atmospheric species occur in the upper atmosphere either naturally as in the aurora or following a high altitude nuclear event. Detailed information of these exchange processes, which control the radiative state of the atmosphere, are obtained using our laboratory simulation facilities and measuring the visible and infrared emission produced by energetic electron irradiation of atmospheric gases. Excitation is accomplished by electrically pulsing an electron beam of 0-5 milliamp over a 500 to 50,000 volt range into a target chamber containing atmospheric gas mixtures at pressures of 1/10,000 to 1 atmosphere.

Recent experiments have concentrated on determining the dynamic behavior of excited gases by observing the evolutionary history of the radiation produced during and after electron impact. The measurement technique of Fourier Time Resolved Spectroscopy is used to obtain the time dependence of the infrared emissions. This technique, developed at AFGL, is based on time gating the signal of a Michelson interferometer-spectrometer at corresponding sampling positions of the interferometer stroke to obtain a series of time sequenced interferograms. Fourier transformation of the series of interferograms gives the entire infrared radiation evolution of the excited gas.

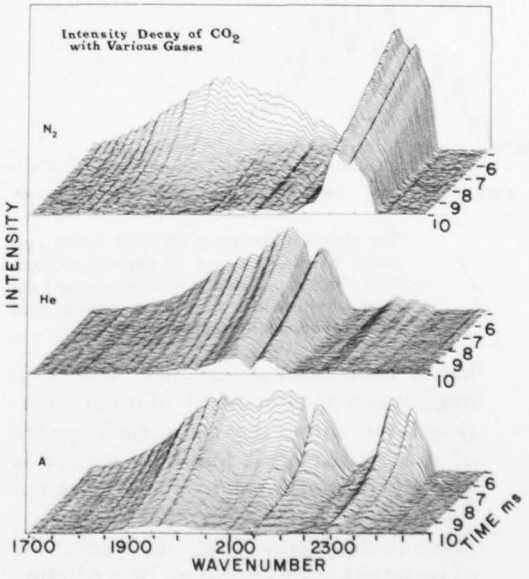

Decay of the infrared emission from carbon dioxide in 100-microsecond intervals following the removal of the electron excitation. The three curves show the differences in the decay in (top to bottom) nitrogen, helium, and argon. Each spectrum has been degraded from the 2-wavenumber resolution achieved in the experiment to 20 wavenumbers, since the detailed spectra would be overlapped and indistinguishable in this type of figure.

Typically the radiation to be observed is weak; hence, the throughput and multiplex advantages of Fourier interferometry are essential to perform the required spectral measurements. The capability of our time resolved technique has been improved so that the spectral region of 1-6 micrometers with 2-wavenumber resolution can be obtained simultaneously in time increments of 10 microseconds.

Earlier measurements of the time-dependent emission of the nitric oxide fundamental bands produced by irradiating mixtures of nitrogen and oxygen gave the composite quenching rate of excited nitric oxide by oxygen and nitrogen. With our increased resolution, the detailed quenching rates of each individual vibrational state comprising the fundamental

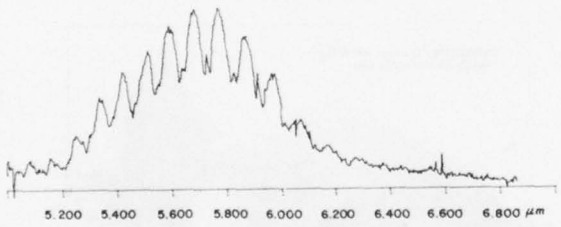

The emission spectrum of nitric oxide produced by the reaction of excited nitrogen with oxygen to form atomic oxygen and excited nitric oxide. A spectral resolution of 0.013 micrometer was achieved.

bands have been determined. Direct simultaneous measurement of each vibrational level shows that the quenching rate of the excited nitric oxide by oxygen is directly proportional to the vibrational state up to level seven. The results of these findings concerning the quenching of nitric oxide are important in predicting the intensity and behavior of the nitric oxide infrared signature in the natural and disturbed atmosphere.

In a related effort, the production of excited oxygen which gives rise to emission at 1.91 micrometers has been observed to be much stronger than predicted. The radiation from this particular state of oxygen is an allowed quadrupole transition which is orders of magnitude smaller than either allowed electric or magnetic dipole radiation. Measurements of this emission showed that at higher oxygen pressures, the excited states of oxygen are perturbed by forming a complex molecule having relaxed selection rules or alternately, the selection rules are relaxed through collision. As a result, the radiation is increased substantially—more in a nitrogen environment than in pure oxygen. The degree of enhancement over

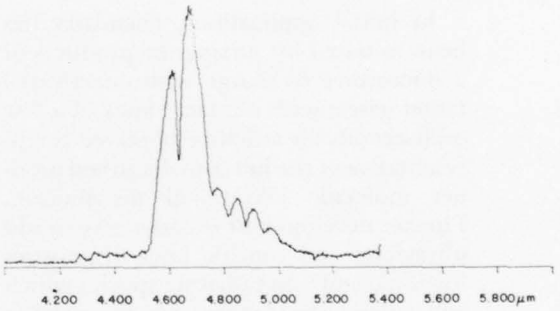

The emission spectrum of carbon monoxide, excited by collisions with vibrationally hot nitrogen. A spectral resolution of 0.013 micrometer was achieved.

the pure quadrupole emission was determined by referring the emission at 1.91 micrometers to the infrared atmospheric bands of oxygen which have their upper excited state in common with that of the 1.91 micrometer emission. Over a pressure range of 0.001 to 300 torr, the enhanced radiation follows the pattern of radiation from two molecules colliding. The rate constant for enhancement in nitrogen has been determined. This type of information is of basic importance to the understanding of molecule-molecule clustering which is now known to be of significance in the D region of the atmosphere.

Preliminary infrared measurements have been performed on carbon dioxide and various gas mixtures subjected to electron bombardment. First observations show that the dominant spectral feature is

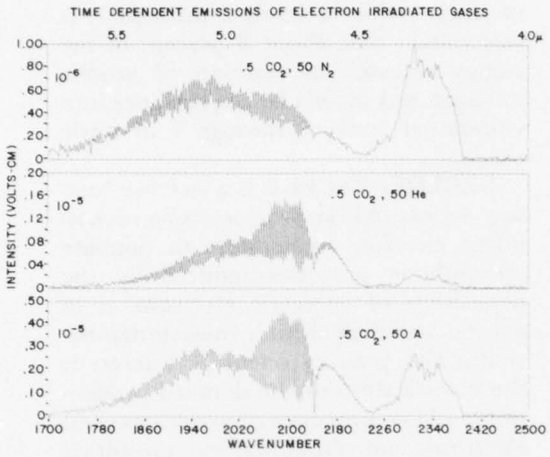

The infrared emission spectra of electron irradiated carbon dioxide gas mixtures at 2-wavenumber resolution, showing the high degree of vibrational excitation of carbon monoxide which results from the subsequent chemical kinetic processes.

that of carbon monoxide which exhibits excitation of the 17th vibrational level. Several infrared atmospheric research problems needing further investigation have been revealed in this preliminary survey and appear to be within the measurement capabilities of our present apparatus. These types of data will allow questions concerning electron-ion recombination rates, vibrational energy exchange rates with various atmospheric species, and vibrational population distributions via specific production processes to be investigated.

To study the IR emission at longer wavelengths (5-25 micrometers) and lower pressures, simulation is accomplished using a large tank, 4½ feet in diameter and 15 feet in length. At these wavelengths, the emission by the room surroundings is larger than that produced by electron excitation of the experimental gases. To overcome this thermal background, the entire internal surface of the tank, transfer optics and IR instrumentation are cooled to liquid nitrogen temperatures. With this added temperature control, the sensitivity of the measurements are effectively increased by one thousand or more and measurements which were previously impossible are now possible.

Molecular Beam Studies: The molecular beam facility is employed to investigate the high velocity collisions occurring at high altitudes (above 300 km) between plume and atmospheric gaseous species. The beam system utilizes isentropic expansion of a gaseous mixture from a heated (approximately 1500 degrees K) supersonic nozzle for beam formation, a time of flight molecular beam detector, a gold-plated chamber where target plume species interact with the beam particles, and an infrared detection system. Beam intensities of 5×10^{18} particles per steradian per second have been achieved with velocities ranging from 1 km/second to 4 km/second. The target species can also be introduced in the form of another counter-flowing molecular beam to achieve higher interaction velocities in the relative coordinate system. The interactions studied so far under varying experimental parameters are excitation of carbon dioxide and first vibrational level of carbon monoxide under impact with high-velocity molecular oxygen, molecular nitrogen and argon beams. No discernible emissions from these plume species have been observed indicating very small cross sections for excitation. Analysis has shown that background photon fluctuations from the room temperature collision chamber are much higher than signals sought. The program will be continued in a liquid nitrogen-cooled collision chamber which is expected to reduce background noise to tolerable levels, and make the measurement of these small cross sections achievable. In this reporting period, vibration-rotation spectra of the second vibrational sequence of the nitric oxide formed in the chemiluminescent reaction of atomic with molecular oxygen yielding

AD-A067 252 AIR FORCE GEOPHYSICS LAB HANSCOM AFB MASS F/G 14/2
REPORT ON RESEARCH AT AFGL JULY 1974-JUNE 1976.(U)
JUN 77 J F DEMPSEY
UNCLASSIFIED AFGL-TR-77-0137 NL

3 OF 3
AD A
067252

END
DATE
FILMED
6-79
DDC

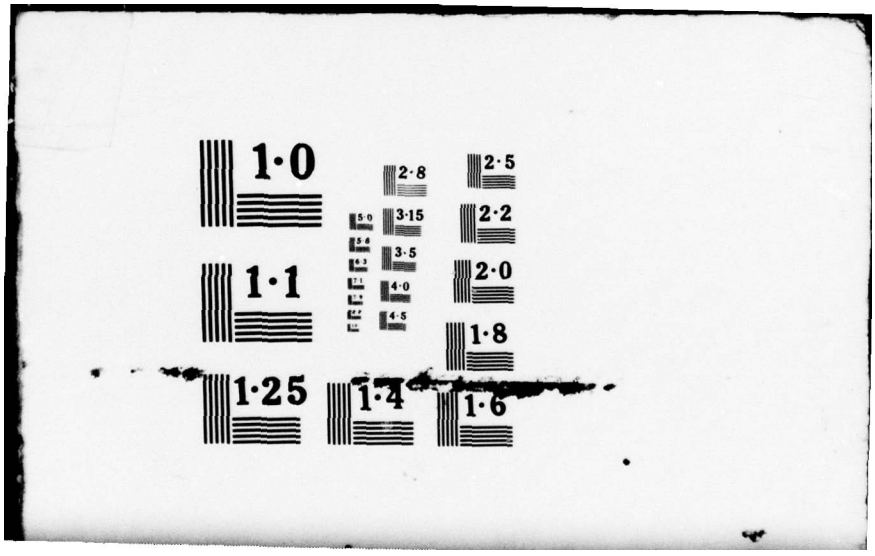
1·0
1·1
1·25
1·4
1·6
1·8
2·0
2·2
2·5
2·8
3·15
3·5
4·0
4·5

excited nitric oxide and atomic oxygen were resolved through the use of an interferometer-spectrometer with a spectral resolution of approximately 15 wavenumbers. The steady-state emission spectra showed features due to molecular species other than nitric oxide which emitted in the spectral region of the first overtone of nitric oxide. It was shown experimentally that the source of these spectral contaminations is the nitrogen dioxide molecule which is probably formed chemically in the reaction cell, undergoing vibrational exchange with excited nitrogen molecules flowing from the microwave discharge source. Infrared signals due to nitrogen dioxide were eliminated by quenching of the excited nitrogen molecules before entry into

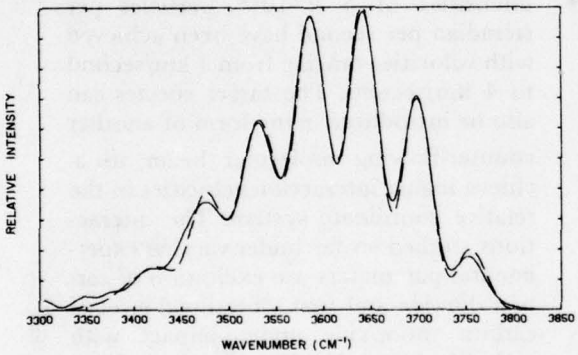

The nitric oxide overtone band from the reaction in which excited atomic nitrogen reacts with molecular oxygen to produce vibrationally excited nitric oxide and atomic oxygen. The solid curve is the experimental result and the dashed curve is the best theoretical fit to the experiment.

the reaction chamber. First overtone bands of nitric oxide were then obtained over the oxygen pressure range of 200 to 600 millitorr. The resulting spectra which showed emission from nitric oxide in the second through seventh vibrational levels were matched to numerically generated nitric oxide spectra. Steady-state number densities for nitric oxide in these levels were obtained and were used to derive partial rate constants for formation of nitric oxide in levels 2 through 7. It was shown that about 8 percent of the energy released in reaction of atomic nitrogen and molecular oxygen goes into vibrational levels 2 through 7 of nitric oxide.

EXCEDE: EXCEDE is a Defense Nuclear Agency/AFGL program using rocket-borne electron accelerators to simulate atmospheric processes induced by the deposition of energetic electrons as in auroras and high altitude nuclear detonations. The primary scientific interest is the investigation of the detailed production and loss processes of various excited electronic and vibrational states resulting in optical and infrared emission as energetic primary electrons and their secondary and all subsequent generation electrons are stopped in the atmosphere. The EXCEDE experiment uses pulsed rocket-borne electron accelerators with well defined excitation conditions of electron energy and power, deposition volume, deposition altitude and dosing duration to provide measurements of time-dependent optical and infrared emissions which are interpreted in terms of chemical processes, reaction rates and photon yields. These data are utilized in various computer codes such as OPTIR and ROSCOE to calculate optical/infrared backgrounds for auroral and nuclear disturbed atmospheres. The codes assess the effects of enhanced atmospheric backgrounds on optical and infrared systems.

The initial rocket in the EXCEDE program, launched October 17, 1974, from White Sands Missile Range, was designated PRECEDE and carried a 2 kW (2.5 kV, 0.8 amp) electron accelerator. The electron source, square wave modulated at 0.5 Hz, was initiated at 95 km on payload ascent and continued through apogee (120 km) to a descent altitude of approximately 80 km, operating for an interval of 180 seconds. On-board measurements included monitors of electron beam volt-

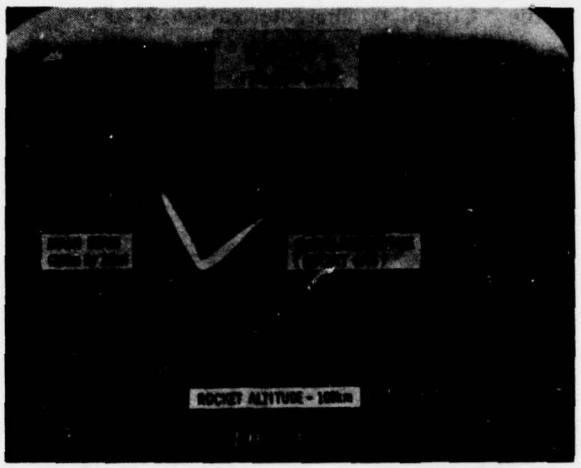

Low light television image of the optical radiation induced in the night atmosphere by the EXCEDE rocket-borne electron accelerator. The camera was located on a radar-controlled ground-based tracking mount and integrated several seconds of observation to produce this image.

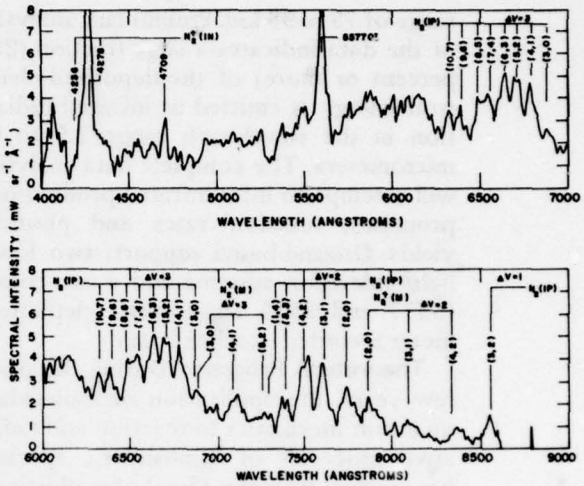

Spectra of the atmospheric emissions induced by the EXCEDE rocket-borne electron accelerator recorded by a ground-based image intensified spectrograph.

age and current and a retarding potential analyzer to determine particle flux and vehicle potential. Ground-based optical systems using radar-controlled tracking mounts provided photometric and spectrographic measurements and photographic and television images of the electron-induced atmospheric emissions. The initial launch confirmed pre-flight estimates of low vehicle potentials (less than 120 volts positive) for an electron-emitting payload in this altitude range and provided excellent data on the altitude dependent radiance of numerous optical and near infrared emissions including the N_2^+ first negative and Meinel systems, N_2 first positive system and $O(^1S)$ emission. These data have been analyzed in terms of production and loss processes including the effects of collisional deactivation. In two subsequent rocket launches (EXCEDE II Test and EXCEDE: SWIR) rocket-based instrumentation was increased substantially and included cryogenic infrared radiometers, photometers and a positive ion mass spectrometer.

The EXCEDE: SWIR rocket-borne electron accelerator experiment was launched from Poker Flat, Alaska, on February 28, 1976 into a quiet night atmosphere. A Sergeant rocket engine carried the 32-inch diameter, 1700-pound payload to an apogee of 99 km providing a total experiment time of approximately 100 seconds. Atmospheric emissions induced by the pulsed electron beam were readily recorded by rocket-based photometers and liquid nitrogen-cooled radiometers as well as by ground-based television and telephotometer instruments. Payload instrumentation functioned as designed including the 3 kW electron accelerator, 22 photometers, 10 liquid nitrogen-cooled radiometer data channels and a positive ion mass spectrometer. Emissions of nitric oxide at 2.7 and 5.4 micrometers and NO^+ at 2.2 and 4.3 micrometers were measured as well as a number of visible emissions considered important precursor species to the infrared chemiluminescent mechanisms. Data were obtained over the altitude

range of 75 to 98 km. Preliminary analysis of the data indicates a large fraction (25 percent or more) of the deposited electron energy is emitted as infrared radiation in the wavelength range 2.5 to 6 micrometers. The complete data analysis will attempt to infer infrared production processes, reaction rates and photon yields. Ground-based support, two low-light television systems and a two-color (5577 and 3914 angstroms) telephotometer recorded excellent data.

Theoretical Program: During the past few years, the application of molecular quantum mechanics to reaction and radiative processes of atmospheric species has reached its highest level of sophistication and accuracy. *Ab initio* molecular calculations are now capable of producing highly accurate wavefunctions, potential energy surfaces and other associated properties of small molecules. This new state-of-the-art technology in computational quantum mechanics has found widespread application to atmospheric processes, where a limited data base of important parameters characterizing chemical reactions and absorption and emission of radiation has been a severe handicap to the successful interpretation of both field and laboratory-simulated atmospheric data and also to the development of accurate atmospheric models.

Recently, the major emphasis of the molecular computational effort at AFGL has been concentrated on accurate calculation of the absolute transition probabilities and line positions of infrared vibration-rotation intensities for selected diatomic molecules. During this reporting period, a very accurate theoretical treatment of the high vibration-rotation transitions in the ground state of nitric oxide has been accomplished. The overtone transitions of this molecule occur around 2.8 micrometers and have been observed in auroras resulting from the chemiluminescent reaction of excited nitrogen atoms with ground state oxygen molecules. Complete characterization of the radiation levels resulting from this reaction requires the absolute intensities of the entire vibration-rotation manifold and these were unavailable from experiments for the higher vibration levels.

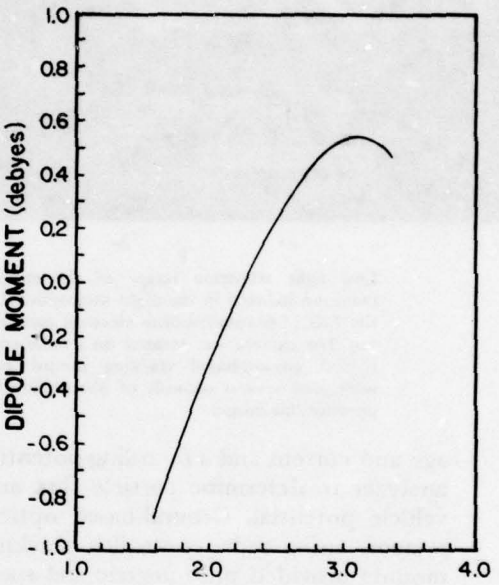

Calculated Electronic Dipole Moment Function of nitric oxide spanning inter-nuclear separations consistent with vibration levels up to the twenty-fifth.

Theoretically, the calculation of these quantities requires an accurate electronic dipole moment function and accurate vibration-rotation wavefunctions. The electronic dipole moment function for nitric oxide was obtained from a multi-configuration self-consistent field analysis. During the calculations, a completely new set of electronic configurations relating to the united atom limit of diatomic molecules was found to be absolutely essential for an accurate representation of the dipole moment function. A complete theory of the vibration-rotation

interaction in nitric oxide was then developed and calculation of the individual multiplet-rotation-vibration line positions and intensities obtained taking full and accurate account of spin-orbit coupling, vibration-rotation coupling and spin uncoupling. The analysis spans vibration states up to the 25th and total angular momentum states up to the 36th rotation state for each vibrational state.

In addition to this large computational effort on nitric oxide, methodology and computational tools for obtaining semi-quantitative wavefunctions and properties for triatomic and larger molecules have been developed. The major problem in such calculations has been the evaluation of the many multi-center integrals which arise when more than two atoms are considered in a system. During the past year, a method and the associated computational software has been implemented at AFGL which reduces the time associated with obtaining polyatomic wavefunctions by over two orders of magnitude. This capability now allows systems which were previously out of the reach of computational quantum mechanics to be treated at a reasonable level of accuracy and economy.

JOURNAL ARTICLES
JULY 1974 - JUNE 1976

BILLINGSLEY, F. P., II
Multiconfiguration Self-Consistent-Field Calculation of the Dipole Moment Function and Potential Curve of NO ($X^2\pi$)
J. of Chem. Phys., Vol. 62 (1975)
Improved MCSCF Dipole Moment Function for NO ($X^2\pi$)
J. of Chem. Phys., Vol. 63 (1 September 1975)
Calculated Vibration-Rotation Intensities for NO ($X^2\pi$)
J. of Mol. Spectros., Vol. 61 (1976)

CHUNG, S. (Univ. of Wis.), and LEE, E. T. P.
Dissociation of the Hydrogen Molecule by Electron Collision
J. of Chem. Phys., Vol. 12, No. 4 (October 1975)

ELTERMAN, L.
Aerosol Measurements Since 1973 for Normal and Volcanic Stratospheres
Appl. Opt., Vol. 16 (1976)
Stratospheric Aerosol Parameters for the Fuego Volcanic Incursion
Appl. Opt., Vol. 14 (June 1975)

FAIRBAIRN, A. R., WOLNIK, S. J., and BERTHEL, R. O.
Oscillator Strengths in the TiO Alpha-Band System
The Astrophys. J., Vol. 193 (Pt. 1) (1 October 1974)

FENN, R. W.
Optical Properties of Aerosols
Chap. 4, Hdbk. on Aerosols, R. Dennis, Ed., Tech. Inf. Ctr., Off. of Public Affairs, U. S. Energy Res. & Dev. Admin. (1976)

FENN, R. W., and MIRANDA, H. A. JR. (Epsilon Labs., Bedford, Mass.)
Stratospheric Aerosol Sizes
Geophys. Res. Ltrs., Vol. 1, No. 5 (September 1974)

FETTERMAN, H. R. (MIT Lincoln Lab., Lexington, Mass.), SCHLOSSBERG, H. R., and BARCH, W. E. (MIT Lincoln Lab., Lexington, Mass.)
Optically Pumped 15.90 μm SF_6 Laser
Appl. Phys. Ltrs., Vol. 26 (March 1975)

GREEN, A. E. S. (Univ. of Fla.), SAWADA, T. (Univ. of Osaka, Japan), and SHETTLE, E. P.
The Middle Ultraviolet Reaching the Ground
Sec. 2.2.1 in The Impact of Climatic Changes on the Biosphere - CIAP Mono. 5, U. S. Dept. of Trnsp., Climatic Impact Assessment Prgm., Rpt. No. DOT-TST-75-55 (September 1975)

HUNT, G. R., SALISBURY, J. W., and LENHOFF, C. J.
Visible and Near Infrared Spectra of Minerals and Rocks: IX. Basic and Ultrabasic Igneous Rocks
Modern Geol., Vol. 5 (1974)

KELLEY, P. L. (MIT Lincoln Lab., Lexington, Mass.), FENN, R. W., MC CLATCHEY, R. A., LONG, R. K. (Ohio State Univ.), and SNELSON, A. (IIT Res. Inst., Chicago, Ill.)
Linear Absorption and Scattering in the Atmosphere
J. of Def. Res. Strat. Warfare (May 1975)

KELLEY, P. L., KILDAL, H. (MIT Lincoln Lab., Lexington, Mass.), and SCHLOSSBERG, H. R.
Highly Selective Excitation of Atoms and Molecules Using Two Photon Processes
Chem. Phys. Ltrs., Vol. 27 (1974)

LOEWENSTEIN, E. V., and SMITH, D. R.
Ltr. to Ed., *Far Infrared Thin Film Beamsplitters: Calculated Properties*
Appl. Opt., Vol. 14 (1975)

LOGAN, L. M., HUNT, G. R., and SALISBURY, J. W.
The Use of Mid-Infrared Spectroscopy in Remote Sensing of Space Targets
Chap. V in Bk., IR and Raman Spectros. of Lunar and Terrestrial Minerals, Ed.: C. Karr, Acad. Press (1975)

MARKHAM, T. P., BUCHAU, J. (Space Phys. Div.), ANCTIL, R. E., and NOXON, J. F. (Harvard Univ., Cambridge, Mass.)
Airborne Study of Equatorial 6300 Å Nightglow
J. of Atm. and Terrestrial Phys., Vol. 37, No. 1 (1975)

MENEELY, C. T., MAJ., and EDWARDS, D. F., RIMSAY, R. L. (Colo. State Univ.)
Diffusion Constant Measurement of Macromolecules in Solutions Containing Particulate Contaminants
Appl. Opt., Vol. 14 (September 1975)

MURPHY, R., COOK, F., and SAKAI, H.
Time Resolved Fourier Spectroscopy
J. of Opt. Soc. of Am., Vol. 65 (May 1975)

MURPHY, R. E., LEE, E. T. P., and HART, A. M.
Quenching of Vibrationally Excited Nitric Oxide by Molecular Oxygen and Nitrogen
J. of Chem. Phys., Vol. 63, No. 7 (1 October 1975)

SALISBURY, J. W., and HUNT, G. R.
Remote Sensing of Rock Type in the Visible and Near Infrared
Proc. of 9th Intl. Symp. on Remote Sensing of Envmt., Vol. 3 (1974)
Meteorite Spectra and Weathering
J. of Geophys. Res., Vol. 79, No. 29 (October 1974)

SALISBURY, J. W., HUNT, G. R., and LENHOFF, C. J.
Visible and Near Infrared: Part X. Stony Meteorites
Modern Geol., Vol. 5 (1975)

SCHLOSSBERG, H. R., and FETTERMAN, H. R. (MIT Lincoln Lab., Lexington, Mass.)
Submillimeter-Wave Optically Pumped Molecular Lasers
Microwave J. (November 1974)
Optically Pumped Vibrational Transition Laser in OCS
Appl. Phys. Ltrs., Vol. 26 (15 March 1975)

SHARMA, R. D., MALT, R. B., HART, R. R. (Mass. Inst. of Technol., Cambridge, Mass.), and PICARD, R. H.
Energy Transfer in Molecular Collisions Far from Resonance
Chem. Phys. Ltrs., Vol. 35, No. 2 (September 1975)

SHARMA, R. D. (Mass. Inst. of Technol., Cambridge, Mass.), and PICARD, R. H.
Distorted-Wave Born Calculation of Near-Resonant Energy Transfer
J. of Chem. Phys., Vol. 62, No. 8 (15 April 1975)

SHETTLE, E. P.
Ltr. to Ed., *Secret Storm*
Comp. Decisions, Vol. 7, No. 1 (January 1975)
Comment on "Atmospheric Aerosol Size Spectra: Rapid Concentration Fluctuations and Bimodality" by T. E. Graedel and J. P. Franey
J. of Geophys. Res., Vol. 80, No. 21 (20 July 1975)

SHETTLE, E. P., and GREEN, A. E. S. (Univ. of Fla.)
Multiple Scattering Calculations of the Middle Ultraviolet Reaching the Ground
Appl. Opt., Vol. 13, No. 7 (July 1974)
The Effects of Atmospheric Ozone and Aerosols on the Middle UV Reaching the Ground
Sec. 5.5 in The Natural and Radiatively Perturbed Tropo. - CIAP Mono. 4, U. S. Dept. of Trnsp., Climatic Impact Assessment Prgm., Rpt. No. DOT-TST-75-54 (September 1975)

SHETTLE, E. P., and KURIYAN, J., (Univ. of Calif. at Los Angeles)
Atmospheric Radiative Transfer Theory (Visible and UV)
Sec. 4.5 in the Natural Strato. of 1974 - CIAP Mono. 1, U. S. Dept. of Trnsp., Climatic Impact Assessment Prgm., Rpt. No. DOT-TST-75-51 (September 1975)

SHETTLE, E. P., NACK, M. L. (Comp. Sci. Corp., Silver Spring, Md.), and GREEN, A. E. S. (Univ. of Fla.)
Multiple Scattering and Influence of Clouds, Haze, and Smog on the Middle UV Reaching the Ground
Sec. 2.22 in The Impacts of Climatic Changes on the Biosphere, CIAP Mono. 5, U. S. Dept. of Trnsp., Climatic Impact Assessment Prgm., Rpt. No. DOT-TST-75-55 (September 1975)

SMITH, D. R., and LOEWENSTEIN, E. V.
A Discussion of Non-Polarizing Angles in Thin-Film Beam Splitters for Michelson Interferometers
Appl. Spectros., Vol. 30, No. 3 (May-June 1976)
Optical Constants of Far Infrared Materials, III: Plastics
Appl. Opt., Vol. 14, No. 6 (June 1975)
Optical Constants of Metal Oxides in the Far Infrared Region
Appl. Opt., Vol. 15 (April 1976)

STAIR, A. T., JR., ULWICK, J. C., and BAKER, K. D., BAKER, D. J. (Utah State Univ.)
Rocketborne Observations of Atmospheric Infrared Emissions in the Auroral Region
Atm. of Earth and the Planets, B. M. McCormac (1975), D. Reidel Pub. Co., Dordrecht, Holl.

VANASSE, G. A., MURPHY, R. E., and COOK, F. H.
Double-Beaming Technique in Fourier Spectroscopy
Appl. Opt., Vol. 15, No. 2 (February 1976)

VOLZ, F. E.
Economical Multispectral Sun Photometer for Measurement of Aerosol Extinction from 0.44 to 1.6 μm and Precipitable Water
Appl. Opt., Vol. 13, No. 8 (August 1974)
Precision and Accuracy of Sun Photometry - A Reply
J. of Appl. Met., Vol. 13, No. 8 (August 1974)
Distribution of Turbidity After the 1912 Katmai Eruption in Alaska
Burden of Volcanic Dust and Nuclear Debris After Injection into the Stratosphere at 40N to 58N
J. of Geophys. Res., Vol. 80, No. 18 (20 June 1975)
Volcanic Twilights from the Fuego Eruption
Sci., Vol. 189 (4 July 1975)

VOLZ, F. E., and SHETTLE, E. P.
Haze in the Stratosphere - From the October 1974 Fuego Eruption
Nature, Vol. 260 (April 1976)

WODARCZYK, F. J., and SACKETT, P. B.
Electronic-to-Vibrational Energy Transfer from Br ($4^2P_{1/2}$) to HF
Chem. Phys., Vol. 12 (1976)

WODARCZYK, F. J., and MAC DONALD, R. G., MOORE, C. B., SMITH, I. W. M. (Univ. of Calif., Berkeley, Calif.)
Vibrational Relaxation of HCl (v=1) by Cl Atoms
J. of Chem. Phys., Vol. 62, No. 8 (15 April 1975)

PAPERS PRESENTED AT MEETINGS JULY 1974 - JUNE 1976

CHUNG, S. (Univ. of Wis.), and LEE, E. T. P.
Dissociation of the Hydrogen Molecule by Electron Collision
27th Ann. Gaseous Elect. Conf., Houston, Tex. (22-25 October 1974)

CLOUGH, S. A.
Vibration-Rotation Effects on the Intensities of Water: Application to ν_2
Mol. Spectros. Symp., Ohio State Univ., Columbus, Ohio (16-18 June 1975)

CONLEY, T. D., and WILSON, R. C. (Boston Coll., Space Data Lab., Newton, Mass.)
Measurements of Positive Ion Mobility in the Mesosphere
Symp. on High Atm. and Space Problems of Atm. Elec., Grenoble, Fr. (30 August 1975)
Positive Ion Mobilities in the Mesosphere
1975 Fall Ann. Mtg. of Am. Geophys. Union, San Francisco, Calif. (8-12 December 1975)

FENN, R. W., SHETTLE, E., and VOLZ, F.
Models of the Optical Properties of Atmospheric Aerosols
23rd Natl. IR Inf. Symp., Naval Postgrad. Sch., Monterey, Calif. (23-25 July 1975)

FETTERMAN, H. R. (MIT Lincoln Lab., Lexington, Mass.), SCHLOSSBERG, H. R., and BARCH, W. E. (MIT Lincoln Lab., Lexington, Mass.)
Optically Pumped 15. 90 μm SF_6 Laser
CLEA Mtg., Wash., D. C. (27-30 May 1975)

GIBSON, F. W.
In Situ Photometric Observations of Optical Scattering Properties of Atmospheric Aerosols
1975 Fall Mtg. of the Opt. Soc. of Am., Boston, Mass. (21-24 October 1975)

HANSEN, D. F., SCHULER, M. P. (HSS, Inc., Bedford, Mass.), and O'NEIL, R. R.
PRECEDE Ground Based Spectrographic Measurements
1975 Fall Ann. Mtg. of Am. Geophys. Union, San Francisco, Calif. (8-12 December 1975)

HORDVIK, A., and SCHLOSSBERG, H.
An Opto-Acoustic Technique for Measuring the Optical Absorption Coefficient in Solids
1975 Fall Mtg. of Opt. Soc. of Am., Boston, Mass. (21-24 October 1975); 5th Conf. on IR Laser Window Mats., Las Vegas, Nev. (1-4 December 1975)

KING, J. I. F.
Parametric Inversion for Real Atmospheric Transmittances
Sec. Conf. on Atm. Radn., Arlington, Va. (29-31 October 1975)

LEIBY, C. C., JR., and PRASAD, B.
Observation of Stimulated Raman Emission at UHF from Laboratory Plasmas
27th Ann. Gaseous Elect. Conf., Houston, Tex. (22-25 October 1974)
Enhanced Coherent Raman Emission from a Theta-Pinch Plasma Experiment
70th Ann. Mtg. of the Am. Phys. Soc., Div. of Plasma Phys., St. Petersburg, Fla. (10-14 November 1975)

MC CLATCHEY, R. A.
High Resolution Atmospheric Transmittance Modeling
IR Inf. Symp., Naval Postgrad. Sch., Monterey, Calif. (23-25 July 1975)
Radiative Properties of the Atmosphere
Sec. Conf. on Atm. Radn., Arlington, Va. (29-31 October 1975)

MC CLATCHEY, R. A., SELBY, J. E. A., and GARING, J. S.
Optical Modeling of the Atmosphere
22nd AGARD Tech. Mtg. on Opt. Propagation in the Atm., The Tech. Univ. of Denmark, Lyngby, Denmark (27-31 October 1975)

MILAM, D. (Lawrence Livermore Lab., Livermore, Calif.), BRADBURY, R. A., and PICARD, R. H.
Statistical Analysis of Laser-Induced Gas Breakdown: A Test of the Lucky Electron Theory of Avalanche Formation
7th ASTM-ERDA-NBS-ONR Symp. on Damage in Laser Mats., Boulder, Colo. (29-31 July 1975)

MURPHY, R., COOK, F., and SAKAI, H.
Time Resolved Fourier Spectroscopy
Opt. Soc. of Am. Mtg., Houston, Tex. (15-18 October 1974)

MURPHY, R. E., FAIRBAIRN, A. R., and ROGERS, J. W., HART, A. M.
Near Infrared Nuclear Spectra Interpretation by Recent Laboratory Results
Def. Adv. Res. Projects Agcy., 4th Strat. Space Symp., Monterey, Calif. (23 September 1975)

MURPHY, R. E., ROGERS, J. W., RAHBEE, A., COOK, F. H., BILLINGSLEY, F. P., and LEE, E. T. P.
LABCEDE Nitric Oxide SWIR Measurements, Analysis and Calculations
Def. Adv. Res. Projects Agcy., 4th Strat. Space Symp., Monterey, Calif. (23 September 1975)

O'NEIL, R. R., HUPPI, E. R., and LEE, E. T. P.
PRECEDE Experiment: Ground Based Telephotometer Measurements of N_2^+ in 3914A and O (^1S) 5577A Emission
1975 Fall Ann. Mtg. of Am. Geophys. Union, San Francisco, Calif. (8-12 December 1975)

O'NEIL, R. R., STAIR, A. T., and ULWICK, J. C.
Project EXCEDE: Artificial Aurora Produced by Rocketborne Electron Accelerators
Symp. on Active Exper. in Space Plasmas, Boulder, Colo. (3-5 June 1976)

PELZMANN, R. F., 1ST LT.
Rocket Observations in the Infrared Using Numerical Integration
148th Mtg. of the Am. Astronom. Soc., Haverford Coll., Haverford, Pa. (21-24 June 1976)

PICARD, R. H.
Laser Induced Damage Mechanisms in Dielectrics
Electro-Opt. Sem., Polytech. Inst. of Brooklyn, Grad. Ctr., Farmingdale, N. Y. (9 January 1976)

PICARD, R. H., MILAM, D. (Lawrence Livermore Lab., Livermore, Calif.), BRADBURY, R. A., and FAN, J. C. C. (MIT Lincoln Lab., Lexington, Mass.)
Threshold Ambiguities in Absorptive Laser Damage to Dielectric Films
7th NBS-ONR-ASTM Symp. on Damage in Laser Mats., Boulder, Colo. (30-31 July 1975)

PICARD, R. H., and WILLIS, C. R. (Boston Univ., Boston, Mass.)
Time-Dependent Projection-Operator Approach to Master Equations for Coupled Systems with Correlations
Ann. Mtg. of Am. Phys. Soc., New York, N. Y. (2-5 February 1976)

PRICE, S. D.
The AFGL Infrared Celestial Survey Program
AIAA 4th Sounding Rocket Technol. Conf., Boston, Mass. (23-25 June 1976)

REIDY, W. P., SHEPHERD, O. (Visidyne, Inc., Burlington, Mass.), O'NEIL, R. R., ULWICK, J. C., and DAVIS, T. N. (Geophys. Inst., Univ. of Alaska), MITCHELL, H. J. (R&D Assoc., Arlington, Va.)
EXCEDE II Test Measurements
1975 Fall Ann. Mtg. of Am. Geophys. Union, San Francisco, Calif. (8-12 December 1975)

ROTHMAN, L. S.
Determination of Valence Force Constants for Water from Vibrational Data
Mol. Spectros. Symp., Ohio State Univ., Columbus, Ohio (16-19 June 1975)

SACKETT, P. B.
Infrared Laser Studies of Vibrational Energy Transfer
Phys. Chem. Res. Gp. Sem., Mass. Inst. of Technol., Cambridge, Mass. (4 December 1974)

SAKAI, H.
High Resolution Fourier Spectroscopy
Opt. Soc. of Am. Mtg., Houston, Tex. (15-18 October 1974)
Measurement of the 3-Micron Methane Band
Mol. Spectros. Symp., Ohio State Univ., Columbus, Ohio (16-18 June 1975)

SANDOCK, J. A., and BURT, D. A. (Utah State Univ.), BIEN, F. (Aerodyne Res., Inc., Burlington, Mass.)
PRECEDE Experiment
1975 Fall Ann. Mtg. of Am. Geophys. Union, San Francisco, Calif. (8-12 December 1975)

SHETTLE, E. P., and FENN, R. W.
Models of the Atmospheric Aerosols and their Optical Properties
22nd AGARD Tech. Mtg. on Opt. Propagation in the Atm., The Tech. Univ. of Denmark, Lyngby, Denmark (27-31 October 1975)

SHETTLE, E. P., FENN, R. W., and VOLZ, F. E.
Atmospheric Aerosols: Models of their Optical Properties
56th Ann. Am. Geophys. Union Mtg., Wash. D. C. (16-20 June 1975)
2nd Conf. on Atm. Radn., Arlington, Va. (29-31 October 1975)

STAIR, A. T., JR., CARPENTER, J. W. (Visidyne, Inc., Burlington, Mass.), and FITZ, H. C., JR. (Def. Nuc. Agcy., Wash., D. C.)
EXCEDE Experiments: Introduction
1975 Fall Ann. Mtg. of Am. Geophys. Union, San Francisco, Calif. (8-12 December 1975)

STAIR, A. T., JR., and ULWICK, J. C.
Infrared Observations in the Auroral Region
Summer Adv. Study Inst., Phys. and Chem. of Atm., Univ. of Liege, Belgium (29 July - 9 August 1974)

ULWICK, J. C.
Optical/Infrared Rocket Probing of the Auroral Atmosphere
1975 Intl. Assoc. for Geomag. and Aeron. (IAGA) Symp., Grenoble, Fr. (25 August - 6 September 1975)

ULWICK, J. C., REIDY, W. (Visidyne, Inc., Burlington, Mass.), and HEGBLOM, E. R. (Boston Coll., Chestnut Hill, Mass.)
Rocket Measurements of the Energy Spectra of Auroral Electrons
1975 Intl. Assoc. for Geomag. and Aeron. (IAGA) Symp., Grenoble, Fr. (25 August - 6 September 1975)

VANASSE, G. A.
Data Compression for Fourier Spectroscopy
Johns Hopkins Univ., Baltimore, Md. (31 March - 2 April 1976)

VOLZ, F. E.
Twilight, Stratospheric Aerosol, and Volcanic Eruptions
Mass. Inst. of Technol., Dept. of Met. (Sem.), Cambridge, Mass. (7 March 1975)
Volcanic Twilight Color Ratios
1975 Fall Mtg. of Opt. Soc. of Am., Boston, Mass. (21-24 October 1975)
Turbidity and Solar Aureole in the Maritime Tropics
2nd Conf. on Atm. Radn., Arlington, Va. (29-31 October 1975)

WESTON, E. B.
Some Needs in Long-Period and Eruptive Variable Star Observations
Am. Assoc. of Variable Star Observers Mtg., McDonnell Planetarium, St. Louis, Mo. (28-30 May 1976)
Characteristics of Variable Stars Seen in Infrared Sky Surveys
148th Mtg. of Am. Astronom. Soc., Haverford Coll., Haverford, Pa. (21-24 June 1976)

WESTON, E. B., and WARES, G. W.
Infrared Sky Surveys and the Spiral Structure of our Galaxy
Am. Assoc. of Variable Star Observers Mtg., McDonnell Planetarium, St. Louis, Mo. (28-30 May 1976)
Contributions of Infrared Sky Surveys to an Understanding of the Spiral Structure of Our Galaxy
148th Mtg. of Am. Astronom. Soc., Haverford Coll., Haverford, Pa. (21-24 June 1976)

TECHNICAL REPORTS
JULY 1974 - JUNE 1976

COOK, F. H., and MURPHY, R. E.
A Synchronous Signal Processing Technique for Repetitive Arbitrary Waveforms
AFCRL-TR-76-0035 (19 January 1976)

GRIEDER, W. F., BAKER, K. D. (Utah State Univ.), STAIR, A. T., JR., and ULWICK, J. C.
Rocket Measurement of OH Emission Profiles in the 1.56 and 1.99 μm Bands
AFCRL-TR-76-0057 (28 January 1976)

HUNT, G. R., and SALISBURY, J. W.
Mid-Infrared Spectral Behavior of Igneous Rocks
AFCRL-TR-74-0625 (23 December 1974)
Mid-Infrared Spectral Behavior of Metamorphic Rocks
AFCRL-TR-76-0003 (6 January 1976)

LOGAN, L. M., HUNT, G. R., LONG, D. A., CAPT., and DYBWAD, J. P.
Absolute Infrared Radiance Measurements of Venus and Jupiter
AFCRL-TR-74-0573 (15 November 1974)

ROGERS, J. W.
Instrumentation Analysis and Data Processing for Rocketborne LWIR Spectrometers (with Application to Rocket A18. 006-2 of 22 March 1973
AFCRL-TR-75-0535 (8 October 1975)

RYAN, T. G., and LEIBY, C. C., JR.
Thermophysical Properties of Thermal Energy Storage Materials - Lif/NaF
AFCRL-TR-75-0263 (8 May 1975)

SAKAI, H.
High-Resolution Fourier Spectroscopy
AFCRL-TR-74-0571 (14 November 1974)

Appendix A

AFGL PROJECTS BY PROGRAM ELEMENT

Program Element	Project Number, Title and Agency
61101F	ILIR Laboratory Director's Fund
61102F	*DEFENSE RESEARCH SCIENCES*
	2303G1 Ion Chemistry
	2303G2 Plume-Atmosphere Interactions
	2309G1 Earth Sciences and Technologies
	2310G1 Infrared and Optical Techniques
	2310G2 Meteorological Research
	2310G3 Upper Atmosphere Composition
	2310G4 Infrared Non-Equilibrium Radiative Mechanisms
	2311G1 Energetic Particle Environment
	2311G2 Electrical Structure of Aerospace
	2311G3 Solar Environmental Research
62101F	*ENVIRONMENT*
	4643 Aerospace Radio Propagation
	6665 Balloon Technology
	6670 Atmospheric Sensing Techniques
	6672 Weather Radar Techniques
	6687 Stratospheric Environment
	6688 Ultraviolet Radiations
	6690 Atmospheric Density and Structure
	6698 Meteorological Satellite Technology
	7600 Geodesy for Naviguidance
	7601 Magnetospheric Effects on Space Systems
	7605 Weather Modification
	7621 Atmospheric Optics
	7628 Geophysical and Geokinetic Effects
	7659 Aerospace Research Instrumentation
	7661 Spacecraft Charging
	7663 Ionospheric Dynamics and Propagation
	7670 IR Properties of the Environment
	8624 Variability of Meteorological Elements
	8628 Terminal Weather Forecasting

In addition to the above continuing Air Force funded projects, AFGL participates in joint programs supported by the following agencies:

1) U. S. Air Force:
   Air Weather Service
   Electronic Systems Division
   Space and Missile Systems Organization
2) Advanced Research Projects Agency
3) Defense Mapping Agency
4) Defense Nuclear Agency
5) National Security Agency

Appendix B

AFGL ROCKET PROGRAM: JULY 1974 – JUNE 1976

Date	Launch Site	Vehicle	Experiment	Scientist	Results
17 Aug 74	WSMR	Ute Tomahawk	Vehicle Potential Stabilization	C. Sherman	Success
4 Sep 74	WRR	Aerobee 200	IR Sources (Hi Star II)	R. Walker	Success
11 Sep 74	WRR	Aerobee 200	IR Sources (Hi Star II)	R. Walker	Partial
17 Sep 74	WRR	Aerobee 200	IR Sources (Hi Star II)	R. Walker	Failure (P)*
17 Oct 74	WSMR	Nike Hydac	Electron Beam (PRECEDE)	O'Neil	Success
13 Dec 74	WSMR	Ute Tomahawk	10" Falling Sphere	Geary	Partial
14 Jan 75	WOPS	Ute Tomahawk	Engineering Test	N. Rosenberg	Success
15 Jan 75	WOPS	Ute Tomahawk	Chemical Release	N. Rosenberg	Partial
17 Jan 75	WOPS	Ute Tomahawk	7" Falling Sphere and Chemical Release	A. Faire N. Rosenberg	Success
17 Jan 75	WOPS	Paiute Tomahawk	Mass Spectrometer, Photometer, E-Field Sensor	R. Narcisi B. Dandekar R. Sagalyn	Partial
17 Jan 75	WOPS	Paiute Tomahawk	Chemical Release, Photometers	R. Good	Partial
26 Feb 75	PFRR	Astrobee D	Gerdien Condenser	J. Ulwick	Success
29 Feb 75	PFRR	Astrobee D	IR and OH Measurements	J. Ulwick	Success
10 Apr 75	CRR	Paiute Tomahawk	Chemical Release, HIBAL Sphere	N. Rosenberg A. Faire	Success
10 Apr 75	CRR	Paiute Tomahawk	Chemical Release	N. Rosenberg	Success
10 Apr 75	CRR	Paiute Tomahawk	Mass Spectrometer, E-Field Measurement	R. Narcisi M. Smiddy	Success
21 Apr 75	CRR	Paiute Tomahawk	Chemical Release, E-Field Measurement	N. Rosenberg M. Smiddy	Success
21 Apr 75	CRR	Paiute Tomahawk	Chemical Release	N. Rosenberg	Success
21 Apr 75	CRR	Paiute Tomahawk	Mass Spectrometer	R. Narcisi	Success
25 Apr 75	CRR	Paiute Tomahawk	Chemical Releases, Photometers	N. Rosenberg	Success
25 Apr 75	CRR	Paiute Tomahawk	Chemical Releases	N. Rosenberg	Success

WSMR – White Sands Missile Range, New Mexico
WRR – Woomera Rocket Range, Australia
WOPS – Wallops Island, Virginia
PFRR – Poker Flat Rocket Range, Alaska
CRR – Churchill Rocket Range, Manitoba, Canada
WTR – Western Test Range, Vandenberg AFB, California
ETR – Eastern Test Range, Cape Canaveral, Florida

*(P) – Payload
*(V) – Vehicle

Appendix B

AFGL ROCKET PROGRAM: JULY 1974 – JUNE 1976

Date	Launch Site	Vehicle	Experiment	Scientist	Results
25 Apr 75	CRR	Paiute Tomahawk	Mass Spectrometer	R. Narcisi	Success
10 Jun 75	WSMR	Aerobee 150	Density by Laser Backscatter	L. Weeks	Partial
7 Aug 75	WSMR	Aerobee 170	Density by Bremsstrahlung	H. Cohen	Success
15 Aug 75	WTR	Paiute Tomahawk	10″ Falling Sphere	A. Faire	Success
18 Sep 75	WSMR	Paiute Tomahawk	Neutral Mass Spectrometer	C. Philbrick	Success
18 Sep 75	WSMR	Paiute Tomahawk	Neutral Mass Spectrometer	C. Philbrick	Success
14 Oct 75	WSMR	Astrobee F	Zodiac IR Flux, Discrete IR Sources	T. Murdock	Success
16 Oct 75	WSMR	Paiute Tomahawk	Dispersion Control Test	E. Mansfield	Partial
2 Dec 75	WSMR	Astrobee D	IR Emissions from OH (Sun)	T. Conley	Success
2 Dec 75	WSMR	Astrobee D	IR Emissions from OH (Horizon)	T. Conley	Success
2 Dec 75	WSMR	Astrobee D	IR Emissions from OH (Sun)	T. Conley	Success
2 Dec 75	WSMR	Astrobee D	IR Emissions from OH (Sun) (Atomic Oxygen)	T. Conley	Success
2 Dec 75	WSMR	Astrobee D	IR Emissions from OH (Horizon)	T. Conley	Success
2 Dec 75	WSMR	Astrobee D	IR Emissions from Atomic Oxygen (Horizon)	T. Conley	Success
3 Dec 75	WSMR	Aerobee 350	IR Sources (Super Hi Star II)	R. Walker	Success
12 Dec 75	WTR	Ute Tomahawk	HIBAL Sphere	A. Faire	Partial
20 Jan 76	CRR	Black Brant IV	Ionospheric Properties at VLF	R. Harvey	Success
23 Jan 76	WOPS	Ute Tomahawk	Neutral Mass Spectrometer	C. Philbrick	Success
23 Jan 76	WOPS	Nike Tomahawk	Chemical Release	W. Vickery	Success
22 Feb 76	PFRR	Paiute Tomahawk	Photomultiplier, Scintillator	L. Weeks	Success
24 Feb 76	WSMR	Aerobee 170	Solar EUV	L. Heroux	Success
3 Mar 76	PFRR	Paiute Tomahawk	10″ Falling Sphere, Photomultiplier, Scintillator	A. Faire L. Weeks	Partial
26 Apr 76	CRR	Paiute Tomahawk	Positive Ion Mass Spectrometer	R. Narcisi	Failure (V)*
1 May 76	CRR	Paiute Tomahawk	Positive Ion Mass Spectrometer	R. Narcisi	Success
18 May 76	WSMR	Aerobee 150	Solar EUV and VUV	L. Heroux	Success
6 Oct 75	WTR	AE-D	Tri-Axial Accelerometer EUV Spectrophotometer	F. Marcos H. Hinteregger	Success
19 Nov 75	ETR	AE-E	Tri-Axial Accelerometer EUV Spectrophotometer	F. Marcos H. Hinteregger	Success
Mar 76	ETR	SOLRAD II	Protons and Alpha Particles	L. Katz	Success
	WTR	S3-1	Accelerometers, Ionization Gauge, and Neutral Mass Spectrometer	F. Marcos C. Philbrick	Success
	WTR	S3-2	Accelerometers, Ionization Gauge, and Neutral Mass Spectrometer	F. Marcos C. Philbrick	Success

APPENDIX C

Air Force Geophysics Laboratory

HANSCOM AIR FORCE BASE, BEDFORD, MASS.

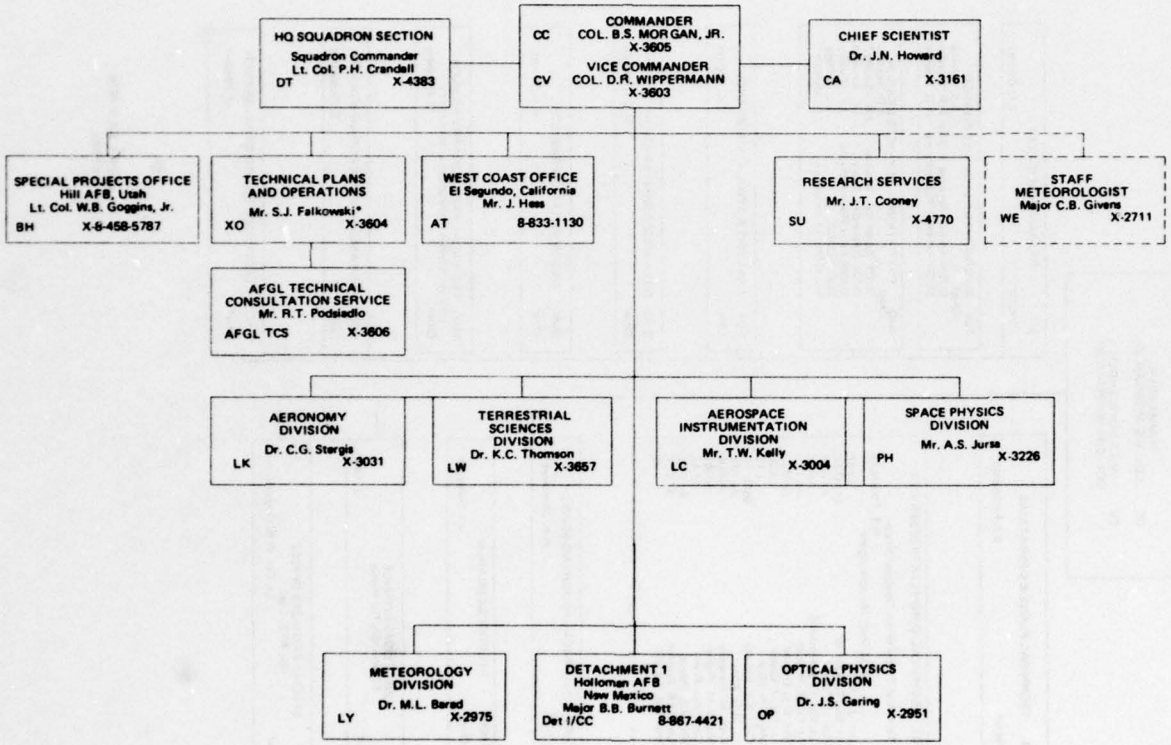

AS OF 1 JULY 1976
* ACTING

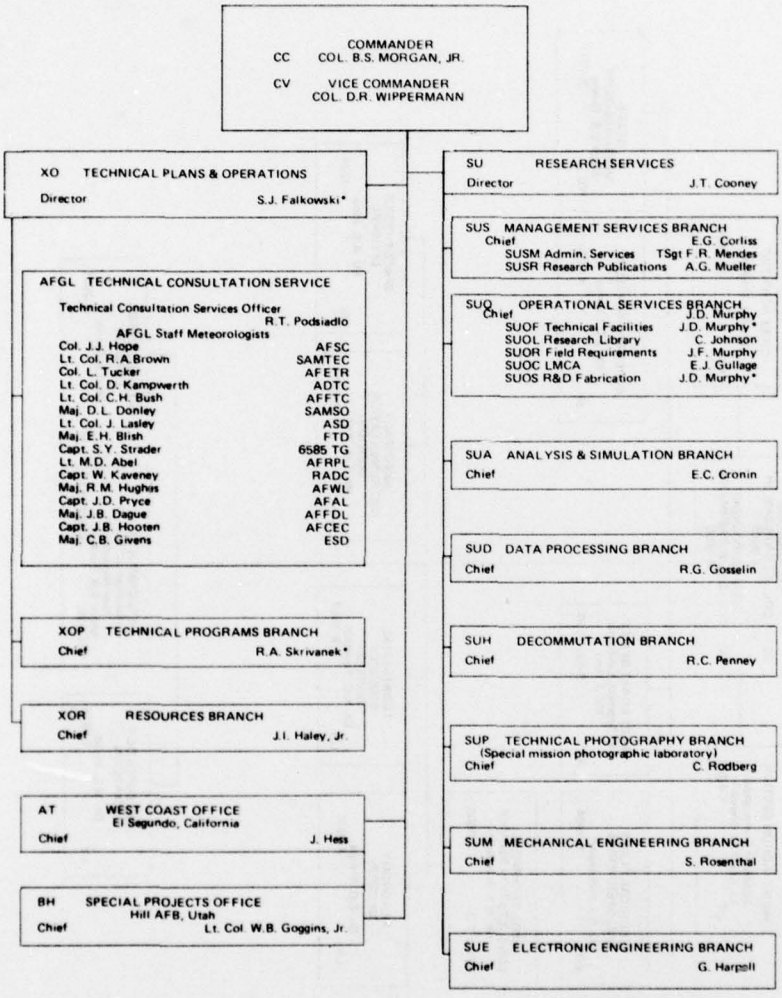

AS OF 1 JULY 1976
* ACTING

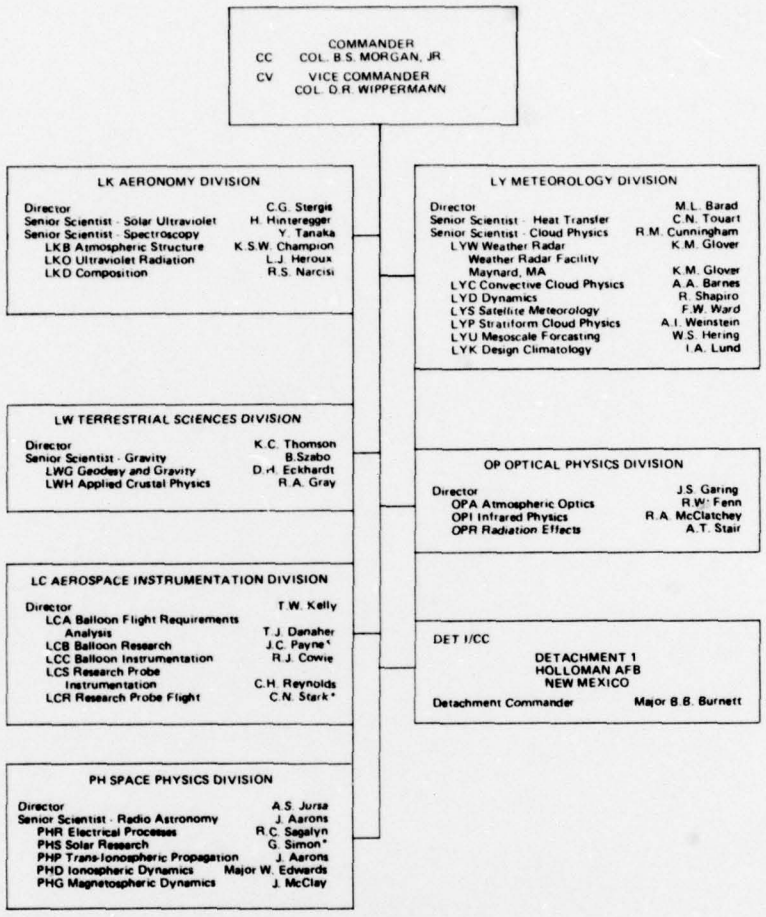

AS OF 1 JULY 1976
* ACTING

☆ U. S. GOVERNMENT PRINTING OFFICE: 1978--700-031--148

Unclassified

SECURITY CLASSIFICATION OF THIS PAGE (When Data Entered)

REPORT DOCUMENTATION PAGE		READ INSTRUCTIONS BEFORE COMPLETING FORM
1. REPORT NUMBER AFGL-TR-77-0137	2. GOVT ACCESSION NO.	3. RECIPIENT'S CATALOG NUMBER
4. TITLE (and Subtitle) Air Force Geophysics Laboratory Report on Research		5. TYPE OF REPORT & PERIOD COVERED Scientific. Interim. July 1, 1974 - June 30, 1976 6. PERFORMING ORG. REPORT NUMBER Special Reports, No. 204
7. AUTHOR(s) John F. Dempsey, Editor		8. CONTRACT OR GRANT NUMBER(s) N/A
9. PERFORMING ORGANIZATION NAME AND ADDRESS Air Force Geophysics Laboratory Hanscom AFB, MA 01731		10. PROGRAM ELEMENT, PROJECT, TASK AREA & WORK UNIT NUMBERS 9993XXXX
11. CONTROLLING OFFICE NAME AND ADDRESS Office of the Chief Scientist (CA) Air Force Geophysics Laboratory Hanscom AFB, MA 01731		12. REPORT DATE June 1977 13. NUMBER OF PAGES
14. MONITORING AGENCY NAME & ADDRESS(if different from Controlling Office)		15. SECURITY CLASS. (of this report) Unclassified 15a. DECLASSIFICATION/DOWNGRADING SCHEDULE N/A

16. DISTRIBUTION STATEMENT (of this Report)

Approved for public release; distribution unlimited.

17. DISTRIBUTION STATEMENT (of the abstract entered in Block 20, if different from Report)

18. SUPPLEMENTARY NOTES

Tech, Other

19. KEY WORDS (Continue on reverse side if necessary and identify by block number)

Geokinetics	Solar Radiations	Trans-Ionospheric Signal
Geodesy	Balloon Technology	Propagation
Gravity	Optical Physics	Rocket Instrumentation
Seismology	Ionospheric Physics	Upper Atmosphere Physics
Meteorology	Magnetospheric Dynamics	Upper Atmosphere Chemistry

20. ABSTRACT (Continue on reverse side if necessary and identify by block number)

This report continues a series of seven Reports on Research at the Air Force Geophysics Laboratory. This report covers a two-year interval. It was written primarily for Air Force and DOD managers of research and development and more particularly for officials in Headquarters Air Force Systems Command, for the Director of Science and Technology (DL), and for the Commanders of and the Laboratories within DL. It is intended that the report will have interest to an even broader audience. → next page

DD FORM 1 JAN 73 1473 EDITION OF 1 NOV 65 IS OBSOLETE

Unclassified

SECURITY CLASSIFICATION OF THIS PAGE (When Data Entered)

cont.

For this latter audience, the report, by means of a survey discussion, attempts to relate the programs to the larger scientific field of which they are a part. The work of each of the Divisions is discussed as a separate chapter. Additionally, the report includes an introductory chapter on AFGL management and logistic activities related to the reporting period. A listing of the publications of each Division during the period follow the chapter describing the research.